Pharmacological and Physiological Manipulation of Ocular Accommodation

Parminder Kaur Randhawa

Doctor of Philosophy

Aston University

July 2016

Aston University

PHARMACOLOGICAL AND PHYSIOLOGICAL MANIPULATION OF OCULAR ACCOMMODATION

Parminder Kaur Randhawa

Doctor of Philosophy

July 2016

Summary

The primary aim of this thesis was to investigate *in-vivo* changes to ocular morphology during ocular accommodation, with particular attention to ciliary muscle changes, using pharmacological agents and physiological stimuli.

To determine the optimum target for accommodation studies, accommodative responses to different stimuli were investigated. Insignificant differences in accommodative responses to a letter target and Maltese cross were found.

Anterior Segment Optical Coherence Tomography (AS-OCT) and semi-automated software were used for *in-vivo* investigation of ciliary muscle morphology. As expected, anti-muscarinic agents reduced the accommodative amplitude, the greatest effect evident with cyclopentolate hydrochloride 1%, which was, in turn, associated with a reduced forward movement of the ciliary muscle, possibly due to the restricted movement of radial and longitudinal fibres.

Pilocarpine nitrate 2% induced a contractile shortening and anterior thickening of the ciliary muscle in both pre-presbyopic and presbyopic eyes. However, pilocarpine does not seem to be a super-stimulus for accommodation. Comparison between cyclopentolate and pilocarpine ciliary muscle morphology further supported the concept that anterior movement of ciliary muscle mass is essential to elicit higher accommodative amplitudes.

Ciliary muscle asymmetry was identified between horizontal and vertical meridians. The findings confirmed a longer ciliary muscle in axial elongated eyes, however, only within the temporal, nasal, and superior muscle quadrants. Nevertheless, during accommodation, anterior thickening and contractile shortening of the muscle was evident for all four quadrants.

The effect of accommodation on posterior eye conformation revealed a homogenous elongation of the posterior pole, with the greatest expansion occurring along the inferior-nasal quadrant, rather than the visual axis. The possibility of a vitreous role in accommodation is discussed.

The studies presented herein suggest a forward movement of ciliary muscle mass is necessary for accommodation. Further research is required to establish whether a mechanical restriction occurs to the muscle with increasing age, resulting in presbyopia. Moreover, investigations are required to explore the variation in ciliary muscle morphology in eyes with ametropia, as well as the likely role of the vitreous in accommodation.

Key words: accommodation, ciliary muscle, anti-muscarinic, parasympathomimetic, retinal contour

ACKNOWLEDGEMENTS

I would like to thank my supervisor Dr Leon Davies and Dr Amy Sheppard for their guidance and theoretical advice for my thesis. Additionally, I would like to thank Dr Richard Armstrong for his statistical advice, Miguel Faria-Ribeiro for his advice and support with analysis for the retinal contour study, Dr Thomas Drew for constructing the Badal Lens systems, Dr Benjamin Coldrick for technical support with the semi-automated software and Professor Ed Mallen for permitting the use of the rig for axial/ eye length measurements.

I would also like to express my gratitude to the participants who volunteered for my studies, and my colleagues in the Optometry Department.

I am grateful to Aston University for supporting my research via the Clinical Demonstratorship.

Thank you to all my friends and family. In particular, I want to acknowledge my sister Sundip, brother Chanveer and husband Ranjit for all their love, support and encouragement.

I reserve my greatest thanks and gratitude to my mum and dad whose unconditional love, support and encouragement have enabled me to achieve my goals. Without them, this thesis would not be possible; Mum and Dad, this is for you.

CONTENTS

LIST OF TABLES

Table **Page**

LIST OF FIGURES

Chapter 1. Accommodation, presbyopia and ocular shape

1.1. Introduction

Ocular accommodation is defined as the adjustment to the dioptric power of the eye (Millodot, 2009), which results from changes within the accommodative apparatus, that constitutes the ciliary muscle, Zonules of Zinn and the crystalline lens. Within the last century, vast research has been conducted to elucidate the processes which produce the rapid change in ocular power, yet, the mechanisms are not fully understood. Research relating to accommodation is important considering a loss of accommodative amplitude occurs with increasing age that affects 100% of the population and subsequently impacts an individual's lifestyle (Holden et al., 2008).

Several theories relating to the possible processes which are involved in accommodation have been established from animal studies (e.g. Bito et al., 1987), since a range of invasive methods can be used to stimulate the accommodative apparatus (i.e. via the Edinger-Westphal nucleus in rhesus monkeys) and visualise the ocular structures (e.g. iridectomised eyes), such as the ciliary muscle that has a primary role in accommodation. However, the lack of *in-vivo* studies in humans has limited our knowledge of the contractility and mobility of the muscle during accommodation and the changes which result with age. Indeed, *in-vitro* studies have documented biological changes that occur with increasing age which may explain the loss in accommodative amplitude in humans (Tamm et al., 1992b; Pardue and Sivak, 2000) and monkeys (Tamm et al., 1992c).

In-vivo studies in humans are dependent on non-invasive instrumentation. Various techniques for investigating the accommodation apparatus have been developed and utilised in accommodation research, such as Scheimpflug photography (Brown, 1973; Dubbelman et al., 2001; Dubbelman et al., 2003; Rosales et al, 2006; Hermans et al., 2007), A-Scan ultrasonography (Glasser and Kaufman, 1999), magnetic resonance imaging (Strenk et al., 1999; Kasthurirangan et al., 2011; Sheppard et al., 2011) and optical coherence tomography (Baikoff et al., 2004, Sheppard and Davies 2010b). Therefore, it could be argued that the higher resolution of instrumentation within recent years has contributed to our understanding of the finite adjustments which occur within the accommodative apparatus and the possible mechanism which results in an increased dioptric power of the eye.

Indeed, investigations of the ciliary muscle using optical coherence tomography has revealed ciliary body asymmetry (Glasser et al., 2001; Sheppard and Davies, 2010b) within the horizontal meridian, as well as the morphological changes which occur during accommodation (e.g. Richdale et al., 2013). Preservation of ciliary muscle contractility with age in humans has been documented (Sheppard and Davies, 2011), suggesting the cause of presbyopia is primarily due to lenticular factors. Yet, removal of the lens substance and replacement with accommodating intraocular lenses fails to restore accommodative ability, with minimal objective increase in accommodative responses reported (Macsai et al., 2006). Considering evidence from *in-vivo* and *in-vitro* studies have provided the basis for the theories behind surgical procedures which aim to reinstate the accommodative amplitude, their lack of success indicates further research is critical relating to the contractility and mobility of the ciliary muscle.

Consequently, the following is a review of the significant findings which have contributed to the field of accommodation and presbyopia, and the key aspects relevant to the present thesis. A detailed account of the anatomical structures within the accomodative apparatus is provided, as well as theories relating to accommodation and presbyopia.

1.2. Anatomy of the accommodative apparatus and auxiliary structures

1.2.1. Crystalline lens

The human lens forms at approximately 28 days gestation (Augusteyn, 2010), when the surface ectoderm overlying the optic vesicle thickens and forms the lens placode. Several foldings occur within the lens placode producing the lens vesicle (Augusteyn, 2010; Kuszak, 1995a) which is completely formed by day 56 (Augusteyn, 2010). The cells on the anterior surface of the lens (the area of the lens towards the cornea) are a single layer of cuboidal cells (Beebe et al, 2001) that structurally form the lens epithelium. The cells are adjoined by interdigitations allowing the structure to change shape and stabilise during accommodation (Cohen, 1965) and functionally secrete a structureless hyaline membrane, which creates the lens capsule, a structure which encases the content of the lens (Kuszak, 1995a; Davson, 2012). The cuboidal cells at the equator and posterior face of the lens eventually differentiate into primary lens fibres (Kuszak, 1995a). The posterior fibres elongate first and lose their nuclei; at the equator the cells arrange into meridional rows and extend forwards and backwards towards the anterior and posterior poles of the lens, respectively. The nuclei within the cells recede as the cells elongate and curve around the poles; eventually the nuclei and other organelles within the fibres disappear (Davson, 2012) creating a transparent

body (Bassnett, 2002). As new fibres are continuously formed beneath the lens epithelium, older fibres are pushed deeper into the lens (Davson, 2012; Augusteyn, 2010; Beebe et al., 2001).

Secondary lens fibres are formed by mitosis from stem cells that exist within the germinative layer, which is a narrow band of cells anterior to the lens equator. Beneath the germinative layer, columnar cells with a hexagonal cross-section known as transitional cells, migrate posteriorly and rotate 180˚ and extend into secondary fibres. The lens growth is continuous throughout life due to the constant formation of secondary lens fibres. The periphery of the lens consists of elongating fibres organised within incomplete shells, referred to as the bow region (Kuszak, 1995a), a term applied since the nuclei of elongating cells remain central as the cells elongate, giving the cells a bow like appearance (Wanko and Gavin, 1959; Kuszak, 1995a; Augusteyn, 2010). The secondary fibres detach from the lens epithelium anteriorly and the lens capsule posteriorly and overlap with newly matured secondary fibres around a polar axis to form sutures (Kuszak, 1995b).

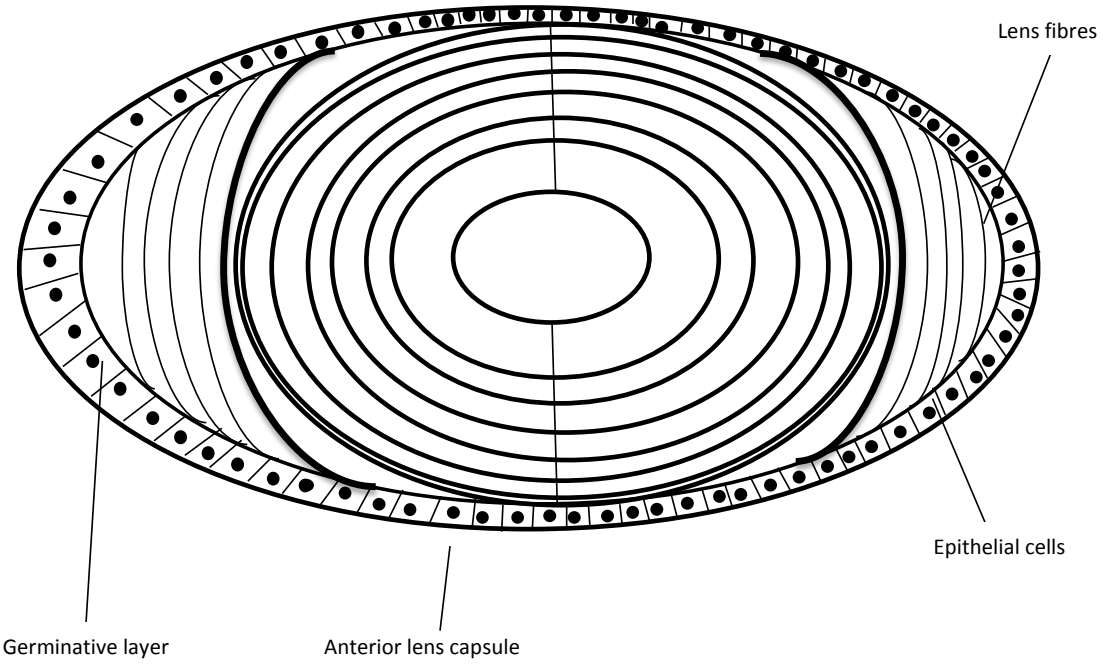

Figure 1-1. Diagram depicting the crystalline lens structure. The thin anterior lens capsule encapsulates the epithelial cells. Secondary lens fibres form within the germinative layer. The concentric lens fibres exist in the deeper layers of the lens. (Diagram based on Kuszak (1995a). The ultrastructure of epithelial and fibre cells in the crystalline lens, pg 309.

The crystalline lenses of most mammals (e.g. mice, rats, guinea pigs, sheep) form anterior and posterior Y-sutures. The posterior sutures are created when the fibres extend to the poles of the lens, more so to the posterior pole than the anterior pole. The fibres overlap and orientate 120˚ to one another, forming three suture branches on the posterior lens surface and one suture branch at the anterior pole (Kuszak, 1995b; Kuszak, 2004). The suture complexes vary between species; for example, the lens fibres in avian eyes form from lens epithelial fibres which are arranged as concentric shells. The fibre ends contact at the anterior and posterior lens, producing a simpler branchless umbilical suture (Kuszak, 2004).

Indeed, the lens can be divided into nuclear, cortical and capsular zones (Sparrow et al., 1986) and the nucleus further subdivided into infantile, foetal and embryonic (Duke-Elder and Wybar, 1961 cited by Augusteyn 2010). Therefore, the different definitions for the regions by research groups can complicate the comparison of the data from *in-vitro* and *in-vivo* investigations of the crystalline lens (Augusteyn, 2010).
Taylor et al (1996) characterized the fibres of eight human lenses (age range 44 to 62 years old) and subdivided the lens into five regions, each defined by the age at which the fibre cells were formed:

- Deep cortex had non-nuclear fibre cells
- Embryonic nucleus formed from the 6 weeks after fertilisation
- Fetal nucleus was defined as containing cell fibres from the 7th week of development until birth
- Juvenile nucleus from the cells formed from birth to puberty
- Adult nucleus defined as the cells formed since puberty

The fibre cells within the adult nucleus are compact as they consume a smaller area (7 ± 2 μm^2) compared to foetal nucleus (35 ± 22 μm^2). Furthermore, the adult and foetal nuclei contribute to the greatest thickness of the lens (21% and 49%, respectively), supporting evidence of the formation of new fibres throughout life, as well as the variation of the growth rates between the regions (Taylor et al., 1996). The capsular thickness increases throughout life, particularly the anterior capsule in comparison to the posterior (Seland, 1974). Consequently the weight of the lens increases with age (Davson, 1980; Glasser and Campbell, 1999): it is 130 mg at 0-9 years of age and 255 mg at 80 to 89 years of age (Davson, 1980).

The lens does not have a nerve supply, nevertheless, muscarinic receptors (G-protein coupled receptors, GCPR; Fryer et al., 2012), have been identified within the anterior

lens epithelium of the human eye, specifically the M3 (Gupta et al., 1994; Collison et al., 2000) and M1 receptor (Collison et al., 2000; Collison and Duncan, 2001). Consequently, activation of membrane potentials are possible when human lenses are placed in acetylcholine solution. Although the receptors remain responsive to acetylcholine throughout life, the amplitude of the response declines with age (at 50 years amplitude of membrane potential is approximately 1.8 mV, at 62 years the amplitude of the membrane potential is approximately 1 mV) (Thomas et al., 1997). Furthermore, the resting potential of the membrane reduces with age. Therefore, it seems muscarinic receptors remain functional throughout life but the magnitude of the electrical pulse of the lens reduces with age (Thomas et al., 1997). Considering the lens is not innervated, it is possible the muscarinic receptors may have a role for cell homeostasis (Nietgen et al., 1999) to prevent the formation of lenticular opacities. For example, it has been suggested the use of parasympathomimetic drugs such as pilocarpine can induce cataracts (Shaffer and Heterington, 1966) due to the disruption of muscarinic receptors within the lens.

1.2.2. The ciliary body

During foetal development, bilateral invaginations of the diencephalon produce the optic vesicles. Folding of the distal portion of the optic vesicles forms the optic cup (Beebe, 1986). The outer margins of the optic cup are in close proximity to the lens vesicle (Graw, 2010) which induce the differentiation of the optic cup into the ciliary body and iris by the expression of genes specific to these structures (Thut et al., 2001). The ciliary body is an anterior extension of the choroid and retina (Tamm and Lütjen-Drecoll, 1996) and lies within the uveal tract and develops in the 11th to 12th week after fertilisation (Forrester et al., 2008 pg 130). The folding of the optic cup produces a bilayered structure which differentiates into the ciliary epithelium; the inner layer produces the non-pigmented epithelium and the outer layer forms the pigmented epithelium (Beebe, 1986; Tamm and Lütjen-Drecoll, 1996; Oyster, 1999 pg 447). The pigmented ciliary epithelium contains melanin (Oyster, 1999) and is continuous with the retinal pigment epithelium (Beebe, 1986), whereas the non-pigmented epithelium is devoid of pigment molecules and is continuous with the sensory retina (Beebe, 1986; Tamm and Lütjen-Drecoll, 1996). The basal face of the non-pigmented epithelium is in contact with the posterior chamber and vitreous body (Tamm and Lütjen-Drecoll, 1996); the morphology and function of the non-pigmented epithelium varies depending on its location (Freddo and Gong, 1971; Tamm and Lütjen-Drecoll, 1996; Streeten 2006).

The ciliary body extends anteriorly from the ora serrata to the iris root and is a unique structure which has three purposes (Freddo and Gong, 1971):

- Producing and secreting aqueous humour into the posterior chamber of the eye;
- Drainage of aqueous humour from the eye;
- Ability to change the focussing power of the eye via changes to the ciliary muscle.

The inner surface of the ciliary body can be divided into two regions (Tamm and Lütjen-Drecoll, 1996): the posterior portion is referred to as the *pars plana* and the anterior portion known as the *pars plicata*, as shown in Figure 1-2.

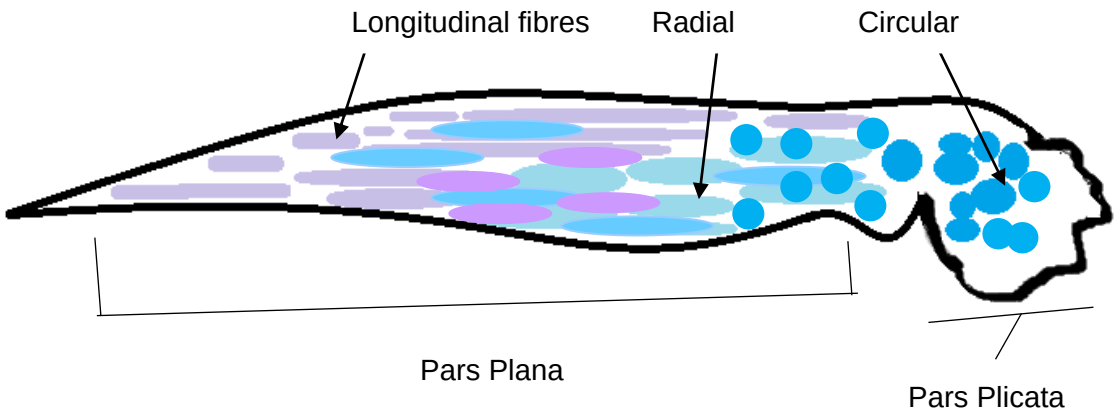

Figure 1-2. The ciliary body can be divided into the *Pars Plana* and the *Pars Plicata.*

The *pars plicata* contains the ciliary processes which are pale radiating undulations consisting of 70-80 ciliary processes, each approximately 0.5 mm wide and 1 mm in height (Tamm and Lütjen-Drecoll, 1996; Streeten, 2006). The ciliary processes secrete aqueous humour (Cole, 1977) and the valleys between the processes anchor the zonular fork (discussed further below*)* (Rohen, 1979; Tamm and Lütjen-Drecoll, 1996). The posterior surface of the iris is continuous with the *pars plicata* (Tamm and Lütjen-Drecoll, 1996) and the anteroposterior length of the *pars plicata* within the adult eye is approximately 2 mm (Streeten, 2006).

The *pars plana* contacts the vitreous body, and contains smooth muscle fibres which form the ciliary muscle (Tamm and Lütjen-Drecoll, 1996).

1.2.3. The ciliary muscle

The ciliary muscle was discovered in the early 1800s and several anatomists are credited for recognising its location, including Phillip Crampton, Ernst Brücke and William Bowman (Harper, 2014). Recent histochemical and ultrastructural examination of the ciliary muscle, within various species, has enhanced our understanding of the muscle's function. Light microscopy of the ciliary muscle of the *gallus domesticus*, a breed of chicken, reveals the muscle has a striated appearance as evident for skeletal muscle (Tedesco et al., 2005). Furthermore, Van der Zypen (1967) suggested the ciliary muscle of the monkey also has a similar structure to skeletal muscle (cited by Flügel et al., 1990), however, cell cultures from human donor eyes (age range 16-91 years) reveal the ciliary muscle is a smooth muscle (Tamm et al., 1991a). The growth of the ciliary muscle has been documented, *in-vitro*, in albino guinea pigs between 1 and 90 days of age since guinea pigs are useful animal models for investigating ocular growth due to their fast development and reproduction in comparison to humans and higher primates (Pucker et al., 2014). The volume of the ciliary muscle increases with normal eye growth, which can be attributed to the muscle becoming longer and thicker as it reaches adult parameters at 90 days of age (Pucker et al., 2014). Furthermore, the development of the nasal and temporal ciliary muscle remains symmetrical throughout life, however, the cells of the nasal ciliary muscle increase in size with age (Pucker et al., 2015). In contrast, the ciliary muscle dimensions are asymmetric within the human and monkey eye, with a longer ciliary muscle length on the temporal side compared to the nasal aspect (Streeten, 2006; Sheppard and Davies, 2010b).

Studies investigating the human ciliary muscle have been conducted for several decades and many aspects of the ultrastructure has been described. The human ciliary muscle consists of tightly contained cells which form bundles and have spaces in between which contain peripheral nerve fibres, fibrils, fibroblasts and connective tissue, specifically collagen (Ishikawa, 1962). The ciliary muscle has the form of a right angled triangle which lies immediately beneath the ciliary processes. The outer surface of the muscle lies against the sclera, with the supra-choroidal lamina lying in between both structures. The ground plate, which contains the elastic lamina extension from Bruch's membrane of the choroid, blood vessels and connective tissue, lies between the ciliary muscle and the ciliary epithelium (Tamm and Lütjen-Drecoll, 1996).

There are three types of muscle fibres which comprise the ciliary muscle. The fibres vary in orientation and are described as longitudinal, radial and circular. The

longitudinal fibres are the outermost fibres which attach loosely to the inner surface of the sclera. The elastic fibres within the tendons of the longitudinal portion extend anteriorly to attach to the elastic fibres of the scleral spur (Tamm et al., 1992a; Tamm and Lütjen-Drecoll, 1996), which is an anterior extension of scleral tissue that extends inwards at the posterior limit of the trabecular meshwork (Freddo and Gong, 1971). The longitudinal fibres are parallel to one another (Ishikawa, 1962) and extend to the posterior chamber where their expansions insert into the anterior choroid (Oyster, 1999). The radial fibres are located towards the centre of the ciliary muscle and they radiate from the anterior chamber angle to the ciliary processes; the inner circular portion runs parallel with the margins of the cornea (Tamm and Lütjen-Drecoll, 1996). The density of connective tissue between the fibres is greater in the radial section compared to the longitudinal fibres (Ishikawa, 1962). The radial fibres extend posteriorly to attach at the elastic lamina of Bruch's membrane (Ishikawa, 1962) which suggests the ciliary muscle may have a role in the movement of the retina and ora serrata during accommodation (Enoch, 1976) and could explain the occurrence of retinal detachments with the use of strong miotics (Westsmith and Abernethy, 1954 cited by Tamm and Lütjen-Drecoll, 1996).

Although the ciliary muscle can be subdivided into separate regions, the histological division is not as defined; rather the longitudinal fibres are mostly present within the outer muscle, whereas the circular fibres predominant in the anterior-inward locations of the muscle and the characteristics gradually change throughout the ciliary muscle (Ishikawa, 1962). Furthermore, during foetal and neonate development, the ultrastructural differences in the smooth muscle fibres are not seen, suggesting the formation of radial and circular fibres occur post-natally (Lütjen-Drecoll et al., 1988a; Forrester et al., 2008 pg 130). Pardue and Sivak (2000) also noted that the muscle groups were not distinguishable in the ciliary muscle from a 1 year old donor, specifically, the orientation of circular fibres.

The differences in the ciliary muscle ultrastructure allows different aspects of the muscle to provide unique functions. The longitudinal portion of the ciliary muscle is connected to the scleral spur (Tamm et al., 1992a) and trabecular meshwork indicating the ciliary muscle may be involved in regulating aqueous outflow (Uga, 1968. Abstract only). The radial and circular regions are located within the anterior muscle, therefore, may have evolved in order to provide an accommodative function (Ebersberger et al, 1993. Abstract only).

The anterior portion of the ciliary muscle has a small cross-sectional area and minimal stiffness in its relaxed state, however, during accommodation it is essential the anterior portion stiffens prior to muscle contraction in order for the muscle to move forward (Flügel et al., 1990). Flügel and colleagues (1990) stated such a function would be possible if different fibres exist such as the fast twitch and slow tonic fibres often observed in skeletal muscle. Comparison of the ciliary muscle and smooth muscle of a blood vessel to skeletal muscle (larynx, diaphragm, pectoral and extraocular muscle) of the cynomolgus monkey revealed the tips of longitudinal muscle fibres have a greater staining for myosin ATPase which resembles the staining of the fast fibres from striated muscle; this suggests the longitudinal muscle tips (anterior attachment of the ciliary muscle to the scleral spur) contract faster than the rest of the muscle and provide an effective stiffness for accommodation (Flügel et al., 1990). Additionally, the existence of microfibrils and myofilaments between smooth muscle cells and the extracellular matrix may be important for maintaining mechanical tension when the ciliary muscle contracts (Tamm and Lütjen-Drecoll, 1996). Further support for various functions of the ciliary muscle are evident from the diverse concentration of proteins within the different locations of the muscle (Flügel-Koch et al., 2009). Considering the posterior ends of the outer longitudinal ciliary muscle insert into Brüchs membrane of the choroid suggests the presence of muscular mechanoreceptors at this region could control the fine movements of the ciliary muscle to maintain an accurate focus during accommodation. Alongside the calretinin-IR terminals within the anterior longitudinal portion of the ciliary muscle, nerve endings between muscle fibres formed close connections with the elastic-like tendons, suggest such a region controls sheer stress during accommodation. Furthermore, intrinsic neurons have also been identified within the various regions of the ciliary muscle suggesting the fine control of accommodation could be controlled internally (Flügel-Koch et al., 2009).

Ciliary muscle dimensions, area of muscle fibre groups and quantity of connective tissue within the muscle have been assessed histologically from human eyes (Tamm et al., 1992b; Pardue and Sivak, 2000) to determine the changes which occur with age. With increasing age, the longitudinal fibres account for the greatest area (range 41-69%) followed by radial fibres (range 25-47%) and circular fibres (range 4-24%) (Pardue and Sivak, 2000). Within older eyes, the circular fibres form bundles near the anterior and internal edge of the muscle, and radial fibres cross obliquely from the scleral spur to the internal edge of the muscle (Pardue and Sivak, 2000).

A reduction to the total length (Tamm et al., 1992b, Pardue and Sivak, 2000) and area (Tamm et al., 1992b) of the muscle has also been shown to occur with advancing age, although there is disagreement as to whether the width increases (Pardue and Sivak, 2000), or remains the same (Tamm et al., 1992b). However, *in-vivo* analysis of the ciliary muscle indicates a reduction in the width at locations representing 50% (CM50) and 75% (CM75) of the ciliary muscle length in presbyopic eyes (Sheppard and Davies, 2010b), which supports evidence for a quantitative decrease in longitudinal fibres (Tamm et al., 1992b).

Within the anterior region of the muscle, at the location of maximum thickness, there is a significant increase in width with age by 2.8 µm/ year nasally and 3 µm/ year temporally (Sheppard and Davies, 2010b). Furthermore, a reduction of the distance between the inner apex and the scleral spur has been observed *in-vitro* (Tamm et al., 1992b, Pardue and Sivak, 2000) and *in-vivo* with similar findings for the nasal and temporal ciliary muscle (reduction of 4.7 µm/ year nasally and 4.1 µm/ year temporally; Sheppard and Davies, 2010b). The findings therefore suggest there is an anterior-inward movement of the ciliary muscle with age. Pardue and Sivak (2000) also identified the anterior length of the muscle becomes shorter whereas the posterior length increases with age suggesting the internal apical edge of the ciliary muscle moves forward with age.

The connective tissue between the ciliary muscle fibre bundles increases with age, particularly within the circular and radial fibre groups (Tamm et al., 1992b, Pardue and Sivak, 2000). The connective tissue within the longitudinal region contributes to 20% of the total area in age groups 50-85 years (Tamm et al., 1992b); in contrast, the connective tissue within the radial portion shows the greatest increase with age. For example, 30-40 year old eyes have connective tissue which contributes to 20% within the region and there is an increase of 1:1 ratio of ciliary muscle fibre to connective tissue with increasing age. The connective tissue within the circular portion also increases with age, with approximately half of the region consisting of connective tissue in eyes older than 60 years (Tamm et al., 1992b), although the increase of tissue does not appear to affect the contraction of the muscle with age (Pardue and Sivak, 2000) as a similar magnitude of contractility has been reported between infant and presbyopic eyes (Van Alphen, 1976).

The possibility for the quantity of fibres within the muscle to alter with age has been reported. Pardue and Sivak (2000) noted an increase of the radial fibres with age and a

fairly stable quantity of circular fibres, whereas Tamm et al (1992b) did not report any change to the area of the radial fibres with age but did report an increase of the circular fibres. The differences in the findings could be due to the sample size as Pardue and Sivak (2000) quantified their data from seven participants, whereas Tamm et al (1992) used data from ninety five eyes and divided their samples depending on horizontal and vertical ciliary muscle orientation. Nevertheless, *in-vivo* findings support the results of Pardue and Sivak (2000) since 25% (CM25) of the ciliary muscle length, which mostly consists of circular fibres, does not appear to alter with age (Sheppard and Davies, 2010b).

1.2.4. Extrinsic innervation to the ciliary muscle

1.2.4.1. Parasympathetic innervation

The multi-unit smooth ciliary muscle also has a dense innervation in order to provide fast contraction and relaxation (Ishikawa, 1962; Lütjen-Drecoll et al., 1988a). The primary extrinsic innervation to the ciliary muscle is provided by the parasympathetic nervous system (Warwick, 1954; Tamm and Lütjen-Drecoll, 1996; Ciuffreda, 1998). It is generally accepted the pre-ganglionic fibres of the ciliary muscle originate at the Edinger-Westphal nucleus, which supplies the autonomic innervation to the eye (Warwick, 1954). The pre-ganglionic nerve cells travel along the third cranial nerve (oculomotor nerve) to the ciliary ganglion where they relay. Consequently, some post-ganglionic fibres travel to the pupil and others travel to the ciliary muscle mostly via the short ciliary nerves. The nerve cells enter the ciliary muscle bundles and although they lose their myelin, the Schwann cells remain (Tamm and Lütjen-Drecoll, 1996). The parasympathetic innervation mediates positive accommodation by providing a rapid change in the focussing power of the eye which has a fast onset of action (1-2 seconds).

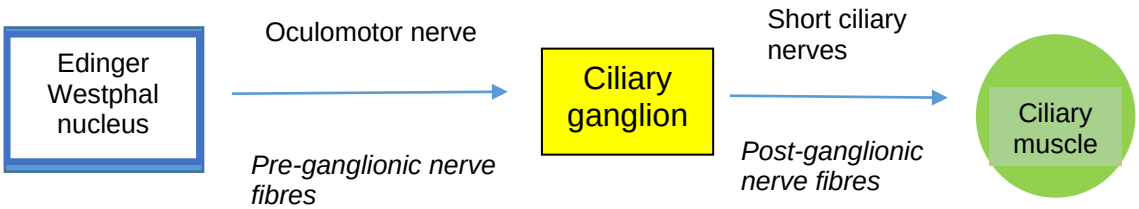

Figure 1-3. Schematic diagram of the parasympathetic pathway to the ciliary muscle.

In-vitro analysis of ciliary muscle from human presbyopic eyes (age range 53 to 91 years) using light microscopy reveals the localization of ganglion cells within the muscle bundles of reticular and circular portion, rather than within the cell bundles

(Tamm et al., 1995). Ganglion cells are located within the inner border of the ciliary muscle whereas the cells are absent within the longitudinal portion. Ganglion cells vary in size between 10 µm and 30 µm, with even distributions throughout the inner regions of the muscle (Tamm et al., 1995). Three types of neuromuscular junctions have been identified in the ciliary muscle of human eyes (Ishikawa, 1962). The first type has a basement membrane between the membranes of the muscle and nerve endings and is the most frequent neuromuscular junction; the second type occurs less frequently than the first and innervates a few muscle cells due to the proximity of the synaptic membranes and the absence of a basement membrane between the muscle and nerve cells; the third type occurs rarely and consists of a larger nerve ending which contacts several muscle cells (Ishikawa, 1962).

The neurotransmitter of the parasympathetic nervous system is acetylcholine which acts upon two classes of cholinergic receptors: nicotinic and muscarinic. Within the autonomic nervous system five subtypes of muscarinic receptors have been identified: M1, M2, M3, M4 and M5 (Hammer et al., 1980; Caulfield and Birdsall, 1998). Muscarinic receptors are present within the ciliary muscle (Lograno and Reibaldi, 1986) and all five receptor subtypes have been identified (Zhang et al., 1995). The M3 receptors are the most abundant within the ciliary body (Woldemussie et al., 1993; Matsumoto et al., 1994; Gil et al., 1997) and are thought to mediate the contraction of the ciliary muscle as established in bovine (Masuda et al., 1998), rhesus monkeys (Poyer et al., 1994) and human tissue (Woldemussie et al., 1993). M1 receptors have been identified within the ciliary processes (Gil et al, 1997) and the ciliary muscle of human tissue (Zhang et al., 1995) and there is a low abundance of M4 receptors in the ciliary body (Gil et al, 1997; Zhang et al., 1995). Such findings are in contrast to bovine eyes where M3 muscarinic receptors dominate within the ciliary processes, and minor amounts of M2 and M4 subtypes are present (Honkanen et al., 1990). There are copious M2 and M3 muscarinic receptors within the circular region of the human ciliary muscle. The presence of both types of receptors within a localised region may indicate that both receptors have a conditional role in modulating the contraction of smooth muscle, like in gastrointestinal smooth muscle (Unno et al, 2003), or the M2 receptor may have a passive role in the presence of the M3 receptor for smooth muscle contraction, as determined in transgenic mice (Matsui et al., 2000). Poyer et al (1994) were unable to exclude the existence of M2 receptors in the longitudinal and circular portion of the rhesus monkey ciliary muscle and suggested the receptors do exist but probably do not mediate the contractile response. The M5 receptor is predominantly present in the longitudinal portion of the muscle (Zhang et al., 1995). The exact

function of the M3 receptor is difficult to determine considering the receptor has also been identified within the human trabecular meshwork (Shade et al., 1996; Wiederholt et al., 1996). Subsequently, the evidence of M2, M3 and M5 muscarinic subtypes within the ciliary muscle impedes a conclusion that the difference in abundance of receptors within each region of the ciliary muscle are responsible for the differential function of aqueous outflow and accommodation (Zhang et al., 1995).

The exact process which produces a contraction of the ciliary muscle is still unknown. Evidence suggests the *in-situ* ciliary muscle of human and cynomolgus monkeys does not contain gap-junctions (Samuel et al., 1996) suggesting electrical activity does not spread from cell to cell. However, *in-vitro* tissue cultures of human ciliary muscle cells indicate gap junctions exist, a finding probably due to the lack of masked expression from the abundant parasympathetic nerve terminals (Tamm et al., 1991a). There is conflicting evidence regarding the major source of ciliary muscle contraction. For example, evidence from an *in-vitro* study on bovine ciliary muscle (Suzuki, 1983) demonstrated the muscle contracts in a solution with high potassium, as well as electrical stimulation of the muscle. However, the responses were abolished with the application of atropine, suggesting the muscarinic receptors are predominantly involved in ciliary muscle contraction. Also, electric simulation of the human ciliary muscle elicits a response which is 85-90% of the maximum produced by carbachol (Lograno and Reibaldi, 1986). Such findings suggest the contraction of the human ciliary muscle is likely to be due to the release of acetylcholine from short ciliary nerve terminals, rather than from the depolarisation of the muscle cells as a consequence of excitation of the muscle cell membrane. However, Lograno and Reibaldi (1986) disagreed and found that the use of the non-selective antagonist atropine reduced the twitch response of the ciliary muscle but did not abolish it when long pulses of electrical simulation were used. Thus, in contrast to Suzuki (1983), the findings suggest the mechanical activity of the ciliary muscle is only partly due to the neurotransmitter acetylcholine (Lograno and Reibaldi, 1986).

1.2.4.2. Sympathetic innervation

There is evidence to suggest the ciliary muscle, like other smooth muscle, has a dual innervation. The diencephalon provides the sympathetic supply to the ciliary muscle; the fibres travel to the lower cervical and upper thoracic regions of the spinal cord, where they synapse in the spinociliary centre of Budge. Second order nerves exit the spinal cord through the cervical and last two thoracic ventral roots. The pre-ganglionic fibres travel up through the cervical sympathetic chain, where they synapse in the

superior cervical ganglion. The third order fibres enter the orbit either with the first division of the trigeminal nerve or individually, where they combine with the long and short ciliary nerves, in such case passing through the ciliary ganglion without synapsing (Cuiffreda, 1998). The neurotransmitter of the sympathetic nervous system is norepinephrine which acts upon two classes of adrenergic receptors: alpha (α) and beta (β).

Sympathetic terminals exist within the ciliary muscle of rhesus and cynomolgus monkeys, which contribute to 1% of the total terminals, suggesting a minimal function of the adrenergic innervation to the ciliary muscle (Ruskell, 1973). Not all mammals exhibit sympathetic innervation to the ciliary muscle, for example, bovine (Suzuki, 1983b).

Van Alphen (1976) investigated the presence of adrenergic receptors on the human ciliary muscle using various selective and non-selective adrenergic agonists, and acetylcholine. The longitudinal and circular segments of the ciliary muscle responded to acetylcholine, however, the catecholamines also induced the relaxation of the ciliary muscle. The non-selective catecholamine, isoproterenol, had the greatest potency for relaxation of the muscle, followed by norepinephrine. Thus, Van Alphen concluded the human ciliary muscle mostly contained beta receptors and possibly a few alpha receptors (Van Alphen, 1976) a finding supported by Zetterström and Hahnenberger (1988). Investigations of the adrenoceptors at the longitudinal and circular portions of the human ciliary muscle, with the use of various adrenoceptor antagonists and agonists, suggests both α_1 and β_2 receptors are present within the circular and longitudinal regions. However, the results indicated inter-individual differences of the ciliary muscle responses to the various agents used, possibly due to the tissue handling and specimens used (Zetterström and Hahnenberger, 1988). In contrast, Lograno and Reibaldi (1986) investigated the human ciliary muscle *in-vitro* of 10 donor eyes and concluded the muscle only comprises β_2 receptors and alpha receptors are absent since the ciliary muscle did not contract with the use of phenylephrine. However, Zetterstom and Hahnenberger (1988) determined phenylephrine only produced a response in 5 of the 12 eyes used and rather noradrenaline, a non-selective adrenoceptor agonist, relaxed the ciliary muscle in all the ciliary muscle tissue samples used. Therefore, the contrasting findings between both studies suggests the sensitivity of the ciliary muscle to phenylephrine is reduced *in-vitro* and cannot be used to rule out the presence of α_1 adrenoceptors.

Although sympathetic innervation to the ciliary muscle has been identified (Tamm and Lütjen-Drecoll, 1996; Rosenfield and Gilmartin, 1998; *review* Gilmartin, 1986) with axons located near the walls of blood vessels and melanocytes of the muscle (Tamm and Lütjen-Drecoll, 1996), there is evidence to suggest the sympathetic nervous system may have an anatagonisitc role in positive accommodation (Cogan 1937; Garner et al., 1983). *In-vivo* electrical stimulation of beta-adrenoceptors of the ciliary muscle within twenty three African green tail monkeys also provides evidence for an antagonistic innervation and that beta receptors have a role in disaccommodation since stimulation of the receptors with isoproterenol reduced the accommodative response. Also, using propranolol, a beta-blocker, prior to the use of isoproterenol, produces a decrease in the accommodative response, but does not eliminate accommodation completely and rather 3-4 D of accommodation remain (Hurwitz et al., 1972). The use of hydroxyamphetamine hydrobromide (an alpha and beta adrenergic agonist) and phenylephrine hydrocholoride (alpha-adrenergic agonist) on eight human volunteers, revealed a reduction in the accommodative amplitude; the greatest reduction occurred with hydroxyamphetamine hydrobromide, suggesting the beta receptors are primarily involved with the antagonism of the parasympathetic innervation to the ciliary muscle (Stephens, 1985). Evidence for a reduced accommodative amplitude, between 10 to 40 seconds after the stimulation of the cervical sympathetic nerve of cynomolgus monkeys, in the presence of a concurrent parasympathetic stimulation, suggests the sympathetic terminals have a minimal role in accommodation due to the slow onset of activity (Törnqvist, 1967). However, the sympathetic innervation may have a significant role for maintaining the accommodative level rather than providing a rapid change in response (Gilmartin et al., 1984) considering the relatively slow time for maximum onset, in comparison to the parasympathetic input. Approximately 30% of the total beta-adrenoceptors present within the anterior segment of human tissue, exist within the ciliary processes (Wax and Molinoff,, 1987) suggesting a role in aqueous outflow (Dafna et al., 1979).

The use of non-selective beta-adrenergic drug timolol maleate within human subjects, produces a 0.85 D myopic shift suggesting the sympathetic innervation of the ciliary muscle may be important for the resting point of accommodation (tonic accommodation) (Gilmartin et al., 1984). A subsequent study to determine whether individual differences in the autonomic tone of the ciliary muscle produced the observed average myopic shift with the use of timolol maleate (Gilmartin et al., 1984) was conducted (Gilmartin and Hogan, 1985). The non-selective beta antagonistic, isoprenaline, was used and the results indicated a mean hyperopic shift of 0.47 D (pre-

isoprenaline = +1.64 ± 0.95, post-isoprenaline = +1.17 ± 0.89) suggesting the sympathetic nervous system has a significant role in maintaining the tonic accommodative state. Furthermore, the lack of oculomotor changes such as vergence, and the minimal changes to the distance refraction and the amplitude of accommodation, suggests the sympathetic input to the ciliary muscle is not significant in the normal visual environment (Gilmartin et al., 1984, Gilmartin and Hogan, 1985). The human ciliary muscle consists of β_2 receptors (Wax and Molinoff, 1987) and within the population, only 15-30% have access to the sympathetic function (Mallen et al., 2005; Vasudevan et al., 2009). Additionally, an *in-vivo* investigation of the human ciliary muscle with the application of 2.5% phenylephrine suggests the α_1 adrenergic receptor agonist does not affect the contractility and dimensions of the ciliary muscle, further supporting the hypothesis the sympathetic innervation has a minimal role in accommodation (Richdale et al., 2012). However, considering the weakest concentration of the drug was used for the study, higher concentrations may have produced observable accommodative changes to the ciliary muscle. Therefore, α_1 adrenoceptors may have a significant role in ocular accommodation particularly at low and midtemporal frequencies in humans (Culhane et al., 1999).

1.2.5. Intrinsic innervation

There is evidence to suggest the ciliary muscle has an intrinsic nerve supply with early studies documenting the neuropeptide, substance P, is present within some varicose nerve terminals, which provides the contraction of the human ciliary muscle (Tamm et al., 1995). Nitric oxide regulates smooth muscle contractility and a vast proportion of nitric producing cells have been identified within the human ciliary muscle (Nathanson and McKee, 1995; Tamm et al., 1995). Nitric oxide relaxes the ciliary muscle of bovine eyes (Wiederholt et al., 1994; Kamikawatoko et al., 1998), therefore, may have a role in facilitating the backward movement of the ciliary muscle during disaccommodation, or possibly provide steady fluctuations to determine the direction of change to induce perfect focus (Tamm et al., 1995). Furthermore, proprioceptors are present within the human ciliary muscle. Within the reticular and longitudinal muscle fibres the receptors may monitor tendon stretch. However, the greatest proportion of receptors are within the anterior region of the ciliary muscle, which contain mostly circular fibres, therefore, may have a mechanical role. Also, the vast concentration of proprioceptors within the circular fibres may provide local regulation for ciliary muscle contraction (Flügel-Koch et al., 2009).

1.2.6. Zonule of Zinn

The Zonule of Zinn are transparent intermediate connections between the ciliary muscle and the crystalline lens. The zonules have two significant roles within the eye: their structural role maintains the position of the crystalline lens (Hanssen et al., 2001) whereas their mechanical role is vital for accommodation whereby forces from the ciliary muscle are transmitted to the crystalline lens. Early studies proposed zonular fibres were comprised of collagen, however, the lack of degradation with collagenase (Raviola, 1971) and the evidence from recent studies using mRNA markers, suggests the main constituent of zonules is fibrillin (*review* Bourge et al., 2007; Hiraoku et al., 2013).

It is unclear how the zonular fibres are synthesised. During embryological development, the invagination of the optic cup results in the non-pigmented region of the ciliary body to lay closest to the lens. Therefore, the attachment of the zonules at the non-pigmented epithelium of ciliary processes, as suggested by various researchers (Rohen, 1979; Farnsworth and Burke, 1977; Raviola, 1971), would be expected in order for the zonules to fulfil their functional and mechanical roles. However, the exact region where zonular insertion occurs has yet to be proved or established in all species, for example, the Japanese monkey (Hiraoka et al., 2013).

A connection of zonular fibres at the basement membrane of the ciliary processes were first identified in rhesus monkeys (Farnsworth and Burke, 1977). Therefore, it is possible that the ciliary epithelial cells synthesize the structural components of zonular fibres (Forrester et al., 2008 pg 37; Levin et al., 2011), evidence for which is supported from *in-situ* hybridization of the guinea pig ciliary epithelium at various stages of ocular development (Hanssen et al., 2001). During foetal development, the non-pigmented epithelium of the ciliary body separates from the lens epithelium, and during this stage, fibrillin-1 mRNA is expressed in the non-pigmented epithelium (Hanssen et al., 2001). Although the eye growth of guinea pigs ceases at 10 months, the expression of fibrillin-1 mRNA persisted within the non-pigmented epithelium (Hanssen et al., 2001), further supporting the hypothesis of zonular production at the non-pigmented ciliary epithelium. Chan et al (1997) investigated the zonular attachment in Sprague-Dawley male rats using a hyaluronan-binding probe. The results indicated the zonules inserted at the *pars plana* over the basement membrane of the ciliary epithelium and the equatorial region of the crystalline lens. Furthermore, evidence for the presence of microfibril bundles of zonular fibres located near the non-pigmented epithelial cell

basement membrane of the ciliary body (Davis et al., 2002; Hiraoka et al., 2013) further supports the hypothesis that zonular fibres originate at the ciliary body. The expression of fibrillin mRNA decreases with age in guinea pigs (Hanssen et al., 2001) and Japanese monkeys (Hiraoka et al., 2010).

The introduction of transmission electron microscopy in the early 1970s enhanced our understanding of the ultrastructure and organisation of the zonule. Three groups of zonules have been located depending on their attachment to the lens capsule (Farnsworth and Burke, 1977; Rohen, 1979; Ludwig et al, 1999). *In-vitro* examination of the zonular fibres in rhesus monkeys aged between 4 and 4½ years, located anterior zonules originating from the valleys between the ciliary processes which inserted into the *pars plana* (Farnsworth and Burke, 1977). Consequently, the architecture of the zonule in 10 human eyes (age range 26-57 years) and 17 cynomolgus monkeys were investigated with electron microscopy. Within the *pars plana*, the zonular fibres form a flat network which interweave at regular intervals. The fibres attach to the non-pigmented epithelium of the ciliary body and form bundles at the posterior end of the ciliary processes before inserting into the ciliary valleys and creating several plexuses described as regular crossings of fine fibrils at constant angles (Rohen, 1979). Furthermore, posterior zonules have been identified in rhesus monkeys which can subdivided into two groups; one group originate from the *pars plana* to insert at the lens capsule, whereas another group course from the *pars plicata* and insert at the lens equator (Farnsworth and Burke, 1977). In contrast, Rohen (1979) described the presence of a zonular fork, which is formed from the anterior division of the plexuses with each end leading to the anterior and posterior lens capsule. Similar findings have also been reported for Japanese monkeys (Hiraoka et al., 2013). Fine zonular fibres also insert at the crystalline lens equator (Rohen, 1979). Interestingly, another set of fibres were also identified underlying the main fibres which attached to the non-pigmented ciliary epithelium of the ciliary valleys and had a course of direction opposite to that of the zonular fork. The fibres connected the zonular plexus with the main fibres, and termed tension fibres, with a possible role as a fulcrum (Rohen, 1979).

Streeten (1977) demonstrated the zonular fibres inserted at the lens capsule but noted there was difficulty distinguishing whether all the fibres covering the lens surface were zonular in origin especially since some fibres were less aggregated. The meridional fibres provided abundant insertions at the lens capsule and were present at various orientations on the lens equator suggesting they may smooth the force from the major zonules, as well as constraining the equator when the major zonules relax during

accommodation. Zonular fibres penetrate the lens capsule by a short distance in cow (Raviola, 1971) and monkey eyes (Raviola, 1971; Streeten, 1977), however, there was a deeper penetration into the human lens capsule with zonules terminating at the lens epithelium. Further studies are required to confirm such a finding considering only one human specimen from a 48 year old donor, was investigated by the author. Additionally, in guinea pigs fibres penetrate deep into the lens capsule and form radial arrangements towards the anterior and posterior apexes (Hanssen et al., 2001). The insertion zones at the crystalline lens capsule is greatest in the anterior lens capsule compared to the posterior surface, and least at the equator (Hiraoka et al., 2013).

The ultrastructure of the zonular apparatus of various primates (Raviola, 1971; Farnsworth and Burke, 1977; Rohen, 1979) is very similar to that in humans. In Japanese monkeys, the fibres at the anterior lens capsule separate to extend radially at the para-polar region and circumferentially at the para-equatorial region, whereas the posterior fibres remain undivided (Hiraoka et al., 2013).

Fine zonular fibrils aggregate to produce zonular bundles (Raviola, 1971; Farnsworth and Burke, 1977; Hiraoka et al., 2013). The fine fibrils have smaller diameters (range from 0.35 – 1 μm) in comparison to the zonular bundles which have a range between 2-30 μm in diameter (Forrester et al, 2008 pg 37), however, in human eyes, the thickness of zonular bundles also varies depending on their location at the crystalline lens (Streeten, 1977). For example, the diameter of the zonular bundles are larger (between 25 to 60 μm) at the anterior and posterior locations of the crystalline lens in their contracted state, compared to the lens equator, where they range from 10 to 15 μm. Thicker bundles at the anterior and posterior insertions of the lens equator, have also been found in 10 month Japanese monkeys (Hiraoku et al., 2013). The thicker fibres at the anterior and posterior locations of the lens is possibly due to their function in accommodation as it is the curvature at these locations which alters the most. Also, the organisation of zonular fibres are finer in a full term Japanese monkey, in comparison to an adult monkey where bundles of fibres exist (Hiraoka et al., 2010). Studies on guinea pigs have also revealed the existence of broader zonular fibres of 25 nm diameter, probably due to the fusion of two singular fibrils, which appear after 25 months of age; the increased thickness may reduce the elasticity of the zonules which could be a contributory factor to presbyopia (Hanssen, 2001).

Ultrasound biomicroscopy has been employed for *in-vivo* imaging of the zonular apparatus in 10 subjects between the ages 14 to 41 years old with refractive errors ranging from -4.50 D to +1.5 D (Ludwig et al., 1999). Fibres were located near the *ora*

serrata which extended to the inner surface of the ciliary muscle and anchor, and possibly, inserted into the muscle apex and departed towards the lens. Additionally, tension fibres and additional zonular fibres were also identified orginiating from the ora serrata and inserting into the lens. However, the researchers used a 34 MHz frequency which identified the large zonular bundles that ranged between 40-80 µm, whereas the individual zonular fibres were much thinner therefore could not be analysed accurately. Hence, there was a large inter-individual variation in the data due to the resolution limit of the instrument employed (Ludwig et al., 1999).

Overall, four bands of zonules were identified which inserted into the lens:

- One band anterior to the lens equator;
- Two bands posterior to the lens equator;
- A weaker band near the lens equator.

Zonular fibres that do not penetrate the posterior lens capsule have also been described in human eyes, indicative of a hyaloid-capsular membrane (Seland, 1974). Further *in-vitro* studies have confirmed a firm attachment of the anterior hyaloid membrane to the ora serrata and posterior lens capsule with the anterior hyaloid membrane fusing with the posterior lens capsule creating the Ligament of Wieger, possibly providing support for the positioning of the lens (Farnsworth and Burke, 1977). Removing the hyaloid membrane reveals zonular fibres attached to the vitreous membrane (Raviola, 1971; Rohen, 1979) which were thought to have a role at strengthening the vitreous base and attaching it to the ciliary body (Rohen, 1979). Streeten (1977) also identified loose perizonular fibrils and suggested they had a possible vitreal origin. Nevertheless, considering the posterior zonule is obstructed by both the anterior zonule and the hyaloid membrane, early studies investigating the zonular apparatus often removed the vitreous and located fine structures which were most likely damaged prior to analysis. Recently, the existence of posterior zonules within presbyopic eyes has been confirmed with a custom made device, which provided radial stretching of donor eyes to reveal the structures involved with accommodation (Bernal et al., 2006). Environmental scanning electron microscopy identified zonules predominantly inserting into the hyaloid membrane of the vitreous rather than having a direct course from the ciliary body to the crystalline lens, and forming strong attachments to the vitreous (Bernal et al., 2006). A zonular attachment between Wiegers ligament and the ciliary processes is also present in rhesus monkeys suggesting the zonule may have a role in the centripetal movement of the ciliary processes during accommodation, supported by evidence of a dampened effect of centripetal movement when the zonule was detached from Wiegers ligament (Croft et

al., 2008). Also, a recent study in rhesus monkeys has shown the anterior hyaloid membrane moves posteriorly during accommodation (Croft et al., 2013a). Significant information regarding the insertion of the vitreous zonules into the lens capsule has been determined with scanning electronic microscopy and ultrasound biomicroscopy in eight human eyes (age range 55 to 100 years old) and twenty three monkey eyes (22 rhesus, 1 cynomolgus) (Lütjen-Drecoll et al., 2010). Consequently, anterior, intermediate and posterior fibres have been recognized, depending on their origin at the vitreous membrane. Within monkey eyes, the anterior vitreous zonules arise from the fibres of the zonular plexus which insert into the vitreous membrane at regular intervals. Furthermore, the periphery of the posterior lens capsule is attached to the fibres of the anterior zonule and the vitreous membrane, the latter structure having a more central insertion into the capsule. The intermediate vitreous zonules bridge the cleft between the vitreous membrane and the intermediate pars plana zonules. Such zonules, separate to produce two strands, one each inserting into the zonular plexus surrounding a ciliary process. The intermediate vitreous zonules do not contact the *pars plana* zonules, however, they do separate into finer fibrils which merge into the vitreous membrane at the ora serrata. Posterior vitreous zonules are located at the regions where the posterior pars plana, ora serrata and vitreous body connect. The ultrastructure of the vitreous zonules is similar between human and the monkey eyes, except that the connection between the pars plana region and the posterior vitreous zonule is greater in humans (humans ~ 3.4 mm, monkey ~ 0.5 mm). The assembly of anterior vitreous zonules to the zonular plexus suggests it may be involved in the fine positioning of the lens during accommodation, whereas the intermediate vitreous zonular fibres attach the vitreous to the *pars plana* possibly to stabilize the vitreous membrane during the forward and inward movement of the ciliary muscle during accommodation. Furthermore, the firm attachment of the posterior zonules to the ora serrata may prevent the detachment of the retina during accommodation (Lütjen-Drecoll et al, 2010). Recently, a new group of zonules have been identified which are possibly involved with the fine tuning and stabilisation of the crystalline lens and zonular fork between accommodation and disaccommodation, especially since they are located closely to the circular muscle fibres (Flügel-Koch et al., 2016).

With increasing age, the distance between the anterior zonular insertion to the posterior zonular insertion increases probably due to the growth of the lens (Ludwig et al., 1999).

1.2.7. Iris

The iris forms from the edge of the optic cup during pre-natal development (O' Rahilly, 1975; Beebe, 1986); the posterior layer of the iris is continuous with the *pars plicata* of the ciliary body (O'Rahilly, 1975; Tamm and Lütjen-Drecoll, 1996). The iris is the anterior extension of the uveal tract which divides the fluid filled compartments of the anterior chamber from the posterior chamber of the eye and has a mechanical function of controlling the amount of light entering the eye.

The iris consists of three layers (Freddo, 1996): the anterior border layer, the stromal layer and the posterior iris layer. The sphincter muscle, a circumferential ring which encircles the pupillary margin is contained within the stromal layer whereas the dilator pupillae, a radial muscle, lies within the anterior layer of the posterior iris layer. Both muscles provide a synergistic role for the iris. In mammals, the sympathetic fibres innervate the dilator pupillae, and alpha and beta adrenoceptors have been located in the iris dilator (Van Alphen, 1976; Van Alphen et al, 1965) with a dual innervation described in rabbits (Van Alphen, 1965; Persson et al., 1971), cats (Ehinger et al., 1968) and cattle (Suzuki and Kobayashi, 1983). Identification of the adrenoceptors within the human iris dilator muscle suggests mostly alpha receptors exist which is supported from pharmacological studies (Van Alphen, 1976). However, an inhibitory cholinergic and excitory adrenergic innervation to the iris dilator muscle could also be present (Yoshitomi et al., 1985; Neuheuber and Schrodl, 2011). Activation of the adrenoceptors within the dilator muscle causes mydriasis (Van Alphen 1965; Van Alphen et al, 1976), however, the cholinergic innervation to the dilator could also have a role for miosis (Yoshitomi et al., 1985) although Persson et al (1971) disagree, and recent evidence suggests $alpha_{1A}$ adrenoceptors regulate sympathetic mydriasis as determined in albino rabbits (Yu and Koss, 2003).

The parasympathetic system innervates the sphincter pupillae via the long ciliary nerves which travel from the third cranial nerve to the sphincter muscle. Few adrenoceptors have been located on the sphincter pupillae muscle of humans (Van Alphen, 1976) and albino rabbits (Persson et al., 1971). The most abundant muscarinic receptor within the iris sphincter is the M3 receptor (Gil et al, 1997; Honkanen et al., 1990; Woldemussie et al., 1993; Eglen et al., 1996), although minimal traces of M2 may also exist as demonstrated in bovine ciliary muscle (Honkanen et al., 1990). Unlike the ciliary muscle, gap junctions exist within the smooth muscle cells of the iris sphincter in human and cynomolgus monkeys (Samuel et al, 1996).

1.2.8. Choroid

The choroid is comprised within the uvea, a structure formed from mesoderm and neuroectoderm during the early stages of foetal development (Mrejen and Spaide, 2013); the choroid extends anteriorly to the *pars plana* where it forms the ciliary body (Nickla and Wallman, 2010). The choroid can be divided into five layers: Bruch's membrane, choriocapillaris, Haller and Sattler's layers and the suprachoroidea (Nickla and Wallman, 2010) and is a highly vascular structure that nourishes the retina (Mrejen and Spaide, 2013; Nickla and Wallman, 2010). Although the choroid is comprised of blood vessels, it also contains connective tissue, pigment and intrinsic choroidal neurons. Also, non-vascular smooth muscle cells have been located within the subfoveal choroid which may stabilize the fovea when the ciliary muscle contracts during accommodation (Flügel-Koch et al., 1996).

The choroidal thickness across the posterior eye varies between adults (Margolis and Spaide, 2009; Ikuno et al., 2010; Ding et al., 2011; Kim et al., 2014) and children (Read et al., 2013a; Read et al., 2013b). The choroid is the thickest at the fovea (Margolis and Spaide, 2009; Ikuno et al., 2010; Ding et al., 2011; Kim et al., 2014) possibly due to the increased metabolic rate within the central macula in comparison to peripheral retinal locations. The nasal (Margolis and Spaide, 200., Ikuno et al.,2010., Ding et al., 2011) and inferior retinal quadrants (Ikuno et al., 2010) have the thinnest choroid. Furthermore, there are variations in subfoveal choroidal thickness between ethnic groups, for example, Korean eyes have a mean sub-foveal choroidal thickness of 307.26 ± 95.18 µm (Kim et al., 2014), the sub-foveal choroidal thickness is 354 µm in Japanese eyes (Ikuno et al., 2010) and 261 µm in Chinese eyes (Ding et al., 2011). The sub-foveal choroidal thickness in Caucasian eyes has been reported between 314 to 346 µm (Rahman et al., 2011; Sanchez-Cano et al., 2014) whereas a thicker choroid has been documented in Afro-Carribean eyes (average 364 µm; Rahman et al., 2011).

Studies on children can provide significant information regarding the changes to the choroid with ocular growth. In early childhood, the choroidal thickness increases before plateauing during adolescence (Read et al., 2013a). Measurements of choroidal thickness from 104 children (mean age 13.1 ± 1.4 years) classified as either myopic (mean spherical equivalent -2.39 ± 1.51 D) or non-myopic (mean spherical equivalent +0.33 ± 31 D) reveals the mean subfoveal choroidal thickness of myopic children was 303 ± 79µm in comparison to non-myopic children where the average subchoroidal

thickness was 359 ± 77μm. The choroidal thickness was greatest within the central retina rather than the peripheral retinal locations (>3 mm diameter from the central foveal zone) with the thinnest choroid at the nasal and inferior nasal retinal locations. The choroid in myopic children was 16% thinner than in non-myopic children, which could not be explained primarily by ocular elongation with refractive error development, thus the authors suggested hyperopic defocus and alterations to the ocular blood flow may also contribute to the thinner choroid (Read et al., 2013b). However, a limitation to the study is the possibility that children within the non-myopic group could become myopic during adolescence, therefore the data reported is not absolute. Genetic factors are known to influence refractive error development (Flitcroft, 2012), thus studies within anisometropic subjects, where genetic factors are controlled, can provide further information about the mechanical factors involved in ocular development. A study on adult non-amblyopic anisometropes (Vincent et al., 2013b) revealed the least myopic eye (eye with the shortest axial length) had a greater choroidal thickness. Moreover, the greatest interocular variation in the choroidal thickness occurred at the fovea. Furthermore, the authors noted their findings were dependent on the degree of axial anisometropia; if the axial anisometropia was less than 0.5 mm, the range of interocular sub-foveal choroidal thickness differences were between 20 μm thinner in the more myopic eye to 40 μm thicker in the more myopic eye. Interestingly, ethnic differences were also noted, with Asian eyes having thicker choroids specifically in the nasal retinal quadrant, compared to Caucasian eyes.

The choroidal thickness is approximately 200 μm at birth and throughout life thins to approximately 80 μm by 90 years of age (Ramratten et al., 1994). A significant negative correlation between subfoveal choroidal thickness and age has been determined in adults (Margolis and Spaide, 2009; Ikuno et al., 2010; Ding et al., 2011; Wei et al., 2013; Kim et al., 2014) and children (Read et al., 2013b). Ding et al (2011) reported a significant subfoveal choroidal thinning within Chinese adults over 60 years of age. In contrast, Kim et al (2014) studied the choroidal thickness in Korean adults and suggested a significant negative correlation between age and choroidal thickness in adults younger than 60 years of age, possibly due to age-related choroidal atrophy which alters less over 60 years of age. With age, Bruchs membrane thickens, the choroiocapillaris thickness decreases, and the choroid thins from 193.5 μm in the first decade of life to 84 μm in the tenth decade (Ramratten et al., 1994).

1.3. Mechanism of accommodation

1.3.1. Historical theories of ocular accommodation

Early theories about the accommodative mechanism date back to 1677, when Descartes correctly identified the increased convexity of the crystalline lens enabled objects at near to be viewed, although the mechanism providing the change was not established (Descartes, 1677 cited by Fincham, 1925). The term ‘accommodation’ was attributed by Porterfield in 1738 to describe the ability of the eye to view objects at a close distance (Atchison and Charman, 2010). Over the centuries, several hypotheses to explain the ability of the eye to change its focussing power have been proposed including the constriction of pupil size, an alteration to the corneal curvature, variation to the axial length and a change to the curvature of the crystalline lens.

In 1801, Thomas Young presented the Bakerian lecture and concluded the primary anatomical structure involved in the accommodative process was the crystalline lens. The evidence was determined by eliminating the possibility of the cornea and axial length as contenders, through several experiments on his own eye. Young noted that the immersion of his eye in water, which neutralised the corneal power, did not prevent accommodation. Furthermore, by clamping two rings, one around the cornea and one close to the posterior pole, a phosphene was created which was overlapping the foveal region, and the size of the phosphene did not alter as the eye accommodated. Thus, Thomas Young concluded that an alteration to the axial length was not responsible for the change in the accommodative amplitude. Although Young was able to confirm the significance of the crystalline lens in accommodation, he suggested the anterior and posterior radii decreased during accommodation to produce a flatter lens (Young, 1801 cited by Atchison and Charman, 2010; Land, 2015).

Hermann von Helmholtz (1924) however acknowledged that the crystalline lens became more convex with accommodation, and suggested the centripetal movement of the ciliary muscle during contraction relaxed the tension on the zonules, enabling the anterior lens equator to move forward and the lens to conform to its natural spherical shape. In contrast, Tscherning proposed that the anterior surface of the crystalline lens became hyperbolic with accommodation due to the contraction of the ciliary muscle, which increased the tension of the zonules. Thus, the elastic contents of the lens are compressed against the stiffer nucleus, increasing the central curvature and flattening the lens periphery (Tscherning, 1904 cited by Fincham, 1925). Furthermore, Cramer suggested during accommodation, the curvature of the lens is altered from the

pressure of the vitreous (Cramer, 1851 cited by Coleman 1986). In 1909, Tscherning further advanced his theory to incorporate the vitreous; he advocated that the contraction of the ciliary muscle produced a centripetal compression of the choroid onto the vitreous, thus increasing the zonular tension and resulting in a hyperbolic anterior curvature of the crystalline lens (Tscherning, 1909 cited by Fincham, 1925).

Understanding of the lenticular changes that occur during accommodation have been provided by Fincham (1925) who investigated the accommodative effect on the anterior and posterior radii of curvature from two 19 year old participants with equal refractive error and similar radii of the anterior crystalline lens surface. The author identified a backward movement of the posterior lens surface with accommodation, but most significantly, that the apex of the surfaces did not become more conic with accommodation. Rather there was a reduction in the radii of curvature of both the anterior and posterior surfaces. Although there was a variation of the anterior surface curvature between individuals, this was attributed to the variances in capsular thickness of the crystalline lens as the capsule was thinnest in the centre and thickest in the periphery. Hence, during accommodation, the central curvature become more convex and the periphery of the lens more concave, thus supporting the von Helmholtz theory of accommodation and possibly explaining the flattening of the peripheral lens which was previously observed by Tscherning (Fincham, 1925).

The vitreal involvement with accommodation is debateable. Coleman (1970) suggested the contraction of the ciliary muscle produces a forward movement of the choroid, which subsequently reduces the volume within the posterior chamber and therefore the vitreous is compressed forward. Subsequently, the anterior lens surface protrudes anteriorly due to the compression force of the vitreous body and the dioptric power of the eye increases, but the posterior lens surface shows minimal change since it is supported by the vitreous. However, Fisher (1982) suggested the possibility of a lower capsular elasticity within the posterior surface in comparison to the anterior lens capsule, could also explain the greater reduction in the anterior radii found during accommodation, especially since accommodation is still possible when the vitreous is absent (Fisher, 1983). Nevertheless, further support for the involvement of the vitreous in accommodation has been provided from evidence investigating the difference in intraocular pressure between the aqueous chamber and vitreous chamber within baboons and chimpanzees. During accommodation, a distribution of pressure from the posterior to the anterior chamber was demonstrated, suggesting the vitreous indeed has a role in accommodation (Coleman, 1986).

1.3.2. Current theories of ocular accommodation

During accommodation the lens thickness increases (Koretz et al., 1984; Drexler et al., 1997; Koretz et al., 1997; Jones et al., 2007; Kasthurirangan et al., 2011) which is primarily due to the thickening of the nucleus (Brown, 1973; Koretz et al., 1984; Koretz et al., 1997; Koretz et al., 2002; Dubbelman et al., 2003; Hermans et al., 2007), which consequently produces a forward movement of the anterior pole of the lens (Brown, 1973; Drexler et al., 1997; Koretz et al., 1997; Koretz et al., 2002) resulting in a reduction to the anterior chamber depth (Brown, 1973; Garner and Yap, 1997; Koretz et al., 1997; Dubbelman et al., 2005; Kasthurirangan et al., 2011; Woodman et al., 2012). The cortical thickness remains unaltered during accommodation (Koretz et al., 1997; Dubbelman et al., 2003), although a thickening of the posterior cortex has been reported with slit-lamp photography (Brown, 1973). However, the results reported from the Scheimpflug images obtained by Brown (1973) were not corrected for the optical distortion as a consequence of the increased curvature of structures anterior to the posterior surface of the lens during accommodation. Therefore, the optical error was included in the results reported by the author. Dynamic changes to the lens thickness during accommodation also support the findings that the cortex remains unaltered during accommodation and an increase to the adult nucleus occurs during accommodation (0.058 ± 0.006 mm/D; Chang et al., 2016. ARVO abstract # 3964).

The increase to the lens thickness is 0.061 ± 0.03 mm/ D (Hermans et al., 2009). Such quantitative data is further supported by three-dimensional MRI results for the accommodative crystalline lens where a mean change in lens thickness of 0.06 ± 0.08 mm/ dioptre of accommodative response has been documented between 0.17 D and 4 D accommodative stimuli, whereas a change of 0.09 ±0.12 mm/ dioptre of accommodative response has been reported between 4 D and 8 D stimuli (Sheppard et al., 2011). A small backwards movement of the posterior lens surface has also been reported (Brown, 1973; Drexler et al., 1997; Croft et al., 2013b) which was recognised by von Helmholtz (1924), although, not thought to be inherent to altering the lens power. The posterior lens surface becomes steeper with accommodation with an increase of 0.46 ± 1.45 mm/ dioptric response (Sheppard et al., 2011). Using the Gullstrand schematic eye, where the crystalline lens has an equivalent refractive index of 1.422, Garner and Yap (1997) calculated the corresponding increase to the lens power as 5.53 D and 3.10 D for the anterior and posterior surface, respectively. Thus, the authors concluded the posterior lens surface contributes significantly to the overall dioptric increase to the eye during accommodation. Therefore, the overall increase to

the axial thickness of the lens provides the greater dioptric power of the eye which is required for viewing near objects.

The radii of curvature of the anterior and posterior lens surface reduces as the lens thickness increases (Fincham, 1925; Brown, 1973; Koretz et al., 2002), which was initially described by von Helmholtz (1924). The reduction is greatest on the anterior surface as reported from several studies. For example, using phakometry (Garner and Smith, 1997), a reduction to the anterior surface radii from 11.54 ± 1.27 mm to 6.59 ± 0.30 mm, and the posterior surface from -6.67 ± 0.97 mm to -5.30 ±0.40 mm has been documented in response to an 8 D stimulus in 11 subjects with a mean refractive error of -1.88 ± 1.64 D and an age range of 18-28 years (mean 21.2 ± 2.62 years). The decrease is similar to recent data acquired from MRI indicating the anterior and posterior radius of curvature reduces by 0.51 ±0.5 mm/ D and 0.14 ±0.13 mm/ D, on the anterior and posterior surface, respectively (Hermans et al., 2009). Sheppard et al (2011) obtained data from nineteen pre-presbyopic participants (mean age 25.8 ± 4.5 years; mean spherical equivalent refractive error -2.38 ± 2.09 D) during relaxed accommodation, and to 4 D and 8 D accommodative demand level. The anterior and posterior radii of curvature reduced with accommodation and the reduction was particularly significant on the anterior surface. Also, the greatest reduction occurred at the lower accommodative demand level (mean reduction was 0.82 ± 1.04 mm/ dioptric response for the anterior surface). Although the capsular thickness of the posterior surface is thinner than the anterior surface (Fincham, 1925), the greatest decrease reported for the anterior lens radii (Rosales et al., 2006) could be due to a greater force applied to the thicker anterior lens capsule (Ziebarth et al., 2005). Dynamic changes to the lens radius of curvature reveals a reduction to the anterior lens radius and a slight increase to the posterior lens surface (Williams et al., 2016. ARVO E-abstract #3959), which further supports the findings obtained during static accommodation.

The lens equatorial diameter reduces with accommodation as a result of the increased axial thickness of the lens (Wilson, 1997; Glasser and Kaufman, 1999; Jones et al., 2007; Kasthurirangan et al., 2011). Kasthurirangan et al (2011) reported the lens equatorial diameter decreased by 0.32 mm during accommodation, although a larger decrease has been recorded from phakometry where the contralateral eye was simulated and convergence occurred (Garner and Yap, 1997). It is unclear from Garner and Yap's study whether the measurements for the radii of curvature were in the same image plane between the relaxed eye and during accommodation. Sheppard et al (2011) documented a greater decrease to the anterior lens diameter than the posterior

surface, and furthermore, the reduction was particularly evident for the lower accommodative stimulus level (between the 0.17 D and 4 D mean change in lens equatorial diameter: -0.14 ± 0.17 mm/ dioptric response; between 4 D and 8 D mean decrease was 0.01 ± 0.16 mm/ dioptric response). Interestingly, the data suggests a possible increase to the equatorial diameter at higher accommodative demand levels. The ratio of the lens thickness to the equatorial diameter increases during accommodation which confirms the lens becomes more spherical (Kasthurirangan et al., 2011), further supporting von Helmholtz's theory of accommodation.

Furthermore, the alteration of the cross-sectional area of the lens has been of interest especially in relation to whether an alteration to the volume of the lens occurs with accommodation. Twenty five participants between 22 and 50 years old accommodated to an 8 D stimulus and images of the crystalline lens were acquired with high-resolution MRI (Strenk et al., 2004a). A significant increase to the cross-sectional area was found that was restricted to the anterior lens surface. The authors suggested the invariance to the posterior surface was probably due to the location of the fetal nucleus. The fetal nucleus is positioned behind the lens equator and considering the structure is not known to change curvature with accommodation, the lack of alteration to the cross-sectional area is probably expected. The cross-sectional area of the anterior surface also increased with the authors suggesting the growth of the lens is restrained to the anterior portion. However, *in-vitro* measurements of the crystalline lens from human eyes aged between 27 and 99 years suggest the lens growth occurs at the equator and the periphery but mostly within the posterior region of the lens (Rosen et al., 2006). Therefore, it is unlikely that the lens growth is restricted to the anterior surface as suggested from the *in-vivo* study by Strenk and colleagues (2004a) especially since the lens is influenced by other anatomical structures such as the ciliary muscle and zonules that may have resulted in the observed findings (Rosen et al., 2006).

The possibility that an overall increase to the cross-sectional area of the lens during accommodation raises questions about the volume changes of the lens. The observed increase to the cross-sectional area suggests the volume of the lens becomes greater with accommodation indicating the lens material is compressed in the relaxed eye, possibly as a result of the protein reorganisation within the lens (Strenk et al., 2004a). However, Rosen and colleagues (2006) suggest the lens dimensions obtained from MRI are underestimated. The researchers used the age groups investigated by Strenk et al (2004a) within their linear regression model to determine the lens volume *in-vivo* and found the volume from Strenk et al (2004a) data was 30% less than expected. It is

possible a reduction in the refractive index of the lens during accommodation provides the increased cross-sectional area and, thus, volume (Jones et al., 2007). Yet, the variation in the refractive index with accommodation is unknown. Hermans and colleagues (2009) used MRI to obtain 3D images of the crystalline lens of five participants (average age 25 years (SD 6.7), MSE -1.3 D (SD 1.03), amplitude of accommodation 5.88 D (SD 0.82)). The MRI images were divided into eight sections and fitted with parametric data in order to determine the alteration of the cross-sectional area and the volume of the lens with accommodation. The authors revealed the cross-sectional area of the lens increased significantly with accommodation from 25.9 ± 0.2 mm^2 to 27.1 ± 0.3 mm^2, and there was a significant decrease to the surface area of the capsular bag with accommodation from 175.9 ± 2.8 mm^2 to 167.5 ±2.9 mm^2. However, there was no change to the lens volume, indicating the lens material is incompressible and rather the elasticity of the capsule is responsible for the observed increase in the cross-sectional area of the lens (Hermans et al., 2009). Data from quantitative optical coherence tomography and imaging processing algorithms also indicate the lens volume remains constant during accommodation (Martinez-Enrique et al. IOVS 2016, ARVO E-abstract 1380). During accommodation, the reduction in the lens surface area seems to be more evident for lower accommodative demands. Sheppard et al (2011) reported a significant reduction to the lens surface area of 4.75 mm^2 between the relaxed accommodative state and 4 D accommodative demand level, whereas a slight insignificant increase occurred to the lens surface between the 4 D and 8 D demand level. However, there was a significant increase to the lens volume from 154.52 ± 19 mm^3 to 158.08 ± 22.89 mm^3 between the relaxed and 8 D accommodative demand. Therefore, the findings support those of Strenk and colleagues (2004a) that the crystalline lens is compressed during the unaccommodated state and the capsule undergoes elastic deformation with accommodation. *In-vitro* data from a bovine lenses suggest the lens volume reduces by 5.3% when stretched (Gerometta et al., 2007), which further supports the evidence from human *in-vivo* studies. Furthermore the authors calculated the cross-sectional area and volume changes during disaccommodation for their modelled human lenses and showed a reduction to the cross sectional area by 7.1% and 2% in a 20 year and 45 year lens, respectively, as well as a 2.6% and 1.7% decrease in the volume for a 20 year and 45 year old lens, respectively. The findings suggests volume is gained by the lens during accommodation and reduces in the relaxed eye, possibly from fluid leaving the lens when it is relaxed. The time frame for which this process can occur is approximately 200 ms (Zamudio et al., 2008), which is within the 3 seconds that the maximum accommodative amplitude is reached and the consequent disaccommodation occurs

(Glasser and Kaufman, 1999). An 11% decrease in the cross-sectional area has also been documented for rhesus and cynomolgus monkeys where 10 D of accommodation is stimulated (Glasser and Kaufman, 1999). During accommodation, alteration of the gradient refractive index (GRIN) of the lens also contributes to the increased power of the crystalline lens (Garner and Smith, 1997; Maceo et al., 2011). Moreover, the lens significantly contributes to the peripheral optics of the eye, with a greater peripheral defocus evident at greater eccentricities and an increased peripheral defocus occurs with increasing lens power during accommodation (Manns et al. IOVS 2016. ARVO E-abstract 1379).

The contraction of the ciliary muscle undeniably initiates the accommodative process, yet, there are limited investigations that have determined the morphological changes to the muscle. An anterior shift of the ciliary body has been reported in human eyes, using ultrasound biomicroscopy, with data suggesting there is contact between the ciliary body and posterior iris (Bacskulin et al., 1995). The ciliary body is occluded by the iris, therefore, it is difficult to view the entire structure with optical techniques (see Instrumentation; Chapter 2). The alteration of the ciliary body can be observed within albino patients using optical coherence tomography since there is minimal pigment within the iris stroma allowing the optical source to penetrate to the ciliary body. Baikoff and colleagues (2004a) documented a contraction of the ciliary body, a centripetal movement of the ciliary sulcus and ciliary body, and a lack of forward movement of the ciliary body during accommodation. The findings are consistent with primate data (Glasser and Kaufman, 1999). However, there are limitations to Baikoff and colleague's data as only one participant with albinism was investigated, therefore, the results may not be representative of the general population. Furthermore, the acquisition of data with optical techniques requires a correction for the distortion which occurs as the light travels through different intraocular media which vary in refractive index, and this correction was omitted by the authors. Also, the analysis of the acquired images were not along the same image plane, therefore, accurate assessment of the ciliary body movement and the conclusions in relation to accommodation cannot be based accurately upon this study (Schachar, 2005).

MRI studies indicate the ciliary muscle contractility remains active throughout life (Strenk et al.,1999) and no inward movement of the ciliary muscle apex occurs with accommodation, although, the anterior muscle mass increases (Strenk et al., 2010). Furthermore, during accommodation a significant decrease to the ciliary ring diameter

occurs (mean change 0.44 mm), although, the circumlental space does not alter (Kasthurirangan et al., 2011).

More recent studies analysing the ciliary muscle during accommodation have shown the muscle thickens anteriorly and thins posteriorly (Sheppard and Davies, 2010b; Lewis et al., 2012; Lossing et al., 2012; Richdale et al., 2013; Shao et al., 2013). The findings correspond with an *in-vitro* study within rhesus monkeys which indicate an increase to the circular region of the ciliary muscle with accommodation, whereas the area of the posterior region reduces (Lütjen-Drecoll et al., 1988a). Sheppard and Davies (2010b) investigated the changes to the ciliary muscle during static accommodation for 4 D and 8 D accommodative demand levels, within fifty pre-presbyopic adults (mean age 25.8 years ± 4.5) with a mean refractive error -2.00 ± 2.62 D. The authors imaged the nasal and temporal ciliary muscle using AS-OCT and identified an asymmetry between both aspects of the ciliary muscle within the relaxed and accommodative states. The temporal ciliary muscle was longer (4810 ± 690 µm) compared to the nasal side (4630 ± 470 µm) during the relaxed state, although the differences were not significant. With accommodation, a contractile shortening was observed in both the temporal and nasal muscle, however, the response for the nasal quadrant was less than the temporal side. The contractile shortening was independent of the axial length and was mainly due to the reduction in the anterior length which comprised 18.5% of the total ciliary muscle length during the relaxed state. With accommodation, the thickness of the ciliary muscle increased anteriorly at the location representing 25% of the total length (CM25) with a mean increase of 7.1 ± 6.4 µm, whereas the thickness measurements at the posterior locations (CM50 and CM75) did not alter significantly with accommodation. The authors identified a greater change to the ciliary muscle parameters between 0.19 and 4 D of accommodation, rather than between 4 D and 8 D accommodative demand levels. For example, the overall length reduced by 80 ± 100 µm per dioptre between 0.19 D and 4 D compared to 50 ± 120 µm between 4 D and 8 D accommodative demand levels. In addition, the anterior length reduced by 60 ± 40 µm and 30 ± 30 µm per dioptre of accommodative response between the 4 D and 8 D demand levels, respectively.

Research investigating the accommodative changes to the ciliary muscle *in-vivo* have also been determined in children aged 9 ± 2.1 years with refractive errors of 0.36 ± 2.41 D (Lewis et al., 2012). The ciliary muscle images were acquired with the Visante AS-OCT for relaxed accommodation, as well as 4 D and 6 D accommodative stimulus levels. The researchers reported that eyes with longer axial lengths had thicker ciliary

muscles in the relaxed state and during accommodation. An anterior thickening of the ciliary muscle was evident with accommodation as determined from the location representing the maximum thickness (CMTMax) and the region corresponding to 1 mm posterior to the scleral spur (CMT1). Thinning of the posterior locations of the ciliary muscle 3 mm posterior to the scleral spur (CMT3) were also reported. Overall, there was an increase of 14.2 µm and 10.4 µm per dioptre of accommodation for CMTMax and CMT1, respectively, whereas CMT3 reduced by 5.4 µm per dioptre of accommodation. The authors concluded eyes with a greater CMTMax were correlated with increased thickening at locations relating to CMT1, as well as shortening within CMT3 during accommodation. Furthermore, the reduced thickening at CMT3 during accommodation was associated with axial length, whereas the thickening at the anterior locations (CMTMax and CMT1) were independent on axial length (Lewis et al., 2012). The overall findings of the contraction of the ciliary muscle longitudinally and radially was in agreement with Sheppard and Davies (2010b). The anterior thickening of the ciliary muscle occurs for all refractive error groups, as reported in young adults during accommodation (Lossing et al., 2012). A summary of the findings by research groups for *in-vivo* ciliary muscle investigation are provided in Table 1.

A reduced movement of the ciliary muscle during accommodation has been reported for myopic subjects in young adults (mean age 25.7 ± 3.7 years), where the length of the ciliary muscle was quantified from scleral and vitreous side (Jeon et al., 2012). The temporal ciliary muscle was imaged and in agreement with previous studies, the ciliary muscle length reduced during accommodation. However, the contractile shortening was only evident for the aspect of the ciliary muscle on the scleral side, which mostly consists of longitudinal fibres. The anterior location (CMT1) was found to increase in thickness with accommodation, whereas a thinning of CMT3 was noted, as with prior studies. Furthermore, the location referring to the maximum thickness of the ciliary muscle and the apical angle increased during accommodation indicating a centripetal movement of the ciliary muscle. A positive correlation was identified between the ciliary muscle length (scleral side) and axial length as well as the region 3 mm posterior to the scleral spur and axial length, thus, agreeing with the findings of Oliveira et al (2005). The authors concluded the anterior thickening of the muscle and the centripetal movement are essential for accommodation, but the movement is reduced in myopic eyes. Investigation of the ciliary body thickness within the unaccommodated eye in children reveal thickness measurements 2 mm and 3 mm posterior to the scleral spur have a strong negative correlation with refractive error (Bailey et al., 2008). The region representing 2 mm posterior to the scleral spur is thicker on the temporal side than the

nasal in the relaxed muscle, whereas with accommodation there is a statistically significant thinning especially on the temporal aspect (Sheppard and Davies, 2010b). Nevertheless, the results also indicate variation between individuals as a thickening of the region was also noted in some participants. CMT2 may therefore be a fulcrum region for accommodation, whereby the location translates from a thinner region to a thicker area with accommodation depending on accommodative effort (Lewis et al., 2012). Measuring the ciliary muscle thickness at fixed locations of the ciliary body does not reflect the movement of the ciliary muscle accurately, since the anterior thickness results perhaps include the forward movement of the muscle during accommodation, thus resulting in the analysis of a different anatomical region. Therefore, as suggested by Sheppard and Davies (2010b), proportional measurements of the ciliary muscle are more likely to provide relevant information of the changes to the ciliary muscle length with accommodation. Various research groups have analysed the data acquired with different methods either using in-built calipers within the Visante AS-OCT (Sheppard and Davies, 2010b, Sheppard and Davies, 2011) or semi-automated software, however, the thickness of the pigmented ciliary epithelium also appears to have been reported in results (Kao et al., 2011; Lossing et al., 2012; Lewis et al., 2012).

			Measurement of Ciliary muscle parameter with relaxed accommodation (µm)					Measurement of Ciliary muscle parameter with accommodation (µm)					
Study	**Age (years)**	**Aspect of ciliary muscle**	TOTAL LENGTH	CMMax	CMT1	CMT2	CMT3	Max accommodative stimulus	TOTAL LENGTH	CMMax	CMT1	CMT2	CMT3
Bailey et al (2008)	11.79 ± 2.31	Nasal	Unknown	Not known	899.43 ± 121.71	601.49 ± 101.55	326.27 ±69.85	-	-	-	-	-	-
Sheppard and Davies (2010b)	25.8 ± 4.5	Temporal (T) and nasal (N)	T: 4810 ± 690 N: 4630 ± 470	-	-	T: 405 ± 58 N: 347 ± 58	-	8 D	T: 4520 ± 610 N: 4440 ± 480	-	-	T: 384 ± 65 N: 340 ± 58	-
Lossing et al (2012)	24.2 ± 1.1	Temporal	Unknown	795.20 ±65.4	774.80 ± 66.3	557.8 ± 80.8	353.7 ± 67.6	4 D	Not known	868.5 ± 83.3	813.9 ± 85.8	535.5 ± 98.2	303..8 ± 70.8
Richdale et al (2013)	30-50 years	Not known	Unknown	870 ± 100	800 ± 100	490 ± 110	270 ± 80	-	-	-	-	-	-
Pucker et al (2013)	8.71 ± 1.51	Nasal	Unknown	809.01 ± 67.63	778.46 ± 65.15	527.87 ±73.13	280.92 ±55.29	-	-	-	-	-	-
Shao et al (2013)	Range 26-47 years	Temporal	Unknown	408 ± 11	406 ± 9	279 ± 12	154 ± 8	4 D		606 ± 12	605 ± 8	309 ± 11	151 ± 9
Jeon et al (2012)	25.70 ± 3.65	Unknown	**Scleral side**: 5518.85 ± 446.41 **Vitreous side**: 5475.37 ± 904.95	582.78 ±88.95	529.32 ± 104.22	396.45 ± 59.26	223.27 ± 26.96	12.5 D	**Scleral side**: 5085.19 ± 646.12 **Vitreous side**: 5339.77 ± 1065.62	724.82 ± 118.02	620.16 ± 165.71	395.63 ± 61.63	176.94 ± 80.67
Oliveira et al (2005)	51.8 ± 16.5	Temporal	Unknown	Not known	Not known	Myopes : 490 ± 115 Emmetropes 362 ± 53	Myopes: 315 ± 79 Emmetropes: 247 ± 49	-	-	-	-	-	

Table 1-1. Summary of *in-vivo* studies investigating the morphology of the ciliary muscle with and without accommodation. The studies within the white background have used the technique AS-OCT, whereas studies using UBM are shown in the grey background.

Although there is variation in technique and analysis procedures between the studies, the overall pattern of changes to the ciliary muscle parameters are similar between studies. The interaction between the crystalline lens and ciliary muscle has recently been assessed dynamically using a combined anterior and posterior optical coherence tomographer (Ruggeri et al., 2016. ARVO E-abstract #3690). The change to the ciliary muscle thickness and crystalline lens thickness between relaxed accommodation and a 2 D accommodative stimulus was analysed. A change of 0.045 mm occured in the cilary muscle thickness and 0.125 mm for the crystalline lens thickness in a 22 year old, whereas a greater change to thickness of the ciliary muscle (change 0.107 mm) occurs in a presbyopic eye and a smaller change in lens thickness (change 0.090 mm). The authors suggested a 0.0005 mm and 0.034 mm change occurs to the ciliary muscle thickness in the 22 year old and 45 year old eye respectively, during the initial phase of accommodation, however, the anterior segment of the ciliary muscle was poorly imaged due to the resolution limits of the instrumentation employed. Considering the anterior segment of the ciliary muscle has been shown to have an important role during accommodation, the results from the study by Ruggeri and colleagues (2016) should be analysed with caution.

Rhesus monkeys have a similar anatomical structure of the accommodative system to humans (Neider et al., 1990) although, the mean accommodative amplitude of rhesus monkeys aged between 1 to 5 years old is greater (Bito et al., 1982) than humans (Duane, 1922). Neverthless, the accommodative amplitude of rhesus monkeys declines at a similar rate to humans (Bito et al., 1982), therefore, the species are ideal animal models for investigating the mechanism of accommodation (Glasser and Kaufman, 1999; Croft et al., 2006a) and presbyopia (Kaufman et al., 1981; Koretz et al., 1987a; Lutjen-Drecoll et al., 1988a; Tamm et al., 1991b; Tamm et al., 1992c; Vilupuru and Glasser., 2005; Wasilewski et al., 2008). Objective techniques are employed to stimulate accommodation in animals, either from the use of pharmacological agents which stimulate the ciliary muscle or electrical stimulation of Edinger-Westphal nucleus via an implanted electrode. Studies reveal an anterior and centripetal movement of the inner apex of the ciliary with the tips of the ciliary processes moving away from the sclera. Moreover, the magnitude and the direction of the movement is similar between the nasal and temporal quadrants of the muscle (Glasser and Kaufman, 1999). However, a greater ciliary body length and ciliary muscle area has been documented for the temporal side compared to the nasal, and no essential differences in ciliary body thickness seems to be evident between both orientations (Glasser et al., 2001). Recent investigations suggest there are differences

in the amplitude of the centripetal movement of the ciliary processes during accommodation with a slightly greater magnitude for the nasal aspect. In addition, when the Edinger-Westphal nucleus is stimulated to produce a supramaximal accommodative response, a greater increase in the centripetal movement has been documented within the nasal quadrant, whereas no difference in movement occurs between the maximum pharmacological stimulation and Edinger-Westphal response for the temporal side (Croft et al., 2006b).

The lens capsule and anterior zonular attachments to the ciliary processes are absent after intracapsular lens extraction, which produces a reduced velocity of the ciliary process movement compared to a normal phakic rhesus monkey eye. Furthermore, extracapsular lens extraction allows zonular attachments to the capsule and Wiegers capsule to remain resulting in a slightly increased velocity of the ciliary processes to be observed. Vitreous strands which extend from the posterior retina and terminating at the pars plana have also been identified which show a centripetal movement during accommodation. Furthermore, a backwards movement of the anterior hyaloid has also been observed in rhesus eyes, which provides evidence against Coleman's theories for accommodation. Furthermore, the absence of the lens and capsule enables a centripetal movement of the ciliary process, only if zonular attachments are not disrupted between the ciliary processes and Wiegers ligaments (Croft et al. IOVS 2016; ARVO E-abstract 1378).

The effect of accommodation on the axial length has also been studied within recent years (see Chapter 7). Garner and Yap (1997) stated accommodation does not alter axial length, however, their data were obtained with ultrasound biomiscroscopy, where the stimulus was presented to the contralateral eye. Consequently, it is presumed that intraocular changes that occur to the eye presented with the accommodative stimulus are equal to the eye from which data are collected. Furthermore, the relatively low resolution of A-scan ultrasonography (150 µm) may have contributed to the lack of axial stretch reported in the study. Nevertheless, a recent investigation using A-scan ultrasonography reported an increase in the axial length of the eye during accommodation, however, the increase was not evident in all subjects (Deshpande, 2012). The author investigated the accommodative effect on the axial length for myopic (25 participants; mean refractive error (MRE) of the right eye -1.93 ± 1.39 D, MRE left eye -2.03 ± 1.09 D), hyperopic (25 participants, MRE right eye + 1.90 ± 1.28 D, MRE left eye +1.69 ± 1.21 D) and emmetropes whose mean refractive error was not stated by the author. Accommodation was stimulated in the left eye as participants viewed

text corresponding to N6 print at two distances, 33 cm and 12.5 cm. Biometric measurements were obtained from the right eye and the results indicated an increase in axial length of 88 µm, 70 µm and 7 µm in emmetropes, myopes and hyperopes, respectively for maximum accommodative demand level. However, there was a reduction to the axial length in 20 subjects, whose refractive error was omitted by the author. Comparison of the results from ultrasound studies suggest the variation in findings may be due to the dissimilar targets used to stimulate accommodation. Recent reports with high-resolution instrumentation indicate an axial elongation with accommodation, which are further explored in Chapter 7.

Schachar disagrees with von Helmholtz's theory for accommodation and instead suggests the equatorial zonules have a key role. Schachar's mechanism of accommodation proposes the contraction of the ciliary muscle increases the tension of the equatorial zonules, which in turn increases the equatorial diameter of the lens resulting in the increased optical power of the eye. Moreover, the anterior and posterior zonules are considered supporting ligaments during the accommodative process (Schachar, 1992; Schachar et al., 1996; Schachar and Bax., 2001; Schachar et al., 2006). Schachar's theory is mathematically supported with non-linear finite element analysis (Schachar and Bax, 2001), indicating the tension applied by the anterior and posterior zonules reduces the central optical power of the lens. Nevertheless, the authors state an increase in the volume of the lens of more than 4% during accommodation could provide a relaxation of the anterior and posterior zonules (and possibly the equatorial zonules) resulting in an increased dioptric power of the eye. However, it is clear from more recent studies that an increase in volume of a magnitude greater than 4% is likely to occur (Gerometta et al., 2007; Zamudio et al., 2008), thus, providing evidence disproving Schachar's mechanism. Support for increased tension of the equatorial zonular fibres during accommodation is provided from evidence that the lens equator moves toward the sclera (Schachar et al., 1996). However, results from primate study indicates a reduction to the equatorial diameter of the lens during accommodation. Also, pharmacological manipulation of the apparatus with pilocarpine shows the lens equator moves away from the sclera, irrespective of whether the nasal or temporal ciliary muscle is imaged, therefore, disagreeing with Schachar's mechanism of accommodation (Glasser and Kaufman, 1999).

Overall, from the literature review, it is evident a significant proportion of studies investigating the accommodative apparatus provide support for von Helmholtz's theory of accommodation.

1.4. Presbyopia

The progressive reduction in the amplitude of accommodation with increasing age is well documented (Donders, 1864; Duane, 1922), with less than half a dioptre of accommodation evident after 50 years of age (Anderson et al., 2014). The term presbyopia is generally applied when the amplitude of accommodation declines below 3 D (Weale, 2000). The aetiology can be attributed to lenticular and extralenticular factors (Gilmartin, 1995), and when considered together, suggest presbyopia is most likely a multifactorial condition due to an ageing accommodative apparatus (Weale, 1989).

Lenticular theories

The crystalline lens continues to grow throughout life due to the addition of new lens fibres (Fisher, 1969; Strenk et al., 1999; Dubbelman et al., 2001; Koretz et al., 2002; Dubbelman et al., 2003; Atchison et al., 2008; Richdale et al., 2008), resulting in an increase of thickness along the sagittal direction (Lowe et al., 1970; Cook et al., 1994; Koretz et al., 1997; Strenk et al., 1999; Allouch et al., 2005), mostly due to the increased thickening of the cortex (Cook et al., 1994, Dubbelman et al., 2003), particularly anteriorly (Dubbelman et al., 2003). Consequently, there is a significant linear increase to the lens weight (Figure 1-3) and cross sectional area (Figure 1-4) with age (Glasser and Campbell, 1999). Furthermore, the anterior chamber depth reduces as a consequence of the increased lens thickening, and from the forward movement of the anterior lens surface (Dubbelman et al., 2001; Koretz et al., 2002). The distance between the cornea and the posterior lens surface increases with age, indicating a backwards movement of the posterior lens surface (Dubbelman et al., 2001; Croft et al., 2016b), although the magnitude of the movement reduces with age (Croft et al., 2016b; Laughton et al., 2016).

Figure 1-4. The weight of the human lens increases linearly with age throughout life. Redrawn from Glasser and Campbell (1999).

Figure 1-5. The lens cross sectional area increases with age. Redrawn from Glasser and Campbell (1999).

The anterior radius of curvature of the unaccommodated lens declines with age (Brown, 1973; Glasser and Campbell, 1999; Dubbelman et al., 2001; Atchison et al., 2008) and although data from Scheimpflug imaging suggests the radius of curvature of the posterior surface also reduces (Dubbelman et al., 2001), results from Purkinje imaging (Atchison et al., 2008), MRI (Kasthurirangan et al., 2011) and *in-vitro* studies (Glasser and Campbell, 1999) suggests there is an insignificant age related change. Overall, the age related changes produce a lens which has a greater curvature in the unaccommodated state, and thus a myopic refractive error should be expected in advanced presbyopes. Yet, it is well documented that the refractive error becomes more hyperopic with increasing age (Wang et al., 1994). The prevention of myopia development may possibly occur from a reduction to the lens refractive index with age, a phenomenon termed the lens paradox (Smith et al., 1992; Brown et al., 1999; Dubbelman and Van der Heijde, 2001; Moffat et al., 2002).

Lenticular theories for presbyopia are based upon the geometric changes to the lens shape and size with increasing age, as well as the reduction in the mechanical properties of the lens substance and capsule. The Hess-Gullstrand theory for presbyopia is purely lenticular and suggests the ciliary muscle contractility is retained throughout life, but the increased lens stiffness that results from advancing age reduces the ability of the muscle to alter the lens shape. Fincham (1937) provided evidence of a reduced ability of the lens capsule to mould the lens material with increasing age possibly due to its declining elasticity (Fisher, 1969), although later studies also incorporate the possibility of lens sclerosis as a contributory factor for presbyopia (Fisher, 1973; Pau and Kranz, 1991).

It is clear the lens stiffness increases with age (Pierscionek, 1993; Pierscionek, 1995; Heys et al., 2004; Weeber et al., 2007), with nucleus stiffness showing the greatest increase with age (Figure 1-6, Heys et al., 2004). A stiffness gradient, rather than a uniform stiffness, seems to explain the rapid decline in accommodative ability evident after 40 years of age (Weeber and Van der Heijde, 2007). Early reports suggested the lens material does not harden with increasing age (Nordman and Mack, 1974). However, removal of the capsule from lens of youthful eyes produces a flattened lens substance and an increased focal length of the lens, yet, decapsulation is ineffective in changing the configuration of the lens substance in older eyes (Glasser and Campbell, 1999). Therefore, lens hardening seems to occur and possibly increases the resistance of the compressive forces from the capsule to change the lens shape in order to induce a significant accommodative response (Glasser and Campbell, 1998; Glasser and

Campbell, 1999). Nevertheless, morphological changes to the lens capsule have also been documented. An increased elastic stiffness and a reduction in the mechanical properties occur with age, therefore, changes to the capsule morphology as well as the increase in lens volume may reduce the ability of the capsule to deform (Krag and Andreassen, 2003). Moreover, the stiffness of the capsule has been documented to increase specifically at the capsularhexis edge after cataract surgery (Pedrigi et al., 2009), which may alter the mechanical properties of the capsule and its ability to deform even when the lens substance has been removed.

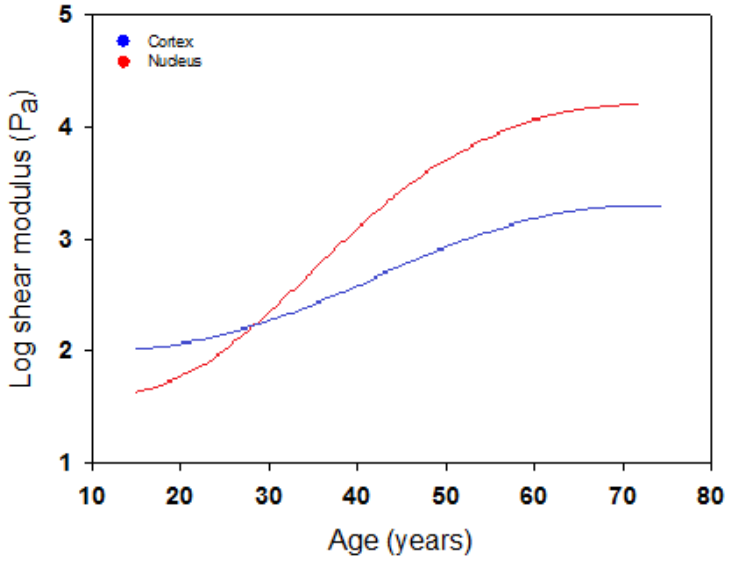

Figure 1-6. Stiffness values of cortex and nucleus as a function of lens age. Redrawn from Heys et al., 2004.

The reduction in the nuclear refractive index and a change in gradient refractive index structure (GRIN) may also contribute to presbyopia development (Moffat et al., 2002), however, evidence relating to the gradient refractive index is equivocal; some studies report the equivalent refractive index remains unchanged with age (Pierscionek, 1997; Glasser and Campbell, 1999), whereas recent evidence suggests there is a reduction (Richdale et al., 2013).

Measurements of the lens equatorial diameter can be obtained using MRI. Although most studies suggest the equatorial diameter remains unchanged with age (Strenk et al., 1999; Jones et al., 2007), a recent study documents an increase of 0.28 mm with age, proposing the lens becomes rounder with age (Kasthurirangan et al., 2011). Data from *in-vitro* studies also indicates lens equatorial diameter increases up to 70 years of age (Glasser and Campbell, 1999), although post-mortem lenses, especially from

young eyes, are known to conform to their accommodated state, therefore may not provide reliable evidence for the age related changes to the lens diameter. Indeed, an increased lens equatorial diameter would reduce the extralenticular space, and a subsequent reduction in the tension from the ciliary muscle at the anterior zonules, which is the mechanism for presbyopia suggested by Schachar (2008). Thus, presbyopia correction surgery based on scleral expansion around the ciliary body has been performed, however, the evidence is equivocal regarding their efficacy. Studies which have measured the amplitude using subjective techniques have either reported an increase in amplitude (Qazi et al., 2002), or no improvement (Hamilton et al., 2002). Furthermore, the restoration of accommodation does not occur for all participants and interestingly, the improvement of the amplitude post-operatively appears to decline such that it is similar to pre-operative accommodation levels, 1 year after surgery (Malecaze et al., 2001). In addition, results from objective methods also suggest scleral expansion surgery does not significantly improve accommodation (Matthews, 1999; Ostrin et al., 2004) suggesting the cause for presbyopia is unlikely to result from an increase in the lens equatorial diameter.

Geometric theory

The geometric theory for presbyopia relates to the changing shape of the crystalline lens with age and the subsequent configuration with the anterior zonules. The distance between the anterior zonules and their insertion at the lens equator increases with age (Farnsworth and Shyne, 1979; Sakabe et al., 1998) resulting in a tangential configuration and thus, preventing a translation of the ciliary muscle force to the lens capsule (Koretz and Handelman, 1986). Consequently, the amplitude of accommodation declines. Strenk and Strenk (2005) provided a modified geometric theory suggesting the reduced zonular tension on the lens is a consequence of the anterior movement of the ciliary sulcus and ciliary muscle with increasing age, possibly as a result from an anterior inward displacement of the iris during lens growth.

Extralenticular theory

The extralenticular theories for presbyopia are related to the contractility of the ciliary muscle. Duane (1925) noted topical instillation of diluted atropine produced a rapid reduction in the accommodative response, specifically in presbyopic individuals, suggesting the ciliary muscle becomes weaker with age. However, Fisher (1977) postulated the contraction of the ciliary muscle actually increases throughout life up to 50 years of age, thus, the reduced accommodative ability documented in advanced presbyopes cannot be explained by the age-related hypertrophy of the muscle.

Although the ciliary muscle has a primary role in accommodation, Fincham (1955) suggested maximum accommodation is due to a combination of ciliary muscle contraction and the ability for the capsule to deform the lens substance, and thus, the reduction in the accommodative ability is due to both factors.

In-vivo evidence from human eyes suggests the contractility of the ciliary muscle is retained throughout life (Strenk et al., 1999; Strenk et al., 2006; Strenk et al., 2010; Sheppard and Davies, 2011; Richdale et al., 2013; Tabernero et al., 2016). Although a slight decline of the contractile ability of the ciliary muscle of early presbyopes has been documented, a considerable contraction is still evident in advanced presbyopes (Strenk et al., 1999). Furthermore, constriction of the ciliary muscle ring diameter is evident during accommodation in pseudophakic eyes, with no significant differences between the contralateral phakic eye (Strenk et al., 2006). Further evidence for a lenticular cause for presbyopia has been provided by Park et al (2008) who reported a manifest centripetal movement of the human ciliary muscle after cataract extraction and Strenk et al (2010) who reported the ciliary muscle of pseudophakic eyes resembles youthful eyes.

Studies employing optical coherence tomography have enhanced our understanding of the morphological and accommodative ability of the aging ciliary muscle. Sheppard and Davies (2011) reported the anterior length of emmetropic eyes reduced with age for both the nasal and temporal quadrants, although there was no significant effect of age on the total length of the muscle. In contrast, there was no change to the anterior length with increasing age for myopic eyes. The authors also reported a reduction to the distance 2 mm posterior to the scleral spur (CMT2) by 2.08 µm/ year, which was only evident within emmetropic eyes and for the temporal ciliary muscle. Also the posterior regions of the ciliary muscle were thinner for the temporal quadrant and the ciliary muscle maximum width increased within the temporal and nasal quadrants. A reduction in the distance between the inner apex and scleral spur was also documented (Sheppard and Davies, 2011). In contrast, Richdale et al (2013) reported an insignificant relationship between age and the ciliary muscle thickness at 1 mm, 2 mm and 3 mm posterior to the scleral spur as well as the maximum thickness and ciliary muscle ring diameter within emmetropic eyes for participants with an age range of 30 to 50 years. Nevertheless, the authors did not report which quadrant of the ciliary muscle was imaged, and also used phenylephrine prior to ciliary muscle acquisition, which may explain the differences to those findings by Sheppard and Davies (2011). However, the multivariate model by Richdale et al (2013) suggested age, lens thickness and the ciliary muscle thickness 3 mm posterior to the scleral spur were

related to accommodative response. Shao et al (2015) simultaneously imaged the ciliary muscle and lens with OCT and documented the amplitude of the ciliary muscle contraction was maintained throughout life, although there was an age related decline to lens shape deformation for each millimetre of increased thickness to the anterior muscle. Moreover, the forward movement of the ciliary muscle positively correlated with the increase to the lens anterior radius of curvature, but there was a negative correlation with lens thickness. Interestingly, the duration to produce the forward movement of the ciliary muscle apex significantly declined with age.

Preservation of human ciliary muscle functionality throughout life is further supported from indirect evidence from the movement of intraocular lenses with accommodative effort (Nakaizumi et al, 1992; Muftuoglu et al., 2005) and lens 'wobbling' in phakic (He et al., 2010) and pseudophakic (Tabernero et al., 2016) after saccadic eye movements, which are suppressed with cycloplegia. The concept for the mechanism of accommodating intraocular lenses are based on the evidence of the contractile ability of the ciliary muscle in presbyopic eyes, however, the accommodative restoration with these lenses remains unclear (Sheppard et al., 2010).

Animal models have significantly contributed to our understanding of presbyopia development. As mentioned in section 1.2.3, the accommodative amplitude of rhesus monkeys and the time course for presbyopia is similar to that in humans. The ciliary muscle of these species undergo age-related changes (Lutjen-Drecoll et al., 1988a) and the ultrastructural changes reduce the contractile response of the muscle to pilocarpine (Lutjen-Drecoll et al., 1988b) and central stimulation via the Edinger-Westphal nucleus (Neider et al., 1990), in contrast to humans. The connective tissue increases in the ciliary muscle of rhesus monkeys (Lutjen-Drecoll et al., 1988a), but to a lesser extent than evident in human tissue (Tamm et al., 1992b). Furthermore, the elastic fibres at the posterior attachment of the ciliary muscle of rhesus monkeys, which are continuous with Bruchs membrane, show age-related stiffening (Tamm et al., 1991b). Thus, the mechanical restriction can explain the cause of presbyopia in rhesus monkeys since severing the posterior attachment from the choroid, restores the contractile response of the muscle to pilocarpine (Tamm et al., 1992c).

Although, inter-species differences exist, recent evidence from human eyes relating to the reduced forward movement of the ciliary muscle with increasing age (Shao et al., 2015) suggests the ultrastructural changes to the posterior attachment of the ciliary muscle may also have a role in human presbyopia development. Indeed, vitreous

zonules have been observed in monkey and human eyes (Lutjen-Drecoll et al., 2010), and, the movement of the strand between the posterior vitreous zonules and lens equator shown to reduce with age (Croft et al., 2016b). Moreover, the forward movement of the ciliary muscle during accommodation in rhesus monkeys seems to contribute to the amplitude of accommodation more so than the centripetal movement of the muscle alone (Croft et al., 2006b).

Cleary, there is considerable evidence to support lenticular theories for presbyopia development. Indeed, significant findings from *in-vivo* studies in humans, suggest the ciliary muscle contractility is retained even in advanced presbyopes, yet, restoration of accommodation using techniques based on the concept of ciliary muscle contractility, have generally been unsuccessful. Therefore, further understanding is required of ciliary muscle mechanics and its functionality in youthful eyes, which could provide essential information to further enhance our understanding of the ciliary muscle and its role in accommodation and presbyopia development.

1.5. Ocular shape variations between emmetropes and myopes

Ocular shape has been investigated in relation to age (e.g. Lim et al., 2011; Lim et al., 2013), refractive error (e.g. Vohra and Good., 2000; Atchison et al., 2004a; Miller et al., 2004; Song et al., 2007; Moriyama et al., 2011; Lim et al., 2011) and pathology (e.g. de Graaf et al., 2005; de Graaf et al., 2007; Munro et al., 2015). Ocular shape is often described by several researchers, however, the generalisation of the term often provides confusion. Direct measurements of ocular shape are possible by using magnetic resonance imaging (MRI) with data suggesting the size and shape of eyes with similar refractive errors significantly vary (Atchison et al., 2004a; Singh et al., 2006).

Investigating the ocular shape in children can provide information about the developmental changes that induce refractive error, which is often difficult to establish in adults with established ametropia. Data from Singaporian-Asian babies, aged between 5 and 17 days old, suggest the globe shape is prolate at birth (Lim et al., 2013). As myopia develops, a greater elongation of eye length and width is evident, whereas emmetropic eyes have an equal stretch in width, height and length dimensions (Lim et al., 2011). Myopic eyes of adults also appear to have a prolate shape, but the greatest elongation occurs in axial length and height compared to width (Atchison et al., 2004a). In contrast, a recent MRI study comparing the shape of the posterior chamber in emmetropes and myopes suggested myopic eyes have a

spherical posterior chamber shape (Gilmartin et al., 2013). Also, comparison of the dimensions of the posterior chamber shape between both eyes of the same individual indicated the vitreous chamber depth ratios were reversed between the right and left eye within the temporal and nasal quadrant, in both emmetropes and myopes (emmetropic RE temporal = 1.040 ± 0.018 and nasal = 1.017 ± 0.013 vs emmetropic LE temporal 1.024 ± 0.015 and nasal 1.039 ± 0.013; myopes RE temporal =1.019 ± 0.013 and nasal = 1.003 ± 0.015 vs LE temporal = 1.009 ± 0.017 and nasal = 1.024 ± 0.016) suggesting processes beyond the optic chiasm may control binocular growth. Moreover, no differences were evident within the vertical plane for both refractive groups (Gilmartin et al., 2013). A temporal-nasal asymmetry has also been documented for some eyes (Singh et al., 2006) and also steeper retinal boundaries have been noted within the nasal quadrant of emmetropic and myopic eyes (Atchison et al., 2004a). Consequently retinal shape can also be determined and some researchers report the findings as 'ocular shape'. Evaluating the retinal shape from mathematical applications of nonrotation symmetrical ellipsoids suggests considerable variation within refractive groups, nevertheless, both emmetropes and myopes display oblate retinal surfaces, although, the degree reduces with increasing myopia (Atchison et al., 2005). Furthermore, an irregular retinal shape has been documented in white and Chinese anisomyopes thus creating a prolate surface within the more myopic eye (Logan et al., 2004). Irregular eye shapes have been reported in eyes with a low myopic refractive error which may be a result of scleral changes that occur prior to the onset of a myopic refractive error (Tabernero and Schaeffel, 2009).

Recently, there has been a renewed interest in the role of peripheral optics on myopigenesis, based on the earlier findings of Hoogerheide and colleagues who concluded that pilots who developed a myopic refractive error initially had a hyperopic peripheral refraction (Hoogerheide et al., 1971). Recent, reports indicate the peripheral retina can influence refractive error development in children (e.g. Mutti et al., 2007; Sng et al., 2011) and animals (e.g. Smith et al., 2005; Smith et al., 2009; Huang et al., 2011). Although studies have been conducted to investigate peripheral refraction, it is clear the sampling at peripheral locations is poorer, resulting in fewer studies measuring the peripheral refraction beyond 40° (Gustafsson et al., 2001; Mathur and Atchison, 2013).

It is clear from the literature that peripheral refraction varies across the retina. Along the horizontal visual field, there is a relative hyperopic peripheral refraction in myopic eyes (Rempt et al., 1971; Love et al., 2000; Logan et al., 2004; Atchison et al., 2005;

Atchison et al., 2006; Chen et al., 2010) whereas, a relative myopic peripheral refraction is apparent in emmetropic eyes (Atchison et al., 2006; Sng et al., 2011). A greater relative peripheral hyperopic refraction has been documented in eyes with central refractive error between -3 D and -4 D, whereas little variation in the hyperopic peripheral refraction has been reported for refractive errors greater than -4 D (Atchison et al., 2006), although fewer subjects with high myopia were included in the study. The authors also found the central refraction appears to have a greater influence on the peripheral refraction along the horizontal meridian rather than the vertical visual field, and also seems to affect the peripheral refraction at temporal visual angles beyond 20° to 25° and beyond 5° of the nasal visual field.

Comparisons between the orthogonal meridians reveal steeper changes in peripheral refractions in the vertical meridian in emmetropic eyes (Atchison et al., 2006). Also, a nasal-temporal asymmetry of the peripheral refraction has been reported for emmetropic and myopic eyes (Feree et al., 1931; Gustafsson et al., 2001; Seidemann et al. 2002; Atchison et al., 2005; Ehsaei et al., 2011; Sng et al., 2011) with the nasal visual field showing greater changes in refraction (Gustafsson et al., 2001; Seidemann et al. 2002; Atchison et al., 2006). Differences in the refraction exist for the oblique meridians of myopic eyes, with the superior-temporal retinal quadrant of myopes revealing smaller shifts in relative hyperopia (Ehsaei et al., 2011). In addition, there is a superior-inferior asymmetry, although, there does not appear to be any variation with increasing myopia (Atchison et al., 2006), however, more studies are required to support the evidence.

Nonetheless, there is great individual variability of the peripheral refractive error in eyes with similar on-axis refractive errors and axial lengths possibly due to differences in the ocular shape (Mutti et al., 2000; Schmid, 2003a). Furthermore, myopes possess a steeper retina than emmetropes, which contributes to the peripheral refractions documented for the different refractive error groups. Differences in peripheral refractive error have also been documented between progressing and non-progressing myopes, specifically, a more hyperopic peripheral refraction in the nasal hemifield of progressing myopes (Faria-Ribeiro et al., 2013). The astigmatic components of the peripheral refraction suggest the retinal shape in progressing myopes is steeper than non-progressing myopes particularly within the nasal quadrant. A probable explanation is a myopic saggital focal image shell in the nasal retina of non-progressing myopes which could inhibit ocular growth, in contrast to a hyperopic sagittal focal length in progressive myopes within the nasal field; such information suggests the position of the saggital

focal length may be important for ocular growth particularly within the nasal retina. Although differences in peripheral refraction between progressing myopes and non-progressing myopes exist, there are no significant differences to the axial length changes with accommodation between these groups (Woodman et al., 2012). Peripheral refraction does not appear to be related to age (Atchison et al., 2005), possibly because the ocular shape has developed and stabilised during adolescence.

Clearly, differences exist in the peripheral refractive profile between refractive groups during distance viewing. However, the implication that near vision may be a factor for myopigenesis has warranted the investigation of peripheral refraction with accommodation (Seidemann et al., 2002; Calver et al. 2007; Davies and Mallen 2009; Ho et al. 2009; Whatham et al. 2009; Tabernero and Schaeffel 2009; Lundström et al. 2009). Calver et al (2007) and Davies and Mallen (2009) reported peripheral refraction was independent of accommodation, therefore, probably does not influence emmetropisation. Other studies have shown the peripheral refractive error becomes more myopic with accommodation (Ho et al., 2009; Whatham et al., 2009; Lundstrom et al., 2009), whereas Tabernero and Schaeffel (2009) found no significant differences for the peripheral retinal profile and accommodation in emmetropes, along the horizontal visual field up to ±45°. Moreover, Davies and Mallen (2009) suggested the periphery of the nasal retina has minimum astigmatism, rather than the fovea, which is in agreement with the findings of Seidemann et al (2002). Peripheral refraction measurements in the vertical meridian have revealed the inferior visual field is more myopic than the superior visual field (Seidemann et al., 2002) and there is inferior-superior retinal asymmetry between emmetropes and myopes with accommodation (Lundström et al., 2009). Also, with accommodation, peripheral refraction measurements at 30˚ of the nasal retina revealed the ocular shape becomes more prolate, although this is not maintained throughout a period of sustained near work (Walker and Mutti, 2002). The steeper retina of myopic eyes in comparison to emmetropes contributes to the measured peripheral refractions observed in different refractive error groups (Schmid, 2003b). Consequently, the variation for peripheral refraction data between refractive error groups and in individuals with the same refractive error is possibly a consequence of the inconsistency in retinal steepness or ocular shape in refractive groups (Mutti et al., 2000; Schmid, 2003b).

Thus, peripheral refraction measurements can only provide assumptions of the ocular shape since the combination of peripheral optics and retinal shape contribute to the results (Verkicharla et al., 2012). Although the retinal contour between refractive

groups has been studied indirectly using peripheral refraction measurements (Logan et al., 2004; Faria-Ribeiro et al., 2013; Nagra et al., 2012), direct measurements using various optical techniques such as A-scan ultrasonography (Logan et al., 2004), MRI (Atchison et al., 2004a, 2004b; Singh et al., 2006; Nagra et al., 2012; Gilmartin et al., 2013) and partial coherence interferometry (Mallen and Kashyap, 2007; Ehsaei et al., 2013) are preferable for evaluating the retinal or ocular shape.

1.6. Aims and objectives of the thesis

The process of accommodation has been investigated for several centuries and although hypotheses for the mechanism of accommodation and presbyopia have been provided, the exact processes are still unknown. The ciliary muscle has an essential role in accommodation as its contraction initiates the morphological changes resulting in an increased in dioptric power of the eye. However, a significant proportion of the literature is based on early research findings from *in-vitro* studies on animals and humans. Recently, *in-vivo* results from animal studies have provided further insight into the morphology of the ciliary muscle during accommodation. Nevertheless, species differences prevnt the generalisation of the possible mechanisms to be related exactly to humans. Research related to the role of the ciliary muscle has been limited in humans thus there is a paucity of literature on the morphological changes of the ciliary muscle during accommodation. In recent years, the advent of high resolution instrumentation, particularly optical coherence tomography, has allowed further *in-vivo* studies of the ciliary muscle in humans to be conducted allowing for greater insight into the role of the ciliary muscle in accommodation under physiological conditions.

Accommodation studies generally use a range of targets to initiate the accommodative response. However, it is unclear which targets allow accurate accommodative responses. Therefore, the aims of the thesis was to determine whether the two commonly used targets, a Maltese cross or letter target, provide significantly different accommodative responses.

The ciliary muscle has a dense innervation as described in the literature review. However, there are no *in-vivo* studies relating to the morphological changes to the ciliary muscle with anti-muscarinic agents such as tropicamide and cyclopentolate or parasympathomimetic agents such as pilocarpine nitrate on the morphology of the ciliary muscle. Indeed, these agents are used frequently for diagnostic and therapeutic agents in ophthalmology, however, they may also provide indications for the ciliary muscle fibre groups that are likely to have a role in accommodation.

Moreover, an asymmetry of the ciliary muscle has been documented from human *in-vivo* studies and animal studies, as explained in the literature review. Yet, it is unknown whether an asymmetry also exists within the vertical meridian, which could enhance our understanding of the structural changes of the ciliary muscle in different meridians. Furthermore, investigating the vertical meridian morphology of the ciliary muscle can enhance our understanding of the relationship between the ciliary muscle dimensions and ametropia.

Consequently, the role of accommodation at the posterior eye is of interest considering the role of the vitreous has been proposed by previous researchers and recent studies suggest there are axial length changes during accommodation. However, it is unclear whether the axial length is the primary locatin for accommodative changes and this is further explored in the present thesis.

Overall, the morphological changes to the ciliary muscle using a range of pharmacological agents as well as physiological stimuli, as well as the physiological effect of accommodation at the posterior eye will be investigated in the present thesis.

Chapter 2. Instrumentation

2.1. Optical Coherence Tomography

Optical coherence tomography (OCT) is a high resolution optical imaging instrument which provides real-time cross sectional images of objects under investigation (Huang et al., 1991; Brezinski and Fujimoto, 1999; Testoni, 2007). The principle is analogous to ultrasound biomicroscopy where sound waves are propagated to the object of interest. The back reflected sound waves are analysed by a detector and the output indicates the mismatch of acoustic waves reflected from the different tissues (Fledelius, 1997). In contrast, optical coherence tomography utilises a light source to provide information for the structural detail of the object under investigation. Therefore, the main difference between both techniques is the source used to form a B-scan from multiple axial scans (A-scans).

The velocity of light is very rapid in comparison to sound (the velocity of sound in water is approximately 1500 m/sec, whereas for light it is approximately 3×10^8 m/sec. Fujimoto et al, 2000). Therefore, spatial information from reflected light echoes are too fast to detect by electronic sensors. To overcome this limitation, instruments exploit the principle of low coherence interferometry with the use of a Michelson interferometer. A low coherent light source travels towards a 50/50 beam splitter which divides the beam into two, resulting in each beam travelling perpendicular to the other. One beam travels along the reference path towards the reference arm, whereas the second beam travels along the sample path towards the structure of interest. When the beam from the light source to the object is equidistant to the beam directed towards the reference mirror, each beam is reflected back along the path to coincide at the detector, as shown in Figure 2-1. The detector analyses the interference of the signal between the reference beam and the beam along the sample path and provides an electrical output. The overall optical path difference (OPD) = sample path length-reference path length (Podoleanu, 2012). Interference only occurs when the optical path lengths are matched and within the coherence length of the light source (Tomlins and Wang, 2005). Therefore, the maximum interference signal will occur when OPD = 0, with the signal strength decreasing as the interference becomes greater than the coherence length of the light source (Podoleanu et al., 2004).

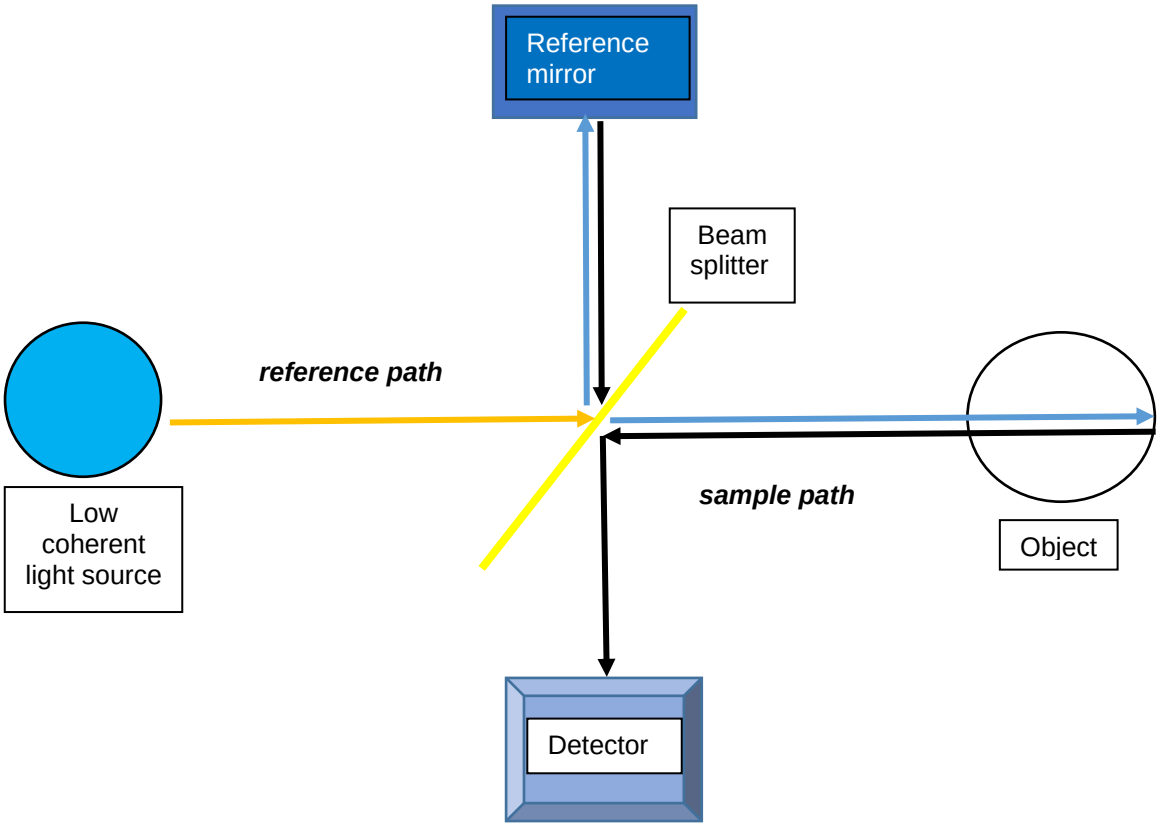

Figure 2-1. A schematic diagram depicting the principle of OCT. A low coherent light source is projected towards the beam splitter which divides the light into two beams, one directed towards the reference mirror (*reference path*) and the other directed towards the tissue of interest (*sample path*). Both beams are backscattered and detected by the interferometer which measures the differentiation of time delay between the beams to provide a measure of distance. Interference only occurs when the reference and sample arm optical path lengths are coordinated within the coherence length of the light.

The performance of optical coherence tomographers are based upon resolution and imaging depth. The bandwidth of the light source determines the axial resolution (Gabriele et al., 2010).The axial resolution of OCT has significantly improved over the last decade, where resolutions less than 10 µm have been achieved. Ultra-high resolution of 3 µm has also been reported with the use of an 800 nm wavelength short pulse solid-state laser to generate low coherence light (Drexler et al., 2001). The transverse resolution is dependent upon the ease to focus the source, and since light is

easier to focus than sound, the resolution of OCT is greater (Fujimoto et al., 2000) than that for ultrasound. High frequency ultrasound, nevertheless, can produce high resolution images but is attenuated within the tissue, therefore penetration is limited to a few millimetres (Fujimoto et al., 2000). For OCT, the depth through which the light beam can travel is dependent upon the centre wavelength of the light source (Gabriele et al., 2010) as well as the absorption and scattering properties of the surface which influence the back-reflection of light. Generally, the light source can penetrate tissue between 1-3 mm which is similar to the resolution achieved from biopsies and histological sections (Fujimoto et al., 2000). The technique is capable of providing high quality data even in the presence of aberrations and unlike ultrasound, the resolution of OCT does not reduce with increasing depth.

The penetration of light to various layers within the tissue sample can be achieved by translating the reference mirror which occurs in a time-domain OCT (Tomlins and Wang, 2005), or stabilising the reference mirror as adopted for frequency domain OCT. Within a frequency domain OCT, reflected frequencies are analysed with a spectrometer to provide spatial information using a Fourier transform (Fercher et al., 1996; Gabriele et al., 2010), unlike time-domain OCT where coherence of light is analysed by a sensor. Therefore, Fourier domain OCT measures the reflected light from various layers simultaneously, whereas time domain instruments measure the echo of light sequentially (Kiernan et al., 2010). Thus, the acquisition rate is faster in a frequency domain OCT compared to time-domain, which is an important consideration during ocular imaging where steady eye fixation may not always be possible. Although the high sensitivity of frequency domain OCT (Leitgeb et al., 2003) makes it attractive for clinical settings, the resolution is limited by the resolution of the spectrometer.

The description of an OCT for use in clinical situations was first demonstrated with a super luminescent diode transmitting a wavelength of 830 nm for axial scanning, thus, creating A-scans and subsequent B-scans (Huang et al., 1991). The authors confirmed the ability of the optical coherence tomographer to produce high resolution images for transparent and non-transparent tissue. Thus, they imaged retinal tissue (a relatively transparent medium), as well as an artherosclerotic plaque (a non-transparent, highly reflective medium). The non-invasive instrument was capable of producing high-resolution images that were comparatively similar to microscopic analysis of histological sections, which emphasised the prospect for the technique in research and clinical environments. Consequently, over the last two decades the advancements in OCT have significantly contributed to the medical field. Nevertheless, the most

abundant application of optical coherence tomography is within ophthalmology and optometry where the advantage of non-contact is valuable for patient comfort.

Frequency domain has been adopted for many commercially available optical coherence tomographers including Cirrus HD-OCT (Zeiss) and Spectralis (Heidelberg Engineering), which produce axial resolutions of 5 µm and 6 µm, respectively (Kiernan et al., 2010). The instruments provide real-time images from the rapid performance, processing and acquisition of data with results displayed very quickly. The transverse and axial scanning of the incident beam across the tissue provides a two dimensional image which is presented as a false-colour or grayscale image (Fujimoto et al, 2000).

Investigation of anterior eye abnormalities has warranted the application of optical coherence tomography for the anterior eye. Although some optical coherence tomographers, such as the Cirrus OCT (Zeiss), have the capability to image the anterior eye with a supplement attachment, it is not currently possible to image the anterior and posterior segment simultaneously due to the high refractive power of the anterior segment (Walsh, 2011). In 1994, Izatt and colleagues proposed the use of posterior segment OCT for anterior eye imaging. The OCT had a super luminescent diode with an 830 nm wavelength with a longitudinal resolution of 10 µm and was mounted onto a slit lamp. The lateral resolution was controlled by the beam diameter which influenced the aperture of the lenses that focussed the beam within the eye. The authors used various aperture lenses to focus the light at different ocular layers to ensure the depth of focus matched the depth of the intraocular structures. The optical data was converted into geometric values by dividing the path length with the refractive index of the separate ocular tissues. Motion defects from involuntary eye movements were removed from the computer analyser. As such, the cornea, iris, sclera and anterior chamber were clearly identified. However, with an 830 nm wavelength, there was significant scattering of light within the anterior eye, which subsequently prevented the optical light source from acquiring data from deeper layers (Izatt et al., 1994).

In 2001, a real-time anterior optical coherence tomographer was developed using a 1310 nm wavelength. The infrared wavelength resulted in less scattering within the ocular media in comparison to an 830 nm wavelength light source. Furthermore, the longer wavelength was able to image deeper ocular structures as it was not absorbed or reflected significantly within the tissue, therefore, providing detailed anatomical data. Thus, the authors established the capability for detailed imaging of the various layers in the iris, scleral spur, anterior chamber angle, anterior lens capsule, and pars plicata of the ciliary body although the increased scattering of light within the sclera hindered the

visibility of the outline of the pars plicata (Radhakrishnan et al., 2001). Another advantage of a longer wavelength is its strong absorption in water, resulting in minimum amount reaching the retina, which means a higher power source can be used allowing data to be obtained faster (Steinert and Huang, 2008).

Hoerauf et al (2002) described a transscleral optical coherence tomographer, where an infrared super luminescent diode producing a wavelength of 1310 nm and a coherence length of 20 µm was attached to a slit lamp. The depth of imaging was 1.8 mm and the axial resolution was approximately 15 µm. Several anatomical structures were imaged including the anterior chamber angle and the iris. Moreover, the ciliary body and longitudinal portion of the ciliary muscle were clearly identified. However, imaging the ciliary body required light to travel through the sclera. The sclera is an inhomogenous medium containing collagen fibrils of different diameters, with variation in refractive indices between the fibrils and scleral tissue, therefore, the anatomical structure increases the scattering of light passing through (Foster and de la Maza, 2013). Furthermore, the signal intensity of the light reduced with increasing depth of tissue therefore preventing the ability to image the zonules (Hoerauf et al., 2002).

Therefore, high-resolution detail of the anterior structures can be obtained *in-vivo* using a longer wavelength of light, which also allows visualisation of deeper structures within the anterior segment due to the reduced scattering properties of the infrared beam within the ocular media. However, a limitation of the longer wavelength incorporated in anterior segment OCT, is the absorption of the wavelength by pigmented structures such as the iris, preventing further penetration of the light waves into deeper ocular tissue.

The Visante *AS-OCT* (Zeiss) was the first commercially available anterior segment OCT. Manufacturer (Carl Zeiss, Meditec) details state the instrument incorporates a super luminescent diode which transmits a light source with a wavelength of 1310 nm. The instrument provides several options for scanning the anterior segment. The high-resolution corneal mode produces 512 A-scans at a rate of 0.25 seconds per line acquisition time, therefore, no motion artefacts are visible. The optical resolution is 18 µm in the axial direction and 60 µm in the transverse direction. Therefore, the instrument has been used to image the internal anterior chamber diameter, white-to-white diameter (Kohnen et al., 2006), anterior chamber depth (Piñero et al., 2008), and anterior chamber angle (Leung et al., 2008). Investigation of the anterior eye is important for intraocular lens implantation where the depth assessment of the anterior

chamber is vital (Baikoff et al., 2004b). Also, imaging the cornea is especially relevant for patients to identify anatomical changes which occur to the cornea after laser refractive surgery (Ustundag et al., 2000).

The SL-OCT (Heidelberg) is also available and uses a 1300 nm superluminescent diode, however, the instrument scans at a lower speed in comparison to the Visante AS-OCT. Recently, the RT-Vue (Optovue) anterior segment optical coherence topographer has become available that has a resolution of 5 µm and employs an 830 nm wavelength light source that is analysed with frequency domain. As such, the acquisition rate is faster than the time domain Visante AS-OCT. Nevertheless, the depth of penetration through tissue is greater with Visante due to the longer wavelength of 1310 nm, therefore providing greater information of deeper anatomical structures (Ramos and Huang, 2009). For this thesis, the Visante AS-OCT has been used for acquiring data for the anterior segment of the eye, and, will only be considered further.

Optical coherence tomographers contain spatial errors resulting from non-telecentric lateral scanning, use of scanners and optical distortion from refraction of light at each intraocular interface. Axial distortion can be significant and causes a greater distortion along the vertical meridian than the horizontal meridian (Podoleanu et al., 2004). Light refracts when there is a change in the refractive index between different mediums and as a non-contact instrument for ophthalmology, the first interface where the refractive index is altered is between the air and cornea interface. As the light beam travels through the ocular media, the values for the refractive index of the various structures is essential to convert the optical path length into physical lengths. Thus, raw images cannot be used to quantify morphological structures as data for the optical path length is provided rather than the geometric values. Various methods have been proposed for correcting the distortion resulting from refraction in custom-made OCT instruments, such as applying Fermats principle (Westphal et al., 2002) and dividing the optical path length by the refractive index of the medium (Wang et al., 2002), however, applying such a principle for peripheral measurements where the deviation of non-parallel rays occurs, is less accurate. Quantifying ocular changes is vital to monitor disease progression, therefore, the correction of distorted images is vital for clinical and research settings.

Various scan modes can be used for capturing anterior eye structures with the Visante AS-OCT, however, the manufacturer does not provide information regarding the

correction factor for each scanning method (Ramasubramanian and Glasser, 2015). An in-built edge-detection algorithm is applied to determine the surface curvature of the cornea and the anterior chamber depth within the instrument (Baikoff, 2006). The accuracy of the data presented from corneal scans with AS-OCT have been investigated using a model eye; the results suggest the residual distortion remains even when images are corrected with in-built software. Nevertheless, the uncorrected images overestimate the corneal and lenticular thickness whereas the anterior chamber depth and surface curvature are underestimated, indicating the in-built software significantly reduces the errors (Dunne et al., 2007). Correction of the images are vital especially when using the data for investigating refractive error since uncorrected images can induce an error of 0.80 D (Ramasubramanian and Glasser, 2015). The Visante OCT has good intrasession and intersession repeatability for corneal parameters (Ramasubramanian and Glasser, 2015).

OCT images of the ciliary muscle have a higher definition than ultrasound biomicroscopy, allowing for easier identification of the scleral spur, which is used as a reference point for analysis. The development of a semi-automated software (Kao et al., 2011) provides data for landmarks at various locations including 1 mm, 2 mm and 3 mm posterior to the scleral spur but no indication of the ciliary muscle length due to the difficulty of detecting the posterior visible limit manually. However, ciliary muscle length is an important measurement considering the length has been reported to reduce with accommodation (e.g. Sheppard and Davies, 2010b) and age (e.g. Tamm et al., 1992b).

2.1.1. Analysis of ciliary muscle images acquired with Visante AS-OCT

Throughout this thesis, the ciliary muscle images obtained with the Visante AS-OCT have been analysed using the semi-automated software described by Laughton et al (2015) to provide quantifiable data for ciliary muscle parameters. The analysis procedure is described below.

To ensure the examiner was masked to the refractive error, ciliary muscle orientation and accommodative demand level, all images were coded prior to image capture. The same examiner (PR) acquired the images and analysed the data. The images were exported as raw DICOM (Digital Imaging and Communications in Medicine) files and saved onto an external hard drive. Previous authors have reported the images are corrected for geometric distortion automatically by the instrument prior to exporting (Kao et al., 2011; Ramasubramanian and Glasser, 2015). Consequently, the images were imported into Matlab R2014b (The Mathworks Inc., Massachusetts, USA). The

images were resized to 512 x 1280 pixels but were not cropped nor reduced in size. The software requires the examiner to identify several landmarks before the data is provided for the various ciliary muscle parameters. Firstly, the location of the scleral spur is located (Figure 2-2) and subsequently the position which is beyond the posterior visible limit of the ciliary muscle is found (Figure 2-3).

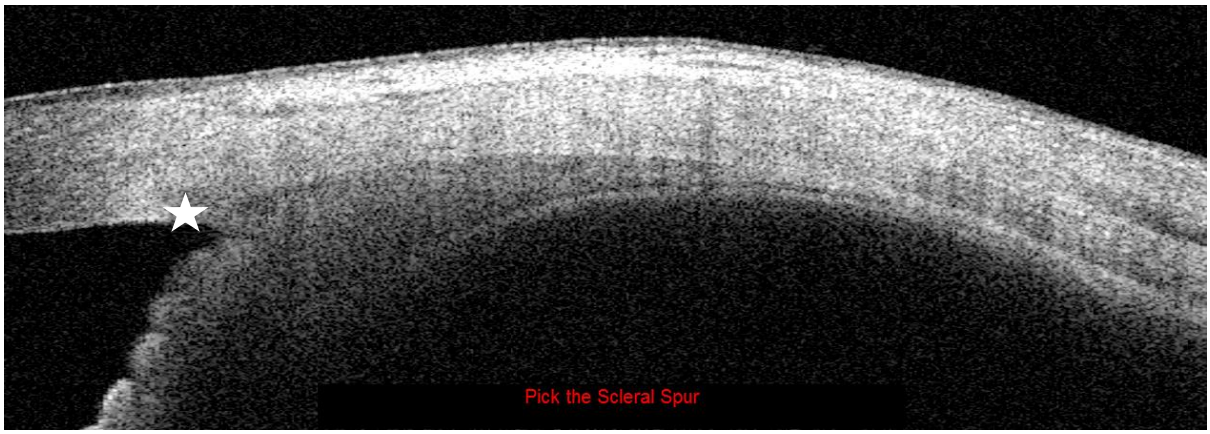

Figure 2-2. The scleral spur is initially identified with the semi-automated software shown with the star on the image.

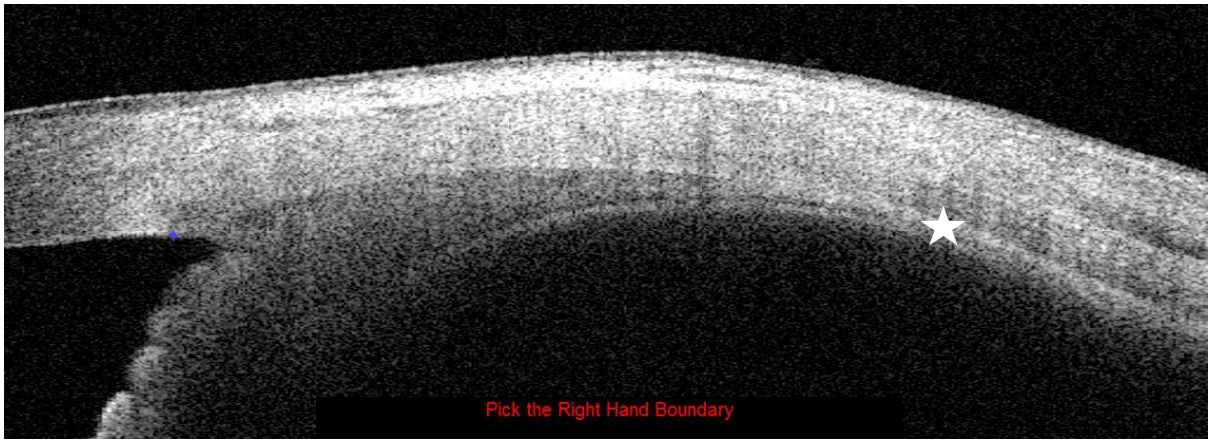

Figure 2-3. The posterior visible limit is shown by the star on the image.

A vertical line appears midway between the points located and the examiner is required to choose the positions relating to the sclera/ciliary muscle boundary and the ciliary muscle/pigmented ciliary epithelium boundary (Figure 2-4).

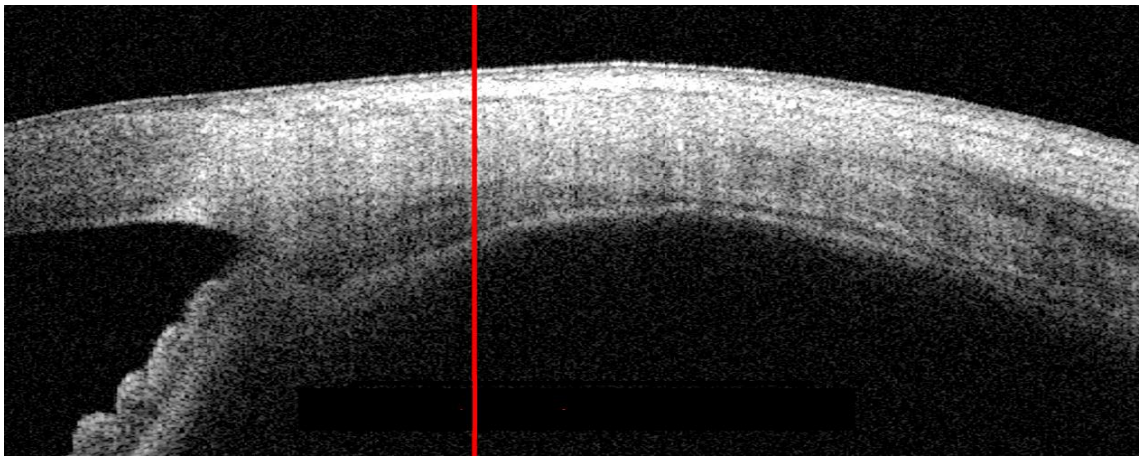

Figure 2-4. The red vertical line is shown from which the superior and inferior limits of the ciliary muscle are located.

Consequently, the software fits 10 vertical lines between the scleral spur and the posterior limit of the ciliary muscle that are separated by 1 pixel intervals every 0.5 mm. This allows the software to determine the ciliary muscle border using a 2nd order Fourier series that is differentiated to fit the ciliary muscle profile. The process is completed separately for the superior and inferior boundaries of the ciliary muscle, with the maximum peak corresponding to the line which crosses the ciliary muscle boundary. As such, a second order polynomial curve is fitted to the ciliary muscle profile (Figure 2-5).

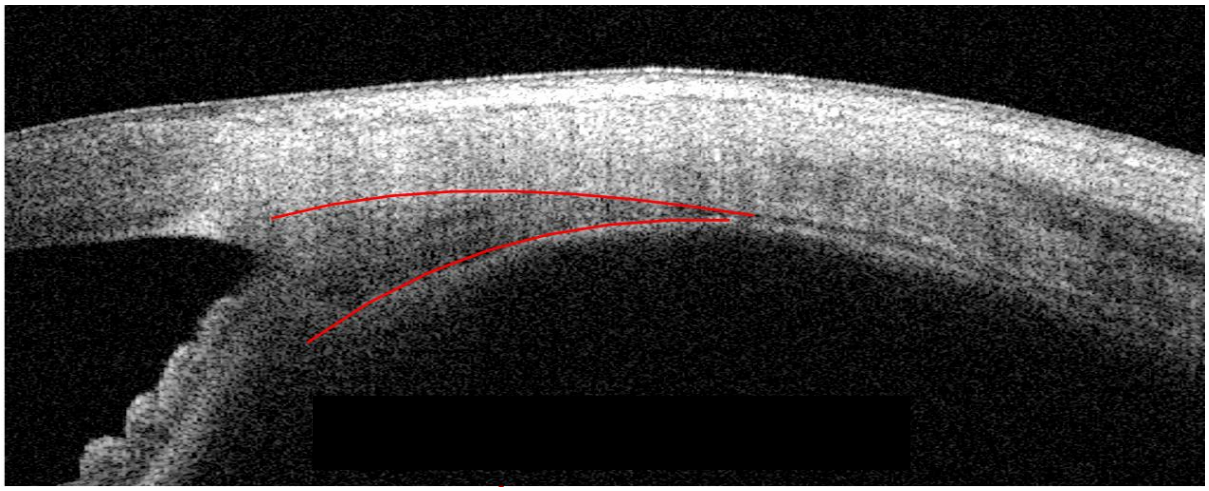

Figure 2-5. The ciliary muscle is outlined with the red curves.

Nevertheless, finding the ciliary muscle/pigmented ciliary epithelium border is more difficult to determine, therefore, the software allows for manual identification of the border to improve the fit of the border if the automated procedure is not suitable. Therefore, the examiner locates three points and a curve is fitted to those locations. In addition, the inner apex must also be manually selected as the image clarity is not as prominent within the region. After the curves have been fitted, the OCT image is converted into a binary image and internal Matlab edge detection algorithms are used to determine the air/sclera interface. The interface is fitted with a second order polynomial curve, followed by a tiered refractive index correction to scleral (n= 1.41) and ciliary muscle tissue (n= 1.38) which corrects the optical distortion that has been well documented within OCT images. The values for the refractive indices are based upon published data from rabbit scleral and ciliary body tissue (Nemati et al., 1997; Nemati et al., 1998). Moreover, the refractive index of bovine muscle tissue (Dirckx et al., 2005) and human cardiac muscle (Tearney et al., 1995) has also been reported as 1.38.

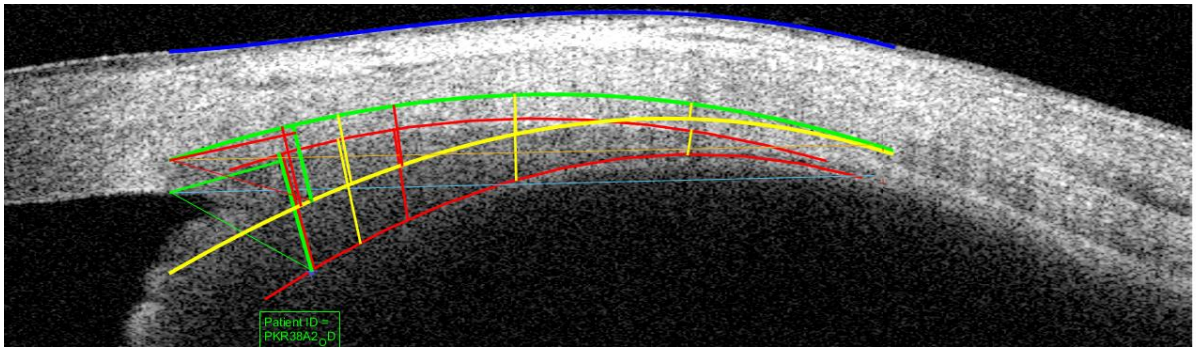

Figure 2-6. The ciliary muscle images are corrected for the refractive indices for the air/scleral interface (green curve) and ciliary muscle tissue (yellow curve).

Considering the difficulty of identifying the posterior visible limit documented (Kao et al., 2011), the software determines the limit automatically by identifying the minimum separation of the curves posteriorly, that have been fitted to the boundary of the ciliary muscle. Determining the posterior visible limit using this technique has produced highly repeatable results (Laughton et al., 2015). Furthermore, the software provides valid and repeatable data for the ciliary muscle parameters (Laughton et al., 2015). Overall, the software provides data for:

- Straight line total distance from the scleral-spur to the posterior visible limit (CM length)
- Ciliary muscle total length measured along the scleral/ciliary muscle boundary (CM length Arc)

- Maximum thickness (CMMAX) which is the perpendicular distance measured from the inner apex to the sclera
- Anterior length measured perpendicularly from the line of maximum thickness to the scleral spur (SS-CM)
- Distance between the scleral spur and the inner apex (SS-IA)
- The thickness measured 1 mm posterior to the scleral spur along the scleral curve (CMT1)
- The thickness measured 2 mm posterior to the scleral spur along the scleral curve (CMT2)
- The thickness measured 3 mm posterior to the scleral spur along the scleral curve (CMT3)
- Thickness measured at 25% of the total curved length of the ciliary muscle (CM25)
- Thickness measured at 50% of the total curved length of the ciliary muscle (CM50)
- Thickness measured at 75% of the total curved length of the ciliary muscle (CM75)

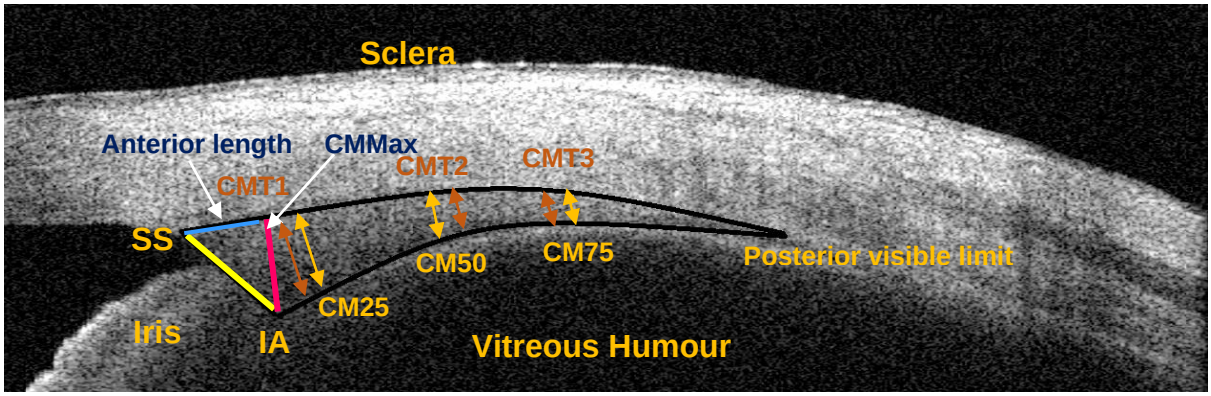

Figure 2-7. The ciliary muscle length and proportional thickness measurements are shown for the temporal quadrant; SS= Scleral spur, IA = inner apex. The anterior length is shown in blue and the maximum ciliary muscle thickness in pink.

2.2. Optical Biometry

The measurement of ocular biometry such as axial length, anterior chamber depth and the corneal radii of curvature is termed ocular biometry. Such measurements are essential for formulae that are used to calculate the intraocular lens power for patients enlisted for cataract surgery. A-scan ultrasonography has frequently been used in the past to obtain biometry measurements (Coleman, 1969; Hoffer, 1980; Shammas, 1982;

Bee and Kiat., 1984), nevertheless, the compromise between the resolution and increasing penetration depth results in a lower longitudinal resolution of approximately 200 µm (Olsen, 1989). Therefore, accurate axial length measurements are not always possible. However, ultrasound biomicroscopy is an essential instrument for determining the axial length when there are dense media opacities (Tehrani et al., 2003; Freeman and Pesudovs, 2005). Nonetheless, ultrasound biomicroscopy requires the use of a topical anaesthetic and is an invasive technique which requires the use of a probe on the cornea, increasing the risk of corneal abrasions and corneal infections.

Axial length is the main determinant for accurate assessment of intraocular lens power, and considering 54% of inaccurate intraocular lens powers can be attributed to errors in axial length measurements (Olsen, 1992), the development of high resolution instrumentation, such as the IOLMaster, has improved the refractive outcome for patients as a result of the improved accuracy of axial length measurements.

2.2.1. Optical biometers: IOLMaster *(Zeiss)* and LenStar LS900 *(Haag-Streit)*

The IOLMaster is a high resolution instrument that uses the principle of partial coherence interferometry (PCI), in order to calculate the axial length of the eye. Infrared light with a wavelength of 780 nm (Santodomingo-Rubido, 2002; Rajan et al., 2002) is directed towards the anterior surface of the cornea which is used as a reference point by the IOLMaster. Consequently, the beam is divided into two by a beam splitter, with each beam directed towards a mirror (Santodomingo-Rubido, 2002). Thus, the principle is analogous to one-dimensional OCT. The advantage of a dual beam is that the instrument is insensitive to longitudinal eye movements (Hitzenberger, 1991). In order to convert optical path lengths into geometrical distances, an average refractive index (n= 1.3549) is used. Precise and accurate axial length measurements can, thus, be obtained in non-pathological (Hitzenberger, 1991) and cataractous eyes (Hitzenberger, 1993). The precision of axial length measurements is 10 µm (Drexler et al., 1998a) and axial length measurements are highly reliable (Vogel et al., 2001), repeatable and valid (Santodomingo-Rubido, 2002). Axial length measurements are acquired along the visual axis of the eye and acquisition is possible for eye lengths within the range of 14-38 mm. Furthermore, the IOLMaster axial length measurements are automatically calibrated to immersion ultrasound (Olsen, 2005).

The LenStar is a newer optical biometer and is also analogous to OCT, however, the instrument utilises a super luminescent diode to produce a short coherent infra-red light source of wavelength 820 nm. The instrument is able to obtain simultaneous

measurements for axial length, lens thickness, anterior chamber depth, retinal thickness and central corneal thickness, along the visual axis. In contrast to the IOLMaster, the LenStar design consists of a rotating prism cube, rather than mirrors, therefore rapid A-scans are obtained quickly (Kaschke et al., 2014). The measurement of the intraocular parameters are precise (Shammas and Hoffer, 2012) and there is good intrasession and intersession repeatability for anterior chamber depth, axial length, keratometry, central corneal thickness and white-to-white distance (Zhao et al., 2013; Buckhurst et al., 2009). According to the technical information provided by the manufacturer (www.haag-streit.com), the corneal thickness measurements have a resolution of 1 µm and measurements can be provided for corneal thicknesses within the range (300-800 µm). The instrument is capable of acquiring data for anterior chamber depth within a range of 1.5-6.5 mm, lens thickness between 0.5 and 6.5 mm, and axial length between 14 and 32 mm. The resolution of the anterior chamber depth, lens thickness, axial length and corneal diameter is 10 µm. As with the IOLMaster, the LenStar defines the axial length as the distance between the anterior corneal surface and the retinal pigment epithelium.

There is moderate agreement between the anterior chamber depth measurements obtained with the IOLMaster and LenStar (Hoffer et al., 2010) possibly attributed to the different techniques used. Considering cycloplegia produces a deeper anterior chamber depth (Mutti et al., 1994), the pre and post-cycloplegia biometric measurements obtained with the LenStar and IOLMaster are reportedly statistically significant (Sheng et al., 2004; Huang et al., 2012).

The LenStar has excellent repeatability with mean intersession differences reported as -0.008 ± 0.020 mm for axial length, 0.001 ± 0.006 for central corneal thickness, -0.024 ± 0.010 for anterior chamber depth, -0.030 ± 0.120 mm for the lens thickness and -0.047 ± 0.240 mm for the corneal diameter (Shammas and Hoffer, 2012). The intraocular measurements obtained are highly reproducible (Cruysberg et al., 2010). The LenStar can also be used to measure the choroidal thickness as determined from the A-scan data, with good repeatability of results (Read et al., 2011).

The refractive index for converting optical distances to geometrical lengths, is proprietary information for the LenStar. However, comparing the axial lengths of model eyes obtained with the IOLMaster and LenStar, Suheimat and colleagues (2015) deduced refractive indices for the cornea (1.340), aqueous (1.341), lens (1.415) and an overall group refractive index (1.354). Due to the unlikely physiological refractive index

for the cornea, the authors reported the instrument possibly calibrates the optical path length to correct for instrument errors.

There is good agreement (Hoffer et al., 2010) and correlation (Holzer, 2009) between the axial length measurements obtained with the LenStar and IOLMaster, although the lengths provided by the LenStar are longer in comparison to the IOLMaster (Buckhurst et al., 2009; Hoffer et al., 2010; Shen et al., 2013). For example, Hoffer and colleagues (2010) reported the mean axial length with the LenStar was 23.72 (SD 1.21) mm and 23.70 (SD 1.20) mm with the IOLMaster, for eyes with clear lenses. Buckhurst and colleagues (2009) reported axial length measurements which were 10 µm longer than the IOLMaster in cataractous eyes, which approximately equates to a refractive difference of 0.03 D and thus is clinically insignificant. Due to the differences which have been documented, some researchers suggest the axial length measurements are interchangeable (Hoffer et al., 2010; Jasvinder et al., 2011), however, Zhao et al (2013) reported the axial length data obtained with the LenStar and IOLMaster, in a myopic population, was not interchangeable since the error produces clinically significant differences for calculating refractive error (difference between 0.62 and 1.00 D). Cruysberg and colleagues (2010) found a statistically significant difference between the axial length measures of both instruments, and although the difference did not produce a clinically significant error for the intraocular lens power calculation, the authors concluded the measurements between both instruments are not interchangeable.

Nevertheless, there is a good correlation of axial length measurements between the IOLMaster and LenStar in eyes with a cataract, as well as pseudophakic, aphakic and silicone oil filled eyes (Rohrer et al., 2009). However, optical techniques cannot always obtain biometric measurements and a recent report suggests the failure rate of axial length acquisition is 62.16% with the IOLMaster and 64.53% with LenStar, for eyes with cataracts, with the greater errors due to posterior subcapsular cataracts (McAlinden et al., 2015). The IOLMaster is capable of measuring the axial length in highly myopic eyes with posterior staphylomas, which is not always possible with the LenStar (Shen et al., 2013). Nevertheless, there is a good correlation between the axial length measurements obtained with the LenStar and IOLMaster for highly myopic eyes (correlation 0.11 mm; Shen et al., 2013). Furthermore, cycloplegia does not have a significant effect on the axial length measurements obtained with the optical biometers (Sheng et al., 2004; Huang et al., 2010; Bakbak et al., 2013). In comparison to applanation ultrasound, the measurements obtained with the IOLMaster are longer. The differences arise because compression of the cornea occurs with the ultrasound

probe and the reflection of the ultrasound source is from the inner limiting membrane compared to the retinal pigment epithelium with IOLMaster (Eleftheriadis, 2003). Generally, non-contact techniques are preferable by patients (Eleftheriadis, 2003; Hoffer et al., 2010) and are therefore used frequently in clinical practice.

The use of partial coherence interferometry and optical low coherence interferometry techniques can be used to obtain peripheral eye length measurements (Hitzenberger., 1991; Schmid, 2003b; Mallen and Kashyap, 2007). Consequently, differences in the retinal contour have been found between emmetropic and myopic eyes, with myopic eyes having a greater axial length and generally longer eye lengths for the peripheral retina (Ehsaei et al., 2013).

The LenStar provides repeatable on-axis and off-axis eye length measurements, although repeatability is poorer at 10° of the nasal retina (Schulle et al., 2013).There is good agreement between the peripheral eye length measurements obtained with the LenStar and IOLMaster and both instruments have good intrasessional (IOLMaster 0.04 (SD 0.04), LenStar 0.02 (SD 0.02)) and interesessional repeatability for peripheral eye length measurements along both the horiozontal and vertical meridains (Verkicharla et al., 2013). However, the authors reported greater intrasessional variability, specifically, at 20°, 25° of the temporal field and 10° and 30° of the superior field with the IOLMaster, and 15° of the temporal field with the LenStar possibly due to the location of the optic disc. The intersessional repeatability for eye lengths was minimal for the central visual field but became less accurate for both instruments as the angle was increased. There is good agreement between both instruments for the measurement of the horizontal and vertical visual fields (mean difference of 0.01 mm (SD 0.07) for the horizontal visual field and 0.02 (SD 0.07) for the vertical visual field). Eye rotation reportedly induces 0.75 D of myopic increase in the refractive error (Seidemann et al., 2002). However, peripheral eye length measurements are valid with the LenStar when eye movements occur (Verkicharla et al, 2013).

2.3. Autorefraction

The Grand Seiko WAM 5500 autorefractor/keratometer (Grand Seiko Co. Ltd., Hiroshima, Japan) is a binocular open-field autorefractor used to provide measurements for refraction, pupil size and keratometry. The instrument has a 12.5 cm x 22 cm open field beam splitter allowing fixation of external targets for distant viewing. An open field autorefractor ensures accommodation is relaxed, and instrument myopia is minimal unlike closed-view autorefractors which use fogging techniques to relax

accommodation and internal viewing targets that may induce instrument myopia (Smith, 1983; Rosenfield and Cuiffreda, 1991). The autorefractor calculates the refractive error using the same principle as the Grand Seiko WR-5100K autorefractor. An infrared ring is imaged onto the retina and focused by a rapidly moving motorized track with an attached lens and the images are analysed in several meridians to calculate the toroidal refractive error. Up to 106 static images can be produced in 1 minute and a range of refractive errors can be measured between ± 22.00 D for the sphere component and ± 10.00 D for the cylinder (Davies et al., 2003) in 0.01 D, 0.12 D or 0.25 D steps, and 1° increments for the cylinder axis (Sheppard and Davies, 2010a). Accurate alignment of the instrument to the visual axis of the eye is possible due to the visibility of the pupil on a colour LCD monitor (Davies et al., 2003).

Validity of the instrument is generally reported as the agreement between the subjective refractive error results and the objective refraction determined with the autorefractor, and good agreement has been reported for the measurement of distance refractive error, indicating good control of accommodation by the instrument (Davies et al., 2003; Sheppard and Davies, 2010a; Aldaba et al., 2015). Sheppard and Davies (2010a) reported statistically, but not clinically significant, differences of the cylindrical and J_0 component of the refractive error between subjective refraction and objective measurements with the Grand Seiko WAM 5500 autorefractor. Nevertheless, the autorefractor is a repeatable and valid instrument for clinical practice and research (Sheppard and Davies, 2010a). Although the autorefractor is open-field for binocular viewing, hypermetropic refractive errors are underestimated, possibly, due to the inability for participants to relax their accommodation completely (Sheppard and Davies, 2010a). Cyloplegia is more effective at eliciting the hyperopic refractive error prior to autorefraction, although relaxing accommodation with fogging lenses are effective in emmetropic eyes (Queiros et al., 2008).

The Grand Seiko WAM 5500 autorefractor can be used to measure the static and dynamic accommodative responses (dynamic mode at a frequency of 5 Hz). Lower stimulus amplitudes have been identified for static accommodative response compared to the dynamic measurements (e.g. for a 2 D stimulus mean static accommodative response 1.41 D and mean dynamic accommodative response 1.54 D), whereas for higher stimulus amplitudes, the static accommodative responses are slightly higher than dynamic (e.g. for an 8 D stimulus, static accommodative response 5.79 D and dynamic accommodative response 5.34 D) and the differences are statistically significant. The variation between the static and dynamic responses is probably due to

individual performance for accommodation tasks and possible accommodative fatigue, rather than differences induced by the instrument itself (Win-Hall et al., 2010). The autorefractor provides repeatable results for the assessment of initial near induced transient myopia and its early decay (Lin et al., 2013) and can also be used to assess the accommodative response in phakic and pseudophakic eyes (Nemeth et al., 2013).

Pupil measurements are also provided for static and dynamic modes by detecting the iris boundary and superimposing a circle of best fit (Sheppard and Davies, 2010a). Pupil measurement are provided in 0.1 mm increments and are possible for pupil sizes greater than or equal to 2.3 mm, although, the maximum pupil size that can be measured by the instrument is unknown. Measurements of the central corneal radius are also possible by analysis of the reflected corneal ring diameter measured in 3 meridians separated by 60° and within the range 5.0 to 10.0 mm (Sheppard and Davies, 2010a).

Chapter 3. Is the accommodative response dependant on the choice of target?

3.1. Introduction

Amplitude of accommodation refers to the maximum accommodative ability of the eye and can be quantified using a range of subjective techniques (push up to blur, pull down to blur, minus lens or dynamic retinoscopy) or evaluated objectively using autorefractors (Wold et al., 2003; Win-Hall et al., 2007; Anderson and Stuebing., 2014). Subjective techniques are dependent upon patient responses for first blur and consequent sustained blur for the object viewed (Rosenfield, 2009) and are influenced by the depth of focus, which is defined as the range of vergences for which an object can be clearly focussed upon the retina. The depth of focus is influenced by pupil miosis as well as the increasing angular size of the object, with closer proximity (Wang and Cuiffreda, 2006). Dynamic retinoscopy is considered an objective technique, however, a subjective input from the examiner is still required to determine the maximum accommodation. Consequently, a greater variation in results have been reported between examiners when assessing the accommodative amplitude with dynamic retinoscopy (Rutstein et al., 1993), nevertheless, the reproducibility is greater than subjective methods (León et al., 2012).

Objective results obtained with autorefractors refer to the optical ability of the eye. Although the instruments do not depend on participant responses, the measurements are influenced by pupil size and instrument design (Win-Hall et al., 2007). For example, as mentioned in Section 2.3, the Grand Seiko WAM 5500 autorefractor is unable to obtain measurements when the pupil size is less than 2.0 mm. Furthermore, the design of binocular open view autorefractors allow viewing of real objects unlike closed-view autorefractors which consequently stimulate proximal accommodation or instrument myopia (Miwa, 1992).

Several studies have compared subjective and objective amplitude of accommodation results, and generally report an over-estimation with subjective techniques (Ostrin and Glasser, 2004; Nemeth et al., 2013; Adnan et al., 2014; Anderson and Stuebing, 2014). Therefore, measuring the accommodative response with objective techniques is more appropriate than using subjective techniques which are known to overestimate the true response (Ostrin and Glasser, 2004). Duane (1912) recorded the amplitude of accommodation with age and although the data was obtained using subjective methods, the study is often cited frequently in relation to the accommodative decline

with age. Recently, evaluation of the objective accommodation from childhood to adulthood has been reported and indicates the amplitude of accommodation increases from preschool to school age, followed by a gradual decrease in early adulthood and a consequent rapid decrease within the mid-forties and onwards (Anderson and Stuebing, 2014).

Values for amplitude of accommodation are not only dependent on the method or technique used but also various factors which influence the ability of the eye to accommodate. It is clear that perceived blur initiates the accommodative response (Cuiffreda, 1998), however, this is dependent upon the stimulus used. Owens (1980) reported optimal accommodative response for targets with a spatial frequency between 3-5 cycles/degree, rather than targets containing higher or lower spatial frequencies, suggesting sharp edges are not essential for the accurate stimulation of accommodation. Furthermore, monocular accommodation is dependent upon luminance contrast with no accommodative response occurring for isoluminant contours (Wolfe and Owens, 1981). Moreover, Fincham (1951) documented that longitudinal chromatic aberration is essential for stimulating accommodation, which is supported by findings that the accommodative response is greatest when the normal chromatic aberration of the eye is present when a target is illuminated by a white light (Aggarwala et al., 1995). In addition, Lovasik and colleagues (1987) reported accommodative responses are not dependent upon the angular subtense of letter targets. Consequently, controlling target sizes, luminance and contrast are essential for studies investigating accommodation.

Thus, a majority of accommodation and presbyopia research utilise Badal optometers which allow independent variation between target size and vergence and provide a linear relationship between the target position and vergence. Furthermore, the angular size of the object remains constant and is independent of the target position and vergence, if the eye is placed at the back focal point of the Badal lens (Badal, 1876 cited by Atchison et al., 1995). Recently, Aldaba and colleagues (2016) reported statistically significant differences between the accommodative responses when real targets were viewed in comparison to stimulating accommodation using a Badal optometer and an optical system (mean difference 0.58 D (SD 0.53)). The authors reported the position of targets in real space as well as the field of view contributed to the documented differences in accommodative responses. Therefore, inaccurate accommodation may occur if inappropriate depth cues are used, especially for high accommodative stimuli (Molins et al., 2016). However, apparent depth cues appear to

be important for stimulating accommodation under closed-loop conditions but are likely to be ineffective under open-view conditions where blur cues are more potent and reduce the effect of perceptually driven accommodative response (Busby and Cuiffreda, 2005).

A wide range of targets are often used to stimulate accommodation, including a single letter target (e.g. Anderson and Stuebing, 2014), a series of letters on a letter chart (e.g. Wold et al., 2003) or a star or Maltese cross (e.g. Aggarwala et al., 1995; Win-Hall et al., 2007; Day et al., 2009). Recently, Win-Hall and colleagues (2007) identified higher accommodative responses for a star stimulus target in comparison to letters of decreasing angular subtense. Although it is evident that stimulation of the accommodative system is dependent on various factors, it is unclear whether there are differences in accommodative responses for the most frequently used stimuli within accommodation studies. The aim of this study was to determine whether a Maltese cross or letters are the most appropriate fixation targets for use in accommodation studies, by assessing the objective accommodative response to each stimuli.

3.2. Methods

The study was conducted in accordance to the tenets of the Declaration of Helsinki. Written and verbal information was provided to participants before they provided written consent for their participation. A favourable opinion was provided by the Life and Health Sciences Ethics Committee at Aston University before the study commenced.

3.2.1. Sample size calculation

The number of participants required for the study was determined from a statistical power test based on a calculation using G*power (version 3.1.9.2; Universitat Kiel, Germany). In order to measure a medium effect size (f=0.25), based on a within-between factors ANOVA design and a required statistical power (1-β) of 95% with an error probability (α) of 0.05, at least 24 participants were required.

3.2.2. Inclusion criteria

Participants were invited to answer questions relating to their ocular and general health to ensure they had no ocular or health concerns or using any medication since amplitude is affected by various factors including recreational and prescribed drugs and general health conditions (Burns et al., 2014). Exclusion criteria included astigmatism which was greater than 1.00 DC, participants with an ocular injury or surgery that

affected the accommodative apparatus. Volunteers who were amblyopic or had a binocular vision condition were also excluded from the study.

Refractive error

The monocular refractive error was measured with the Grand Seiko WAM 5500 autorefractor from each eye (Sheppard and Davies, 2010), whilst the contralateral eye was occluded with an eye patch. Subjects viewed a Maltese cross target (average target luminance and Michelson contrast was 34.0 cd/m^2 and 82%, respectively) within a Badal lens system. The Badal lens system consisted of a +5.00 D full aperture lens (diameter 10 cm) with a Maltese cross target placed at the focal point of the lens (20 cm) allowing a measure of the refractive error at 0 D of accommodation. The constant angular subtense of the Maltese cross target was 6.8˚ horizontally and vertically. Participants were classified as emmetropic if the MSE was within the range -0.50 D to +0.75 D and myopic if MSE was less than -1.00 D.

Visual acuity

Visual acuity was determined using a logMAR visual acuity chart with the subject's habitual refractive error. Visual acuity was measured monocularly and binocularly to ensure a visual acuity of at least 0.00 logMAR.

3.2.3. Procedure

Prior to data collection, the refractive error of the myopic participants were corrected with a soft daily contact lens (*Nelfilcon A*; water content 69%) in order to ensure the participants were functionally emmetropic. The over-refraction with the contact lens in-situ was determined with the autorefractor and all participants were within +0.50 D.

The objective accommodation was determined with the Grand Seiko WAM 5500 autorefractor from the right eye only with the contralateral eye occluded. In order to ensure the maximum accommodative amplitude was determined for all participants, a Badal lens system with an auxiliary lens was used to increase the ocular vergence range (Atchison et al., 1995). The Badal lens system consisted of a full aperture convex lens (+5.00 D) which was placed 20 cm from the eye, and an external gantry that was fixed onto the autorefractor, as shown in Figure 3-1. The gantry had a full aperture convex (+5.00 D lens, 4 cm diameter) auxiliary lens which was placed 40 cm from the larger full aperture lens, to stimulate 0 D demand level. The auxiliary lens was moved to stimulate 1 to 8 D in 1 D steps accommodative demand levels.

The targets used for the study were a Maltese cross target (average Michelson contrast 82 %) and a high contrast (100%) ETDRS letter chart. Room illuminance was approximately 300 lux and the average target luminance was 50 cd/m^2. The targets were placed against a wall 2.5 m behind the autorefractor, and reflected in a mirror which was placed 5 m from the target (Figure 3-2). The constant angular subtense of the Maltese cross target was 0.86 ° horizontally and vertically.

To ensure the targets were aligned to the visual axis of the eye, participants were asked to report whether the targets were positioned in the centre of the infrared measurement circle which appears when the autorefractor is obtaining measurements. Minor adjustments to the target positions were made until the object was within the infrared ring and thus, any data obtained prior to alignment were discarded before analysis. The vertex distance for the autorefractor was set as 0 mm and the results displayed in 0.12 D steps.

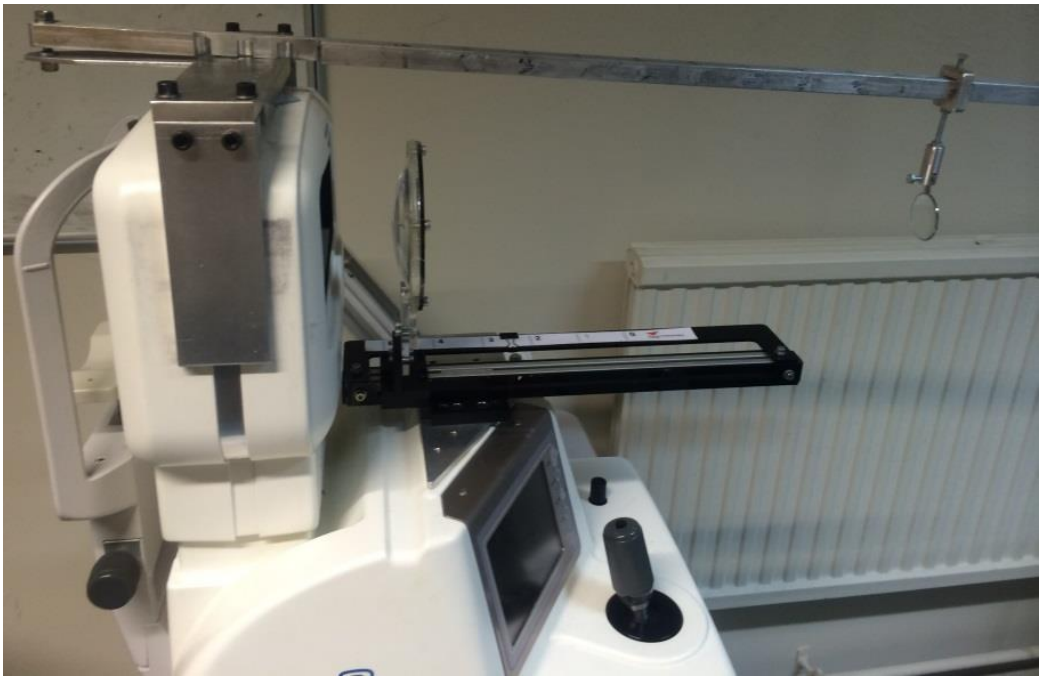

Figure 3-1. The Grand Seiko WAM 5500 autorefractor with a metal gantry and Badal lens system setup.

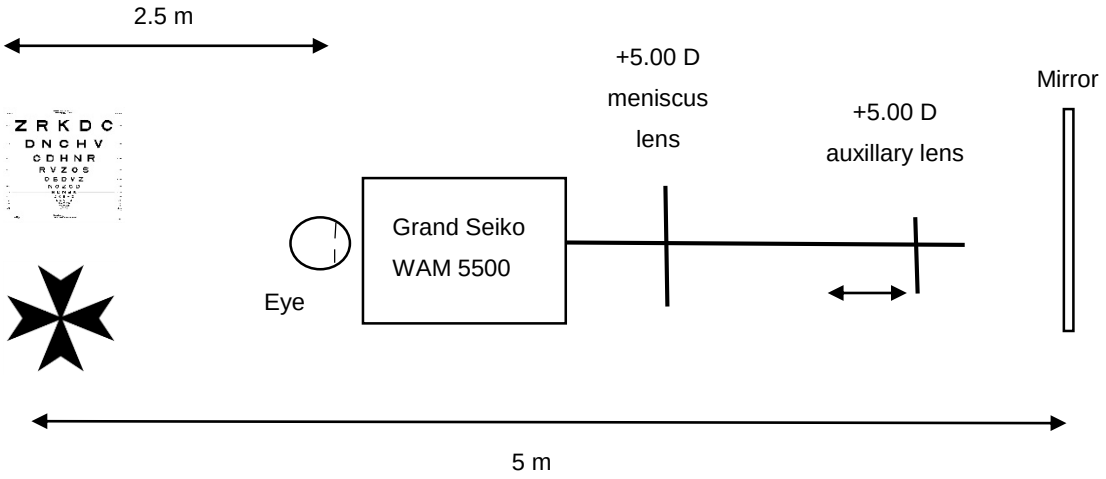

Figure 3-2. Schematic diagram showing the WAM 5500 placed 2.5 m away from the target. the target is placed 5 m away from the mirror. The +5.00 D meniscus lens is fixed in position and the auxillary lens is moved to stimulate accommodation.

The participants were instructed to view the lowest line of letters they could read clearly on the letter chart and to continue focussing on one of the letters on the line. For the Maltese cross, the participants were instructed to view the centre of the cross and to ensure it remained clear as the auxiliary lens was moved towards the eye to stimulate accommodation. The target and accommodative demand levels were randomised and the static objective accommodative response was recorded for each level.

Once data collection was completed, the contact lens was removed from the myopic participants and the eye health checked with the slit lamp.
The results were converted to the mean spherical equivalent and the accommodative response calculated for each accommodative demand level.

3.2.4. Statistical analysis

A Shapiro-Wilk test (SPSS Statistics 21; SPSS Inc., Illinois, USA) revealed normal distribution of the data for the accommodative response for all demand levels. Therefore, assumptions of normality and homogeneity of variance were met. A within-between repeated measures analysis of variance (ANOVA) was performed (Armstrong et al., 2011) to determine whether there was a difference in the accommodative response and target choice. To determine whether there was a significant relationship between refractive error and target choice, a within-between repeated measures ANOVA was performed. A within-between repeated measures ANOVA was also conducted to determine whether there was a significant effect of accommodative

responses to target choice within each refractive error group. There was non-sphericity for the accommodation term as well as the refractive error term, as assessed with Mauchley's test of sphericity ($p < 0.05$), therefore, Greenhouse Geiser results are reported. Post-hoc comparisons were determined using Bonferroni correction.

3.3. Results

Accommodative responses of inexperienced observers are often weaker than those who are practiced at accommodation tasks (Horwood and Riddell, 2010). Therefore, for this study, 40 participants were recruited to account for attrition of data due to poor accommodative responses. Consequently, data are presented for 35 participants due to the inability for 5 participants to accommodate efficiently to all stimulus levels presented in this study. The mean age and refractive error of the cohort was 20.2 (SD 1.9) years and -1.30 D (SD 1.96), respectively. There were 13 myopes (mean age 20.6 (SD 1.8) years, mean refractive error -3.26 D (SD 0.98)) and 22 emmetropes (mean age 19.9 (SE 1.41) years, mean refractive error -0.14 D (SD 0.50)).

Table 3-1 shows the mean accommodative response for all participants to the letter target and Maltese cross target and the mean difference between the accommodative responses to both stimuli. The accommodative response to the letter target was greater than the Maltese cross for all accommodative demand levels, except 7 D, which is also shown in Figure 3-3. There was a lag of accommodation for all accommodative demand levels.

Accommodative demand (D)	**Accommodative response for letter target (D)**	**Accommodative response for Maltese cross target (D)**	**Mean difference in accommodative response between letter and Maltese cross target (D)**
0	0.22 (SE 0.07)	0.22 (SE 0.07)	0
1	0.53 (SE 0.08)	0.38 (SE 0.11)	0.15 (SE 0.09)
2	1.26 (SE 0.09)	1.11 (SE 0.11)	0.15 (SE 0.08)
3	2.21 (SE 0.11)	2.03 (SE 0.05)	0.18 (SE 0.11)
4	3.23 (SE 0.09)	2.92 (SE 0.12)	0.31 (SE 0.11)
5	4.02 (SE 0.09)	3.82 (SE 0.10)	0.21 (SE 0.11)
6	4.91 (SE 0.09)	4.66 (SE 0.11)	0.25 (SE 0.09)
7	5.40 (SE 0.22)	5.45 (SE 0.12)	-0.05 (SE 0.24)
8	5.89 (SE 0.20)	5.72 (SE 0.19)	0.18 (SE 0.19)

Table 3-1. The mean accommodative response to a letter target and Maltese cross target, and the mean difference between the accommodative responses of both targets for 35 participants. The response is reported as the MSE with the standard error.

The accommodative response to the letter target was statistically significant for all stimulus demand levels ($F_{376.96}$, p<0.001) and post-hoc analysis revealed the mean differences were statistically significant between baseline and all accommodative stimuli levels (p<0.001). The pairwise comparisons were highly significant (p<0.001) between all accommodation levels, except, between the 6 D and 7 D demand levels (mean difference -0.48 D (SE 0.22, p=1.00) and between 7 D and 8 D demand levels (mean difference -0.50 (SE 0.24), p= 1.000).

There was also a highly significant effect of participant accommodative responses to the Maltese cross target for all accommodation demand levels ($F_{782.39}$, p= 0.000). Post-hoc analysis for the Maltese cross data revealed statistically significant differences between baseline accommodation level and all accommodative stimuli used in the study (p= 0.000). The pairwise comparisons were highly statistically significant between all accommodation levels (p=0.000) except between 7 D and 8 D demand levels (mean difference -0.27 (SE 0.098), p= 0.367). There was no significant difference between the average accommodative responses for the letter target or the Maltese cross ($F_{1.91}$, p= 0.172) or significant interaction between accommodation and target chosen ($F_{0.561}$, p= 0.640).

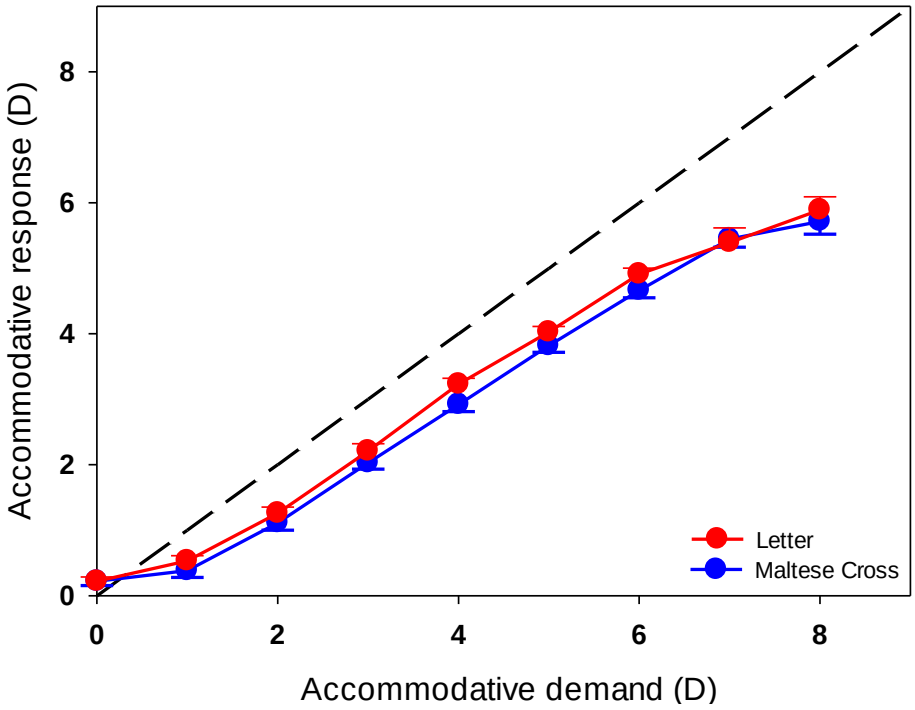

Figure 3-3. The accommodative response to a letter target and Maltese cross for each accommodative demand level. The linear black line represents the accommodative response which equals the accommodative demand.

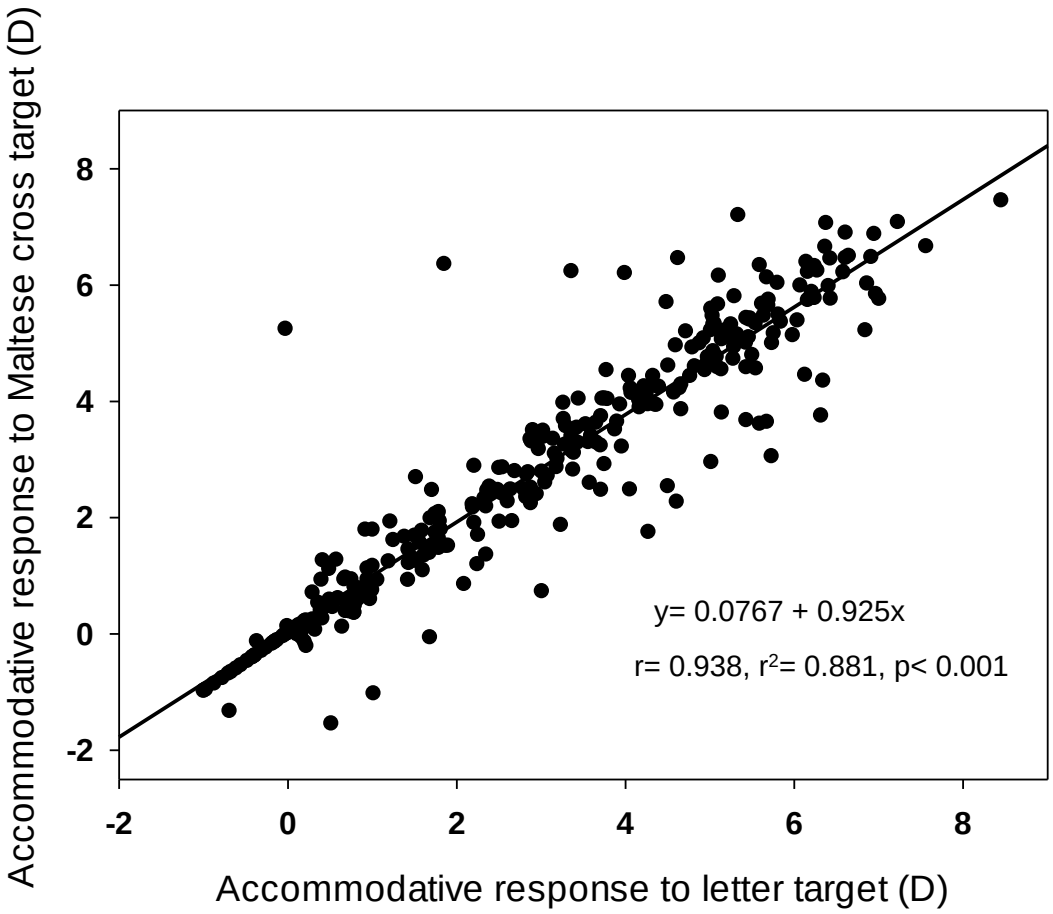

Figure 3-4. Comparison of the accommodative responses (D) between the letter target and Maltese cross target. The responses were significantly correlated ($p < 0.001$) with larger amplitudes measured using the letter target as indicated by the intercept.

Regression analysis was performed with the accommodative response to the letter target plotted on the *x*-axis and the accommodative response to the Maltese cross target plotted on the *y*-axis. There was a significant correlation between the accommodative responses for the letter target and Maltese cross target, as seen in Figure 3-4, with larger responses evident for the letter target as indicated by the intercept for the line of best fit.

Difference versus the mean analysis also indicates greater accommodative responses to the letter target in comparison to the Maltese cross (mean difference 0.076 D), as shown in Figure 3-5.

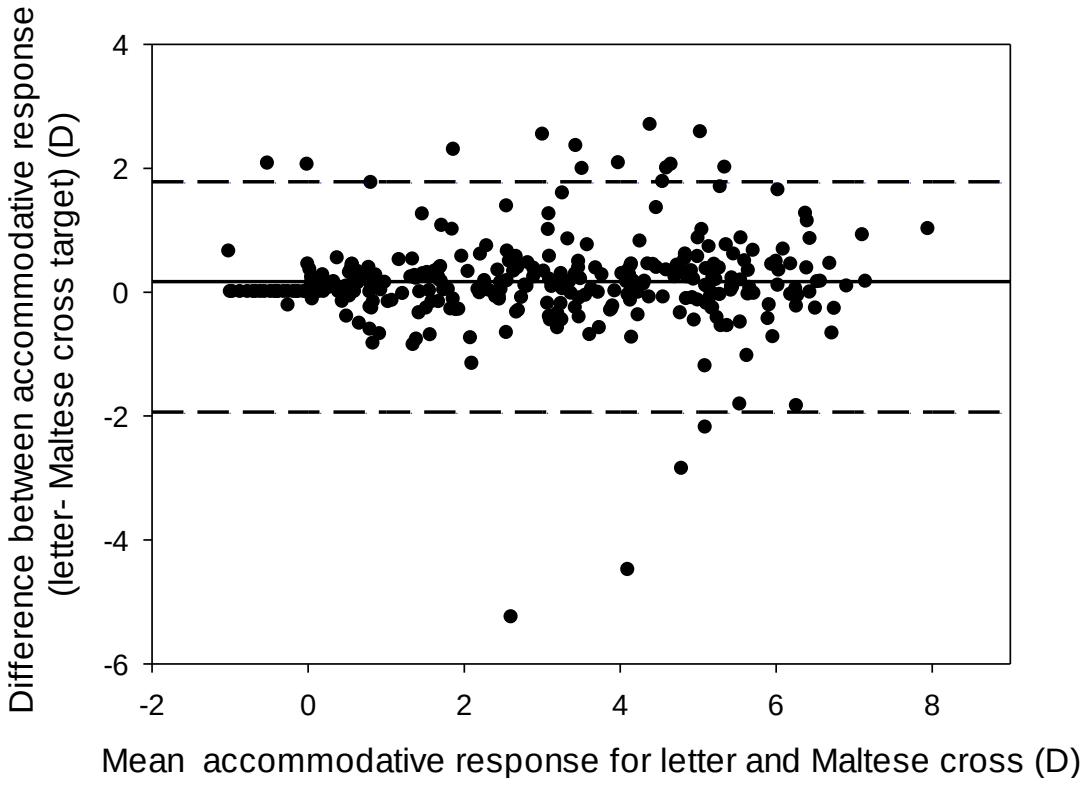

Figure 3-5. Comparison of the accommodative responses (D) between the letter target and Maltese cross target. Mean difference was 0.076 D, 95% confidence limit, -1.93 to + 1.78 D.

Accommodative demand (D)	Accommodative response for letter target (D)		Accommodative response for Maltese cross target (D)	
	Emmetropes	Myopes	Emmetropes	Myopes
0	0.17 (SE 0.09)	0.30 (SE 0.09)	0.17 (SE 0.09)	0.30 (SE 0.09)
1	0.57 (SE 0.07)	0.56 (SE 0.18)	0.48 (SE 0.11)	0.22 (SE 0.22)
2	1.28 (SE 0.10)	1.22 (SE 0.20)	1.23 (SE 0.11)	0.91 (SE 0.24)
3	2.31 (SE 0.15)	2.03 (SE 0.17)	2.08 (SE 0.09)	1.99 (SE 0.21)
4	3.18 (SE 0.08)	3.31 (SE 0.20)	2.98 (SE 0.11)	2.81 (SE 0.23)
5	4.00 (SE 0.09)	4.07 (SE 0.20)	3.92 (SE 0.10)	3.64 (SE 0.22)
6	4.93 (SE 0.09)	4.89 (SE 0.21)	4.76 (SE 0.11)	4.50 (SE 0.24)
7	5.18 (SE 0.33)	5.75 (SE 0.20)	5.58 (SE 0.13)	5.22 (SE 0.25)
8	5.96 (SE 0.21)	5.78 (SE 0.41)	5.86 (SE 0.24)	5.47 (SE 0.34)

Table 3-2. The mean accommodative response to each accommodative demand of the letter target and Maltese cross target for emmetropes (n= 22) and myopes (n= 13). The response is reported as the MSE with the standard error.

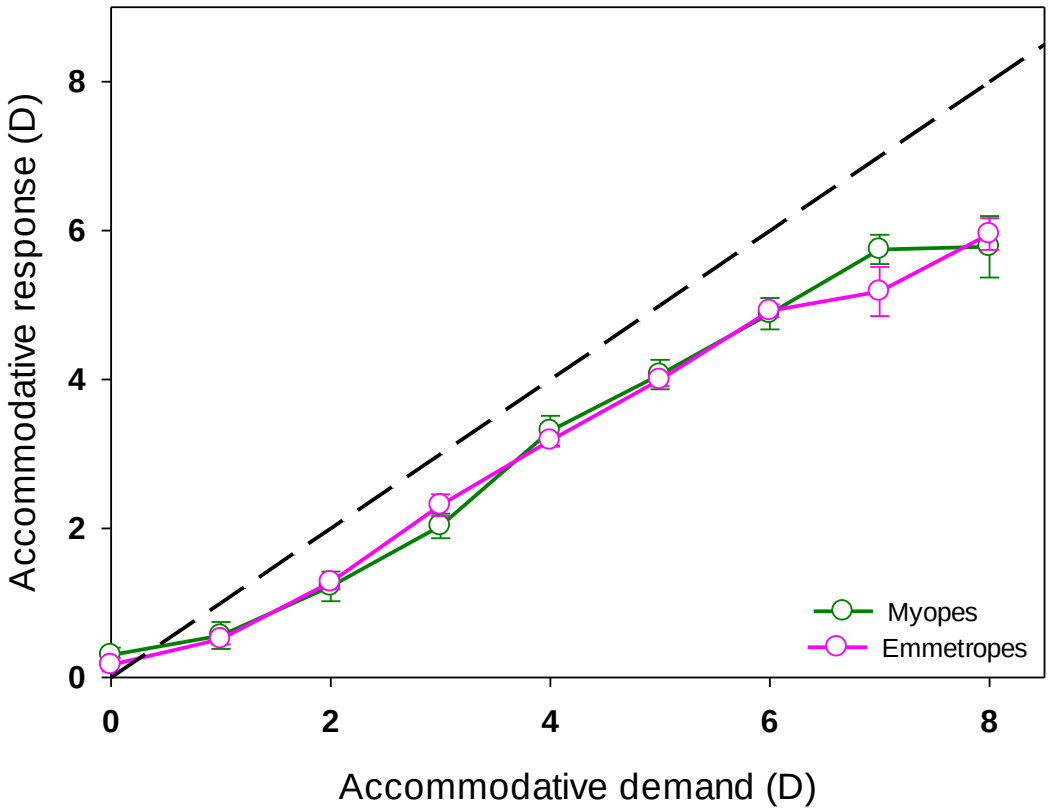

Figure 3-6. The mean accommodative response (D) for each dioptre of accommodative demand for the letter target between emmetropes (n= 22) and myopes (n= 13). The error bars represent ±1 SE of the mean.

Table 3-2 shows the accommodative response per dioptre of accommodative demand for emmetropes and myopes separately, for the letter and Maltese cross target used for this study. The accommodative response per dioptre of accommodation to the letter target for emmetropes and myopes, is shown in Figure 3-6, and it can be seen the accommodative responses were similar between emmetropes and myopes, for all demand levels. Myopes showed a weaker accommodative response to a 3 D stimulus, but had a greater response for a 7 D compared to the emmetropes. The responses to the Maltese cross target is depicted in Figure 3-7, and it can be seen that the accommodative responses were greater for the emmetropes than the myopes, for all demand levels. However, there was no significant interaction between refractive error and accommodative response to the letter target ($F_{1.061}$, p= 0.37) or Maltese cross target ($F_{0.270}$ p= 0.79). Furthermore, there was no significant differences between accommodative responses elicited by the emmetropes and myopes to the letter target ($F_{0.047}$, p= 0.83) or Maltese cross target ($F_{1.821}$, p= 0.19).

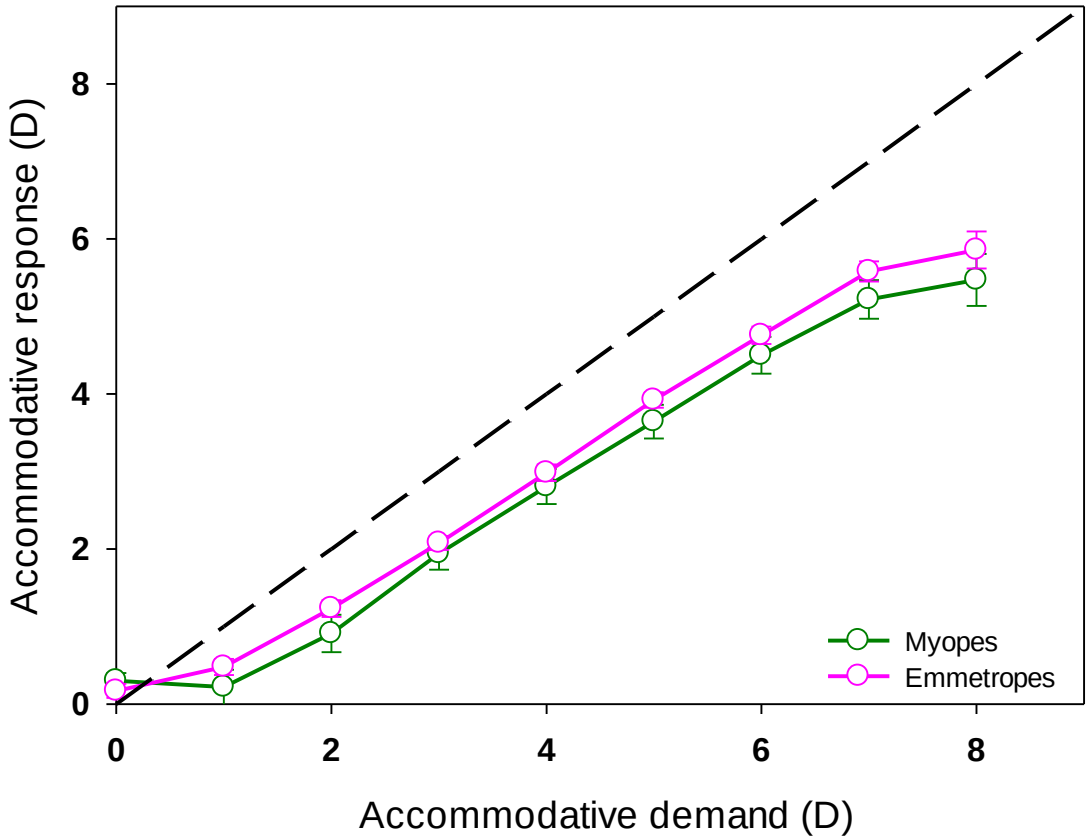

Figure 3-7. The mean accommodative response (D) for each dioptre of accommodative demand for the Maltese cross target between emmetropes (n= 22) and myopes (n= 13). The error bars represent ± 1 SE of the mean.

Within each refractive group, the use of a letter target or Maltese cross did not produce a significant difference to the accommodative response (emmetropes $F_{0.218}$, p= 0.64; myopes $F_{1.921}$, p= 0.18).

3.4. Discussion

The results from this study indicate that both the letter target and Maltese cross elicit significant accommodative responses for a range of accommodative demand levels, in young adults with a range of refractive errors. Furthermore, the results suggest the choice of target for stimulating the accommodative system may be more important when considering ametropia since a greater lag of accommodation was evident in myopic participants when the Maltese cross target was used, which suggests the resolution of a central 'dot' is not as accurate when compared to letter targets. Studies investigating the accommodative apparatus generally use a letter target or Maltese cross in order to produce defocus blur which stimulates the accommodative response

(Campbell and Westheimer, 1960). Eventhough the results for the current study indicate the accommodative response to a letter target is greater compared to the Maltese cross, overall, there were no significant differences for the accommodative response to each target nor between refractive error groups, suggesting either target can be used for accommodation studies.

For the current study an ETDRS chart consisting of letters of decreasing size was used since the type of letter used to stimulate accommodation does not appear to have a significant effect on the accommodative stimuli-response curves of emmetropes and myopes (Yeo et al., 2006; Radhakrishnan et al., 2015). Participants were instructed to resolve the smallest line of letters they could see clearly since smaller letters are known to improve the accuracy of the accommodative system (Tucker and Charman, 1975; Seidemann and Schaeffel, 2003) regardless of the ametropia (Schmid et al., 2005). In agreement with Schmid et al (2005) no significant differences were evident in the accommodative responses for the myopic and emmetropic participants in the current study, when a letter target was used. The likely increase in accuracy in accommodative response to a letter target is probably because identification of smaller letters requires discrimination of the strokes within the letter, whereas larger letters are resolved by their edges (Majaj et al., 2002). A similar explanation can also be related to the central dot of the Maltese cross target as it does not have fine detail that requires accurate resolution, and therefore probably explains the lower accommodative responses measured in comparison to the letter target. Nevertheless, the cognitive effect of using letters compared to the Maltese cross may also explain these differences in accommodative response.

The accommodative stimulus-response curves, shown in this study, follow the pattern described by Cuiffreda and Kenyon (1983), where an initial non-linear portion of the curve indicates the tonic accommodation level; this portion is shown between 0 D and 1 D accommodative demand levels and represents the accommodative lead. Consequently, a linear zone representing a proportional increase of the accommodative response to the accommodative demand level, is shown between 2 D and 6 D accommodative demand levels. The accommodative response then increases for the 7 D and 8 D demand levels, however, the responses are not linear with the increase in the accommodative demand level. Overall, inspection of the stimulus-response curves for the whole cohort indicates the maximum objective amplitude of accommodation occurred to a 7 D accommodative demand level.

There are various methods for altering the vergence of the target to stimulate accommodation, including moving the target distance or using minus lenses to stimulate blur. Minus lenses produce a minified image of the object viewed and there is conflicting evidence about the use of concave lenses for stimulating accommodation, especially since some individuals are unable to accommodate accurately to optical blur (Abbott et al., 1998). Some reports suggest minus lenses provide reliable measurements of the accommodative results in younger participants (Ostrin and Glasser, 2004; Wold et al., 2003), whereas, a greater error in accommodative response (i.e. accommodative leads at low demands and greater lags at higher demand levels) has also been reported (Yeo et al., 2006). Nevertheless, the average amplitude of accommodation for the cohort analysed for this study was to the letter target for a 7 D demand level, where the mean accommodative response was 5.40 D (SE 0.22) which is comparable to the findings by Anderson and Stuebing (2014), who measured objective accommodation using a similar protocol as the present study, and reported a maximum amplitude of accommodation of 5.98 (SD 1.36) D for their cohort between 21 and 25 years of age. Moreover, Win-Hall and colleagues (2007) documented a maximum accommodative amplitude of 5.67 (SE 0.15) D using minus lenses for their cohort with a slightly higher mean age range (25.6 ± 2.26 years) and refractive error range (between -5.75 D to +2.75 D), than analysed for this study. In contrast, Wold et al (2003) used a Hartinger optometer and reported an amplitude of accommodation of 7.00 ± 0.91 D for their young cohort (age range 23 to 28 years and a 36 year old participant). Differences in methodology can explain the variances in the stimulus-response curves between emmetropes and myopes since no significant differences have been reported between the accommodation error of emmetropes and myopes when the target distance is altered (Yeo et al., 2006), although using negative lenses either produces a similar accommodative accuracy between emmetropes and myopes (Radhakrishnan et al., 2015), or a lesser accommodative accuracy in myopes than emmetropes (Yeo et al., 2006).

Indeed, it is evident from the literature there are various factors which affect the accommodative response including blur cues, chromatic aberration and an alteration to target size (Kruger and Pola, 1986) with greater target sizes over-estimating the amplitude of accommodation (Rosenfield and Cohen, 1995). Furthermore, a reduction of the contrast target below the contrast threshold can reduce the accommodative response to the tonic level (Rosenfield et al., 1994), although, a recent study indicates a reduction in contrast between 90% and 60% does not have significant effect on the accommodation response curves for emmetropes and myopes (Schmid et al., 2005).

Therefore, a Badal optometer was used in the current study to control for these factors. Although recent studies indicate depth cues should be used with Badal optometers when stimulating the accommodation system, especially for higher accommodative demand levels (Aldaba et al., 2016), the lack of depth cues used with the Badal optometer within the present study did not produce large accommodative lags, and rather the amplitude was similar to previous studies (Win-Hall et al., 2007; Anderson and Stuebing, 2014), suggesting the accommodative responses of emmetropes and corrected myopes are similar for real targets whether size and disparity cues are present (Seidel et al., 2005).

In addition, accommodation was stimulated monocularly within the present study, therefore, reducing the effect of convergence accommodation. Although, similar accommodative lags have been reported whether a target is viewed under monocular (lag of 0.18 D per dioptre of accommodation) or binocular conditions (lag of 0.17 D per dioptre of accommodation), the lags become greater under monocular conditions when larger letters are used (Seidemann and Schaeffel, 2003). Lags of accommodation have been reported by many researchers. McBrien and Millodot (1986) identified a greater lag of accommodation in myopes compared to emmetropes, when a reading print target was used. The myopes were divided into early onset myopes (myopia development before 13 years of age) and late-onset myopes (myopia development at 15 years or later), however, the mean refractive error for each group was not reported. A larger lag of accommodation was noted for the higher stimulus levels between the late-onset myopes and the hypermetropic cohort (a difference of 0.45 D lag), whereas, a difference of 0.29 D in accommodative lag to a 5 D stimulus was evident between the late onset myopes and emmetropes. These reported differences are greater than identified in the current study where a mean difference of 0.07 D in accommodative lag was found between emmetropes and myopes for a 5 D letter target. However, the myopes were not classified by the onset of their refractive error in the current study. The differences in the lag of accommodation between the current study and McBrien and Millodot (1986) may be due to the method of stimulating vergence since the authors varied the distance of the target, therefore incorporating proximal cues in their results, although the angular subtense remained constant.

Pupil size decreases as accommodation is stimulated, thus increasing the depth of focus of the eye. However, Individuals with larger pupil sizes during relaxed accommodation may exhibit less pupil miosis during accommodation resulting in greater spherical aberrations and a consequent lag of accommodation compared to

individuals with smaller pupils. Lags of accommodation have often been reported as greater in myopic individuals, therefore, the relationship between ametropia and pupil size and accommodation is of interest. Although it has been suggested that myopes have larger pupils (Hirsch and Weymouth, 1949), most studies seem to support the hypothesis that pupil size is not dependent on refractive error (Jones, 1990; Winn et al., 1994; Charman and Radhakrishnan, 2009), and therefore, unlikely to influence accommodative responses (Charman and Radhakrishan, 2009). McBrien and Millodot (1986) suggested the greater accommodative lag evident in myopic individuals was possibly due to the greater parasympathetic innervation to the ciliary muscle which would render the individual myopic. However, a combination of environmental and genetic factors contribute to myopia development and although the greater lags have been confirmed by several studies (Millodot, 2015), the inaccurate accommodative response often reported in myopes is likely a possible consequence of myopia development (Mutti et al., 2006). Indeed, pupil miosis occurs during accommodation, thus, increasing the depth of focus of the eye. Although the findings in this study revealed greater lags of accommodation for the higher demand levels, the greater lag is not likely to result from miosis and the consequent increased depth of focus (Seidemann and Scaheffel, 2003). Moreover, the greater difference in the lag of accommodation between the emmetropes and myopes was only evident when the Maltese cross target was used, indicating the target choice rather than refractive error produced the differences in lag. Nevertheless, it would have been of interest to investigate whether there was significant pupil miosis during accommodation between the refractive groups to determine whether pupil size confounded the results.

Although the findings from this study suggest that stimuli consisting of letter targets or a Maltese cross can provide accurate accommodative responses, the data were only obtained from young observers. However, presbyopes are known to produce lower accommodative responses when the accommodative system is stimulated with minus lenses in comparison to pharmacological stimulation with pilocarpine (Ostrin and Glasser, 2004). Therefore, target choice may not be a significant factor for presbyopes. Nevertheless, identifying whether accommodative responses differ when different targets are used should be investigated in presbyopes, especially since significant research relating to the performance of accommodating intraocular lenses is assessed using non-pharmacological techniques. Furthermore, the present study did not confirm the refractive error with cycloplegia, however, all participants had an eye examination within 12 months of participating in the study, within the optometry clinics at the university, where significant latent hypermetropia would have been identified.

In conclusion, accurate accommodative responses are possible to a high contrast letter target or Maltese cross, for a young cohort who are experienced to accommodation tasks. Nevertheless, the choice of target may be important for accommodation studies investigating the differences in the accommodative responses between refractive error groups, for which a letter target should be considered.

3.5. Summary

- The aim of the study was to determine whether a significant difference in accommodative response was evident to a Maltese cross target and letter targets. Furthermore, whether differences in the accommodative response was evident between emmetropes and myopes was also investigated for each of the targets
- Objective accommodative responses were evaluated from a pre-presbyopic cohort
- The main findings were:
    - The accommodative response to a letter target is greater than a Maltese cross, however, there were no significant differences in the responses between the targets
    - There were no significant differences in the accommodative response between emmetropes or myopes for the letter or Maltese cross target
- The findings suggest both a Maltese cross and letter target can elicit accurate accommodative responses in young participants, and are suitable target choices for accommodation research.

Chapter 4. Can topical anti-muscarinic agents be used to differentially identify ciliary muscle fibre groups?

4.1. Introduction

The non-selective muscarinic antagonists, tropicamide and cyclopentolate, are essential agents for use in clinical practice due to their cycloplegic and mydriatic properties, which aid the examination of refractive error and ocular health. They are the most frequently used anti-muscarinic agents as they have a rapid onset for mydriasis and cycloplegia, as well as a fast recovery from these effects. Various studies have documented statistically significant differences between non-cycloplegic and cycloplegic refractions (Egashira et al., 1993; Twelker et al., 2001; Mimouni et al., 2016), indicating the importance of cycloplegic refractions as the gold-standard for epidemiological studies in children and adults up to 50 years of age (Morgan et al., 2015). Nevertheless, the depth of cycloplegia and mydriasis is dependent upon various factors such as iris colour (Manny et al., 1993), corneal permeability (Siu et al., 1999) as well as the concentration of the agent used (Lovasik, 1986).

There are many reports suggesting inadequate cycloplegia in individuals with dark irides, especially in early studies, where results were obtained using subjective methods (e.g. Milder and Riffenburgh, 1953; Dillon et al., 1977; Lovasik, 1986). In contrast, measuring residual accommodation with objective methods indicates an insignificant effect of iris colour on the measurement of refractive error, accommodation or alteration to ocular components (Mutti et al., 1994). The depth of cycloplegia is important for clinical and research practice since it is vital an adequate cycloplegic effect occurs before the assessment of refractive error. Manny and colleagues (1993) investigated residual accommodation after instillation of cyclopentolate 1%, and their results suggested minimal residual accommodation in participants with lighter irides. However, the time course for cycloplegia was dependent on iris colour with a longer duration (30-40 minutes) documented in individuals with darker irides (Manny et al., 1993). Furthermore, the authors reported variability for the time course of maximum cycloplegia with 40% of participants reaching maximum cycloplegia within 15 minutes post-instillation and 22% of their participants not showing a maximum cycloplegic effect before 45 minutes. Retention of residual accommodation after cycloplegia is probably related to ethnicity as greater amplitudes of accommodation have been reported in Hispanic participants (Manny et al., 2001). Although a greater dose or concentration of the anti-muscarinic agent increases the degree of mydriasis and cycloplegia (Barbee and Smith, 1957), the risk of an adverse reactions also increases (Jones et al., 1991).

The use of a topical anaesthetic prior to the instillation of tropicamide appears to *prolong* its cycloplegic effect (Mordi et al., 1986a), whereas, a faster onset of cycloplegia occurs when used prior to cyclopentolate (Lovasik, 1986).

There is conflicting evidence within the literature relating to the most appropriate agent for cycloplegic refractions. For example, a less effective cyloplegia occurs with the use of tropicamide (Milder, 1961; Mordi et al., 1986a; Lovasik, 1986; Mutti et al., 1994) such that the depth of cycloplegia is approximately 60-70% in comparison to atropine (Milder, 1961). Yet, comparison of the latent hyperopia elicited between tropicamide and cyclopentolate within healthy children (mean age 8.8 ± 2.0 years) indicates invariant differences (tropicamide: +0.77 ± 0.45 D, cyclopentolate: +0.91 ± 0.57 D) and a clinically insignificant latent hyperopic bias with cyclopentolate, suggesting both agents are suitable for cycloplegic refractions in children (Egashira et al., 1993). Twelker and colleagues (2001) have also reported insignificant differences of the cycloplegic results obtained using two drops of 1% tropicamide in comparison to 1% cyclopentolate in children with a mean age 5.7 ± 0.7 years.

Considering both tropicamide and cyclopentolate are competitive antagonists to acetylcholine and compete for muscarinic receptors within the iris and ciliary body, the documented differences for cycloplegia indicate the agents may alter the morphology of these anatomical structures differently. Mutti and colleagues (1994) determined the effect of 1% tropicamide and 1% cyclopentolate on the ocular components of 20 hyperopic children (age range 6-12 years). The authors reported the residual amplitude of accommodation, measured objectively, was greater with the use of tropicamide than cyclopentolate. Furthermore, biometric measurements, obtained with A-scan ultrasonography, revealed statistically significant differences between both agents for anterior chamber depth (mean difference +0.07 ± 0.10 mm), crystalline lens thickness (mean difference -0.03 ± 0.05 mm) and crystalline lens power (mean difference -0.65 ± 0.69 D). Similarly, Drexler et al (1997) also documented changes to ocular biometry after instillation of 1% tropicamide and 1% cyclopentolate for two myopes (MSE -1.75 D and -4.00 D) and one emmetrope (MSE -0.375 D). Although the myopic refractive error was uncorrected during data acquisition and the age range of the participants was unspecified, the authors reported no significant differences to the anterior chamber depth (difference of 61. 2 µm) or lens thinning (difference of - 51.6 µm) between both agents. Comparison of the differences between the lens thinning data reported by Drexler et al (1997) and Mutti et al (1994) is possibly due to the different methodology employed for ocular biometry measurements, as well as the sample size analysed.

Significant differences have also been reported between tropicamide and cyclopentolate for measurements of refractive error, lens thickness (difference 0.04 mm) and anterior chamber depth (difference 0.59 mm) as well as the posterior radii of curvature (difference 0.16 mm) in young children (mean age 6.36 (SD 0.8) years), whereas for older children (mean age 16.74 (SD 0.7) years), significant differences are only evident for lens thickness (difference 0.04 mm) and the anterior radius of curvature (difference 0.45 mm; Owens et al., 1998). Although the results suggest the anti-muscarinic agents have a greater effect on a younger age group, the differences reported by the authors may also have occurred due to the different dose of agents used in the study: two drops of 1% tropicamide were instilled after administration of proparacaine in the young children, whereas, only one drop of 1% cyclopentolate was instilled in older children.

Tropicamide and cyclopentolate increase the anterior chamber depth (Sheng et al., 2004; Arici et al., 2014; Sander et al., 2014), which is most likely to occur from the reduction in lens thickness. Interestingly, the increased depth has also been reported with the use of tropicamide in pseudophakic eyes (Kriechbaum et al., 2003), suggesting anti-muscarinic agents produce similar effects in presbyopes and pre-presbyopes. However, the effect of anti-muscarinic agents on the axial length is equivocal; some studies suggest tropicamide and cyclopentolate do not alter the axial length significantly, as measured with the IOLMaster (Sheng et al., 2004; Arici et al., 2014; Adler et al., 2015), whereas measurements obtained with the LenStar indicate a reduction to the length after the instillation of homatrapine (Sander et al., 2014). However, the conflicting data are probably due to the type of anti-muscarinic agent used as homatropine is known to produce a greater cycloplegic effect.

The choroid extends anteriorly to the ciliary body (Nickla and Wallman, 2010) and there is evidence to suggest anti-muscarinic agents may have an effect on choroidal thickness, with a significant decrease in subfoveal choroidal thickness documented after the use of *tropicamide* (Kara et al., 2014), whereas a thickening to the sub-foveal and para-foveal choroid has been documented with *homatropine* (Sander et al., 2014). In contrast, Kim et al (2012) used Mydria-P, a combination of tropicamide and phenylephrine (tropicamide 5 mg/ml, phenylephrine 5mg/ml), in 59 participants, whose age range was not specified. The results indicated no significant differences in the choroid before and after drug instillation.

Overall, it is evident that refractive error and intraocular biometry are altered differently depending on the anti-muscarinic agent used. Although ocular biometry measurements have been reported in children and adults, the findings are generally limited to the anterior chamber depth, lens thickness and axial length. However, the effects of anti-muscarinic agents on the contraction and mobility of the ciliary muscle have not been studied *in-vivo*, even though the ciliary muscle contraction initiates the accommodative response and has an abundance of muscarinic receptors which are the site of action for these agents.

Consequently, the aims of the study were to identify the morphological changes that occur to the ciliary muscle with anti-muscarinic agents, and to define regions within the ciliary muscle that are involved in accommodation. Ocular biometry was also investigated with the agents. Residual accommodation was also assessed for a sub-group of participants to determine the depth of cycloplegia with each anti-muscarinic agent.

4.2. Methods

The study was conducted in accordance to the tenets of the Declaration of Helsinki. Written and verbal information was provided to participants before they provided written consent for their participation. A favourable opinion was provided by Aston University Research Ethics Committee before the study commenced.

4.2.1. Sample size

The number of participants required for this study was calculated from a statistical power test using G*power (version 3.1.9.2; Universitat Kiel, Germany). In order to measure a medium effect size (f=0.25), based on a within subject ANOVA design and a desired statistical power (1-β) of 90% with an error probability (α) of 0.05, at least 26 participants were required.

4.2.2. Participants

Volunteers were recruited from the optometry undergraduate cohort through email announcements.

Inclusion criteria

Participants were invited to answer questions relating to their refractive history, ocular history and general health. Healthy participants were recruited with no history of ocular injury, surgery or pathology and no general health concerns. Exclusion criteria included

participants who had an ocular or systemic disease, participants who had an ocular injury, trauma or surgery which affected the cornea, or accommodative apparatus. Volunteers who were amblyopic or had a binocular vision condition were also excluded from the study. Due to the greater lag of accommodation documented for myopic individuals (e.g. Abbott et al., 1998; Mutti et al., 2006) and the lower amplitude of accommodation evident in corrected hypermetropes (Maheswari et al., 2011), only participants with emmetropic refractive errors were recruited for the study.

Visual acuity

The procedure has been described in Chapter 3 section 3.2.2.

Refractive error

The procedure for determining the refractive error has been described in Chapter 3 section 3.2.2. Participants were classified as emmetropic if the MSE was within the range -0.50 to +0.75 DS.

4.2.3. Procedure

Accommodative response determined with Grand Seiko *WAM 5500*

The procedure for determining the accommodative response was replicated from Chapter 3, section 3.2.3. The stimulus used for this study was the ETDRS letter chart which was placed 2.5 metres behind the participant and 5 metres away from the mirror.

Visante AS-OCT

Ciliary muscle images were acquired with the Visante AS-OCT (Carl Zeiss, Meditec) from the right eye only with the left eye occluded. All images were obtained from the temporal ciliary muscle due to its greater contractility during accommodation (Sheppard and Davies, 2010a).

To obtain images from the right eye, the participant placed their chin on the left side of the chin rest and forehead against the forehead rest, whilst the contralateral eye was occluded with a patch. Firstly, the participant viewed the internal fixation star of the instrument, whilst the chin rest and forehead rest were adjusted by the examiner who was guided by the real-time video AS-OCT video screen, until a high resolution corneal profile was visible (shown in Figure 4-1). An image of the cornea with a bright central reflex through the optic axis was captured. The bright reflex represents the vertex of the cornea, where the spatial distortion is equal to zero and signifies the optic axis of

the instrument. All images were captured in high-corneal mode which provided an axial resolution of 8 µm, a scanning depth of 3 mm and scanning area of 10 mm.

Figure 4-1. The image shows the cornea of the right eye imaged in high resolution corneal mode prior to imaging the ciliary muscle.

To image the full length of the temporal ciliary muscle, the participant viewed a 5 x 5 grid of high contrast (90%) letters of 0.8 logMAR (Figure 4-2) within a bespoke Badal lens system consisting of a +10 D lens. Letters were chosen to ensure consistency of the targets throughout the study. The rig was placed external to the AS-OCT (on the left side of the instrument) at a 40˚ angle which represents the minimum horizontal eye movement required to ensure the participant can view the letter target without obstruction from the instrument itself. The external gaze is necessary in order for the instrument to scan through the sclera, which reduces the optical distortions of the light beam since it penetrates through a flatter plane in comparison to the cornea (Laughton et al., 2015). A further advantage for imaging through the sclera is light waves do not have to pass through iris pigmentation, which obstructs the penetration of light, thus preventing the visualisation of the ciliary muscle. The participants were instructed to focus on a single letter at all times and to ensure it remained clear. Participants were instructed to keep their gaze as still as possible, whilst a real-time image of the ciliary

muscle was viewed on the screen of the AS-OCT. Considering the participant was aligned in primary position, minimal vertical movements were required to ensure the ciliary muscle was visible on adduction. In order to image the temporal ciliary muscle, the scanning plane was adjusted to 0˚ for horizontal ciliary muscle measurements and three images were acquired. The Badal lens system allowed data acquisition for relaxed accommodation and for the maximum accommodative response.

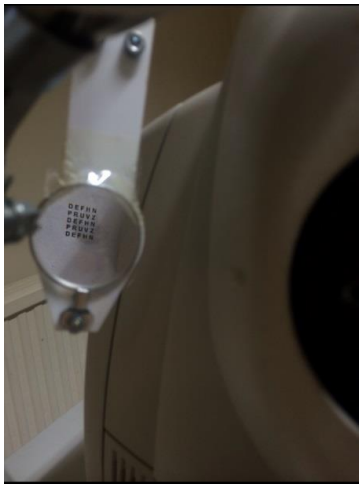

Figure 4-2. The 5 x 5 letter grid used as a target for the study.

LenStar LS900

Axial length, corneal thickness, anterior chamber depth and crystalline lens thickness were acquired with the LenStar LS900 biometer (Figure 4-3) from the right eye only with the left eye occluded. A Badal lens system was used consisting of a +10 D achromatic doublet lens and a 5 x 5 letter grid of the same description used during ciliary muscle acquisition. The letter grid was retro-illuminated and viewed through an 8% reflection pellicle beamsplitter that was placed at a 45° angle, allowing simultaneous viewing of the letter target and the light beam from the LenStar. Three measurements were obtained and the mean result was calculated for each parameter.

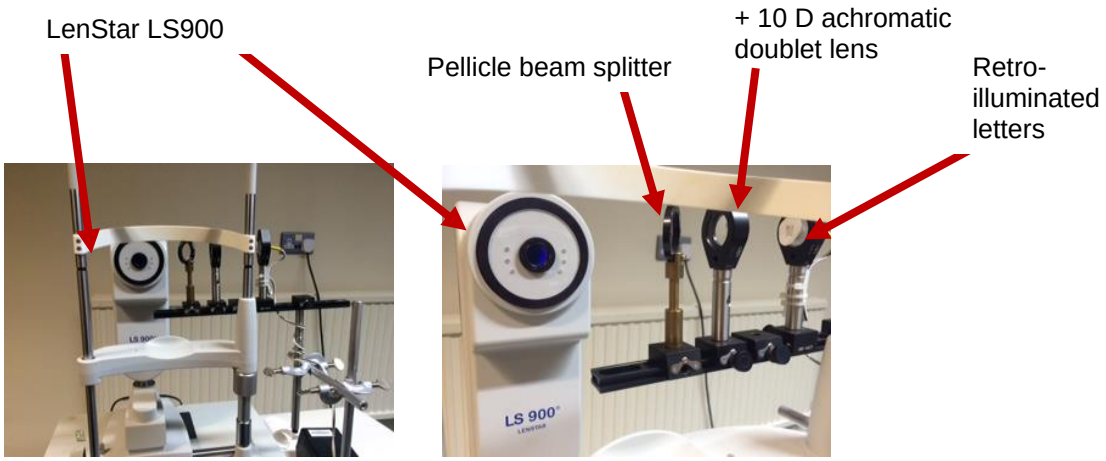

Figure 4-3. The LenStar LS900 and rig used for biometry data.

Health examination prior to drug instillation

The anterior eye was examined with a slit lamp and the anterior chamber angle was graded to ensure the participant was not at risk of angle closure. Intraocular pressure was determined with the i-care tonometer (Davies et al., 2006). Furthermore, iris colour was determined and classified using the classification system defined by Seddon et al (1990).

Instillation of anti-muscarinic agent

After baseline data for refractive error, accommodative response, ocular biometry and ciliary muscle were obtained, one drop of 0.5 % proxymetacaine (*Minims* preparation) was instilled into the lower fornix of the right eye followed by 1 drop of 1% tropicamide or 1% cyclopentolate hydrochloride (*Minims* preparations) which was randomly selected. Participants were instructed to close their eyes and occlude the punctum for 30 seconds to reduce systemic absorption of the agent.

Subsequently, data was acquired every 10 minutes post-instillation of the anti-muscarinic agent. Ciliary muscle images were obtained during relaxed accommodation and for the maximum accommodative amplitude at each time interval. Due to the variability in the literature relating to the time course of the anti-muscarinic agents to achieve maximum cycloplegia and reports of a delayed onset of mydriasis in comparison to cycloplegia, the end point for this study was classified when the accommodative response was returning with tropicamide and when three consecutive accommodative responses were the same with cyclopentolate. Ocular biometry was obtained once the end point for the study was reached.

The participants attended for a second visit between 4-8 days after the first visit. Proxymetacaine (0.5%) was instilled followed by the anti-muscarinic agent which was not administered on the first visit. The same procedure for administration of the agent and data acquisition were followed as the first visit.

At the end of each visit, intraocular pressure was determined with the i-care tonometer and a leaflet provided to the patients regarding the instillation of the drug and advice relating to adverse effects.

4.2.4. Statistical analysis

A Shapiro-Wilk test (SPSS Statistics 21; SPSS Inc., Illinois, USA) revealed normal distribution of the parameters analysed for the study. Therefore, assumptions of normality and homogeneity of variance were met. A repeated measures analysis of variance (ANOVA) was performed to determine the effect of the anti-muscarinic drug on the ciliary muscle parameters and the amplitude of accommodation. A paired t-test was conducted to determine the effect of cyclopentolate on ocular biometry. Greenhouse Geisser results are reported and post-hoc comparisons were determined using Bonferroni correction (Armstrong et al., 2011).

4.3. Results

4.3.1. Ciliary muscle results

The ciliary muscle images were analysed as described in Chapter 2. Due to the variability in the time course of each agent to have its maximum cycloplegic effect, thirty six participants were recruited to account for attrition. The maximum effect of tropicamide was more variable than cyclopentolate. The end point for tropicamide was reached at 30 minutes for two participants and 50 minutes for three participants, therefore these data were excluded as the majority of participants had a maximum cycloplegic effect at 40 minutes. Due to the failure of the AS-OCT instrument during data collection, one participant's data was lost. Therefore data is presented up to 40 minutes for tropicamide and 50 minutes for cyclopentolate. The cohort consisted of thirty emmetropic participants (MSE -0.04 D (SD 0.40)) and mean age 19.8 (SD 1.5) years. Twenty six participants had a dark brown iris (grade 5) and four participants had a green or light brown iris (grade 4). Due to the unequal distribution of iris colour within the cohort, the effect of iris colour and cycloplegia was not analysed.

The amplitude of accommodation at baseline varied between the participants; twenty six participants were able to accommodate up to the 6 D demand level, whereas four

participants were able to accommodate up to the 7 D demand level. Therefore, during ciliary muscle acquisition, each individual's maximum amplitude of accommodation was stimulated, in order to determine the maximum mobility and contractility of the ciliary muscle. The results were pooled in order to determine the mean for the cohort. Baseline data for the ciliary muscle at relaxed accommodation and during maximum accommodation was obtained at the first visit, and the mean results are shown in Table 4-1 and Figure 4-4, 4-5, 4-6 and 4-7. The physiological changes to the ciliary muscle during accommodation indicated a thickening at CMT1 (mean 6.1 µm (SE 7.0)), CM25 (mean 22.2 µm (SE 9.7)), CM50 (mean 12.5 µm (SE 11.5)), CM75 (8.0 µm (SE 8.0)) and CMMax (mean 8.9 µm (SE 5.2)). Furthermore, there was a shortening of the ciliary muscle length (CMLengthArc, mean reduction 520.3 µm (SE 140.5)) and there was a reduction in the distance between the scleral spur and the inner apex (SS-IA, mean 14.0 µm (SE 13.7)), indicating a centripetal movement of the muscle. Moreover, there was a reduction to the anterior length (SS-CM, mean reduction 25.2 µm (SE 14.9)). Paired t-tests were conducted and revealed a significant effect of accommodation on the ciliary muscle thickness at CMT2 ($F_{3.035}$, p= 0.005), CMT3 ($F_{5.202}$, p= 0.000), CM25 ($F_{-2.274}$, p= 0.031) and a contractile shortening of the ciliary muscle length arc ($F_{3.703}$, p= 0.001).

Ciliary muscle parameter	**Average measurement (µm) during relaxed accommodation (0 D stimulus)**	**Average measurement (µm) during maximum accommodation**
CMT1	618.5 (SE 5.1)	624.6 (SE 6.4)
CMT2	418.6 (SE 6.7)	399.3 (SE 8.1)
CMT3	256.2 (SE 8.0)	224.3 (SE 9.1)
CM25	523.0 (SE 8.2)	545.2 (SE11.6)
CM50	273.9 (SE 10.1)	285.4 (SE 13.5)
CM75	111.4 (SE 6.3)	119.5 (SE 8.9)
CMMAX	601.4 (SE 4.1)	610.3 (SE 5.5)
SS-IA	1178.6 (SE 11.5)	1164.6 (SE 12.5)
SS-CM	1036.0 (SE 13.3)	1010.8 (SE 13.7)
CMLength Arc	5884.6 (SE 149.6)	5364.3 (SE 155.2)

Table 4-1. The mean (± 1 SEM) measurements for the ciliary muscle parameters during relaxed accommodation and at the amplitude of accommodation.

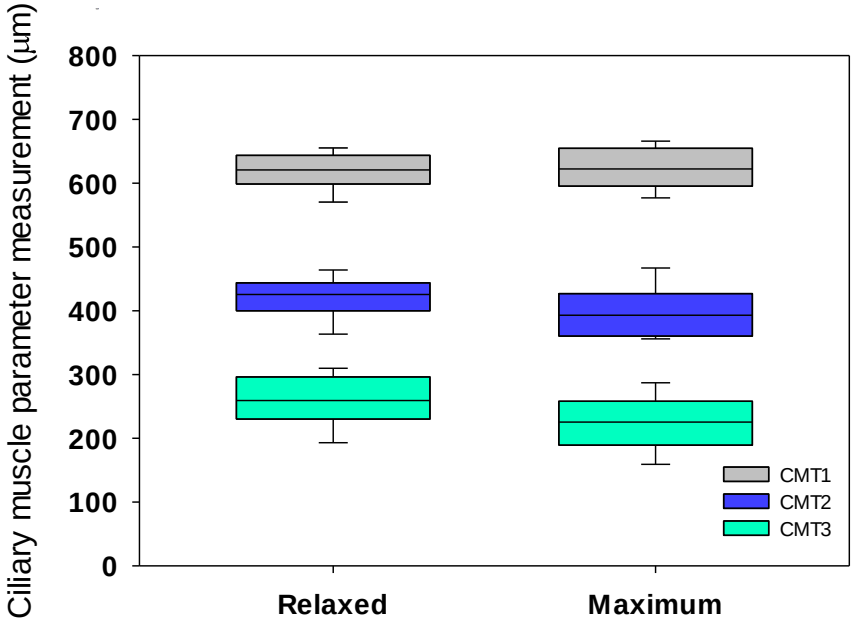

Figure 4.4. A box and Whisker plot showing the CMT1, CMT2 and CMT3 ciliary muscle parameter measurements during relaxed and maximum accommodation.

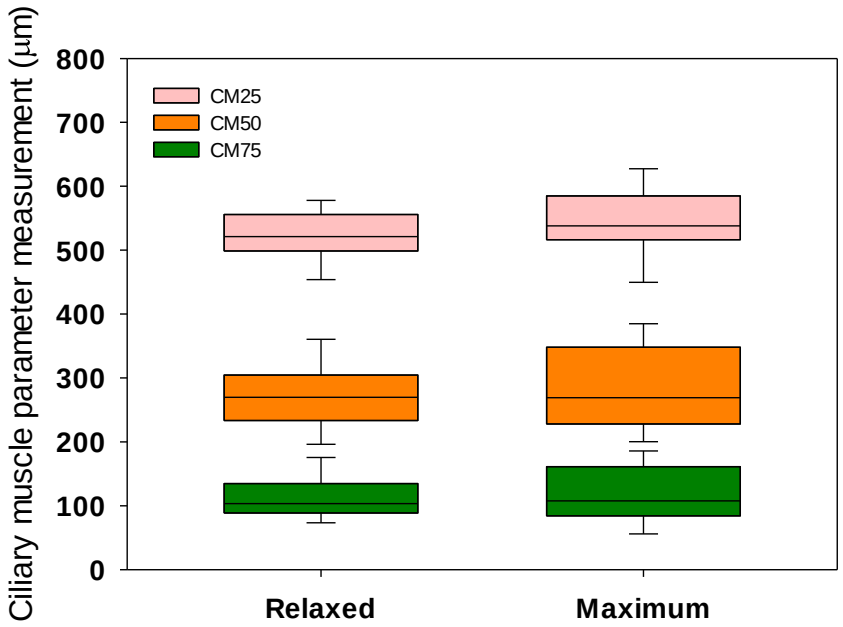

Figure 4.5. A box and Whisker plot showing CM25, CM50 and CM75 ciliary muscle parameter measurements during relaxed and maximum accommodation.

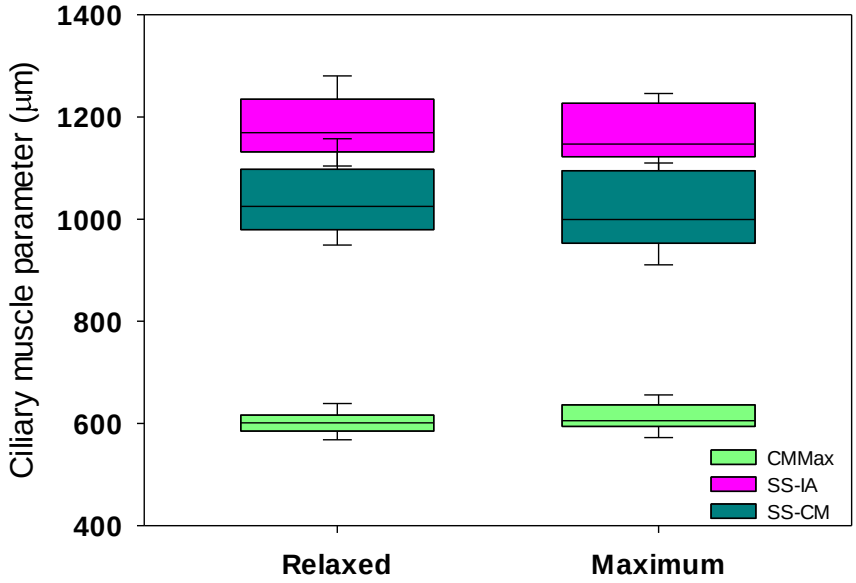

Physiological accommodation at baseline and maximum accommodation (D)

Figure 4.6. A box and Whisker plot showing CMMax, SS-IA and SS-CM ciliary muscle parameter measurements during relaxed and maximum accommodation.

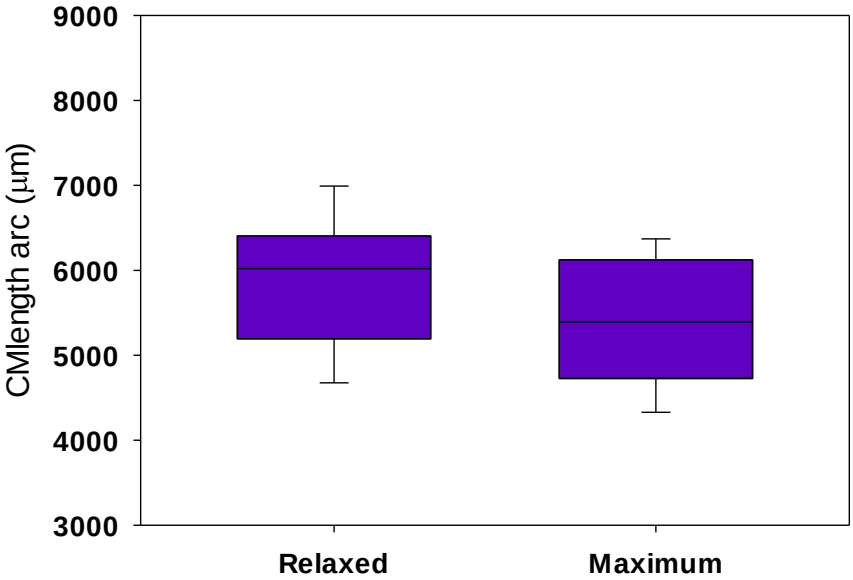

Physiological accommodation at baseline and maximum accommodation (D)

Figure 4.7. A box and Whisker plot showing CMLengthArc measurements during relaxed and maximum accommodation.

The effect of tropicamide on the ciliary muscle morphology during relaxed accommodation (0 D demand level), is shown in Appendix 1 Table A1-1. Within 20 minutes post-instillation, there was an increase in thickness throughout the muscle. The distance between the scleral spur and inner apex increased (SS-IA, $F_{0.804}$, p= 0.503) and the anterior length increased (SS-CM, $F_{0.511}$, p= 0.703) and CMLengthArc reduced ($F_{1.328}$, p= 0.268), suggesting the ciliary muscle mass moved anteriorly during the initial 20 minutes of agent instillation. Between 20 and 30 minutes post-instillation, there was a reduction in thickness at CM25, CM50 and CM75. There was a significant effect of tropicamide on the thickness at CM25 only ($F_{2.806}$, p= 0.038), although post-hoc comparisons did not reveal any significant mean differences between time intervals. After 20 minutes post-instillation, CMT1 increased in thickness whereas CMT2 and CMT3 remained invariant. Furthermore, there was an increase in ciliary muscle length arc, CMMax and minimally for SS-IA, suggesting the anterior movement of the ciliary muscle mass was occurring but at a lesser extent.

The effect of cyclopentolate on the measurements of the ciliary muscle parameters during relaxed accommodation (0 D demand level), are shown in the Appendix 1 Table A1-2. Within 20 minutes post-instillation of cyclopentolate, there was a thinning at CMT3, a thickening at CM25, CM50 and CM75 and the ciliary muscle length shortened suggesting an anterior movement of ciliary muscle mass. The distance between the scleral spur and inner apex, as well as the anterior length, reduced up to 10 minutes, and then subsequently increased. Cyclopentolate produced a significant thickening at CM25 ($F_{2.836}$, p= 0.032) specifically between 0 and 40 minutes (mean difference 20.0 µm, p= 0.038), an insignificant thickening at CM50 ($F_{2.358}$, p= 0.062) and a significant thickening at CM75 ($F_{1.605}$, p= 0.040), specifically between 0 and 20 minutes (mean difference 23.0 µm, p= 0.040). There was a significant effect of cyclopenolate on the ciliary muscle length arc ($F_{2.865}$, p= 0.026), although post-hoc comparisons revealed the effect was not significant between specific time intervals. There was an insignificant effect of cyclopentolate at CMMax ($F_{1.605}$, p= 0.179), distance between the scleral spur and inner apex (SS-IA; $F_{1.446}$, p= 0.223) and SS-CM ($F_{1.103}$, p= 0.359).

To determine the effect of the anti-muscarinic agents on the contractility of the ciliary muscle, and therefore their effect on the accommodative ability, the changes to the ciliary muscle at baseline and at regular intervals post-instillation of tropicamide and cyclopentolate were calculated. The results are shown in Appendix 1: Table A1-3 and A1-4, respectively.

The change to the thickness over time for CMT1 is shown in Figure 4-8 A, and the differences and similarities between both anti-muscarinic agents is evident from the graph. Tropicamide reduced the accommodative ability within the region up to 20 minutes, represented by the thinning within the region up to 20 minutes. Between 20 minutes and 40 minutes there was an increase to the thickness, indicating contraction of the muscle fibres during accommodation was possible within the region. There was a significant effect of tropicamide on the ciliary muscle thickness ($F_{5.72}$, p= 0.024) but an invariant interaction between ciliary muscle thickness and time ($F_{1.90}$, p= 0.13) at CMT1.

Cyclopentolate also altered the accommodative ability of the ciliary muscle fibres within CMT1 over time. For example, it is evident from Figure 4-8 A that the contraction of the ciliary muscle was still possible 10 minutes post-instillation of cyclopentolate, as indicated by the thickening within the region. However, between 10 and 20 minutes post-instillation, there was a reduction to the thickness with a mean difference indicating a minimal contraction of the muscle fibres (mean difference -18.5 µm (SE 10.8)). This was followed by a slight increase in thickness of the ciliary muscle region between 20 and 30 minutes (mean difference 4.1 µm (SE 8.1)), followed by a further reduction in contractility between 30 and 40 minutes (mean difference -10.4 µm (SE 10.0)). There was a consequent increase in the ciliary muscle thickness between 40 and 50 minutes mean difference (9.1 µm (SE 9.60)). There was an insignificant effect of cyclopentolate on ciliary muscle thickness ($F_{0.09}$, p= 0.77), time ($F_{0.68}$, p= 0.61) and interaction between ciliary muscle thickness and time ($F_{1.66}$, p= 0.16) at CMT1.

The thickness of the ciliary muscle at 2 mm posterior to the scleral spur (CMT2) is shown in Figure 4-8 B. At baseline (0 minutes), prior to the instillation of either agent, there was thinning of the region during accommodation. Between baseline (0 minutes) and 10 minutes post-instillation, there was an increase to the thickness by 20.2 µm (SE 7.30) when tropicamide was used, and an increase of 27.2 µm (SE 7.73) when cyclopentolate was used, suggesting a reduced contractile ability within the region during accommodation. Consequently, there was an indication of the contractile ability returning between 10 and 20 minutes for both agents as evident from the thinning within the region with accommodative effort. However, the contraction of the ciliary muscle during accommodation reduced after 20 minutes for both agents up to 40 minutes for tropicamide and 50 minutes for cyclopentolate, as shown on the graph. Cyclopentolate produced a greater effect on the ciliary muscle contractility at CMT2 compared to tropicamide, as seen on the graph.

There was a significant change to the ciliary muscle thickness at CMT2 with tropicamide, ($F_{11.19}$, p= 0.002), time effect of the agent ($F_{5.16}$, p= 0.002) and interaction between ciliary muscle thickness and time ($F_{2.72}$, p= 0.04). Pairwise comparisons revealed the significant interaction occurred between 0 and 30 minutes (mean difference 13.0 µm (SD 4.0), p= 0.042) and 0 and 40 minutes (mean difference 17.0 µm (SE 4.0), p= 0.09). Cyclopentolate did not significantly affect the ciliary muscle thickness ($F_{3.86,}$ p=0.06) but had a significant effect on the ciliary muscle thickness over time ($F_{3.57}$, p= 0.009) and a significant interaction between ciliary muscle thickness and time ($F_{2.94}$, p=0.03) with pairwise comparisons indicating near significance between 0 and 50 minutes (mean difference 14.0 µm (SE 5.0), p= 0.059).

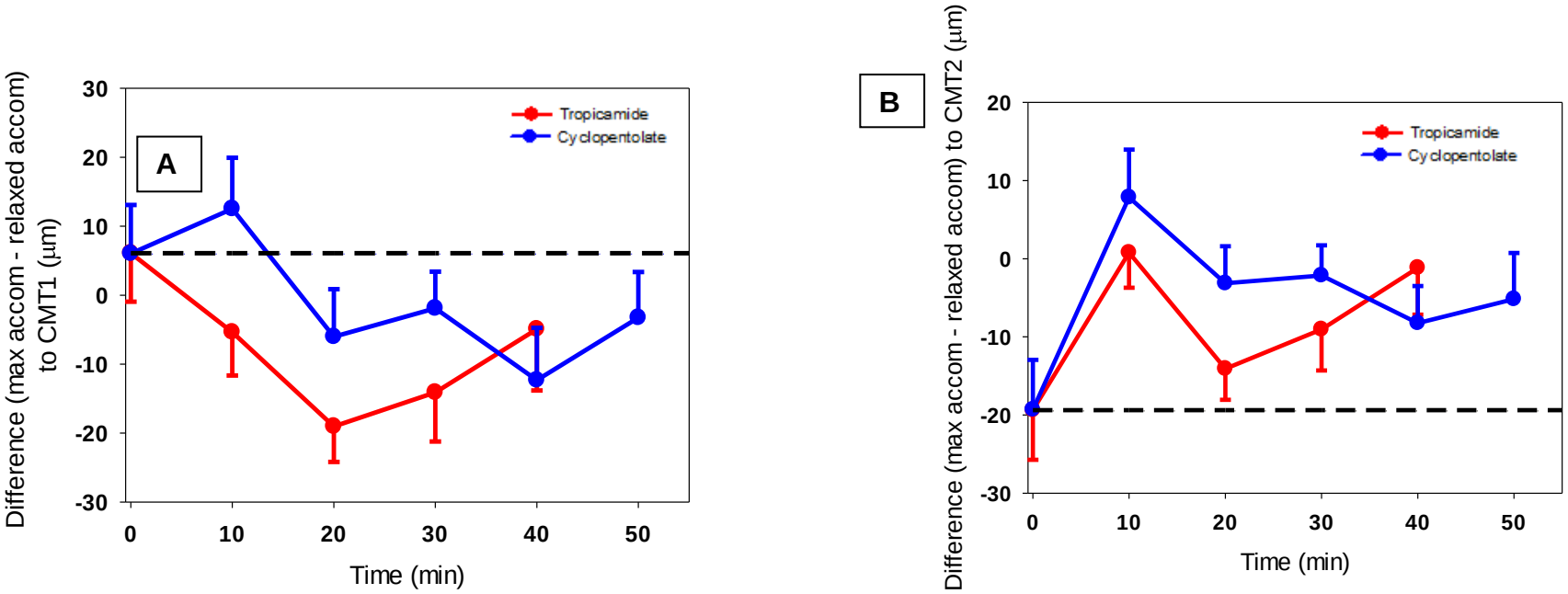

Figure 4-8. The difference in thickness between the measurement at the maximum objective amplitude of accommodation and during relaxed accommodation for A: CMT1 and B: CMT2 over time for cyclopentolate (mean + 1 SEM) and tropicamide (mean – 1 SEM). 0 minutes refers to baseline measurements (pre-instillation of the agent).

CMT3 represents the ciliary muscle thickness 3 mm posterior to the scleral spur. From Figure 4-9 A, it is evident the ciliary muscle contractility is prevented 10 minutes post-instillation of tropicamide, as indicated by the increase in thickness of the ciliary muscle (mean difference between maximum accommodation and relaxed accommodation CMT3: 2.45 µm (SE 4.17) and cyclopentolate (mean difference between maximum accommodation and relaxed accommodation CMT3: 2.8 µm (SE 5.3)). The ciliary muscle contractility appears to return between 10 and 20 minutes, more so for tropicamide than cyclopentolate. Tropicamide produced a significant increase to the ciliary muscle thickness ($F_{16.35}$, p= 0.000), time ($F_{8.33}$, p= 0.000) and interaction between ciliary muscle thickness and time ($F_{6.39}$, p= 0.000). The effect of time was significant between 0 and 10 minutes (mean difference -17.0 µm (SE 4.0), p= 0.005), 0 and 20 minutes (mean difference 18.0 µm (SE 5.0), p= 0.011), 0 and 30 minutes (mean difference 19.0 µm (SE 5.0), p= 0.004) and 0 and 40 minutes (mean difference 19.0 µm (SE 5.0), p= 0.006). With cyclopentolate, there was a significant effect of ciliary muscle thickness ($F_{6.38}$, p= 0.017), time ($F_{7.08}$, p= 0.000) and interaction between ciliary muscle thickness and time ($F_{7.00}$, p= 0.000). Post-hoc tests indicated the only times of significance were between 0 and 10 minutes (mean difference -15.0 µm (SE 5.0), p= 0.04), 0 and 30 minutes (mean difference 20 µm (SE 5.0), p= 0.01), 0 and 40 minutes (mean difference 20.0 µm (SE 5.0), p= 0.009) and 0 and 50 minutes (mean difference (19.0 µm (SE 4.0), p= 0.003).

The changes which occur to the region representing 25% of the ciliary muscle length are shown in Figure 4-9 B. Prior to the instillation of the anti-muscarinic agents, there was a thickening within the region during accommodation (mean 22.2 µm (SE 9.8)). However, post-instillation of the anti-muscarinic agent there was a reduction in the contractile ability within the region, as indicated by the reduced thickness with accommodation up to 20 minutes for both agents. There was a consequent increased thickening between 20 minutes and 30 minutes (mean increase tropicamide 32.6 µm (SE 9.4), cyclopentolate 16.0 µm (SE 8.2)), indicating the contractile ability with accommodation was returning. Both anti-muscarinic agents follow a similar pattern but the effect of tropicamide is slightly greater than cyclopentolate. There was minimal change to the thickness between 30 minutes and 40 minutes for tropicamide (mean thickening 0.50 µm (SE 11.8)), indicating a maximum effect of the agent had occurred. With cyclopentolate, the thickness reduced further indicating inability for the ciliary muscle fibres to contract with accommodation between 30 minutes and 40 minutes (mean thickening -2.4 µm (SE 9.3)). Only the interaction between ciliary muscle

thickness and time was significant for both anti-muscarinic agents at CM25 (tropicamide $F_{4.73}$, p= 0.004; cyclopentolate $F_{3.75}$, p= 0.007).

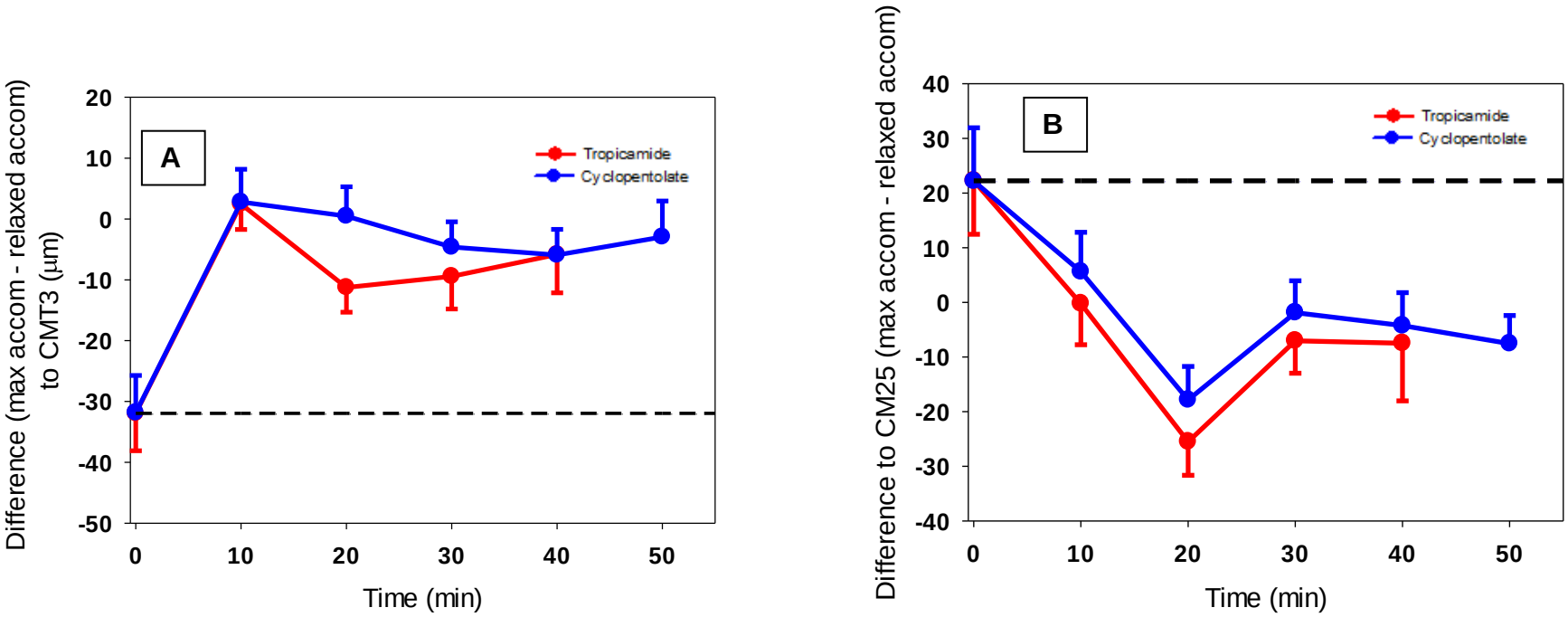

Figure 4-9. The difference in thickness between the measurement at the maximum objective amplitude of accommodation and during relaxed accommodation for A: CMT3 and B: CM25 over time for cyclopentolate (mean + 1 SEM) and tropciamide (mean – 1 SEM). 0 minutes refers to baseline measurements (pre-instillation of the agent).

Figure 4-10 A and B shows the changes to the ciliary muscle at 50% (CM50) and 75% (CM75) of the ciliary muscle length, respectively. Both anti-muscarinic agents produced a thinning to the regions within 20 minutes post-instillation of the agents, indicating a minimal contractile ability during accommodation within this time. The effect of tropicamide on the contractile ability within the regions appeared to reduce after 20 minutes as there was an increase in thickness at CM50 between 20 and 30 minutes (mean increase 22.8 µm (SE 11.0)) and CM75 (mean increase in thickness 11.0 µm (SE 7.3)). Also, the thickness at CM50 continued to increase between 20 and 40 minutes with cyclopentolate (mean increase was 21.9 µm (SE 12.3)) and at CM75 (mean increase 7.9 µm (SE 6.9)) suggesting the muscle fibres within the region were able to contract with accommodative effort. Overall neither anti-muscarininc agent produced a significant effect on the ciliary muscle thickness or time effect at both CM50 and CM75.

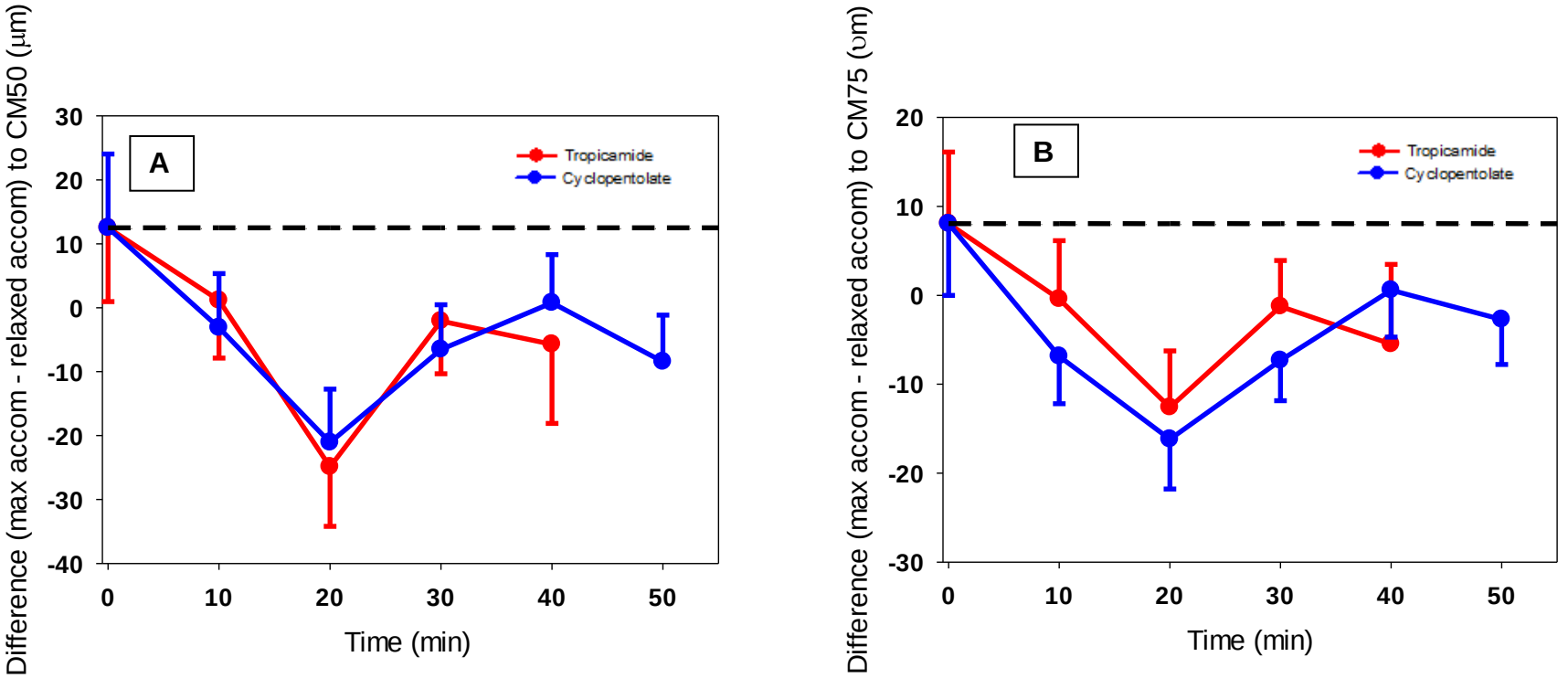

Figure 4-10. The difference in thickness between measurement at the maximum objective amplitude of accommodation and during relaxed accommodation for A: CM50 and B: CM75 over time with cyclopentolate (mean + 1SEM) and tropicamide (mean – 1 SEM). 0 minutes refers to baseline measurements (pre-instillation of the agent).

The anti-muscarinic agents also altered the region representing the ciliary muscle maximum thickness (CMMax), as shown in Figure 4-11 A. There was a reduction in thickness up to 20 minutes post-instillation of tropicamide (mean reduction 18.3 µm (SE 6.1)), indicating the region was unable to respond to an accommodative stimulus, however, there was an increase in thickening (mean increase 12.9 µm (SE 8.1)) between 20 minutes and 40 minutes post-instillation, indicating the contractile ability of the muscle to the accommodative stimulus returned. The pattern is similar to the profile show in Figure 4-8 A for CMT1. There was no significant effect of tropicamide on the ciliary muscle thickness ($F_{0.03}$, p= 0.865) but the change to the thickness over time was statistically significant ($F_{2.83}$, p= 0.04). There was no significant interaction between ciliary muscle thickness and time.

The effect of cyclopentolate at CMMax was similar in profile to the effect of the agent at CMT1 where there were two phases of a reduction in thickness followed by an increase in thickness. Between 0 and 10 minutes, the thickness increased by 5.4 µm (SE 6.7) followed by a reduction in thickness of 20.2 µm (SE 8.3) between 10 and 20 minutes. Subsequently, there was an increase in thickness between 20 and 30 minutes (mean increase 9.8 µm (SE 6.5)) and a further thinning within the region between 30 and 40 minutes (mean reduction 10.1 µm (SE 7.1)) The interaction between ciliary muscle thickness and time was significant for this region ($F_{2.61}$, p= 0.03).

Furthermore, cyclopentolate produced an increase to the distance between the scleral spur and inner apex of the ciliary muscle (SS-IA up to 10 minutes post-instillation (mean increase 19.5 µm (SE 20.0)), as shown in Figure 4-11 B, indicating centripetal movement of the muscle was restricted during accommodation. There was a consequent reduction in the inner apex which reached baseline levels at 30 minutes, indicating a return of the centripetal movement. The inner apex further reduced between 30 and 40 minutes (mean reduction 16.8 µm (SE 18.4)). Neither the distance ($F_{2.17}$, p= 0.15), time ($F_{1.31}$, p= 0.27) or the interaction between accommodation and time ($F_{1.07}$, p= 0.38) were significant. With tropicamide, there was a reduced distance between the inner apex and the scleral spur up to 30 minutes post-instillation indicating a centripetal movement of the muscle was possible with accommodation. The centripetal movement increased between 30 minutes and 40 minutes. However, the distance ($F_{2.44}$, p= 0.13), accommodation ($F_{1.41}$, p= 0.25) and the interaction between accommodation and time ($F_{1.29}$, p= 0.28) were invariant.

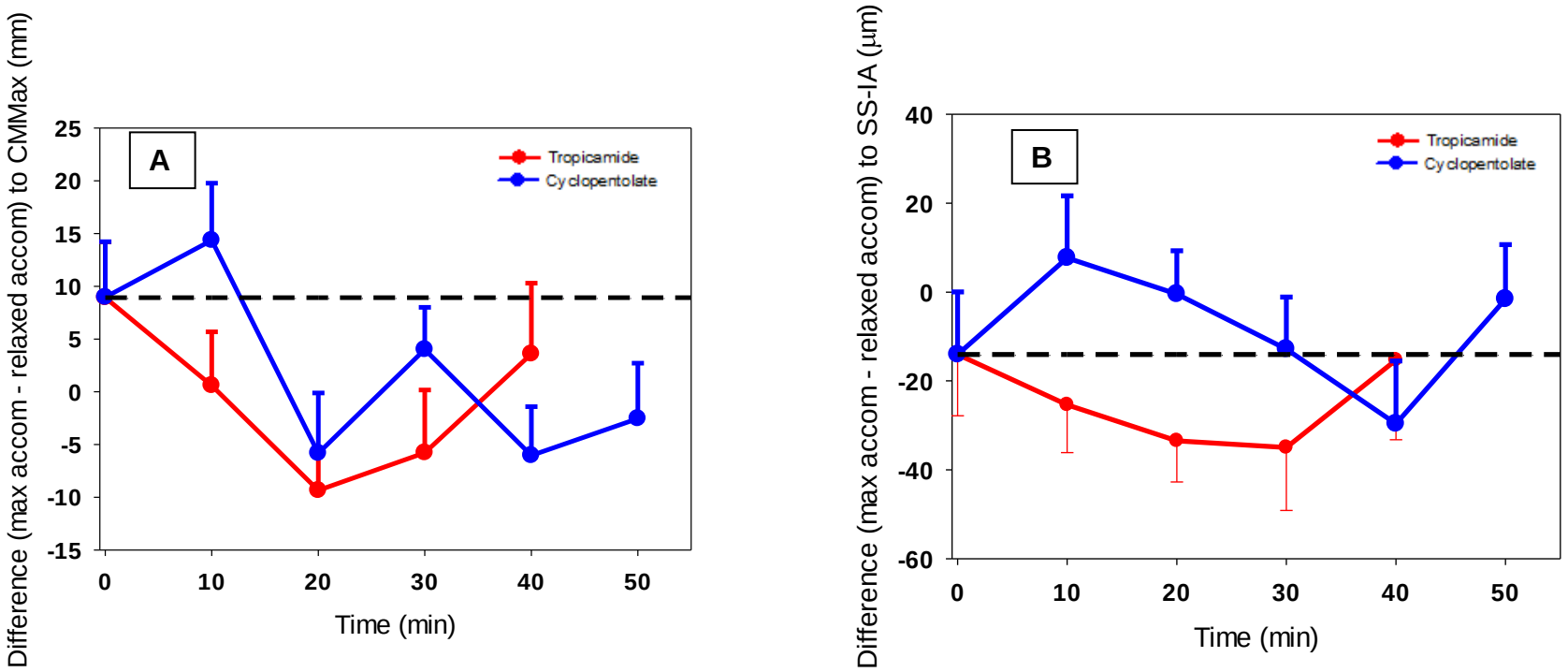

Figure 4-11. The difference between the maximum objective amplitude of accommodation and during relaxed accommodation for A: CMMax and B: SS-IA over time with cyclopentolate (mean + 1 SEM) and tropicamide (mean – 1 SEM). 0 minutes refers to baseline measurements (pre-instillation of the agent).

There was a reduction to the anterior length (SS-CM) between 0 and 10 minutes post-instillation of tropicamide, which did not differ to the baseline level, indicating accommodative ability within the region was possible. Furthermore, the anterior length shortened with accommodation between 10 and 30 minutes post-instillation (mean reduction 15.5 µm (SE 18.6)), as shown in Figure 4-12 A, suggesting the ciliary muscle was still able to contract in the presence of tropicamide. At 40 minutes, the anterior length was near baseline level. For cyclopentolate, the anterior length increased between baseline and 20 minutes (mean increase 25.9 µm (SE 19.9)) followed by a reduction between 20 and 40 minutes (mean reduction 33.9 µm (SE 16.4)). There was a significant effect of tropicamide ($F_{22.34}$, p= 0.00) and cyclopentolate ($F_{5.99}$, p= 0.02) on the anterior length. The anterior length and centripetal movement returned to baseline levels at 40 minutes post-instillation of tropicamide.

There was an increase to the ciliary muscle length (CMLength Arc) between 0 and 20 minutes for both tropicamide (mean increase 698.6 µm (SE 169.7)) and cyclopentolate (mean increase 814.3 µm (SE 169.5)), with a greater increase evident for cyclopentolate, suggesting the contractile shortening with accommodation was reduced in the presence of the anti-muscarinic agents. The ciliary muscle length reduced between 20 and 30 minutes in the presence of tropicamide (mean reduction 293.7 µm (SE 162.8)), as shown in Figure 4-8 B, indicating the ciliary muscle was able to contract during accommodation. However, there was an elongation of the ciliary muscle between 30 and 40 minutes (mean increase 185.9 µm (SE 201.1)) which indicates the contractile ability of the ciliary muscle was reduced during accommodation. A similar profile was evident with cyclopentolate, where the contractile ability of the muscle during accommodation was slightly evident between 20 and 40 minutes (mean reduction 398.1 µm (SE 144.0)), although an increase in length between 40 and 50 minutes (mean increase 168.6 µm (SE 111.6)) occurred, indicating the inability of the muscle fibres to contract to the accommodative stimulus. There was a significant interaction between ciliary muscle length arc and time for tropicamide ($F_{4.58}$, p= 0.003) and cyclopentolate ($F_{6.71}$, P= 0.00).

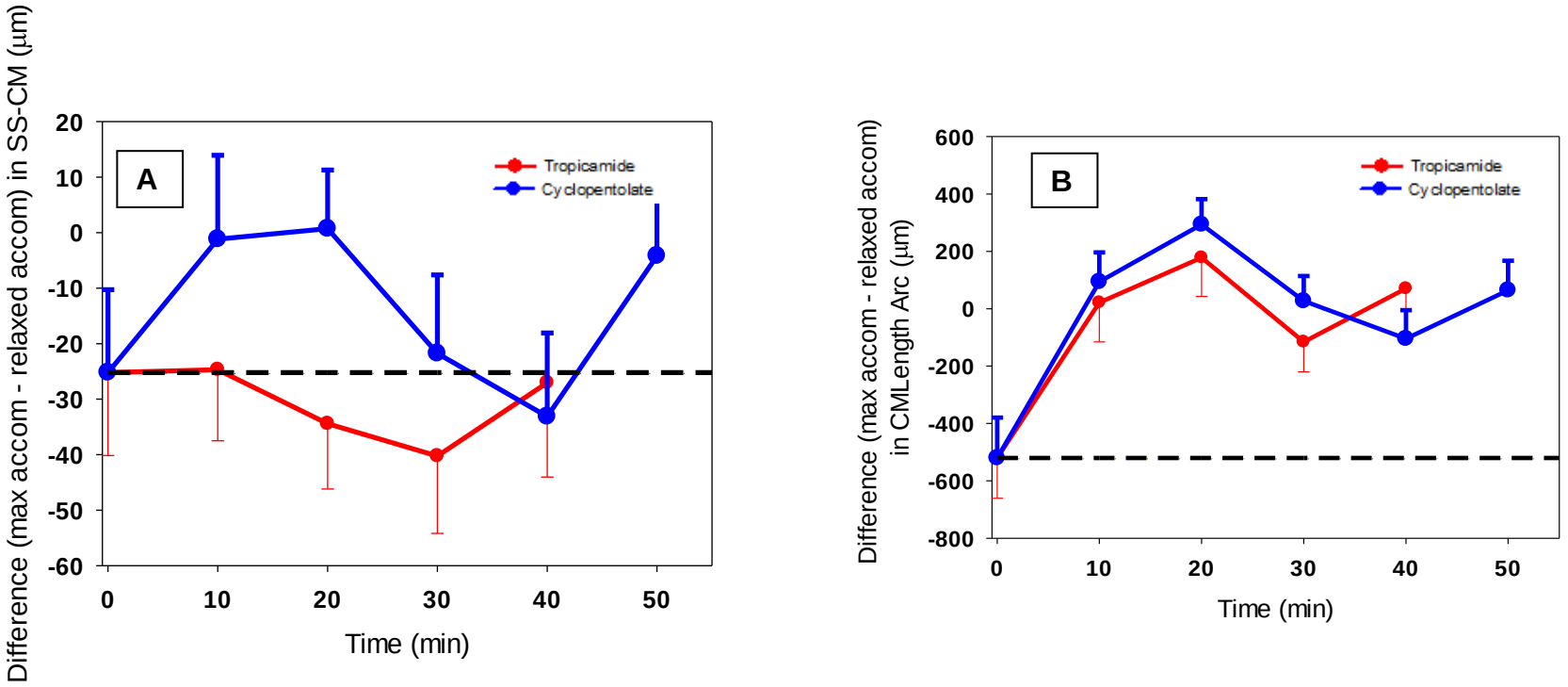

Figure 4-12. The difference between the measurement at the maximum objective amplitude of accommodation and during relaxed accommodation for A: SS-CM and B: CMLengthArc over time with cyclopentolate (mean +1 SEM) and tropicamide (mean – 1 SEM). 0 minutes refers to baseline measurements (pre-instillation of the agent).

There were no significant differences between the effect of tropicamide and cyclopentolate on the ciliary muscle parameters (p> 0.05).

4.3.2. Ocular biometry data

In order to investigate the effect of anti-muscarinic agents on the intraocular parameters, ocular biometry measurements were obtained prior to the instillation of the agent, and at the end of the study when the end point was achieved. However, the shorter duration of the cycloplegic effect with tropicamide meant the final measurement for biometry was obtained when the accommodative response was returning. In contrast, the cycloplegic effect with cyclopentolate was still evident at the end point of data collection. Consequently, ocular biometry data are only presented for data obtained using cyclopentolate. Moreover, ocular biometry was acquired with the LenStar, however, data for all biometric parameters (corneal thickness, lens thickness, axial length and anterior chamber depth) could only be obtained from 11 participants included in the study. Therefore, biometric data has been presented for these participants only (mean age 19.9 (SD 1.9) years, MSE (-0.01 D (SD 0.32)) which are shown in Table 4-2. The axial length data acquired during maximum accommodation (pre and post-instillation) has been corrected using the equations listed in Chapter 6, section 6.2.5.

To determine the change to the intraocular parameters prior to instillation of cyclopentolate and data acquired at the end of the study, where the maximum cycloplegic effect was achieved, paired sample t-tests were performed. Prior to the instillation of cyclopentolate, there was a significant increase to the lens thickness with accommodation (t= -3.67, p= 0.004) and reduction to the anterior chamber depth (t= 8.96, p= 0.000), whereas the increase in corneal thickness and the reduction in axial length was not significant. The ocular biometry measurements obtained at the end of the study in the presence of cyclopentolate, indicates some accommodative ability was still possible, as there was a reduction in the anterior chamber depth and an increase in lens thickness at the maximum accommodative amplitude. However, these changes were not significant (lens thickness t= -1.78, p= 0.10, anterior chamber depth t= 2.02, p= 0.07). Furthermore, the axial length did not significantly decrease (t= 1.30, p= 0.22) and the corneal thickness did not significantly reduce (t=0.18, p= 0.86).

There was a significant reduction to the anterior chamber depth (t= -6.58, p= 0.000) between the relaxed accommodative level at baseline and at the end of the study, but an invariant thinning of the lens (t= 1.61, p= 0.14), an insignificant reduction to the

corneal thickness (t= 0.26, p= 0.79), and an invariant reduction to the axial length (t= 0.18, p= 0.86).

Intraocular parameter	Measurement during relaxed accommodation prior to instillation of cyclopentolate	Measurement at the maximum amplitude of accommodation prior to instillation of cyclopentolate	Measurement during relaxed accommodation at end point	Measurement at the maximum amplitude of accommodation at end point
Corneal thickness (µm)	542.94 (SE 11.55)	544.79 (SE 11.35)	542.61 (SE 11.39)	541.09 (SE 11.41)
Anterior Chamber Depth (mm)	2.92 (SE 0.05)	2.69 (SE 0.07)	3.06 (SE 0.05)	3.05 (SE 0.05)
Lens thickness (mm)	3.57 (SE 0.09)	3.88 (SE 0.11)	3.48 (SE 0.10)	3.51 (SE 0.09)
Axial Length (mm)	23.42 (SE 0.25)	23.39 (SE 0.23)*	23.36 (SE 0.24)	23.36 (SE 0.21) *

Table 4-2. The mean (± 1 SEM) changes to the intraocular parameters during relaxed accommodation and at the maximum accommodative amplitude pre-instillation of cyclopentolate and at the end point of the study. The asterisk data represents the corrected axial lengths.

4.3.3. Amplitude of accommodation

Prior to the instillation of the anti-muscarinic agent, the objective accommodation was measured for all participants to determine their amplitude of accommodation. All participants (n= 30) were able to accommodate to a 6 D stimulus (average accommodative response 4.86 D (SD 0.56)), and 26 participants were able to accommodate to a 7 D stimulus (average accommodative response -5.43 D (SD 0.75)).

The maximum residual accommodation was required at each time interval post-instillation of the anti-muscarinic agent, in order to stimulate the maximum accommodation when ciliary muscle images were acquired. Therefore, the amplitude of accommodation at each time interval was recorded. Nevertheless, it was of interest to determine whether differences in the residual accommodation were evident between both anti-muscarinic agents. Therefore, data was obtained from a sub-set of participants whose accommodative response was obtained per dioptre of accommodative demand, between 0 and 7 D at regular time intervals, for both visits. The sub-group consisted of 21 participants (mean age 19.7 (SD 1.8) years, MSE -0.09 D (SD 0.42)) and data is presented in Table 4-3 and Figure 4-13 for tropicamide and Table 4-5 and Figure 4-14 for cyclopentolate. However, for Figure 4-14, the data has only been shown up to 40 minutes for easier inspection of the graph as similar responses were obtained at 40 minutes and 50 minutes post-instillation.

Prior to the instillation of either anti-muscarinic agent, there was an increase in the accommodative response for each dioptre of accommodative demand which was significant between all demand levels (p=0.000), except between 7 D and 8 D demands. Between 7 and 8 D the accommodative response began to plateau (mean difference -0.21 D, p=1.00) indicating the maximum accommodative amplitude was achieved at the 7 D accommodative demand level.

The instillation of tropicamide reduced the accommodative response, however, inspection of Figure 4-13 indicates approximately 25% of the residual accommodation was present for each dioptre of accommodative demand up to 4 D demand level at 40 minutes. Tropicamide produced a significant effect on accommodation ($F_{69.29}$, p= 0.00), and the accommodative response over time ($F_{70.97}$, p= 0.00) as well as a significant interaction between time and accommodation ($F_{64.37}$, p= 0.00). Post-hoc comparisons revealed the significant effect of tropicamide upon the accommodative response only occurred between baseline (0 minutes) and 10 minutes post instillation (mean difference 1.56 D, p= 0.00), indicating no significant reduction to the accommodative response between all other time points.

There was a reduction in the accommodative response after the instillation of cyclopentolate which produced a significant reduction to the accommodative response ($F_{39.17}$, p= 0.00). The accommodative response with cyclopentolate was significantly dependant on time ($F_{209.06}$, p= 0.000) and there was an interaction between time and accommodation ($F_{170.67}$, p= 0.000). Post-hoc comparisons revealed statistically significant differences in accommodative responses at all time levels except between

20 and 30 minutes (mean difference 0.154 D, p= 0.55), 20 and 40 minutes (mean difference 0.16 D, p= 0.36), and 40 and 50 minutes (mean difference= 0.03 D, p= 1.00), suggesting the maximum reduction in the objective amplitude occurred at 20 minutes. There was a significant difference in residual accommodation at all accommodative demand levels between tropicamide and cyclopentolate ($F_{25.92}$, p= 0.00).

Accommodative Stimulus (D)	Time (min)				
	Baseline	10	20	30	40
0	-0.07 (SE 0.08)	-0.04 (SE 0.12)	-0.07 (SE 0.15)	-0.11 (SE 0.13)	-0.13 (SE 0.14)
1	0.53 (SE 0.06)	0.40 (SE 0.07)	0.37 (SE 0.07)	0.35 (SE 0.08)	0.39 (SE 0.12)
2	1.27 (SE 0.10)	0.86 (SE 0.10)	0.74 (SE 0.10)	0.74 (SE 0.10)	0.77 (SE 0.13)
3	2.15 (SE 0.10)	1.39 (SE 0.16)	1.30 (SE 0.14)	1.26 (SE 0.15)	1.32 (SE 0.15)
4	3.16 (SE 0.09)	1.64 (SE 0.20)	1.29 (SE 0.19)	1.45 (SE 0.19)	1.58 (SE 0.17)
5	4.02 (SE 0.10)	1.70 (SE 0.26)	1.20 (SE 0.22)	1.38 (SE 0.22)	1.43 (SE 0.23)
6	4.83 (SE 0.11)	1.50 (SE 0.25)	1.10 (SE 0.23)	1.18 (SE 0.27)	1.09 (SE 0.20)
7	5.64 (SE 0.11)	1.48 (SE 0.23)	0.98 (SE 0.16)	1.07 (SE 0.22)	1.14 (SE 0.23)

Table 4-3. The mean (± 1 SEM) accommodative response (D) to the accommodative stimulus (D) over time for tropicamide.

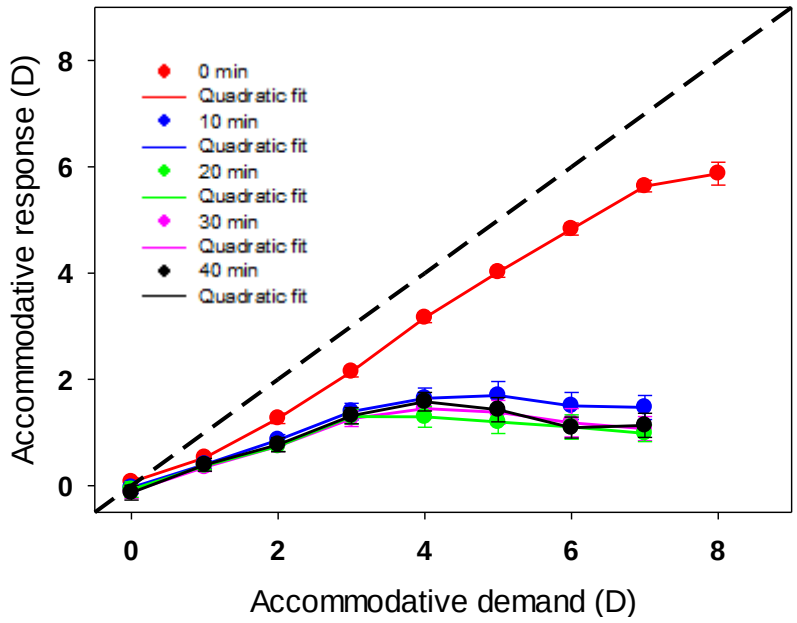

Figure 4-13. The accommodative response per dioptre of accommodative demand for 21 participants over time with tropicamide. The error bars represent 2 SEM. 0 minutes refers to the baseline measurement.

Accommodative Stimulus (D)	Time (min)					
	Baseline	10	20	30	40	50
0	-0.07 (SE 0.08)	0.17 (SE 0.13)	0.26 (SE 0.12)	0.36 (SE 0.13)	0.43 (SE 0.12)	0.46 (SE 0.14)
1	0.53 (SE 0.06)	0.26 (SE 0.08)	0.09 (SE 0.07)	0.03 (SE 0.10)	0.03 (SE 0.07)	0.09 (SE 0.08)
2	1.27 (SE 0.10)	0.50 (SE 0.07)	0.31 (SE 0.08)	0.23 (SE 0.11)	0.28 (SE 0.09)	0.21 (SE 0.09)
3	2.15 (SE 0.10)	0.86 (SE 0.11)	0.45 (SE 0.13)	0.28 (SE 0.13)	0.23 (SE 0.11)	0.22 (SE 0.10)
4	3.16 (SE 0.09)	0.99 (SE 0.18)	0.40 (SE 0.12)	0.21 (SE 0.13)	0.17 (SE 0.10)	0.11 (SE 0.10)
5	4.02 (SE 0.10)	0.92 (SE 0.21)	0.45 (SE 0.15)	0.17 (SE 0.11)	0.14 (SE 0.10)	0.08 (SE 0.09)
6	4.83 (SE 0.11)	0.94 (SE 0.22)	0.40 (SE 0.15)	0.09 (SE 0.10)	0.10 (SE 0.10)	0.06 (SE 0.07)
7	5.64 (SE 0.11)	0.84 (SE 0.20)	0.43 (SE 0.13)	0.18 (SE 0.10)	0.10 (SE 0.09)	0.10 (SE 0.09)

Table 4-4. The mean (± 1 SEM) accommodative response (D) to the accommodative stimulus (D) over time for cyclopentolate.

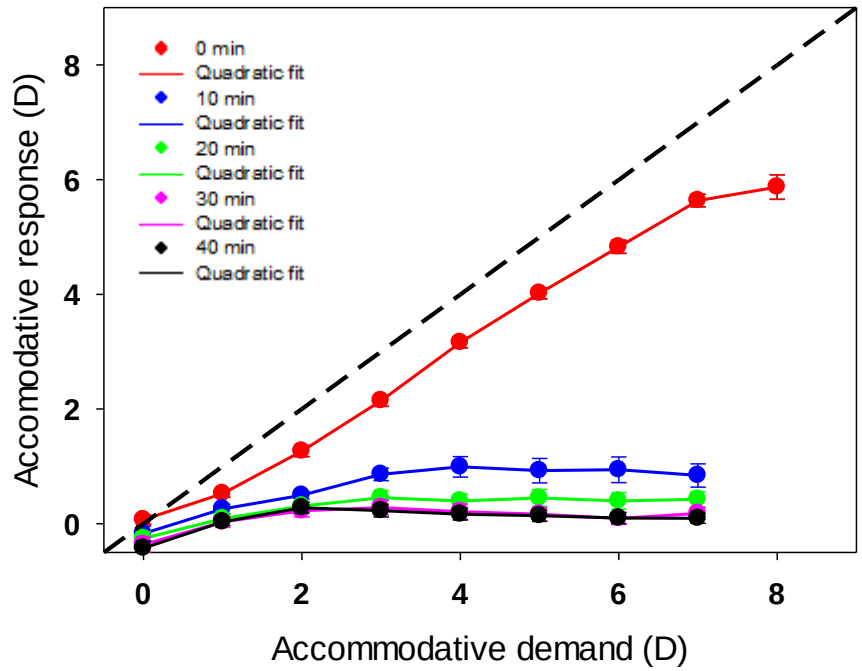

Figure 4-14. The accommodative response per dioptre of accommodative demand for 21 participants over time with cyclopentolate. The error bars represent 2 SEM. 0 minutes refers to the baseline measurement.

4.4. Discussion

Contraction of the ciliary muscle initiates changes to the intraocular components, resulting in the increased dioptric power of the eye. Indeed, significant research has contributed to our understanding of the muscle fibres predominantly involved in accommodation, however, a limitation of previous investigations is the determination of the ciliary muscle morphology *in-vitro* (e.g Pardue and Sivak, 2000). The results from

this present study provide the first *in-vivo* data to explore the ciliary muscle fibre groups which have a possible role in accommodation.

The results from the present study indicate both anti-muscarinic agents produce an anterior shift of the ciliary muscle mass within 20 minutes post-instillation. Also, both agents alter the contractility and mobility of the ciliary muscle during accommodation, resulting in the reduction of the accommodative response. Generally, the greatest reduction to the contractility and mobility of the ciliary muscle also occurred within 20 minutes after the agent was instilled. Although the profile for the changes to the ciliary muscle were similar with both anti-muscarinic agents, especially at the proportional measurements of CM25, CM50 and CM75, there were notable differences at the anterior length and the region representing the scleral spur to the inner apex. The most important difference was the ability for cyclopentolate to reduce the centripetal movement, specifically up to 20 minutes, whereas the movement was still possible when tropicamide was used. This probably explains why the residual accommodation was much greater for tropicamide in comparison to cyclopentolate.

Moreover, the greatest reduction in accommodative amplitude occurred within 20 minutes after the instillation of cyclopentolate and within this time the thickness measurements at CM25, CM50 and CM75 were also reducing. Moreover, the ciliary muscle length was increasing indicating the accommodative ability was restricted. A similar profile was also noted after the instillation of tropicamide. Indeed, *in-vitro* studies have shown that the anterior ciliary muscle consists of circular fibres and there is a gradual change in muscle orientation between the anterior and posterior muscle from radial to longitudinal fibres (e.g. Pardue and Siavk, 2000). Therefore, the significant findings from the current study suggest that all fibre groups are involved in accommodation, and that circular fibres alone are not solely responsible for eliciting an accommodative response.

After 30 minutes post-instillation of cyclopentolate, contraction of the ciliary muscle was evident during accommodation as the ciliary muscle length shortened and the thickness at CM25, CM50 and CM75 increased in response to the accommodative stimulus. Although the contraction of the ciliary muscle was possible, it did not reach baseline levels throughout the duration of the study, which probably explains the continued reduction in the accommodative response, since the ciliary muscle contraction was unable to alter the lens thickness significantly. Further support for the inability of the ciliary muscle to increase the lenticular power when the contractile ability

of the muscle was returning, is evident by thinning of the lens which was documented at the end of the study. A possible explanation for the lenticular thinning evident in the presence of the anti-muscarinic agents could be an indirect consequence of the increased lengthening of the ciliary muscle, which may stretch the zonular fibres and therefore stretch the lens. Moreover, the lens capsule contains muscarinic receptors (Gupta et al., 1994; Collison et al., 2000; Collison and Duncan, 2001), therefore, the anti-muscarinic agents may have had a direct effect on the lens, thus producing the elongation and consequent thinning.

Muscarinic receptors are located throughout the ciliary muscle. M_2 and M_3 receptors are prominent within the circular region whereas M_5 receptors are predominant within the longitudinal region. Although both anti-muscarinic agents reduces the ability of the ciliary muscle to alter its thickness during accommodation at all locations analysed, the data suggests tropicamide had a greater effect on the ciliary muscle contractility within the anterior portion, notably, CMT1 and CM25, whereas cyclopentolate produced a greater effect at the posterior locations, CMT3 and CM75. Similar effects between both agents were noted within the central region, CM50. Therefore, tropicamide seems to have a greater affinity for the M_2 and M_3 muscarinic receptors. Indeed, a greater affinity of M_3 receptors by tropicamide have been reported within the iris sphincter (German et al., 1999). Furthermore, cyclopentolate appears to alter the morphology of the complete muscle, but more so at the longitudinal fibres which predominantly contain M_5 muscarinic receptors. Considering cyclopentolate affected the posterior regions of the muscle more than tropicamide, could explain why the ciliary muscle length did not reduce when accommodation was stimulated, in comparison to tropicamide, therefore suggesting the longitudinal regions of the ciliary muscle were unable to contract and are consequently likely to be involved in accommodation. Overall, the findings from the current study further support evidence of the importance of a contractile shortening and anterior thickening required for accommodation (Sheppard and Davies, 2010a).

The anti-muscarinic agents significantly reduced the accommodative response, which suggests the muscarinic receptors are mainly responsible for ciliary muscle contraction during accommodation, therefore supporting *in-vitro* findings reported by Suzuki (1983). During the time course of the study, neither anti-muscarinic agent paralysed the ciliary muscle completely, as a residual accommodation was evident. Such responses may be due to the intrinsic innervation of the muscle, which consists of nitric oxide synthase positive nerve cells (Tamm et al., 1995). However, the minimal residual

accommodation evident with cycloplegia suggests the intrinsic innervation is unlikely to have a significant role for producing an accommodative response.

An increase in the axial length during accommodation has been reported (Shum et al., 1993; Read et al., 2010a), and considering a reduction in axial length was noted from this study, it suggests accommodation was not possible post-instillation of cyclopentolate. A possible cause for the reduction in axial length is the increase in choroidal thickness which has been reported with the use of anti-muscarinic agents (Sander et al., 2014).

Previous studies investigating the depth of cycloplegia with anti-muscarinic agents, have reported the depth of cycloplegia using subjective methods, often with participants viewing a near target (Priestley and Medine, 1951; Gettes and Leopold, 1953; Gettes and Belmont, 1961; Lovasik, 1986). However, near targets provide depth and blur cues and stimulate proximal accommodation, therefore over-estimating the amplitude of accommodation. Less residual accommodation has been demonstrated when a distance target (0.30 ± 0.25 D) is used in comparison to a near target (0.75 ± 0.53 D; Rosenfield and Linfield, 1986). Consequently, the combination of subjective techniques and near targets which have been used in early studies investigating the cycloplegic effects of tropicamide and cyclopentolate (e.g. Gettes and Leopold, 1953; Gettes, 1954; Gettes and Belmont, 1961, Amos, 1978) may have over-estimated the depth and duration for maximum cycloplegia. There is a general consensus within the literature that the duration taken for maximum cycloplegia with tropicamide is 30 minutes and 60 minutes for cyclopentolate (Merrill et al., 1960; Milder, 1961; Pollack et al., 1981). The findings from the present study indicate the residual accommodation was greater after using tropicamide and accommodative responses were still possible at low demand levels (less than 4 D) when tropicamide was used as a cycloplegic agent, although the magnitude of the responses were approximately half of that achieved under physiological conditions. Therefore, unlike previous studies which suggest tropicamide is an adequate cycloplegic agent (Egashira et al., 1993), the findings from this study indicate the depth of cycloplegia is greatest with cyclopentolate and should be the agent used for cycloplegic refractions, at least for young adults. Moreover, the data obtained with the objective method and a distant target in the current study, indicates the maximum cycloplegia occurred at 20 minutes post-instillation of cyclopentolate and 10 minutes post-instillation for tropicamide indicating the onset of cycloplegia is longer with cyclopentolate, at least for eyes with dark brown irides, which is in agreement with Manny et al (1993). Since the majority of participants

recruited for this study had dark irides, proxymetacaine 0.5% was used prior to the instillation of tropicamide or cyclopentolate to increase corneal permeability (Green and Tonjum, 1971), allowing for a greater penetration of the agent at the ciliary muscle. Consequently, the duration of cycloplegia may differ if a topical anaesthetic was not used, especially as evidence from young Chinese participants suggests a rapid onset of the cycloplegic effect in comparison to controls (Siu et al., 1999).

Although topical anaesthetics do not significantly alter the magnitude or rate of onset for mydriasis (Haddad et al., 2007), the effect of the topical anaesthetic on the ciliary muscle morphology is unknown. Therefore, the results found from this study relating to the duration and depth of cycloplegia as well as the morphology of the ciliary muscle may have been influenced by the use of a topical anaesthetic. Considering the effect of prior instillation of a topical anaesthetic to anti-muscarinic agent has not been investigated in relation to ciliary muscle morphology, it would be of interest to determine whether a significant effect occurs.

Indeed, the study was limited by the inability to obtain refraction measurements and ocular biometry measurements simultaneously to ciliary muscle acquisition, which would have provided more information relating to the lenticular and ciliary muscle changes in order to determine whether the lens thinning occurred at a specific time level and the coinciding ciliary muscle parameters during that time. Furthermore, the shorter cycloplegic effect with tropicamide affected the ability to obtain ocular biometry measurements, therefore a comparison of the intraocular parameters with both anti-muscarininc agents could not be achieved. Only young adults with emmetropic refractive errors were recruited for this study, therefore differences in ciliary muscle morphology and ocular biometry may exist between patients with ametropia. Cyloplegia is possible in myopic children (Manny et al., 1993; Lin et al., 1998; Owens et al., 1998) and biometry measurements during cycloplegia have been obtained (Mutti et al., 1994). Myopic children are known to have thinner lenses (Zadnik et al., 1995; Mutti et al., 1998), and a recent report suggests the use of tropicamide results in a thinner and more posterior placed lens in myopic children compared to emmetropes, as well as smaller changes in the anterior segment (Yuan et al., 2015). Therefore, it would be of interest to determine if the same effects occur in myopic adult eyes. Furthermore, there are reports that anti-muscarinic agents such as atropine and pirenzepine slow down the progression of myopia (Tan et al., 2005; Lee et al., 2006., Fan et al., 2007); therefore, the effect of these agents on ciliary muscle morphology is of interest to determine whether there are significant differences in the ciliary muscle characteristics

between emmetropic and myopic eyes which could provide insight into myopia progression. Moreover, pirenzepine and atropine have greater anti-muscarinic effects, therefore, may have provided more information regarding the regions of the ciliary muscle which are involved with accommodation.

Overall, the results from this study indicate anti-muscarinic agents alter ciliary muscle morphology and reduce its contractility, therefore, reducing the accommodative ability of the muscle. Both anti-muscarinic agents showed similar profiles to the reduction in thickness of the muscle in the presence of an accommodative stimulus. However, the greatest reduction in accommodative amplitude occurred with cyclopentolate, which was most likely due to the reduction in centripetal movement and anterior thickening. In contrast, a centripetal movement was still evident with tropicamide. Therefore the results confirm circular fibres within the anterior region of the ciliary muscle are essential for accommodation, in order to produce the centripetal movement and anterior thickening during accommodation. Yet, even though the centripetal movement is necessary for accommodation, as shown from this study, the reduction in centripetal movement cannot explain the full reduction in amplitude, since the centripetal movement was possible in eyes treated with tropicamide, although the amplitude decreased. Rather, the lack of contractile ability of the muscle fibre groups within CM50 and CM75, as well as the contractile shortening, indicates the contraction of the radial and longitudinal fibres are essential to produce the forward movement of the muscle during accommodation.

4.5. Summary

- The main aim of the investigation was to determine the morphological changes which occur to the ciliary muscle *in-vivo* with tropicamide and cyclopentolate in order to identify which regions of the ciliary muscle are involved with accommodation
- Pre-presbyopic emmetropic participants were recruited and attended two visits. The agent instilled at the first visit was randomly chosen and the remaining agent was instilled at the second visit.
- The main findings were:
    - 20 minutes after instillation of the anti-muscarinic agent, when accommodation was relaxed, there was an anterior movement of ciliary muscle mass

    - When accommodation was stimulated, the greatest reduction in the contractility and mobility of the ciliary muscle occurred within 20 minutes post-instillation of either agent
    - When accommodation was stimulated, both agents reduced the thickness at CM25, CM50 and CM75 within 20 minutes of instillation
    - A centripetal movement was still evident after tropicamide instillation. In contrast, the movement was restricted with cyclopentolate
- Overall, the findings suggest circular fibres have a role in producing an anterior shift of ciliary muscle mass during accommodation whereas radial and longitudinal fibres possibly have a significant role in the contractile shortening.

Chapter 5. Is pilocarpine a super-stimulus for ciliary muscle contraction?

5.1. Introduction

Pilocarpine is a parasympathomimetic agent that is effective at the muscarinic receptors of autonomic effector cells (Hopkins and Pearson, 2007), thus, producing pupil miosis and contraction of the ciliary muscle within the eye.

Pilocarpine is used as a treatment option for glaucoma (Hopkins and Pearson, 2007), and also within ophthalmological research, where it is frequently administered to induce accommodation in pseudophakic participants to determine the efficacy of accommodating intraocular lenses (Langenbucher et al., 2003; Findl et al., 2003; Findl et al., 2004; Koeppl et al., 2005b; Kriechbaum et al., 2005). The studies assume pilocarpine is a super-stimulus for accommodation (Koeppl et al., 2005a), however, ciliary muscle contraction induced from pilocarpine has not been studied directly and rather indirect measurements of pharmacologically stimulated accommodation have been determined from anterior chamber depth measures, which reveal a small but significant movement of accommodating intraocular lenses (Koeppl et al., 2005b; Kriechbaum et al., 2005), although the increase to amplitude of accommodation is minimal (less than 0.50 D; Findl et al., 2003). Although a weak correlation has been demonstrated between pharmacological and near-stimulated accommodation for intraocular lens movement, the ability of pilocarpine to produce a significant intraocular lens movement suggests the agent may contract the ciliary muscle fibres to a greater extent than possible under physiological conditions, and therefore, produce an anterior shift of the ciliary body toward the scleral spur (Kriechbaum et al., 2005).

The effect of near stimulated and pilocarpine stimulated accommodation on anterior chamber depth, lens thickness and distance of the anterior and posterior lens surface, has been investigated in phakic individuals (Koeppl et al., 2005a). Data from 10 emmetropic pre-presbyopes (mean age 24 years) revealed no difference between the two accommodation stimulus methods for the reduction to the anterior chamber depth, increase to lens thickness or forward movement of the posterior lens surface. In contrast, results from 11 emmetropic presbyopes (mean age 58 years) demonstrated accommodative ability during near-stimulated accommodation as evident from the reduction in the anterior chamber depth (27 ± 29 µm) and a thickening of the lens (10 ± 15 µm). However, pilocarpine produced a significant movement of the anterior lens surface as well as a significant increase to the lens thickness (mean thickening 50 ± 46

μm). The change in biometric measurements were significantly different between pharmacological and physiological manipulation of the accommodative system, suggesting pilocarpine provides a greater accommodative effect in presbyopic individuals. A greater objective amplitude of accommodation with pilocarpine has been reported within presbyopic participants in comparison to pre-presbyopes, nevertheless, the magnitude between blur-stimulated and pilocarpine stimulated amplitude for an age range 46-50 years is approximately 0.50 D (Ostrin and Glasser, 2004), indicating pilocarpine does not induce a substantial increase in accommodation.

Clearly, pilocarpine does induce accommodative changes. Early reports with ultrasonic biometry also revealed a thickening of the lens (mean thickening 0.32 mm) and a reduction to the anterior chamber depth (reduction 0.29 mm) when pilocarpine 2% was administered in pre-presbyopes (Abramson et al., 1972). Parasympathomimetic agents produce greater amplitudes in primates (between 11 and 34 D of accommodation; Koretz et al., 1987; Bito et al., 1982; Crawford et al., 1989; Vilpuru and Glasser, 2002) in comparison to the direct stimulation of the Edinger-Westphal nucleus which stimulates between 10 D and 18 D of accommodation (Koretez et al., 1987; Crawford et al., 1989; Vilpuru and Glasser, 2002). Furthermore, within rhesus monkeys the movement of the ciliary processes are greater when pharmacological agents are instilled, in comparison to Edinger-Westphal stimulation, whereas a greater movement of the lens edge is elicited with electrical stimulation, suggesting both methods of accommodation stimulation may alter ciliary muscle morphology differently (Ostrin and Glasser, 2007). Pilocarpine stimulated accommodation produces a statistically significant reduction in the anterior chamber depth (-1.54%), but not lens thickness in guinea pigs (Ostrin et al., 2014). Although Ostrin and colleagues (2014) attempted to image the ciliary body, poor identification of the ciliary body boundary prevented analysis of the structure. However, the authors discussed the possibility of an underdeveloped ciliary muscle in guinea pig eyes compared with humans and monkeys, since repeated doses of pilocarpine were required to elicit the reported findings.

Variability of the accommodative response has been documented in monkeys (e.g. Wendt et al., 2008) and humans (Abramson et al., 1973; Wold et al., 2003; Ostrin and Glasser, 2004; Koeppl et al., 2005a). Abramson and colleagues (1973) reported lens thickening in all presbyopic participants, however, only 85% of eyes showed a reduction in anterior chamber depth (Abramson et al., 1973). A possible cause for the variation in humans may be iris colour especially since greater amplitudes (mean 8.90

D) can be achieved in eyes with lighter irides, in comparison to dark irides (mean 3.53 D; Wold et al., 2003), whereas in monkeys, the method of pilocarpine administration is the most likely cause for the variability (Wendt and Glasser 2010). Moreover, variability of the effect of pilocarpine within the accommodative apparatus is also evident within guinea pigs where an increase in lens thickness does not always occur (Ostrin et al., 2014).

Pupil miosis which results from the use of pilocarpine restricts the ability to obtain objective refraction measurements with autorefractors, therefore, the duration and time for the maximum effect of the agent cannot always be determined easily. However, the Hartinger coincidence refractometer, which is based on the Scheiner principle, can provide refraction data for miotic pupils that are 1 mm or 2 mm in size (Fincham, 1937). Consequently, the maximum effect of pilocarpine 6% has been reported as 33 minutes in a youthful group with a mean age of 26 years (Wold et al., 2003). An early study suggests the effect of pilocarpine occurs within 15 minutes, with maximum effect occurring between 45 and 60 minutes post-instillation within presbyopic eyes (Abramson et al., 1973), whereas a maximum effect has been reported between 30 and 60 minutes in pseudophakic eyes (Kriechbaum et al., 2005). In order, to overcome the pupil miosis some researchers utilise phenylephrine (Ostrin and Glasser, 2004) due to the minimal effect on the accommodative amplitude (Mordi et al., 1986a). Furthermore, low dose phenylephrine (2.5%) does not affect the ciliary muscle dimensions or contractility for moderate accommodative stimuli (Richdale et al., 2012). However, high concentrations of phenylephrine (3 drops of 10%) have been utilised to overcome miosis in order to investigate the wave front aberrations during pilocarpine stimulated and blur stimulus (physiological) accommodation within young phakic participants with a mean age of 27 years (Plainis et al., 2009). The researchers reported an exponential decrease of pupil miosis with time before plateauing between 60 and 90 minutes. However, there was variability in the change to the pupil diameter per dioptre change in accommodative response (between 0.29 mm per dioptre to 1.54 mm per dioptre), possibly due to the inconsistency of accommodative responses induced by pilocarpine.

Examination of histological ciliary muscle sections from donors aged between 1 and 107 years old, which have been treated with pilocarpine, reveal an overall shortening to the ciliary muscle length and posterior length and a narrowing of the ciliary muscle width, indicating the ciliary muscle maintains its contractility throughout life (Pardue and Sivak, 2000).

Pilocarpine is utilised in accommodation research and is often referred to as a super-stimulus for accommodation. However, it is evident the effect is variable between individuals as established from refraction measurements and ocular biometry. Yet, the influence of the agent upon the ciliary muscle contractility and morphology has not been determined *in-vivo*. Such analysis could provide insight into the regions of the muscle, and consequently, the muscle fibre groups, which have a role in accommodation. Furthermore, the variability of pilocarpine between pre-presbyopes and presbyopes suggests the effect of pilocarpine between the different age groups may differ.

Consequently this study aimed to determine whether pilocarpine is a super-stimulus for accommodation by investigating the effect of the agent on the ciliary muscle morphology *in-vivo*, within pre-presbyopic and presbyopic eyes. Furthermore, the investigation of the ciliary muscle fibre groups which are likely to be involved in accommodation were further explored by comparing data from a sub-group of participants who participated in the study detailed in Chapter 4.

5.2. Methods

The study was conducted in accordance to the tenets of the Declaration of Helsinki. Written and verbal information was provided to participants before they provided written consent for their participation. A favourable opinion was provided by Aston University Research Ethics Committee before the study commenced.

5.2.1. Sample size

The number of participants required for this study was calculated from a statistical power test using G*power (version 3.1.9.2; Universitat Kiel, Germany). In order to measure a medium effect size (f=0.25), based on a within subject ANOVA design and a desired statistical power (1-β) of 90% with an error probability (α) of 0.05, at least 26 pre-presbyopic and 26 presbyopic participants were required.

5.2.2. Participants

Volunteers were recruited from the optometry undergraduate cohort through email announcements.

Inclusion criteria

The same inclusion criteria was used as outlined in Chapter 4, section 4.2.2, for recruiting pre-presbyopic and presbyopic participants. Only emmetropic individuals were included, for the same reasons explained in the previous chapter. In addition, myopic individuals were excluded due to the increased risk of retinal detachment documented in myopes with the use of miotics (Singh, 1985).

Visual acuity and refractive error

The procedure has been described in Chapter 3, section 3.2.2. Participants were classified as emmetropic if the MSE was within the range -0.50 to +0.75 DS.

5.2.3. Procedure

Accommodative response determined with Grand Seiko *WAM 5500*

The procedure for determining the accommodative response was replicated from Chapter 3, section 3.2.3 and is referred to as physiological accommodation throughout this chapter. The stimulus used for this study was the ETDRS letter chart which was placed 2.5 metres behind the participant and 5 metres away from the mirror (see Figure 3-2). The maximum objective accommodation was determined for each participant. The pre-presbyopes and presbyopes were instructed to keep the lowest line of letters they could see clear as the objective accommodative response was measured for all demand levels.

Visante AS-OCT

The ciliary muscle images were acquired from the temporal aspect, as described in Chapter 4, section 4.2.3. The ciliary muscle images were acquired during relaxed accommodation and per dioptre of accommodation up to the individually determined amplitude of accommodation.

LenStar LS900

Ocular biometry measurements were obtained at relaxed accommodation and at the maximum amplitude for each participant, using the same procedure outlined in Chapter 4, setion 4.2.3.

Health examination prior to drug instillation

The same procedure was completed as described in Chapter 4, section 4.2.3.

Instillation of parasympathomimetic agent

After baseline data were obtained for refractive error, objective accommodation, ocular biometry and ciliary muscle images, one drop of 0.5 % proxymetacaine (*Minims* preparation) was instilled into the lower fornix of the right eye followed by 2 drops of 2% pilocarpine nitrate (*Minim* preparations). Participants were instructed to close their eyes and occlude the punctum to reduce systemic absorption of the agent for approximately 30 seconds.

The badal system used for the autorefractor, AS-OCT and LenStar were set to ensure a 0 D accommodative demand level since pharmacological stimulation of the ciliary muscle provided the accommodative response. Data for refractive error, ocular biometry and ciliary muscle images were acquired every 10 minutes post-instillation of the agent. However, pupil miosis produced pupil sizes less than 2.3 mm, the minimum size required for measurements with the autorefractor, therefore, data for refractive error measurements could not be obtained for all participants at all time intervals examined. The end point of the study was determined from ocular biometry, when three consecutive anterior chamber depth measurements were the same.

At the end of each visit, intraocular pressure was determined with the i-care tonometer (Davies et al., 2006) and a leaflet provided to the patients regarding the instillation of the drug and advice relating to adverse effects.

5.2.4. Statistical analysis

A Shapiro-Wilk test (SPSS Statistics 21; SPSS Inc., Illinois, USA) revealed normal distribution of the parameters analysed for the study. Therefore, assumptions of normality and homogeneity of variance were met. A repeated measures analysis of variance (ANOVA) was performed (Armstrong et al., 2011) to determine the effect of physiological accommodation on the ciliary muscle parameter as well as the effect of pilocarpine on the ciliary muscle parameter over time. A repeated measures ANOVA was also conducted for the ocular biometry data to determine the effect of pilocarpine on the intraocular parameters. Greenhouse Geisser results are reported and post-hoc comparisons were determined using Bonferroni correction.

5.3. Results

In order to account for attrition due to the variability from the time course of the agent to produce its maximum accommodative effect, 35 pre-presbyopic participants were recruited for the study. Due to poor physiological accommodative responses (n= 1) the

inability to obtain anterior chamber depth measurements at all time intervals (n= 1), inadequate pupil miosis suggesting an insufficient effect of the agent at the muscarinic receptors (n= 3), these data were excluded. The end point for the study was reached at 60 minutes for 27 participants and 70 minutes for three participants. Therefore, data are presented for 27 participants whose end point was achieved at 60 minutes with a mean refractive error -0.18 (SD 0.48) D and mean age 19.6 (SD 0.36) years. Iris colour was classified according to the criteria by Seddon et al (1990). Twenty four participants had dark brown irides (grade 5) and three participants had a light brown or green iris (grade 4).

Recruiting emmetropic presbyopic participants within the inclusion criteria defined for this study was difficult, and overall, four presbyopic participants were able to participate with a mean refractive error 0.01 (SD 0.49) and mean age 45.8 (SD 4.78) years. All participants had an iris colour of grade 4. Due to the small sample size, the observed power for all the ciliary muscle parameters investigated were determined. The post-hoc results indicated there was insufficient power for the presbyopic sample size included in the present study.

Figure 5-1 shows the physiological objective accommodative response for the accommodative demand levels tested in this study. Twenty four pre-presbyopic participants were able to accommodate to all demand levels up to 8 D whereas 3 participants were only able to accommodate to the 7 D demand level. It is clear from the graph, there is a greater variability in the accommodative response at the higher demand levels (7 D and 8 D) as indicated by the larger error bars. As expected, the amplitude of accommodation for presbyopes was lower than the pre-presbyopes; there was a gradual increase in the accommodative response up to 3 D and it is clear from Figure 5-1, the response declined at 4 D demand levels and above.

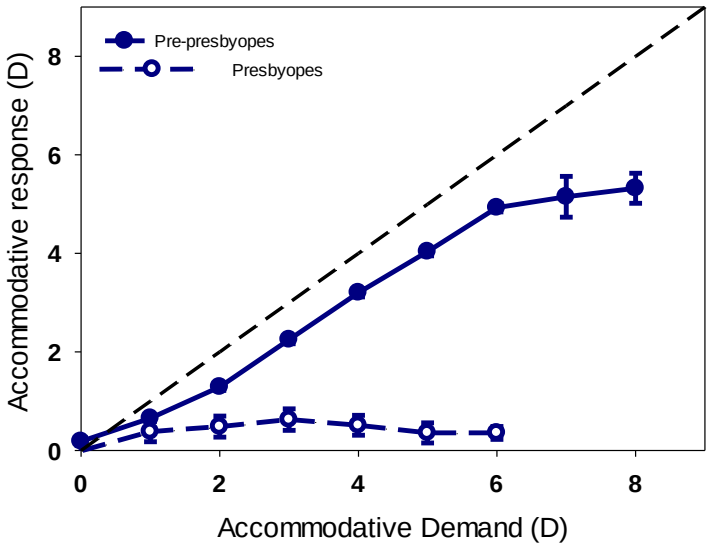

Figure 5-1. The accommodative demand-response curve for 27 pre-presbyopes and 4 presbyopes, during blur-driven (physiological) accommodation.

The results for the ciliary muscle parameters at each accommodative demand level tested, are shown in Appendix 2 Table A2-1 for the pre-presbyopes and Table A2--2 for the presbyopes. Analysis of the mean baseline data between both groups reveals the presbyopic ciliary muscle is shorter and also thinner than the pre-presbyopic muscle.

5.3.1. The effect of physiological accommodation on ciliary muscle morphology within a pre-presbyopic and presbyopic cohort

Since all pre-presbyopic participants were able to accommodate to the 7 D demand level, the physiological response of the ciliary muscle for every accommodative demand level between 0 D and 7 D were obtained, prior to the instillation of pilocarpine. Ciliary muscle images were acquired up to the 5 D demand level for the presbyopic cohort, prior to the instillation of pilocarpine.

There was an insignificant effect of accommodation on the ciliary muscle thickness at CMT1 within the pre-presbyopic muscle ($F_{1.579}$, p= 0.652) and presbyopic muscle ($F_{0.276}$, p= 0.797), as well as an insignificant accommodative effect at CMT2 for pre-presbyopes ($F_{0.825}$, p= 0.538) and presbyopes ($F_{1.324}$, p= 0.335). As shown in Figure 5-2 A, the ciliary muscle thickness at CMT3 for the pre-presbyopes significantly reduced for all accommodative demand levels ($F_{8.882}$, p= 0.000), with post-hoc pairwise comparisons indicating the significant changes were between 0 D and 6 D (mean difference 20.0 µm, p= 0.015) and between 0 D and 7 D demand levels (mean

difference 29.0 µm, p= 0.000). Although there was an indication of a reduced thickening within the region for the presbyopic cohort, especially up to the 3 D demand level, theses changes were not significant ($F_{1.324}$, p= 0.335). There was a thinning within CM25 region up to 2 D demand level, which was of a greater magnitude within the presbyopes than the pre-presbyopes, as shown in Figure 5-2 B. There was significant thickening at CM25 within the pre-presbyopic ciliary muscle ($F_{4.190}$, p =0.002) specifically between the 2 D and 6 D demand level (mean difference 25.0 µm, p= 0.035). However, the effect of accommodation at CM25 was insignificant within the presbyopic cohort ($F_{0.831}$, p= 0.484). Figure 5-2 C shows the ciliary muscle thickness at CM50 and it is clear there was a thinning within the region for the 1 D and 2 D accommodative demand levels within the pre-presbyopic cohort, and up to the 3 D demand level for the presbyopic cohort. There was a thickening of the pre-presbyopic ciliary muscle between 2 D and 3 D accommodative demand levels, and between 4 D and 6 D accommodative demand levels. However, there was no significant effect of accommodation on the thickness of the muscle at CM50 for the pre-presbyopic cohort ($F_{1.989}$, p= 0.085) or presbyopic cohort ($F_{1.528}$, p= 0.294). There was no significant effect of accommodation at CM75 for the pre-presbyopic ($F_{0.580}$, p= 0.716) or presbyopic cohort ($F_{1.386}$, p= 0.323).

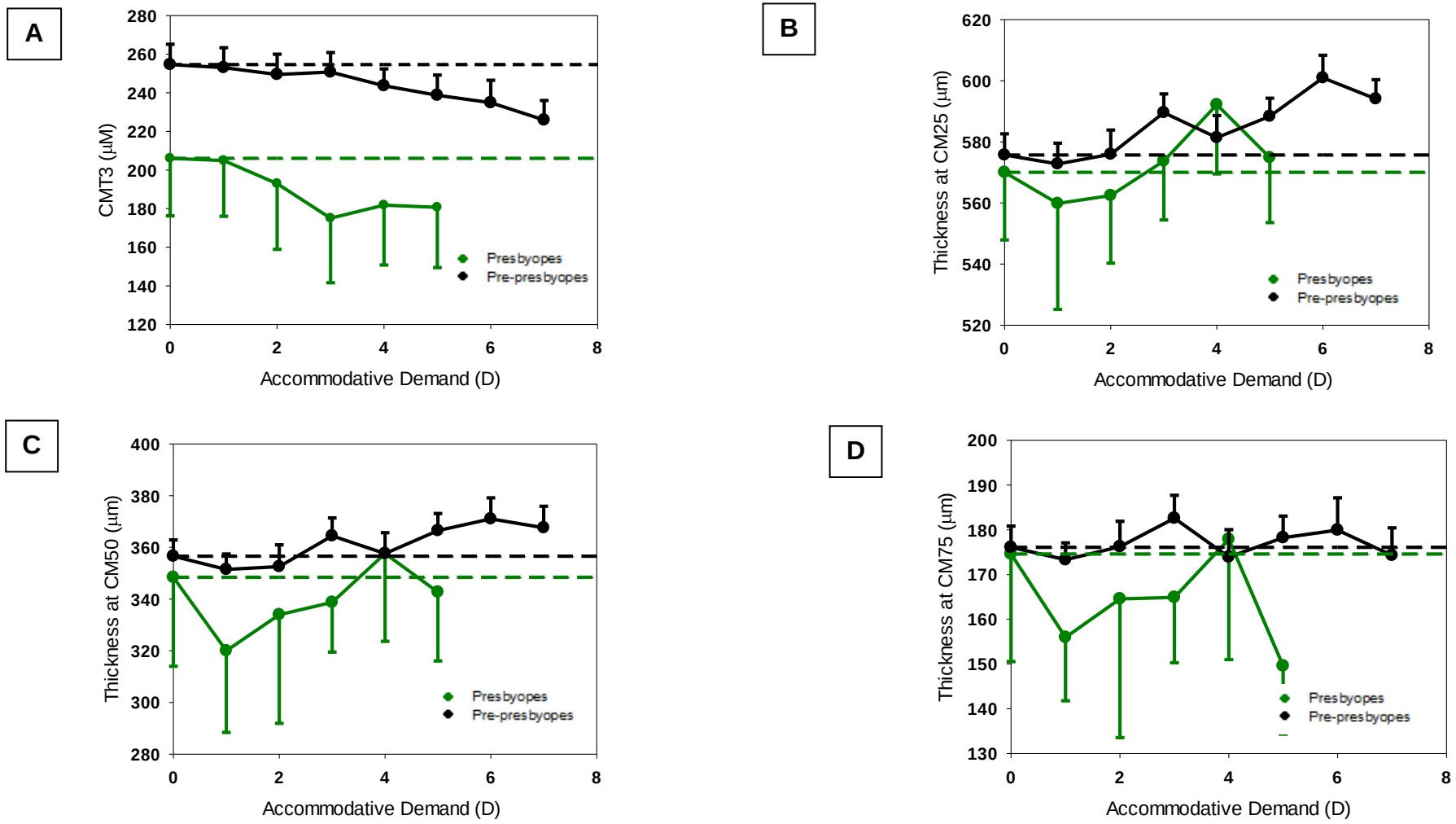

Figure 5-2. The ciliary muscle thickness at various accommodative demand levels A: CMT3, B: CM25, C: CM50 and D: CM75 for the pre-presbyopes (mean + 1 SEM) and presbyopes (mean – 1 SEM).

The ciliary muscle thickness at CMMax significantly increased with accommodative effort within the pre-presbyopes ($F_{4.400}$, p= 0.001) as seen in Figure 5-3 A, although there were no significant mean differences between the thicknesses at the different demand levels. There was also a significant reduction to the ciliary muscle length with accommodation within the pre-presbyopic cohort ($F_{5.712}$, p= 0.000), particularly between 0 D and 5 D demand levels (mean difference 0.19 µm, p= 0.041), 0 D and 6 D demand levels (mean difference 234.0 µm, p= 0.016) and 0 D and 7 D demand levels (mean difference 280.0 µm p= 0.020), as shown in Figure 5-3 B suggesting the contractile shortening of the ciliary muscle is greatest at higher accommodative demand levels. Furthermore, within the pre-presbyopic cohort there was a significant effect of accommodation on the anterior length ($F_{3.479}$, p= 0.007), particularly between 0 D and 7 D demand levels (mean difference 56.0 µm, p= 0.032), as seen in Figure 5-3 C. There was also a significant effect of accommodation on the distance between the scleral spur and inner apex, which became shorter with accommodation indicating a possible forward movement of ciliary muscle mass and a centripetal movement ($F_{2.519}$, p= 0.039), although there were no significant mean differences to the distance between different demand levels.

Within the presbyopic cohort, there was an insignificant effect of accommodation at CMMax ($F_{1.642}$, p= 0.265), distance between the scleral spur and inner apex (SS-IA; $F_{1.152}$, p= 0.377), the anterior length ($F_{1.317}$, p= 0.337) and the ciliary muscle length arc ($F_{4.136}$, p= 0.064).

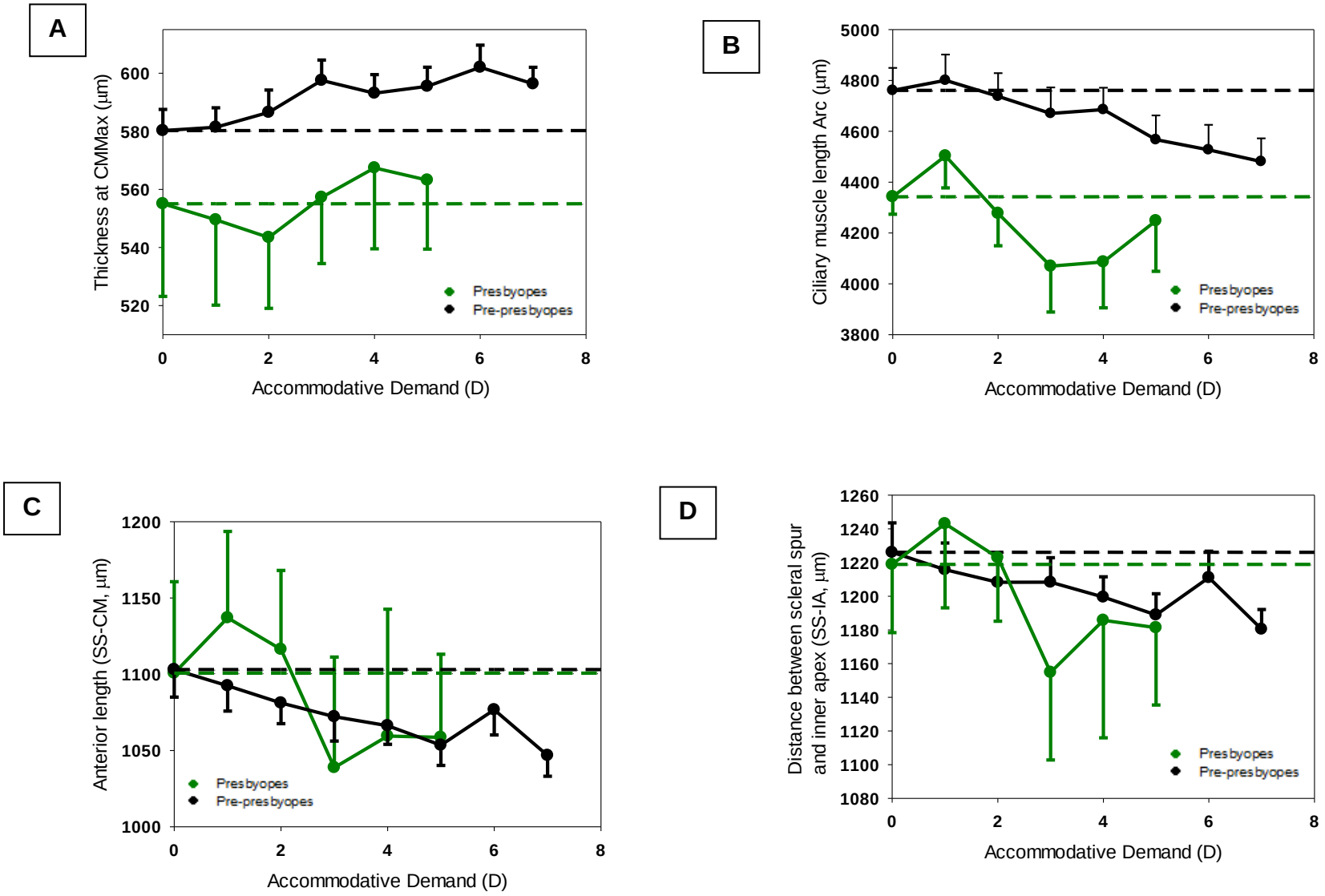

Figure 5-3. Mean (1 SEM) ciliary muscle parameter at various accommodative demand levels. A: CMMax, B: ciliary muscle length arc, C: anterior length (SS-CM), D: SS-IA for the pre-presbyopes and presbyopes.

5.3.2. The effect of pilocarpine stimulated accommodation on ciliary muscle morphology within a pre-presbyopic and presbyopic cohort

Post-instillation of pilocarpine revealed a significant reduction to the thickness at 3mm posterior to the scleral spur (CMT3) over time ($F_{5.518}$, p= 0.002), particularly between baseline (0 minutes) and 50 minutes (mean difference in CMT3 34µm, p= 0.013), within the pre-presbyopic cohort (see Figure 5-4 A). Although there was a reduction to the ciliary muscle thickness within CMT3 of the presbyopic cohort, the thinning was insignificant ($F_{2.204}$, p= 0.226).

Pilocarpine also produced a statistically significant thickening at CM25 within the pre-presbyopic cohort as seen in Figure 5-4 B, indicating a contraction of the ciliary muscle ($F_{2.992}$, p= 0.015), although not between any particular time intervals as indicated from the post-hoc comparisons. There was an increased thickening at CM25 post-instillation of pilocarpine within the presbyopic cohort up to 30 minutes, however, the effect of pilocarpine on the thickness was insignificant ($F_{1.119}$, p =0.389). Pilocarpine produced a significant thickening to CM50 over time within the pre-presbyopic cohort ($F_{2.782}$, p= 0.022), which was nearly significant between baseline (0 minutes) and 20 minutes (mean difference 0.026 µm, p= 0.055). There was an insignificant effect of pilocarpine on the thickness at CM50 within the presbyopic cohort ($F_{1.48`}$, p= 0.292). Pilocarpine produced two phases of thickness changes at CM75 within the pre-presbyopic muscle, although the effect of the agent over time was insignificant ($F_{1.017}$, p=0.409). A thickening within the region was evident up to 20 minutes, which reached baseline levels at 30 minutes, before increasing in thickness again. However, there was an insignificant effect of pilocarpine on the ciliary muscle thickness within the region over time within the presbyopic cohort ($F_{1.428}$, p= 0.306).

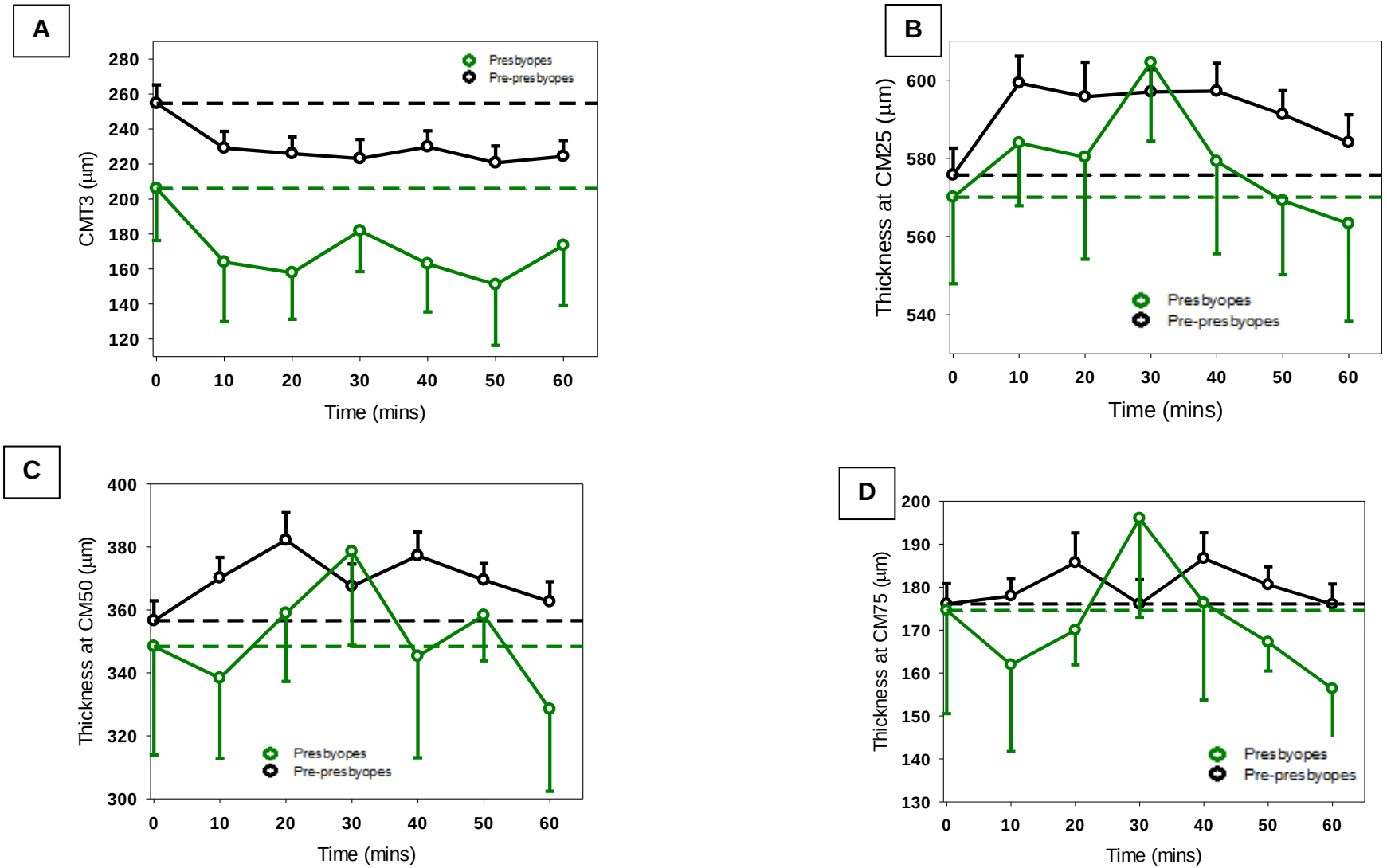

Figure 5-4. The ciliary muscle thickness over regular time intervals post-instillation of pilocarpine for pre-presbyopes (mean + 1 SEM) and presbyopes (mean – 1 SEM). 0 minutes refers to baseline measurements. A: CMT3, B: CM25, C: CM50, D: CM75.

The thickness at CMMax increased between baseline and 10 minutes post-instillation of pilocarpine which was significant ($F_{3.070}$, p=0.015) for the pre-presbyopes (mean difference 21 µm, p= 0.026). A gradual decrease in thickness consequently occurred, indicating the effect of pilocarpine was reducing, although no significant differences between time intervals were evident from post-hoc comparisons. A similar profile is also evident for the presbyopes as seen in Figure 5-5 A, although the increased thickening was insignificant ($F_{0.365}$, p= 0.686). Pilocarpine produced a significant shortening of the anterior length over time within the pre-presbyopic cohort ($F_{3.972}$, p= 0.008), although there were no significant post-hoc comparisons for time intervals. Within the pre-presbyopic cohort, pilocarpine also significantly reduced the distance between the scleral spur and inner apex over time ($F_{3.021}$, p= 0.025), indicating a centripetal movement was possible. However, post-hoc pairwise comparisons did not reveal significant differences to the ciliary muscle thickness influenced by pilocarpine between any particular time intervals. Pilocarpine induced a significant contractile shortening of the ciliary muscle ($F_{8.839}$, p= 0.000), which was significant between baseline and all time intervals (p <0.005), indicating the contractile shortening is a vital aspect for accommodation.

There was an insignificant effect of pilocarpine on the reduction to the anterior length ($F_{2.157}$, p=0.220), distance between the scleral spur and inner apex (SS-IA; $F_{2.762}$, p= 0.164) and ciliary muscle length arc ($F_{4.136,}$ p= 0.064) within the presbyopic cohort.

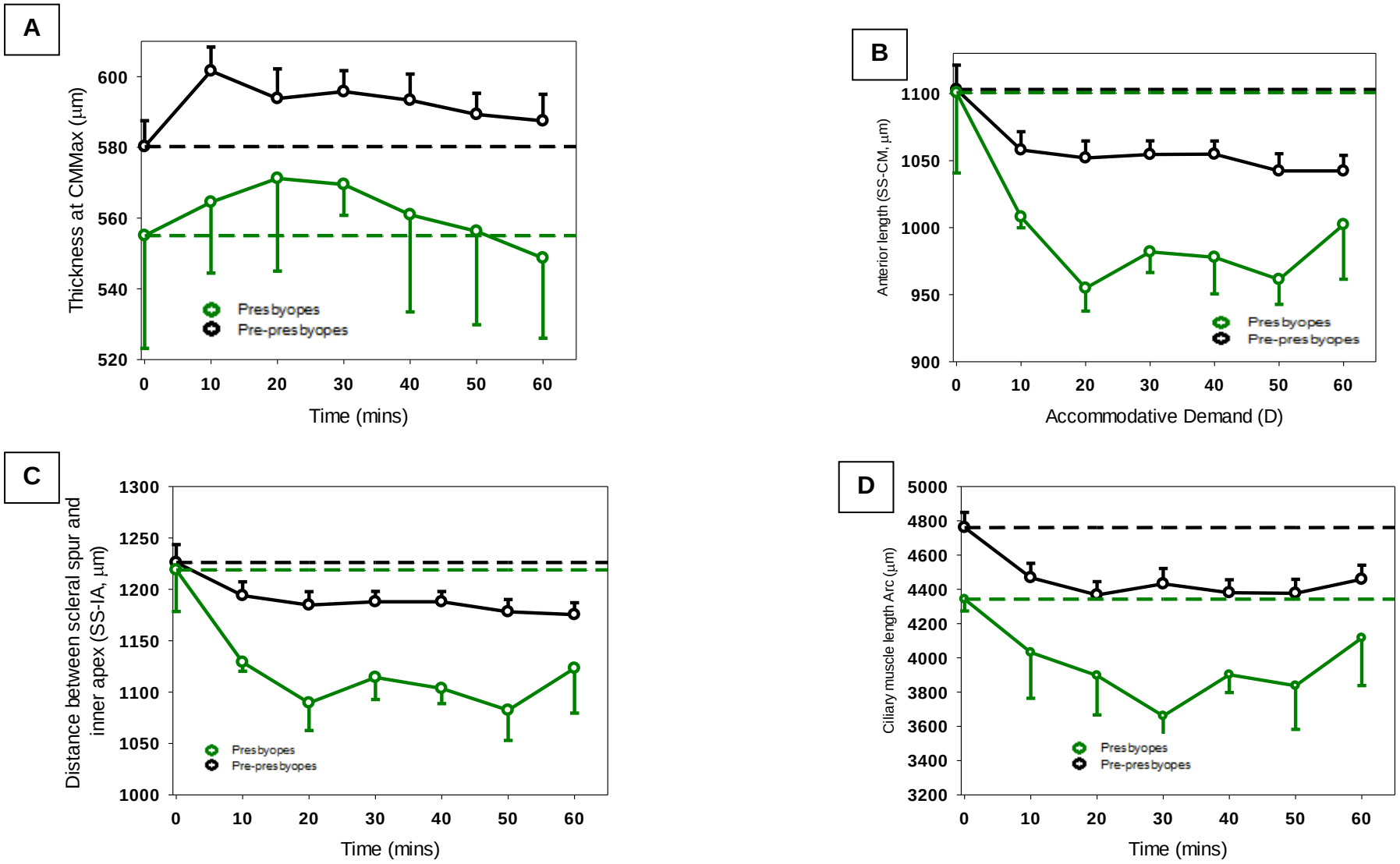

Figure 5-5. Ciliary muscle parameter over time with pilocarpine. A: CMMax, B: anterior length (SS-CM), C: SS-IA, D: CMLength Arc for the pre-presbyopes (mean + 1 SEM) and prebyopes (mena – 1 SEM).

5.3.3. Ocular biometry and pilocarpine

Ocular biometry measurements were taken for each participant prior to the instillation of pilocarpine and every 10 minutes post-instillation. Within the pre-presbyopic cohort, the corneal thickness, anterior chamber depth and axial length measurements were obtained from all participants. However, lenticular thickness was difficult to obtain in a majority of the participants at all time intervals assessed within the study. Therefore, complete data for lens thickness for the duration of the study was obtained from 8 participants. In contrast, the lens thickness measurements were acquired from all the presbyopic participants. For the 8 pre-presbyopic participants, the mean lens thickness at baseline was 3.62 mm (SE 0.08), and the thickness increased 10 minutes post-instillation of pilocarpine (mean 3.75 mm (SE 0.13)), and 20 minutes (mean 3.79 mm (SE 0.12)), followed by a reduction in thickness at 30 minutes (mean 3.78 mm (SE 0.13)) which continued until the end point of the study (at 60 minutes the mean thickness was 3.76 mm (SE 0.13)). There was a significant effect of pilocarpine on the lens thickness ($F_{6.601}$, p= 0.027) specifically between 10 and 20 minutes (mean difference 0.44 mm, p= 0.026).

Within the presbyopic cohort, a similar pattern was evident. There was an increase in lens thickness from baseline (mean thickness 4.41 (SE 0.02) mm) to 10 minutes (mean thickness 4.48 (SE 0.02) mm) and 20 minutes (mean thickness 4.49 (SE 0.02) mm) which remained constant up to 60 minutes, when a reduction in thickness was evident (mean thickness 4.48 (SE 0.03) mm). For both groups, the lens thickness did not return to baseline levels throughout the duration of the study and was thicker than baseline levels at the end of the study (60 minutes).

The corneal thickness, anterior chamber depth and axial length measurements for all the pre-presbyopic cohort are shown in Table 5-1, and the presbyopic cohort is shown in Table 5-2. There was an insignificant effect of pilocarpine on the corneal thickness within the pre-presbyopic ($F_{0.512}$, p= 0.499) and presbyopic ($F_{0.719}$, p= 0.502) cohort. There was also an invariant change to the axial length within the pre-presbyopic ($F_{0.685}$, p= 0.425) and presbyopic ($F_{3.209}$, p= 0.269) cohort. However, axial length measurements for each time interval post-instillation of pilocarpine, have not been corrected for the error induced as a consequence of the reduced anterior chamber depth and increased lenticular thickness which occurs during accommodation, since a measurement of lens thickness was not possible for a majority of pre-presbyopic participants. Also, objective refraction measurements could not be obtained for all

participants with the autorefractor, in order to approximate lens thickness measurements using Norrby's equations (2005).

Pilocarpine produced a gradual and insignificant change to the anterior chamber depth of the pre-presbyopic cohort ($F_{26.418}$, p= 0.363). There was a gradual decrease in the anterior chamber depth for the presbyopic cohort within 20 minutes post-instillation of pilocarpine, followed by a steep decrease at 30 minutes (shown in Figure 5-6) suggesting the maximum effect of pilocarpine was achieved. There was an insignificant change to the anterior chamber depth with pilocarpine within the presbyopic cohort ($F_{1.785}$, p= 0.260).

Ocular parameter	**Time (min)**						
	0	10	20	30	40	50	60
Corneal thickness (µm)	540 (SE 6.32)	539.57 (SE 6.19)	538.73 (SE 6.15)	539.16 (SE 5.99)	537.89 (SE 6.07)	538.07 (SE 6.00)	537.57 (SE 6.05)
Anterior chamber depth (mm)	3.03 (SE 0.05)	2.94 (SE 2.89)	2.89 (SE 0.05)	2.88 (SE 0.05)	2.88 (SE 0.05)	2.89 (SE 0.05)	2.90 (SE 0.05)
Axial length (mm)	23.63 (SE 0.16)	23.58 (SE 0.17)	23.56 (SE 0.17)	23.56 (SE 0.17)	23.55 (SE 0.17)	23.56 (SE 0.17)	23.56 (SE 0.17)

Table 5-1. Ocular biometry measurements at each time interval post-instillation of pilocarpine for 27 pre-presbyopes. 0 minutes refers to baseline. Data are presented as the mean ± 1 SE. The raw axial length data are presented.

Ocular parameter	Time (min)						
	0	10	20	30	40	50	60
Corneal thickness (µm)	527.92 (SE 20.02)	529.42 (SE 19.47)	529.92 (SE 19.36)	529.67 (SE 19.86)	530.42 (SE 20.08)	529.33 (SE 19.18)	529.50 (SE 19.59)
Anterior chamber depth (mm)	2.76 (SE 0.14)	2.73 (SE 0.13)	2.68 (SE 0.12)	2.50 (SE 0.15)	2.67 (SE 0.12)	2.68 (SE 0.13)	2.67 (SE 0.12)
Axial length (mm)	23.83 (SE 0.42)	23.84 (SE 0.42)	23.93 (SE 0.46)	23.82 (SE 0.41)	23.82 (SE 0.42)	23.82 (SE 0.42)	23.82 (SE 0.42)

Table 5-2. Ocular biometry measurements at each time interval post-instillation of pilocarpine for 4 presbyopes. 0 minutes refers to baseline. Data are presented as the mean ±1 SE. The raw axial length data are presented.

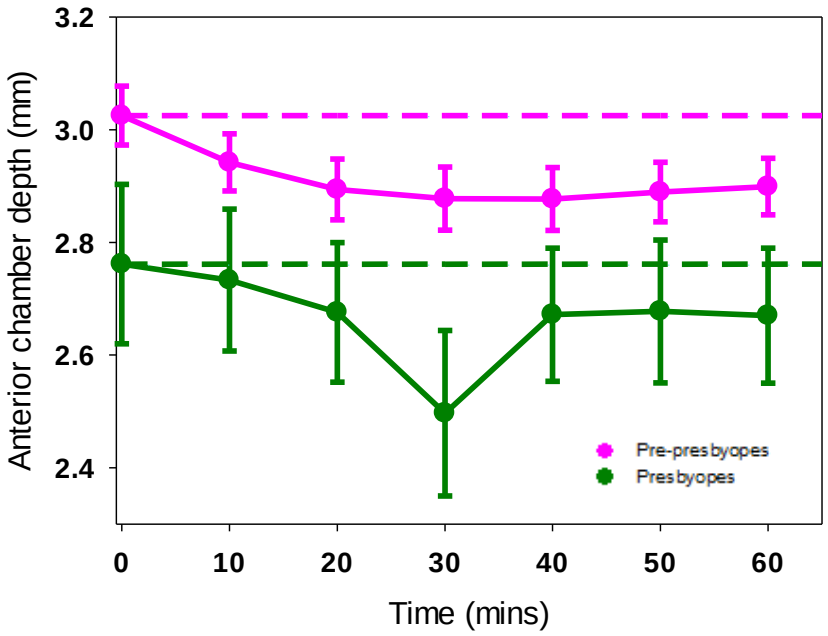

Figure 5-6. The mean (± 1 SEM) anterior chamber depth at regular time intervals post-instilation of pilocarpine. 0 minutes refers to baseline.

5.3.4. Objective refraction measurements

During the time course of the study, pilocarpine produced pupil miosis, therefore measurements of objective refraction with the Grand Seiko WAM 5500 autorefractor could not be obtained from 2 participants with green irides (grade 4) and 4 participants with dark brown (grade 5) irides, within the pre-presbyopic cohort. The data which could be obtained from the 21 remaining participants were recorded at each time interval. 10 minutes post-instillation revealed a mean accommodative response of 0.93 D (SE 0.15), at 20 minutes the mean was 1.83 D (SE 0.22), 30 minutes the mean response was 2.10 D (SE 0.27), at 40 minutes the mean response decreased to 2.09 D (SE 0.30), which further declined at 50 minutes (mean 1.74 D (SE 0.22) and 60 minutes (mean 1.44 D (SE 0.22)). Therefore, the maximum accommodation response induced with pilocarpine was slightly over 2 D and the maximum effect of pilocarpine occurred at 30 minutes. Figure 5-7 shows the variability in the accommodative responses at each time interval, by the larger error bars.

Within the presbyopic cohort the objective refraction measurements were unable to be measured for 3 of the 4 participants at each time interval since the pupil size was smaller prior to the instillation of pilocarpine and the miosis increased after the instillation of the agent, preventing further measurements with the autorefractor. Therefore, autorefraction data for the presbyopes has not been analysed.

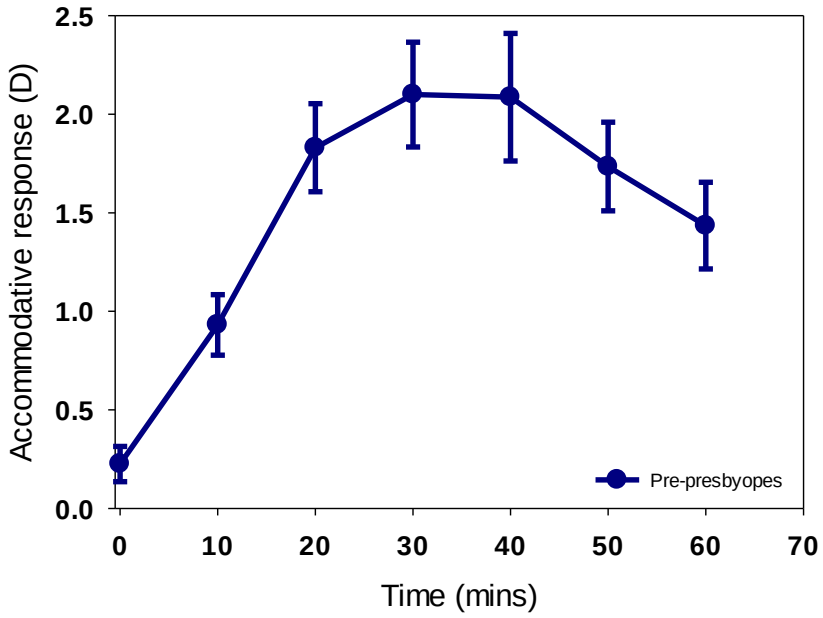

Figure 5-7. The accommodative response curve over time for 21 pre-presbyopes during pilocarpine stimulated accommodation (mean ± 2 SEM).

5.3.5. Comparison of the ciliary muscle morphology with pilocarpine and cyclopentolate in a sub-group of participants

A sub-group of participants (n= 10) participated in the study described in Chapter 4, and the current study. In order to gain a greater understanding of the regions within the ciliary muscle which are most likely involved in accommodation, the data for the sub-group of participants obtained under maximum cycloplegia with the use of cyclopentolate, were compared to the data obtained after the instillation of pilocarpine. Cyclopentolate therefore induced a maximally relaxed ciliary muscle, whereas, pilocarpine caused a contraction of the ciliary muscle. The washout period between both studies was 2 months. The average age of the participants was 19.8 (SE 0.70) years and mean refractive error was -0.14 D (SE 0.13). Eight participants had a dark brown iris (grade 5) and two participants had a green or light brown iris (grade 4). The autorefraction data could not be obtained from one participant throughout the duration of study due to pupil miosis, therefore their results were omitted from the amplitude of accommodation data. The maximum physiological accommodation for the remaining 9 participants was 6.07 D (SE 0.35), and the maximum accommodation achieved with pilocarpine stimulated accommodation was 2.71 D (SE 0.65) at 40 minutes.

Figure 5-8 and 5-9 shows the results for ciliary muscle thickness and length. Cyclopentolate produced a thickening 3 mm posterior to the scleral spur (CMT3) over time specifically up to 30 minutes, whereas pilocarpine produced a thinning within the region up to 30 minutes, as seen in Figure 5-8 A. There were no significant differences to the ciliary muscle thickness between the agents within the region. Both cyclopentolate and pilocarpine increased the thickening within CM25 over time, although the increase was greater with pilocarpine, therefore indicating a contraction of the ciliary muscle within the region. The likely cause of the thickening with cyclopentolate was probably due to the ciliary muscle mass moving anteriorly over time. The differences to the ciliary muscle thickness were significant between both agents ($F_{19.910}$, p= 0.000). Similar profiles were also evident for CM50 and CM75, as seen in Figure 5-8 C and D, and the difference in the thickening between both agents were also significant (CM50: $F_{15.590}$, p= 0.001; CM75: $F_{10.975,}$ p= 0.004). Both pilocarpine and cyclopentolate produced a greater distance between the scleral spur and inner apex, although the difference between both agents were not significant ($F_{0.514}$, p= 0.483). Both agents increased the anterior length, and there was an invariant difference between both agents within the region ($F_{1.187}$, p= 0.290). Ciliary muscle length arc reduced over time with cyclopentolate, specifically within 30 minutes, possibly due to a

forward movement of the ciliary muscle mass. Pilocarpine produced a contractile shortening of the muscle over time, and the difference in length between both agents was significant ($F_{16.572}$, p=0.001).

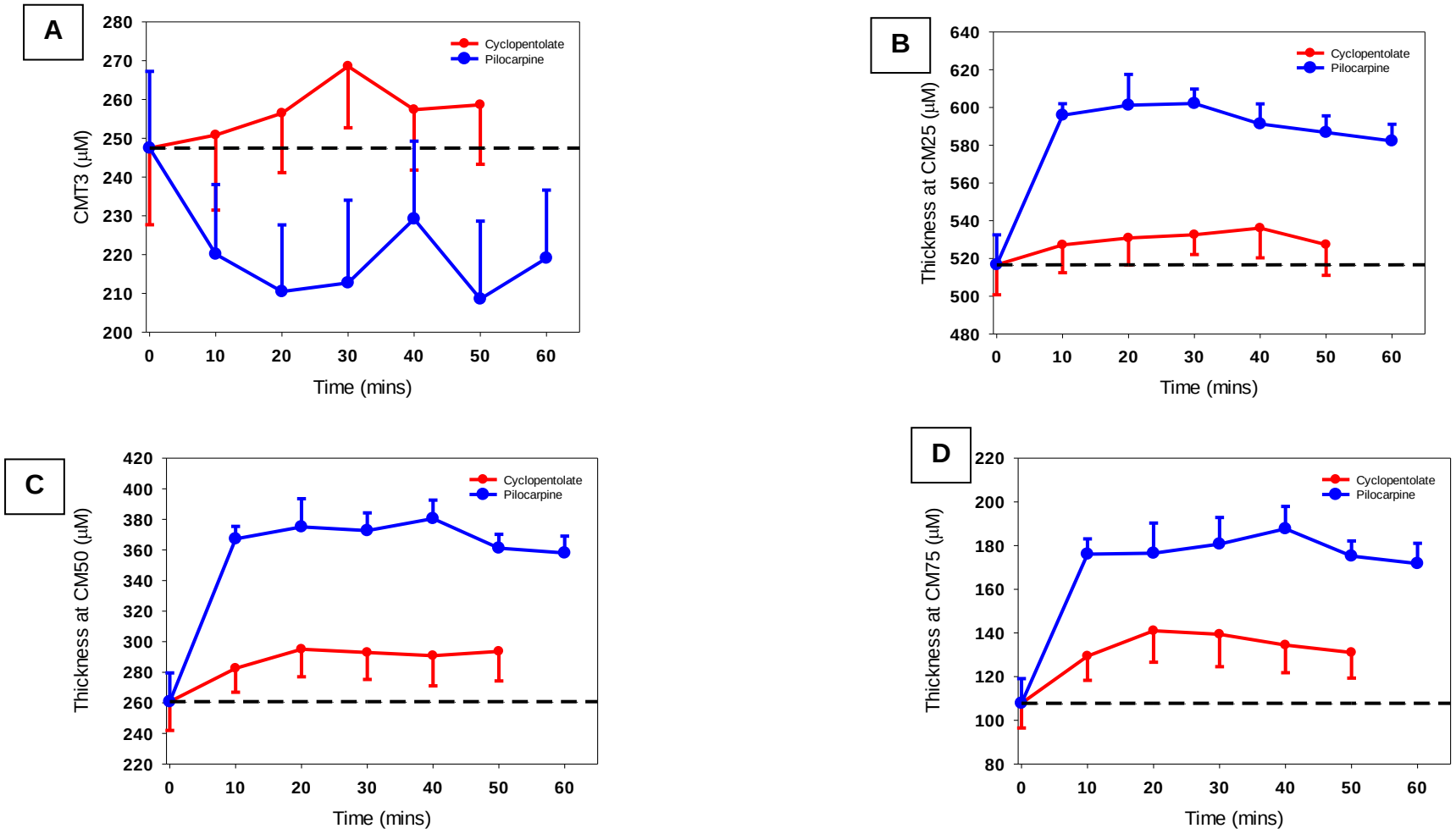

Figure 5-8. The ciliary muscle thickness over regular time intervals for 10 participants. Data is presented for post-instillation of pilocarpine (mean + 1 SEM) and cyclopentolate (mean – 1 SEM). 0 minutes refers to baseline measurements. A: CMT3, B: CM25, C: CM50 D: CM75.

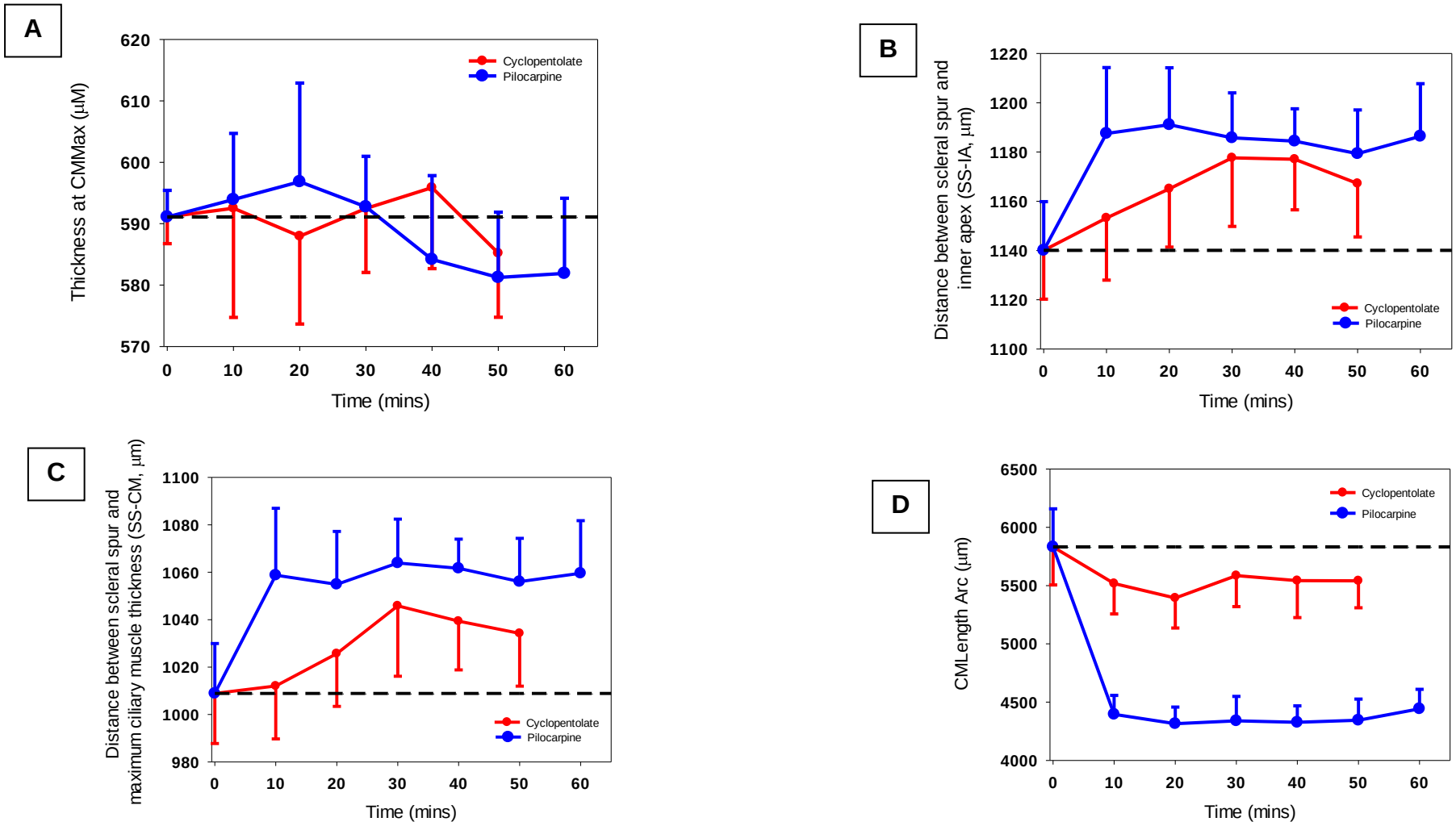

Figure 5-9. The ciliary muscle measurement over regular time intervals for 10 participants. Data is presented for the post-instillation of pilocarpine (mean + 1 SEM) and cyclopentolate (mean – 1 SEM). 0 minutes refers to baseline measurements. A: CMMax, B: SS-IA, C: SS-CM, D: CMLength Arc.

5.4. Discussion

The results from the current study provide *in-vivo* data for the effect of pilocarpine on the ciliary muscle morphology, within pre-presbyopic and presbyopic human participants, as well as further insight into the accommodative mechanism of the human ciliary muscle. The results have shown, for the first time, that pilocarpine produces an anterior movement of the ciliary muscle as indicated by the increased thickening, centripetal movement and contractile shortening, which was evident in pre-presbyopic and presbyopic participants. However, the amplitude of accommodation achieved, as determined from the pre-presbyopic cohort, is less than that achievable under physiological stimulation of the accommodative apparatus. Interestingly, evidence from the current study indicates that a centripetal and apical thickening is not solely responsible for accommodation but the increased thickening within the muscle and the contractile shortening, are essential for providing the forward movement of the muscle to achieve maximum accommodation.

Comparison of ciliary muscle morphology between presbyopes and pre-presbyopes indicates a shorter and thinner ciliary muscle within the presbyopic cohort, which is in agreement with *in-vitro* findings of a reduction in ciliary muscle length and width with age (Tamm et al., 1992b). Such findings may be explained by the possible reduction in the quantity of longitudinal fibres and consequent posterior thinning of the muscle with age (Tamm et al., 1992b). Furthermore, the lens thickness of the presbyopic cohort was greater than the pre-presbyopes at baseline, a finding which is well documented within the literature (e.g. Dubbelman and Van der Heijde, 2001).

During physiological manipulation of the accommodative apparatus, the ciliary muscle thinned posteriorly as indicated by the significant reduction in thickness at CMT3, and increased in thickness anteriorly as suggested by the thicker measurements at CM25 and CMMax. There was a reduction in anterior length, a decrease in the distance between the scleral spur and inner apex and a contractile shortening. These findings support current evidence of *in-vivo* ciliary muscle changes during accommodation (Sheppard and Davies, 2010b; Lewis et al., 2012; Lossing et al., 2012; Richdale et al., 2013; Shao et al., 2013). Furthermore, the presbyopic cohort demonstrated a reduction in thickness at CMT3, up to the maximum mean accommodative demand level (3 D), thus supporting evidence of a posterior thinning within the presbyopic ciliary muscle during accommodation (Sheppard and Davies, 2011) and also the relevance of CMT3 during accommodation (Richdale et al., 2013). Although the thickness of the

presbyopic ciliary muscle at CM25, CM50, CM75 and CMMax increased above baseline when the 4 D demand level was simulated, a thinning was evident for the 1 D demand level, suggesting the increased depth of focus due to miotic pupils, may provide up to 1 D accommodation and ciliary muscle contraction is not required. The reduction in anterior length, ciliary muscle length arc and distance between scleral spur and inner apex was only evident between the 2 D and 3 D demand levels, indicating the contraction and mobility of the ciliary muscle was not possible beyond 4 D, and therefore explains the reduced accommodative responses for demand levels of 4 D and greater. Sheppard and Davies (2011) also found the anterior region of the ciliary muscle, represented by CM25 and the anterior length remained responsive to an accommodative stimulus throughout life, and contractile shortening was evident even when presbyopia was well established (Sheppard and Davies, 2011), which is supported by the findings from the current study.

Pilocarpine is often inferred to as a super-stimulus for accommodation (Koeepl et al., 2005b; Kriechbaum et al., 2005) and although pilocarpine induced a significant shortening and anterior thickening of the ciliary muscle, the findings were only significant for the pre-presbyopic cohort. The results from the current investigation support findings of an anterior and inward movement of the ciliary muscle during accommodation (e.g. Lewis et al., 2012), and the maintenance of contractile ability of the muscle with age (Sheppard and Davies, 2011) which may occur if neurotransmitter and synthesis binding remains constant throughout life, which has been demonstrated in the rhesus monkey (Gabelt et al., 1990). The present study provides the first *in-vivo* results relating to the effect of pilocarpine on ciliary muscle morphology. The results indicate the ciliary muscle length 30 minutes after pilocarpine instillation was 3.66 mm (SE 0.23), which is shorter than the pilocarpine treated ciliary muscle length determined *in-vitro* for a similar age group 24-48 hours after death (length of 4.01 mm (SD 1.11); Pardue and Sivak, 2000). Therefore, the differences may be a consequence of oedema in tissue at post-mortem.

The results from the sub-group data suggest the increased thickening within CM25, CM50, CM75 and the contractile shortening of the muscle are likely to have a significant role in accommodation. Indeed, studies from rhesus monkeys reveal that the loss of forward movement in the ciliary body of older monkey eyes, produces a greater reduction to the accommodative amplitude, and, although a 12% loss in centripetal movement occurs in older eyes compared to younger eyes, it is not enough to produce the 57% reduction in centripetal *lens* movement or the 76% reduction in

accommodative amplitude (Croft et al., 2006b), therefore, suggesting a forward and centripetal movement of the ciliary muscle is required for maximum accommodation. Consequently, the present study supports the hypothesis that a restriction to the ciliary muscle mobility and consequent hinderance to the forward movement of the muscle, could explain the reduced accommodative amplitude which occurs with increasing age. Croft and colleagues (2013a) suggested the possible cause of the reduced forward movement that may result with increasing age is the restricted movement of the vitreous zonules, which prevent a forward movement of ciliary muscle mass and ciliary muscle apex thickness, therefore, reducing the accommodative amplitude. Indeed, the increased thickness within the apex of the muscle reduces the tension on the anterior zonules and enables a centripetal movement of the lens, however, the forward movement of the vitreous zonule and ciliary muscle together provides a greater increase to the lens thickness, during accommodation (Croft et al., 2013b). Nevertheless, the increase in connective tissue (Tamm et al., 1992b; Pardue and Sivak, 2000) and the inability of acetylcholine to stimulate the ciliary muscle nerves due to the larger proportion of tissue around nerve fibres may also contribute to the reduced ability of the muscle to forward during accommodation with increasing age.

There are several reports for the variability for the effect of pilocarpine on the accommodative response as well as the time course for maximum effect (Wold et al., 2003; Kriechbaum et al., 2005; Plainis et al., 2009). Indeed, a variable effect of pilocarpine on the ciliary muscle morphology was documented in the present study, where an increase in distance between the scleral spur and inner apex (SS-IA) and the anterior length was found for the sub-group of participants, in comparison to the mean data from the 27 participants, where a reduction to the anterior length and distance between the scleral spur and inner apex was evident. Autorefraction data could not be obtained from all the presbyopes within the study, however, the ciliary muscle data for the main study with 27 participants, suggests the maximum effect of pilocarpine occurs at 30 minutes at least in pre-presbyopic individuals, indicating studies which obtain measurements for intraocular biometry after administration of 2% pilocarpine at 30 minutes post-instillation (Koeppl et al., 2005b) are valid. Plainis et al (2009) reported a maximum accommodative response occurs between 38 and 85 minutes post-instillation of pilocarpine, however, the authors used phenylephrine alongside pilocarpine which may explain the large variation for the duration of the agent.

It is clear measurements of accommodative response and intraocular biometry after the instillation of pilocarpine should be obtained at regular time intervals, rather than assuming the maximum effect occurs at one time point due to the variability in the time

course of the drug. Subsequently, pilocarpine stimulated accommodation may not provide essential information about accommodating intraocular lenses, if measured at one interval for all participants, due to the variation in effect of the agent (Plainis et al., 2009).

Although refraction data could not be acquired at each time interval for all participants involved in the study, the accommodative effect of pilocarpine was monitored from anterior chamber depth measurements. There was evidence of a reduced anterior chamber depth and increased lens thickness within all participants, therefore indicating the contractile shortening and anterior thickening of the muscle produced by pilocarpine, resulted in an increase to the lens thickness and decrease in the anterior chamber depth for both the presbyopic and pre-presbyopic cohort. Although these findings provide evidence for accommodation, the magnitude determined from autorefraction did not reveal responses as great as that reported by Wold et al (2003) or Plainis et al (2009).

During ciliary muscle contraction, a redistribution of muscle mass occurs increasing within the posterior region, which may exert pressure on the peripheral vitreous (Busaaca, 1955 cited by Cumming et al., 2001). The results of the current study seem to support this finding of an increased muscle mass posteriorly, since pharmacological manipulation of the ciliary muscle with pilocarpine produced a significant thickening within the posterior locations of the ciliary muscle, CM50 and CM75, in comparison to the maximally relaxed muscle induced by cyclopentolate. However, the effect of this increased muscle mass was only evident during pharmacological manipulation of the accommodative apparatus, suggesting the greater increase is not possible under physiological conditions to produce pressure at the peripheral vitreous.

The present investigation is not without its limitations. The sample size of the presbyopic participants was limited and resulted in, greater variability for the reported ciliary muscle and biometry data was documented. Although the findings suggest the contractility and mobility of the ciliary muscle is sustained in presbyopia, and the maximum effect of pilocarpine occurs at 30 minutes post-instillation, the insufficient power of the sample size in the present study warrants further investigation with larger sample sizes to confirm these findings. The current study also investigated the ciliary muscle of emmetropes due to the risk of pilocarpine on ocular health in ametropic individuals. Considering the ciliary muscle morphology differs between individuals with ametropia (Sheppard and Davies, 2010b), it would be of interest to determine whether similar findings are evident in ametropic individuals. Furthermore, pupil miosis

prevented the acquisition of refraction data for 6 pre-presbyopic participants and 3 presbyopic participants. Although other researchers have used phenylephrine to produce mydriasis, the combination of pilocarpine and phenylephrine was avoided in this study due to the risk of an adverse event, especially since a high concentration of phenylephrine can induce systemic side effects (Fraunfelder, and Scafidi, 1978). Moreover, the axial length data obtained throughout the study could not be corrected for the error induced by the increased lens thickness and reduction in the anterior chamber depth, therefore the raw data has been included.

Overall, the study has shown pilocarpine stimulated accommodation induces a forward movement of the ciliary muscle, an anterior and posterior thickening as well as a contractile shortening, which are significant within the youthful eye. Similar findings are also evident within presbyopic eyes, but were insignificant. Importantly, the forward movement of the muscle as indicated by CM25, CM50, CM75 and the contractile shortening, may have a greater role for eliciting high accommodative amplitudes. Moreover, although pilocarpine produced a contraction of the ciliary muscle, the amplitude of accommodation was less than under physiological conditions, suggesting the agent is unlikely to be a super-stimulus for accommodation.

5.5. Summary

- The study investigated whether pilocarpine is a super-stimulus for accommodation by investigating the effect of the parasympathomimetic agent on the ciliary muscle *in-vivo* within pre-presbyopic and presbyopic eyes
- Furthermore, data from a sub-group of participants were used for comparison to data from Chapter 4, to further identify which regions within the ciliary muscle have a role in accommodation
- The main findings were:
    - The accommodative responses were less with pilocarpine compared to physiological accommodation, suggesting pilocarpine is not a super-stimulus for accommodation
    - Pilocarpine produced a significant decrease in thickness at CMT3 and a statistically significant increase in thickness at CM25 and CM50 within the pre-presbyopic cohort
    - There was a significant increase in maximum thickness within the anterior ciliary muscle 10 minutes post-instillation of pilocarpine within

the pre-presbyopic cohort. There was a subsequent gradual decrease in thickness
    - There was a significant decrease in anterior length, SS-IA and contractile shortening in the pre-presbyopic cohort post-instillation of pilocarpine
    - The findings of an anterior thickening and contractile shortening of the ciliary muscle post-instillation of pilocarpine was also evident for the presbyopic cohort although the findings were not significant
- The results suggest:
    - Increased thickening at CM25, CM50 and CM75 as well as the contractile shortening of the muscle are likely to have a significant role in accommodation
    - Consequently, forward movement of the ciliary muscle possibly allows for greater accommodative responses to be elicited than centripetal movement alone

Chapter 6. *In-vivo* investigation of the alteration to the ciliary muscle morphology within the horizontal and vertical meridians in relation to accommodation and ametropia

6.1. Introduction

In-vivo investigations of the human ciliary muscle using high-resolution instrumentation have revealed a sectorial contraction of the muscle during accommodation: regions within the anterior portion of the muscle thicken, and areas within the posterior region of the muscle thin (Sheppard and Davies, 2010b; Lewis et al., 2012; Lossing et al., 2012; Richdale et al., 2013; Shao et al., 2013).

Several *in-vitro* studies have examined the ultrastructure of the muscle and the relationship with accommodation, yet, few studies have reported the orientation of the muscle investigated. Tamm and colleagues (1992b) analysed the ciliary muscle within the horizontal and vertical meridians to determine age related changes, but found no significant differences in morphology between the orientations, therefore reported collated data.

Considering the accommodative triad consists of convergence, investigations of the ciliary muscle have generally been restricted to the horizontal meridian. A nasal-temporal asymmetry of the muscle has been identified in humans (Sheppard and Davies, 2010b) and rhesus monkeys (Glasser et al., 2001; Croft et al., 2006a), therefore, indicating variation in the ciliary muscle morphology exists depending on orientation. Such findings are unsurprising considering there is asymmetry within ocular shape (Singh et al., 2006) and peripheral refraction measurements (Charman and Radhakrishnan, 2010) between horizontal and vertical meridians as well as *within* either meridian (see Chapter 1, section 1.5). Furthermore, the eye is not a spherical ocular shape but is longer in the anteroposterior direction and equatorially compared to height (Bron et al., 1997). In addition, myopic eyes show a greater stretch in the horizontal meridian compared to the vertical (Singh et al., 2006), thus producing a prolate eye. Furthermore, a recent study documented a greater elongation of the pupil diameter and the posterior lens capsular surface within the vertical meridian during accommodation, as determined with an extended scan depth optical coherence tomographer (Leng et al., 2014). Therefore, if asymmetry exists within the biometric architecture of the accommodative apparatus and the ocular shape, could there also be

a variation within the ciliary muscle dimensions as well as the magnitude of contraction during accommodation, depending on the muscle orientation?

There is a significant interest between the association of ciliary muscle and refractive error development. Van Alphen reported the ciliary muscle stretched with ocular growth and suggested a thinner muscle would be present in eyes undergoing axial elongation (1986). However, recent studies using ultrasound biomicroscopy suggest the ciliary body is thicker in eyes with the greater myopic refractive error (Oliveira et al., 2005; Muftuoglu et al., 2009), particularly within the posterior locations of the ciliary body. Consequently, these reports indicate a positive correlation between the ciliary body thickness at 2 mm and 3 mm posterior to the scleral spur, and axial length (Oliveria et al., 2005). The thicker measurements at the posterior locations of the muscle have also been identified in children (Bailey et al., 2008), although a study in young adults suggest the overall ciliary muscle length and the anterior length is longer in eyes with greater axial lengths, but the muscle is not necessarily thicker (Sheppard and Davies, 2010b). Interestingly ocular volume is a better predictor of ciliary muscle thickness as a greater correlation has been reported in comparison to axial length (Buckhurst et al., 2013).

Further analysis of the relationship between ciliary muscle thickness and refractive error suggests differences exist between refractive groups. A thicker posterior ciliary muscle has been documented for high myopic refractive errors and a thicker anterior ciliary muscle in hyperopic refractive errors; the thicker apical region in hyperopic eyes may result from the greater workload expected in hyperopic eyes, as is known to occur within skeletal muscle during exercise (Pucker et al., 2013). Also, gender differences have been reported, with females having a greater thickness within the anterior ciliary muscle (Pucker et al., 2013). An association between ciliary body thickness and accommodative microfluctuations suggests a thicker ciliary body may stabilize the high frequency portion of the accommodative response (Schultz et al., 2009).

Overall, the ciliary muscle has been investigated in relation to accommodation and refractive error, yet, studies have mostly identified the alteration of the muscle in one quadrant, specifically within the horizontal meridian. An asymmetry of the muscle has been identified within the horizontal meridian during accommodation, therefore, although the ciliary muscle is a sphincter, the morphology and contraction of the muscle is not symmetrical. Consequently, establishing the muscular changes within the vertical meridian may identify similarities and differences between the horizontal and

vertical quadrants that could enhance our understanding of the changes which occur to the muscle during accommodation.

The aim of this study was to investigate the alteration to the ciliary muscle thickness and length during accommodation at four locations: temporal, nasal, inferior and superior quadrants. The results were also analysed in relation to ametropia to provide further insight into the relationship of ciliary muscle morphology with axial length in emmetropic and myopic refractive groups.

6.2. Methods

The study was conducted in accordance to the tenets of the Declaration of Helsinki. Written and verbal information was provided to participants before they provided written consent for their participation. A favourable opinion was provided by Aston University Research Ethics Committee before the study commenced.

6.2.1. Sample size

The number of participants required for this study were calculated from a statistical power test using G*power (version 3.1.9.2; Universitat Kiel, Germany). In order to measure a medium effect size (f=0.25), based on a within-between subject ANOVA design and a desired statistical power (1-β) of 95% with an error probability (α) of 0.05, at least 24 participants were required.

6.2.2. Participants

Volunteers were recruited from the optometry undergraduate cohort through email announcements.

Inclusion criteria

Participants were invited to answer questions relating to their refractive history, ocular history and general health. Healthy participants were recruited with no history of ocular injury or surgery, no ocular pathology and no general health concerns. Exclusion criteria included participants who had an ocular or systemic disease, participants who had an ocular injury, ocular trauma or ocular surgery which affected the cornea, lens or ciliary apparatus and astigmatism greater than 1.00 DC. Volunteers who were amblyopic or had a binocular vision condition were also excluded from the study.

Visual acuity

The visual acuity was determined as decribed in Chapter 3, section 3.2.2.

Refractive error

The monocular refractive error was measured with the Grand Seiko *WAM* 5500 autorefractor from each eye (Sheppard and Davies, 2010a), whilst the contralateral eye was occluded with an eye patch. Subjects viewed a Maltese cross target (average target luminance and Michelson contrast was 34.0 cd/m^2 and 82%, respectively) within a Badal lens system. The Badal lens system consisted of a +5.00 D full aperture trial lens with a Maltese cross target placed at the focal point of the lens (20 cm) allowing a measure of the refractive error at 0 D of accommodation. The constant angular subtense of the Maltese cross target was 6.8˚ horizontally and vertically. Participants were classified as emmetropic if the MSE was within the range -0.50 to +0.75 DS and myopic if the MSE was less than -1.00 D.

6.2.3. Procedure

Accommodative response determined with Grand Seiko *WAM 5500*

The health of the anterior eye was examined of the myopic participants with a slit lamp prior to the correction of the refractive error with a spherical daily soft contact lens (*Nelfilcon A,* Alcon; water content 69%) to render participants functionally emmetropic. After the contact lens was inserted, a settling time of five minutes was allowed. The contralateral eye was occluded with a patch and an over-refraction was performed with the Grand Seiko *WAM 5500* autorefractor whilst the participant viewed an external fixation target within a Badal lens system. The over-refraction results were within ±0.50 DS for all subjects. Subsequently, the monocular objective accommodative response of the right eye for the three demand levels (0.17 D, 4 D and 8 D) was determined for all emmetropic and myopic individuals as the subjects viewed a Maltese cross target in free space. Three measurements were taken at each position and a final overall result was provided by the autorefractor, which was recorded. The order of the measurements for the accommodative response was randomised.

Visante AS-OCT

Ciliary muscle images were acquired from the right eye with the Visante AS-OCT (Carl Zeiss, Meditec). Images were obtained for the nasal, temporal, inferior and superior quadrants. The myopic participants remained functionally emmetropic with the contact lens *in-situ*. To obtain images from the right eye, the participant placed their chin on the left side of the chin rest and forehead against the forehead rest, with the contralateral

eye occluded with a patch. The AS-OCT was setup as described in Chapter 4, section 4.2.3.

To image the full length of the nasal and temporal ciliary muscle, the participant viewed a Maltese cross target within a bespoke Badal lens system consisting of a +10 D lens, as shown in Figure 6-1.

Figure 6-1. The rig consisted of a Badal lens system with a +10 D lens and a Maltese Cross target. The rig was placed at a 40˚ angle to the instrument in order to image the ciliary muscle.

Figure 6-2. The temporal ciliary muscle of the right eye was imaged on adduction as the participant viewed a Maltese Cross target within a Badal lens system.

To acquire images of the ciliary muscle in the vertical plane, an external rig with a Badal lens system consisting of a +10 D lens, a beam splitter and a Maltese cross target was used. The beam splitter was positioned at 45˚ to reflect the target, as shown in Figure 6-3. The participant was able to view the Maltese cross when they looked upwards and the scanning plane was adjusted to 90˚ to capture the inferior ciliary muscle image. For some participants, the lower lid hindered the image of the ciliary muscle, therefore, the lid was held down during image acquisition. To image the superior ciliary muscle, the rig was adjusted so the arm was positioned inferiorly as shown in Figure 6-4, allowing the participant to look down to view the target, and the upper lid was held open. Again the scanning plane was positioned to 90˚. The angular subtense of the Maltese Cross was 5.8° and contrast was 90%.

Figure 6-3. The rig was placed to the side of the AS-OCT and the arm adjusted to enable imaging of the inferior muscle.

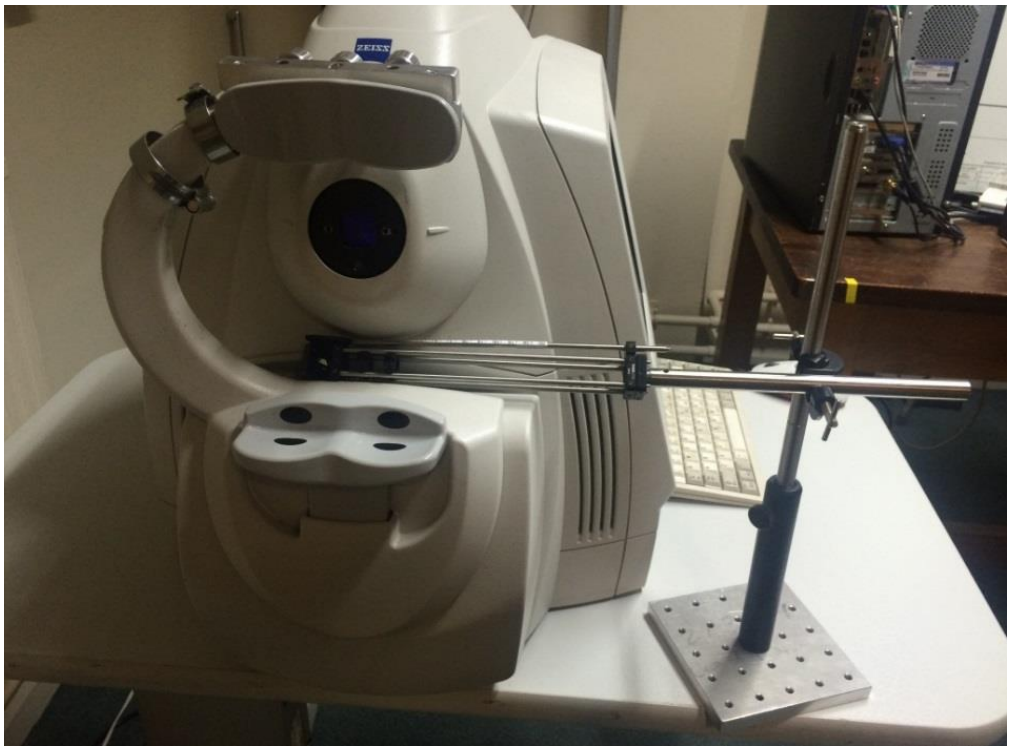

Figure 6-4. The rig was placed to the side of the AS-OCT and the arm adjusted in order for the participant to view the Maltese cross within the Badal lens system as they looked down, allowing image acquisition of the superior ciliary muscle.

Several consecutive images were obtained and overall three images which clearly depicted the full length of the ciliary muscle, were saved for each accommodative demand level within the four quadrants of the ciliary muscle. Images were randomised in respect to accommodative demand level and quadrant.

The images were coded to ensure the examiner analysing the images was masked to the refractive error, ciliary muscle quadrant and the accommodative demand level.
After ciliary muscle image acquisition, the contact lens was removed from the myopic participants and the axial length was measured with the IOLMaster (Zeiss).

Axial length
On-axis axial eye length measurements were obtained from the right eye (contralateral eye occluded with a patch) with the Zeiss *IOLMaster* with relaxed accommodation (0.17 D) and at the 8 D accommodative demand level. A metal frame was placed around the forehead/chin rest of the IOLMaster to which a badal rig system was attached using the same setup as described by Mallen and Kashyap (2007). The rig consisted of a badal optometer, a high contrast Maltese target which was illuminated by an LED light and a beamsplitter (50% transmission/ 50% reflection). The power of the badal lens was +20.8 D (Edmund Optics). The rig was attached to the top of the metal frame mount so measurements could be obtained for the axial length. The rig was adjusted to ensure the Maltese cross target within the rig was aligned with the pupil centre of the right eye, which was confirmed when the patient reported the beam from the *IOLMaster* coincided with the Maltese cross target. The target was reflected onto the beam splitter and placed at the far point by using a push-up method: the Badal lens was slowly moved down towards the beam splitter until the subject reported the Maltese cross target appeared clear. It was then moved away from the beam splitter until the subject reported it first became blurred and then moved towards the beam splitter until the subject reported it appeared clear again; this ensured there was no accommodation at the far point confirming accommodation was relaxed. Five measurements were obtained for 0 D and 8 D accommodative demand level.

6.2.4. Analysis software

Ciliary muscle images
The ciliary muscle data was analysed using the semi-automated software as described in Chapter 2.

6.2.5. Axial length error during accommodation

The IOLMaster uses a refractive index of 1.3549 to convert the optical path length to a geometric path length for the wavelength used by the instrument (780 nm). However, during accommodation, the crystalline lens thickness increases and the optical path length calculated is consequently overestimated. Therefore, the error to the axial length induced for each individual has to be calculated, in order to determine the change to the length with accommodation. Atchison and Smith (2004b) used the Gullstrand no. 1 (exact) eye and assumed the vitreous chamber depth remains unchanged with accommodation. Thus, the authors reported an error of 18 µm to the axial length for a 10 D accommodative stimulus. In our study, in order to calculate the error associated with the axial length during accommodation, the change to the crystalline lens thickness and anterior chamber depth were required for each participant. Thus, the lens thickness and anterior chamber depth for each demand level have been calculated based on the equations provided by Norrby (2005) (equation 1.0 and 1.1, respectively). In equation 1.0 and 1.1, *A* represents the age in years and *D* refers to the accommodative stimulus level. A homogenous refractive index for the crystalline lens was used (n=1.413) based on the Gullstrand simplified schematic eye, whereas the refractive indices for corneal thickness (CT), anterior chamber depth (ACD) and vitreous chamber depth (VCD) was used from Gullstrands exact schematic eye (Atchison and Smith, 2004b). Since the vitreous chamber depth is assumed to remain unaltered during accommodation, the baseline axial length was subtracted from the sum of the CT, ACD and LT for each of the accommodative demand levels to determine the vitreous chamber depth at each demand level. The average refractive index of the eye (n_{ave}; equation 1.4) was determined by using the disaccommodated values for each of the biometric parameters, since the overall alteration to the refractive index of the eye during accommodation is still not fully understood. The error induced from the axial length could be obtained and subtracted from the axial length measured during each accommodative stimulus level, to obtain the corrected axial length measurements.

$$LT = 2.93 + 0.0236A + D\,(0.058 - 0.0005\,A) \quad (1.0)$$

$$ACD = 3.87 - 0.010 * age - D\,(0.048 - 0.0004\,A) \quad (1.1)$$

$$VCD = AL - CT - ACD - LT \quad (1.2)$$

$$OPL = (CT \times 1.376) + (ACD \times 1.336) + (LT \times 1.413) + (VCD \times 1.336) \quad (1.3)$$

$$n_{ave} = [(CT/AXL) \times 1.376] + [(ACD/AXL) \times 1.336] + [(LT/AXL) \times 1.413] + [(VCD/AXL) \times 1.336] \quad 1.4$$

$$E = (OPL/ n_{ave}) - AXL_{disaccommodated} \quad 1.5$$

$$AXL_{corrected} = AXL_{accommodated} - E \quad 1.6$$

6.2.6. Statistical analysis

A Shapiro-Wilk test (SPSS Statistics 21; SPSS Inc., Illinois, USA) revealed normal distribution of the data for the axial length at relaxed accommodation and for the 8 D accommodative demand level. The ciliary muscle parameters also exhibited normal distribution for both accommodative demand levels. Therefore, assumptions of normality and homogeneity of variance were met. In order to determine the relationship between the axial length and the ciliary muscle parameters for each quadrant investigated, separate linear regression analyses were determined. A repeated measures analysis of variance (ANOVA) was performed with two within subject factors (i.e. accommodation and quadrant) to determine the effect of quadrant and accommodation, as well as the interaction between both factors on the ciliary muscle parameter. There was non-sphericity for the interaction term as assessed with Mauchley's test of sphericity ($p<0.05$), therefore, Greenhouse Geisser results are reported. Post-hoc comparisons were determined using Bonferroni correction. The effect of refractive error on the ciliary muscle parameters was determined by a within-between ANOVA.

6.3. Results

To allow for data attrition resulting from poor quality images which would affect the detection of the ciliary muscle edge and the posterior visible limit of the images acquired with AS-OCT, 40 participants were recruited (MSE -1.66 D (SD 1.93)) with a mean age of 20.7 years (SD 2.1). The cohort consisted of 18 emmetropes (MSE -0.21 D (SD 0.52), age 20.4 years (SD 1.5)) and 22 myopes (MSE -2.85 D (SD 0.90), age 21.0 years (SD 2.4)).

Figure 6-5 A shows the correlation between axial length and refractive error for the cohort within this study, and as expected, the refractive error decreases with increasing axial length. The average refractive error and axial length for all 40 participants was -1.66 D (SE 0.30) and 24.18 mm (SE 0.14), respectively. For the emmetropic participants, the average refractive error was -0.21 D (SE 0.09) and average axial length 23.71 mm (SE 0.22). The myopic participants had a mean refractive error of -

2.85 D (SE 0.40) and average axial length of 24.57 mm (SE 0.15). The frequency distribution of the axial lengths are represented in Figure 6-5 B for emmetropes and Figure 6-5 C for myopes. It is evident there is an overlap of axial lengths between the different refractive groups. The assumption of homogeneity of variances were met, for the average axial lengths between emmetropes and myopes, as assessed by Levene's test for equality of variances (p= 0.065). An independent sample t-test revealed a statistically significant difference in the axial length at baseline between the emmetropic and myopic participants ($t_{-3.218}$, p= 0.002).

Figure 6-6 and Figure 6.7 shows results for the analysed ciliary muscle parameters during relaxed accommodation and 8 D accommodative demand. The ciliary muscle thickness and length varied across the different quadrants. On average, for relaxed accommodation, the inferior ciliary muscle was thickest (CMMax 0.62 mm (SE 0.01)). The temporal ciliary muscle was the longest (CMLength arc 4.99 mm (SE 0.08)) and the nasal ciliary muscle was the shortest (CMLength arc 4.44 mm (SE 0.07)).

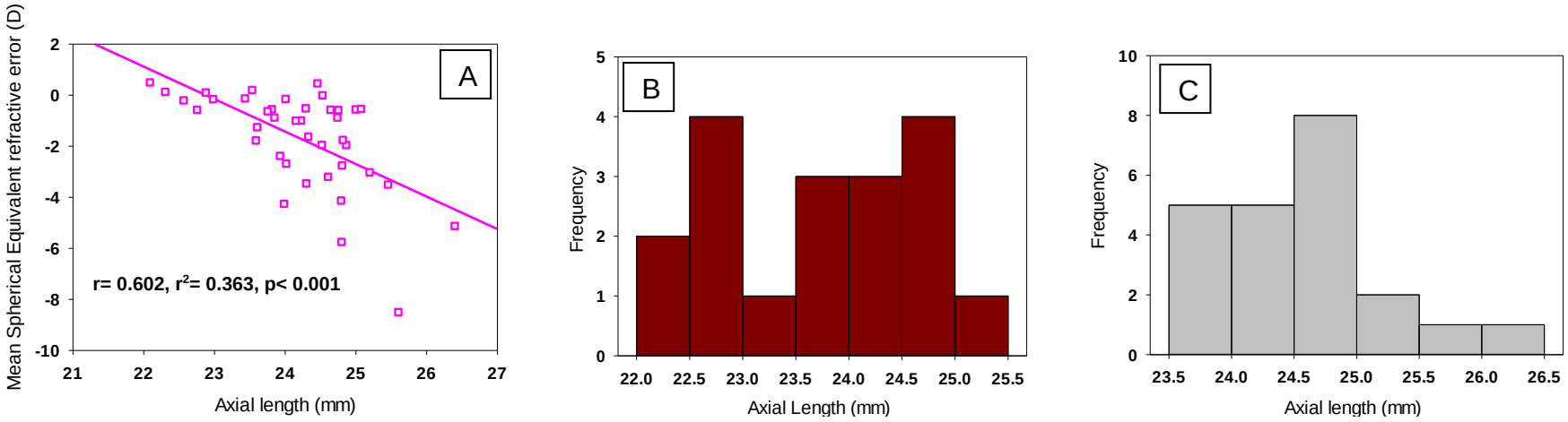

Figure 6-5. A. The correlation between axial length and refractive error for the cohort of participants included in the study. **B** Histogram representing the frequency distribution of the axial length of emmetropes. **C** Histogram representing the frequency distribution of the axial length of myopes.

6.3.1. Correlation between ciliary muscle parameters and axial length

During relaxed accommodation, there was a positive correlation of ciliary muscle length arc (CMLength Arc) with increasing axial length as shown in Figure 6-6 A, which was statistically significant for the temporal (r= 0.510, r^2 = 0.261, p< 0.001), nasal (r= 0.506, r^2 = 0.256, p< 0.001) and superior (r= 0.442, r^2 =0.195, p= 0.004) quadrants, as shown in Table 6-1. Interestingly, the length of the inferior ciliary muscle did not vary with increasing axial length (r = 0.019, r^2 = 0.00035, p= 0.91).

CM parameter (µm)	Temporal	Nasal	Inferior	Superior
CMLENGTH ARC	**r = 0.510**	**r = 0.506**	r = 0.019	**r = 0.442**
CMT1	r= 0.212	r= 0.578	**r= 0.089**	r= 0.166
CMT2	**r = 0.452**	**r = 0.527**	r= 0.014	r = 0.300
CMT3	**r= 0.610**	**r= 0.542**	r= 0.031	r= 0.365
CM25	r = 0.022	r = 0.27	r = 0.046	r = 0.080
CM50	r = 0.080	r = 0.055	r = 0.040	r = 0.031
CM75	r = 0.236	r = 0.064	r = 0.097	r = 0.045
CMMAX	r = 0.127	**r = 0.448**	r = 0.043	r = 0.124
SS-IA	**r = 0.366**	**r = 0.522**	r = 0.135	r = 0.202
ANTERIOR LENGTH	**r = 0.364**	**r = 0.451**	r = 0.134	r = 0.191

Table 6-1. The correlation between axial length and ciliary muscle parameter, during relaxed accommodation, as determined from linear regression analysis. The values in bold represent a statistically significant correlation.

As shown in Figure 6-6 B, there is an increase of the ciliary muscle thickness 2 mm posterior to the scleral spur (CMT2), for the temporal (r= 0.452, r^2 = 0.20, p= 0.003) and nasal (r= 0.527, r^2 = 0.28, p< 0.001) quadrants. Although the superior muscle thickness increased as the axial length became longer, the correlation was not significant (r= 0.300, r^2 = 0.09, p= 0.06). The inferior muscle thickness within this anterior location remained relatively constant with increasing axial length (average 0.41 mm (SE 0.01); r= 0.014, r^2 = 0.0002, p= 0.93).

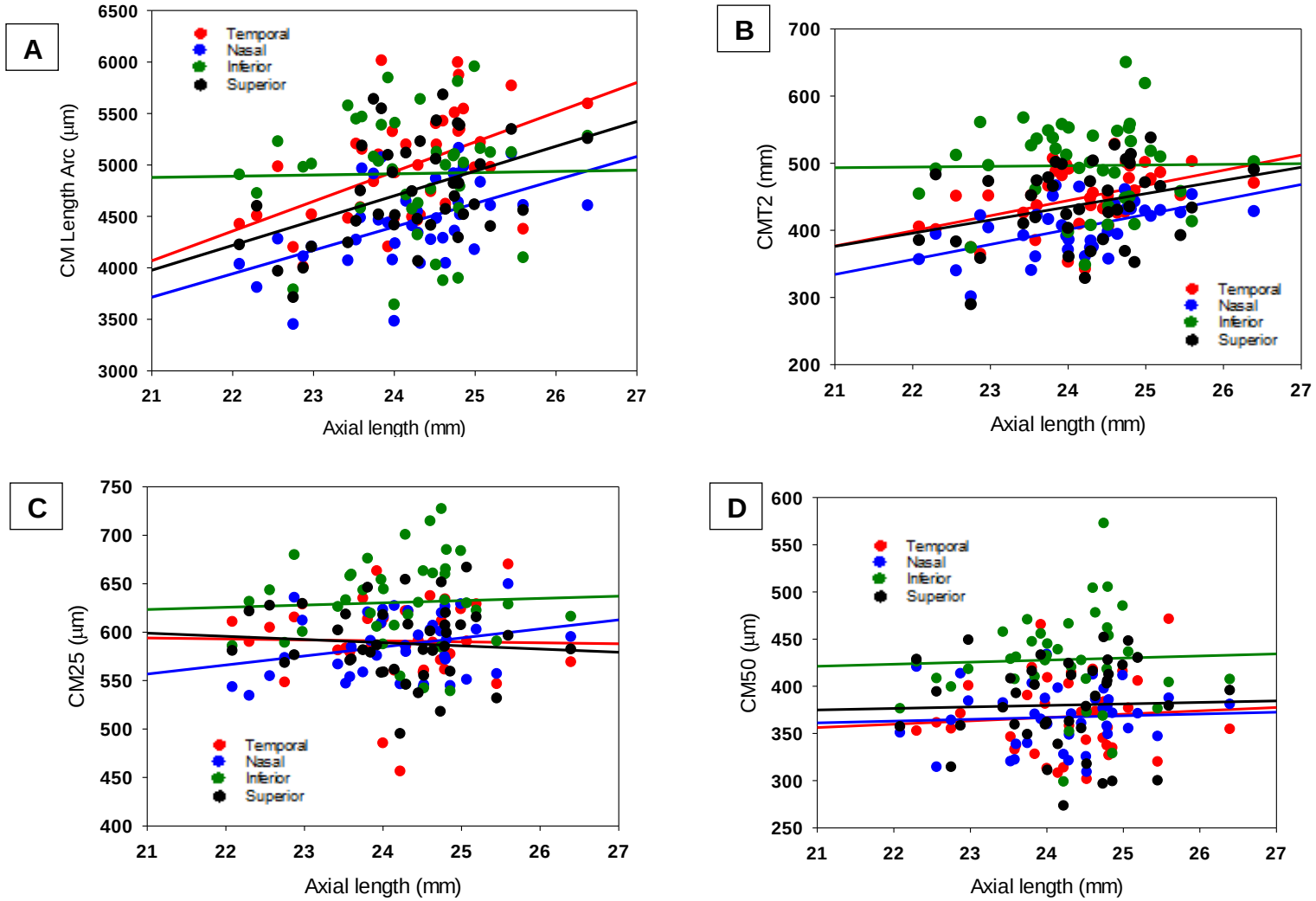

Figure 6-6. The correlation between axial length and A: ciliary muscle length (CM Length Arc), B: CMT2, C: CM25 D: CM50 for the four ciliary muscle quadrants during relaxed accommodation.

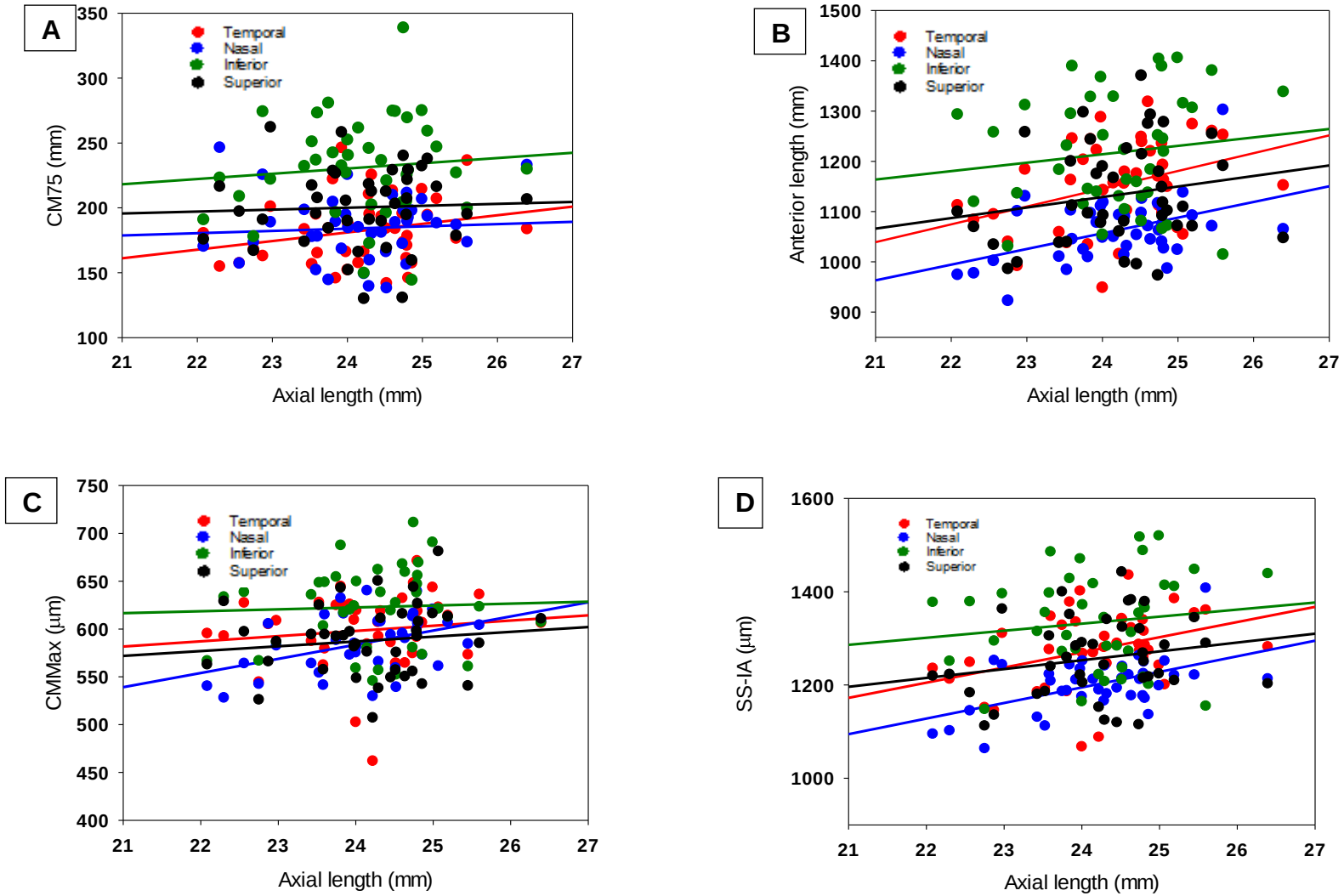

Figure 6-7. The correlation between axial length and A: CM75, B: anterior length, C: maximum ciliary muscle thickness, D: scleral spur to inner apex for the four ciliary muscle quadrants during relaxed accommodation.

The region representing the thickness at 25% of the ciliary muscle length (CM25) varied depending on the quadrant. There was an increase in thickness for the nasal quadrant as axial length increased (r= 0.268, r^2= 0.071, p= 0.09), whereas the inferior muscle remained relatively stable (inferior: r= 0.046, r^2= 0.0021, p= 0.78). There was a minimal insignificant negative correlation between the temporal and superior quadrants with increasing axial length (temporal: r= 0.023, r^2= 0.0005, p= 0.89; superior r= 0.08, r^2= 0.0064, p= 0.62) as shown in Figure 6-6 C.

Furthermore, the thickness at CM50 was independent of axial length for the temporal, inferior and superior quadrants, whereas for CM75 there was an indication for the temporal muscle to thicken as axial length increased (r= 0.236, r^2=0.056, p= 0.14). Also, during relaxed accommodation, the anterior length comprised 23%, 23.8%, 24.8% and 23.8% of the total ciliary muscle length for the temporal, nasal, inferior and superior muscle, respectively. The anterior length increased for all four quadrants as axial length elongated as shown in Figure 6-7 B, which was only significant for the horizontal meridian (temporal: r= 0.364, r^2= 0.13, p= 0.02; nasal: r= 0.45, r^2= 0.20, p= 0.003).

There was a significant positive correlation for the maximum ciliary muscle thickness (CMMax) within the nasal quadrant with increasing axial length (r= 0.448, r^2= 0.20, p=0.04) as shown in Figure 6-7 C. For the inferior quadrant, CMMax was not dependent on axial length (r= 0.043, r^2= 0.0016, p= 0.79), whereas the temporal and superior muscle showed a minimal positive correlation (temporal r= 0.127, r^2= 0.017, p= 0.43; superior: r= 0.124, r^2= 0.014, p= 0.45). The results for CMMax, CM25 and CMT2 together refer to the anterior portion of the ciliary muscle and although there was a positive correlation between the thicknesses in each of these parameters as a function of axial length within the nasal quadrant, the posterior locations of the muscle were invariant with axial length (CM50: r= 0.0552, r^2=0.00305, p= 0.74; CM75: r= 0.064, r^2=0.0041, p= 0.70). A statistically significant increase for SS-IA occurred for the nasal (r= 0.52, r^2 = 0.27, p <0.001) and temporal (r= 0.127, r^2= 0.016, p= 0.02) quadrants.

6.3.2. Alteration to ciliary muscle morphology with accommodation

During accommodation, there was a contractile shortening of the ciliary muscle which was greatest for the temporal (average reduction CMLength arc 210.9 µm (SE 57.3)) and inferior quadrant (average reduction CMLength arc 207.9 µm (SE 104.5)), with minimal shortening occurring within the nasal quadrant (average reduction CMLength arc 76.2 µm (SE 46.1)), as seen in Figure 6-8 A. The contractile shortening of the ciliary muscle length arc was dependent on accommodation (accommodation $F_{18.62}$, p= 0.000) and quadrant (quadrant $F_{19.68}$, p= 0.000). Post-hoc comparisons using Bonferroni correction revealed the reduction to the ciliary muscle length arc was statistically significant in the temporal quadrant compared to the nasal (mean difference 47.9 µm (SE 0.047)) and superior (mean difference 23.3 µm (SE 55.0)), whereas the inferior length arc significantly reduced compared to the nasal quadrant (mean difference 41.0 µm (SE 6.8)). There was no significant interaction between quadrant and accommodation to the length of the muscle ($F_{0.860}$, p= 0.46). Figure 6-10 A shows the change to the ciliary muscle length arc with accommodation as a function of axial length. Although the overall reduction to the ciliary muscle length occurred for all four quadrants during accommodation, the change between the maximum and relaxed accommodative demand level reduced within the inferior muscle for axial lengths greater than 25.27 mm.

The location representing 2 mm posterior to the scleral spur (CMT2) was analysed due to the possibility of the region acting as a fulcrum during accommodation (Lewis et al., 2012). On average, there was a thinning of CMT2 during accommodation within the temporal (mean reduction 16.6 µm (SE 5.3)), nasal (mean reduction 6.0 µm (SE 6.7)) and superior quadrants (mean reduction 15.0 µm (SE 6.6)), whereas the inferior quadrant thickened (mean 11.0 µm (SE 11.0)), as seen in Figure 6-8 B. The thickness within the region was dependent on quadrant ($F_{66.01}$, p= 0.000) but not accommodation ($F_{3.86}$, p= 0.06). Post-hoc comparisons revealed the mean differences in quadrants were only statistically significant for the temporal when compared to the nasal (mean difference 38.0 µm (SE 5.0)) and inferior (mean difference -62.0 µm (SE 8.0)), but not when compared to the superior aspect (mean difference 9.0 µm (SE 7.0)). There was no significant interaction between quadrant and accommodation ($F_{2.52}$, p= 0.06). Figure 6-10 B also shows the change to CMT2 with accommodation for all quadrants as axial length increases. Within the inferior muscle, the thinning at CMT2 reduced with axial lengths greater than 23.45 mm (r= 0.20, r^2= 0.04, p= 0.22).

CM25 thickened with accommodation within the nasal and inferior quadrant, whereas the temporal and superior quadrants remained invariant with accommodation, as seen in Figure 6-8 C. The thickness was dependent on accommodation ($F_{10.13}$, p= 0.003) and quadrant ($F_{49.67}$, p= 0.000). Post-hoc pairwise comparisons revealed the mean differences to the thickness were significant for the inferior muscle when compared to the temporal (mean difference 50 µm (SE 6.0)), nasal (mean difference 52.0 µmm (SE 6.0)) and superior quadrants (mean difference 53.0 µm (SE 5.0)). There was also a significant interaction between quadrant and accommodation for CM25 ($F_{3.13}$, p= 0.03). Figure 6-10 C shows the change in CM25 in relation to axial length. As axial length increased, there was a negative correlation for CM25 with accommodation for the inferior (r= 0.112, r^2 = 0.012, p= 0.49) and nasal (r= 0.24, r^2= 0.06, p= 0.14) quadrants, indicating less thickening occurred, whereas the temporal (r= 0.03, r^2= 0.0006, p= 0.89) and superior (r= 0.021, r^2= 0.0004, p= 0.90) quadrants had a relatively constant thickening irrespective of axial length.

As shown in Figure 6-8 C, the only quadrant which altered in thickness at CM50 with accommodation was the inferior. The effect of accommodation was invariant on ciliary muscle thickness at CM50 ($F_{2.65}$, p= 0.11), however, the ciliary muscle thickness significantly varied depending on quadrant ($F_{67.55}$, p= 0.000). Pairwise comparisons revealed significant differences for the means between the inferior quadrant when compared to the remaining quadrants. There was a significant interaction between quadrant and accommodation for CM50 ($F_{3.64}$, p= 0.02). There was no significant correlation between axial length and change in CM50 with accommodation for the temporal (r= 0.050, r^2= 0.0025, p= 0.76), nasal (r= 0.07, r^2= 0.0049, p= 0.67), inferior (r= 0.069, r^2= 0.0048, p= 0.67) or superior (r= 0.16, r^2= 0.025, p= 0.329) quadrants.

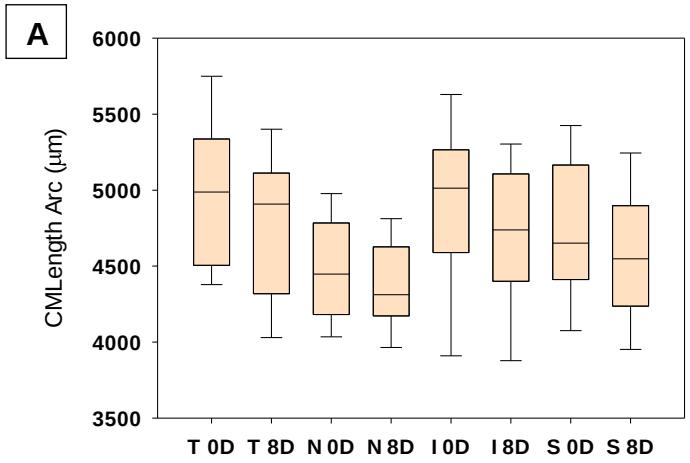

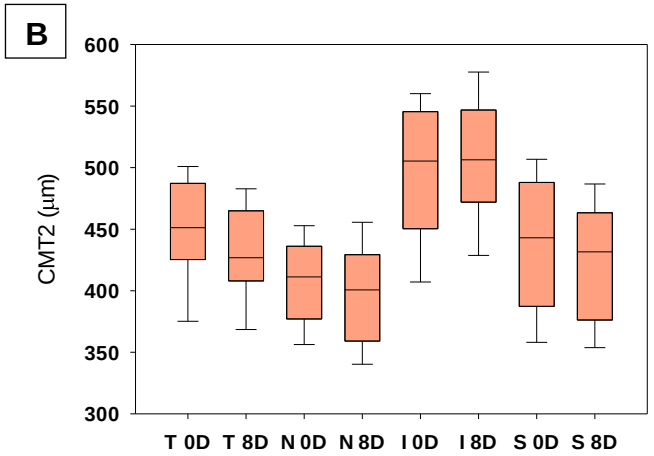

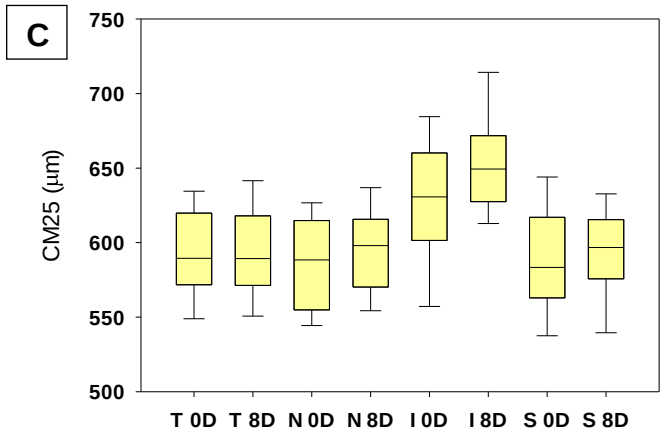

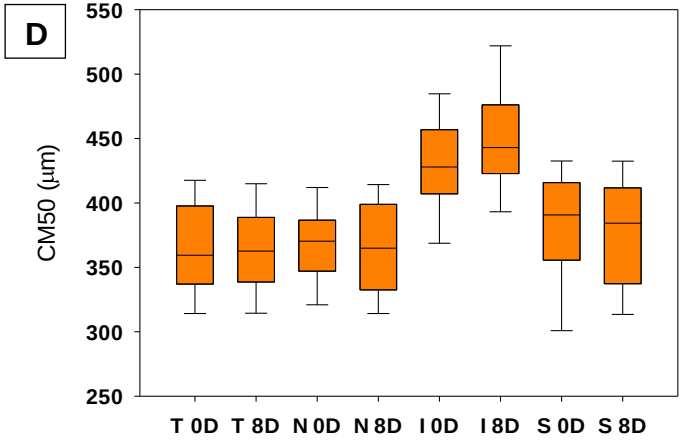

Figure 6-8. Box and whisker plots showing the thickness of the ciliary muscle at temporal (T), nasal (N), inferior (I) and superior (S) orientations for 0 D and 8 D accommodative demand levels.

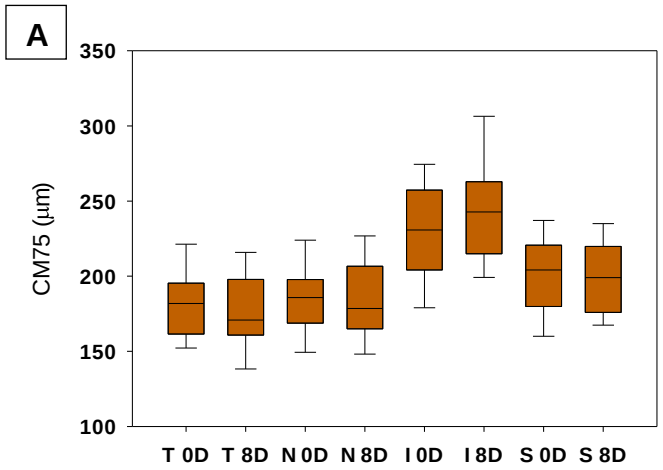

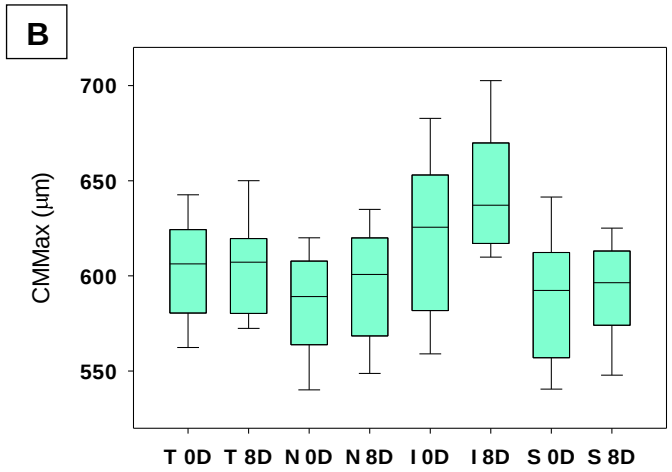

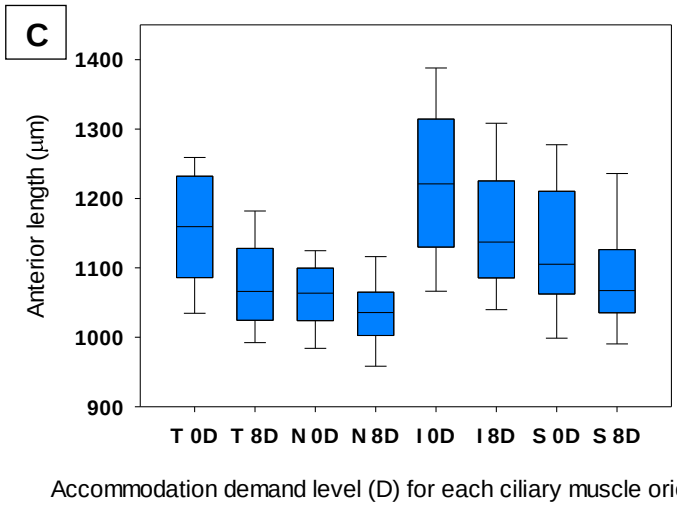

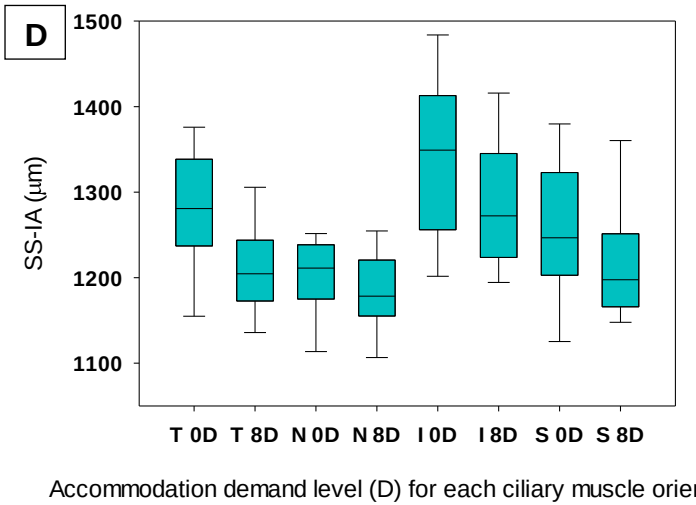

Figure 6-9. Box and whisker plots showing the ciliary muscle parameter at temporal (T), nasal (N), inferior (I) and superior (S) orientations for 0 D and 8 D accommodative demand levels.

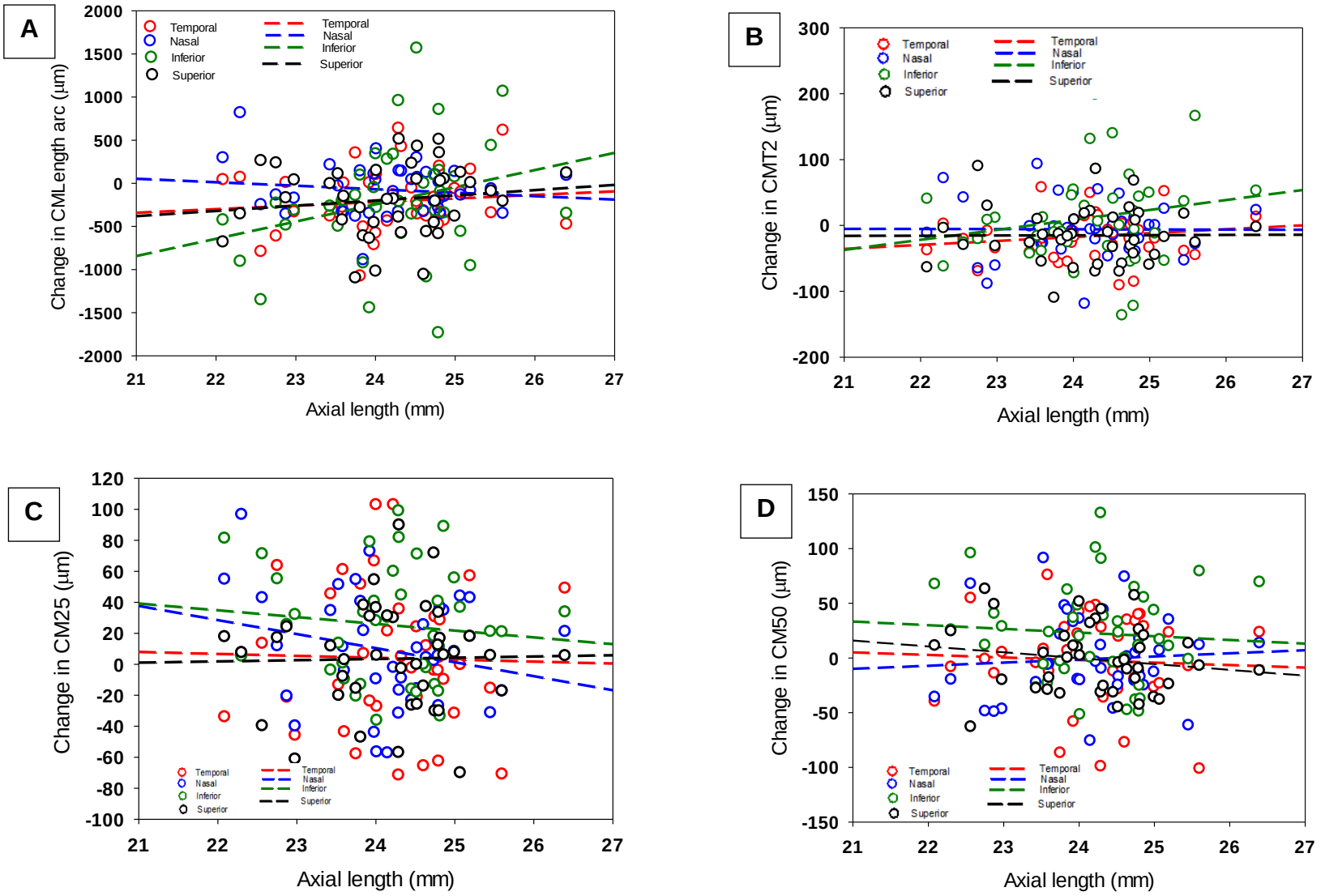

Figure 6-10. The correlation between axial length and A: ciliary muscle length (CM Length Arc), B: CMT2, C: CM25 D: CM50 for the four ciliary muscle quadrants between 8 D and 0 D demand level.

As seen in Figure 6-9 A, the thickness at the posterior region of the ciliary muscle (CM75) slightly reduced with accommodation in the temporal and superior quadrants, but increased in thickness within the inferior quadrant. There was no significant effect of accommodation ($F_{0.16}$, p= 0.691) on the thickness, although there was a statistically significant effect of quadrant ($F_{54.35}$, p= 0.69), notably the inferior quadrant when compared to the remaining orientations. The interaction between quadrant and accommodation were not significant ($F_{2.10}$, p= 0.11). Furthermore, with increasing axial length, the temporal (r= 0.15, r^2= 0.023, p= 0.34), superior (r= 0.11, r^2= 0.011, p= 0.51) and inferior (r= 0.13, r^2= 0.018, p= 0.41) quadrants reduced in thickness, whereas the nasal quadrant became thicker (r= 0.12, r^2= 0.014, p= 0.47), although the correlations were not significant (see Figure 6-11 A).

On average, the ciliary muscle maximum thickness (CMMax) increased during accommodation for the temporal, nasal and inferior quadrants as seen in Figure 6-9 B, whereas the superior thickness remained stable. The greatest change occurred for the inferior quadrant (relaxed accommodation average 623.0 µm (SE 7.0), maximum accommodation average 647.0 µm (SE 6)). The change to the maximum thickness was dependent on quadrant ($F_{50.70}$, p= 0.000). Pairwise comparisons between the mean differences for the inferior quadrant with the temporal, nasal and superior revealed significant mean differences of 33.0 µm (SE 5.0), 44.0 µm (SE 5.0) and 46.0 µm (SE 5.0), respectively. CMMax was also influenced by accommodation ($F_{13.84}$, p= 0.001) and there was a significant interaction between quadrant and accommodation ($F_{3.376}$, p= 0.02). As axial length increased, the change to the thickness with accommodation within the superior and temporal ciliary muscle became greater although there was no significant correlation (temporal: p= 0.49; superior: p= 0.45). However, there was a negative correlation for the nasal muscle indicating the muscle becomes thinner although not significantly (r= 0.221, r^2 = 0.049, p= 0.17). The inferior quadrant remained relatively constant (r= 0.036, r^2= 0.015, p= 0.45). There was a reduction to the anterior length and SS-IA with accommodation for all quadrants. The effect of quadrant and accommodation as separate factors were significant on the anterior length (quadrant $F_{29.64}$, p= 0.000; accommodation $F_{38.18}$, p= 0.000) and SS-IA (quadrant $F_{30.18}$, p= 0.000; accommodation $F_{31.34}$, p= 0.000), although the interaction between accommodation and quadrant was invariant for both parameters. There was a greater reduction to SS-IA and anterior length for shorter axial lengths for the inferior quadrant as seen in Figure 6-11 C and D, respectively.

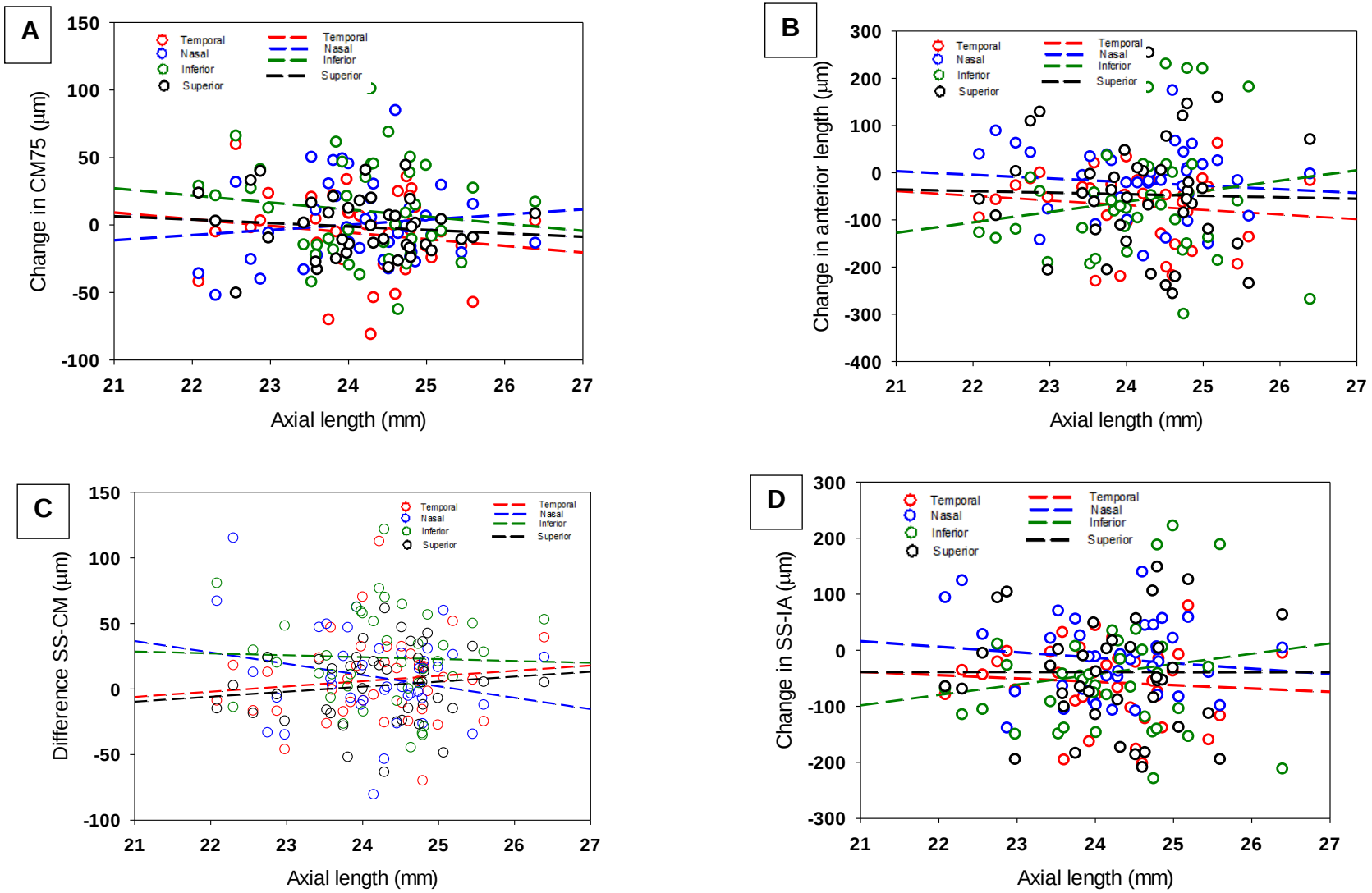

Figure 6-11. The correlation between axial length and A: CM75, B: anterior length, C: maximum ciliary muscle thickness, D: scleral spur to inner apex for the four ciliary muscle quadrants between 8 D and 0 D demand level.

6.3.3. Refractive error effect on ciliary muscle parameter for each quadrant with accommodation

The ciliary muscle parameters for 0 D and 8 D accommodative demand levels for emmetropic and myopic groups are depicted in the box and whisker plots (Figure 6-12 and Figure 6-13) and Table A3-2 in the appendix. The ciliary muscle length arc for relaxed accommodation was longer in myopes for the temporal (average 5185.0 µm (SE 110.0)), nasal (average 4631.0 µm (SE 70.0)) and superior (average 4939.0 µm (SE 92.0)) quadrants, whereas the inferior ciliary muscle was generally slightly longer in emmetropes (average 4933.0 mm (SE 132.0)), as seen in Figure 6-12 A. The interaction for quadrant and refractive error for the ciliary muscle length arc was statistically significant ($F_{3.96}$, p= 0.02), however, the interaction between accommodation and refractive error was insignificant ($F_{0.21}$, p= 0.65). Furthermore, the interaction between accommodation, refractive error and quadrant was not significant ($F_{1.13}$, p= 0.34).

As seen in Figures 6-12 and Figure 6-13, the ciliary muscle thickness (CMT2, CM25, CM50, CM75 and CMMax) were invariant between refractive groups, although there was a significant interaction between quadrant and refractive error for CMT2 ($F_{5.10}$, p= 0.004) and CMMax ($F_{3.52}$, p= 0.02). There was also a significant interaction between quadrant, accommodation and refractive group for CM25 ($F_{3.41}$, p= 0.02) and CMMax ($F_{4.05}$, p= 0.009). For SS-IA there was a statistically significant between refractive groups ($F_{7.203}$, p= 0.011) but there was no significant interaction between accommodation and refractive error ($F_{0.06}$, p= 0.81), quadrant and refractive error ($F_{1.39}$, p= 0.25) or quadrant, refractive error and accommodation ($F_{1.22}$, p= 0.31). Figure 6-13 D shows the anterior length between refractive groups and during accommodation. There was a significant difference in the anterior length between refractive groups ($F_{10.24}$, p= 0.003), but there was no significant interaction of refractive error and quadrant ($F_{1.40}$, p= 0.25), refractive error and accommodation ($F_{0.16}$, p= 0.70) or accommodation, refractive error and quadrant ($F_{0.87}$, p= 0.46).

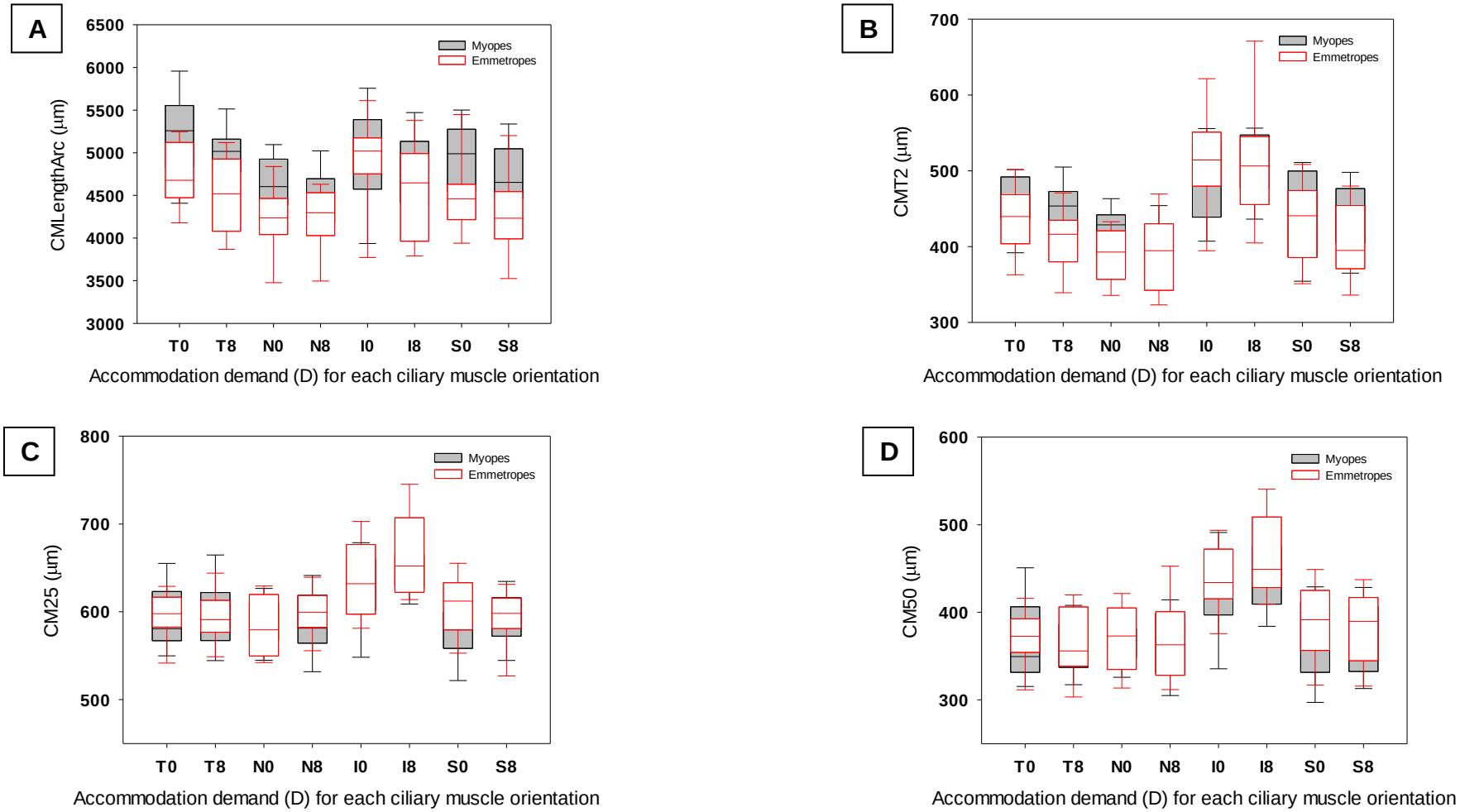

Figure 6-12. Box and whisker plots showing A) CMLengthArc, B) CMT2, C) CM25 and D) CM50 during relaxed accommodation (0 D) and maximum accommodation (8D) for the temporal (T), nasal (N), inferior (I) and superior (S) ciliary muscle orientations, in emmetropes and myopes.

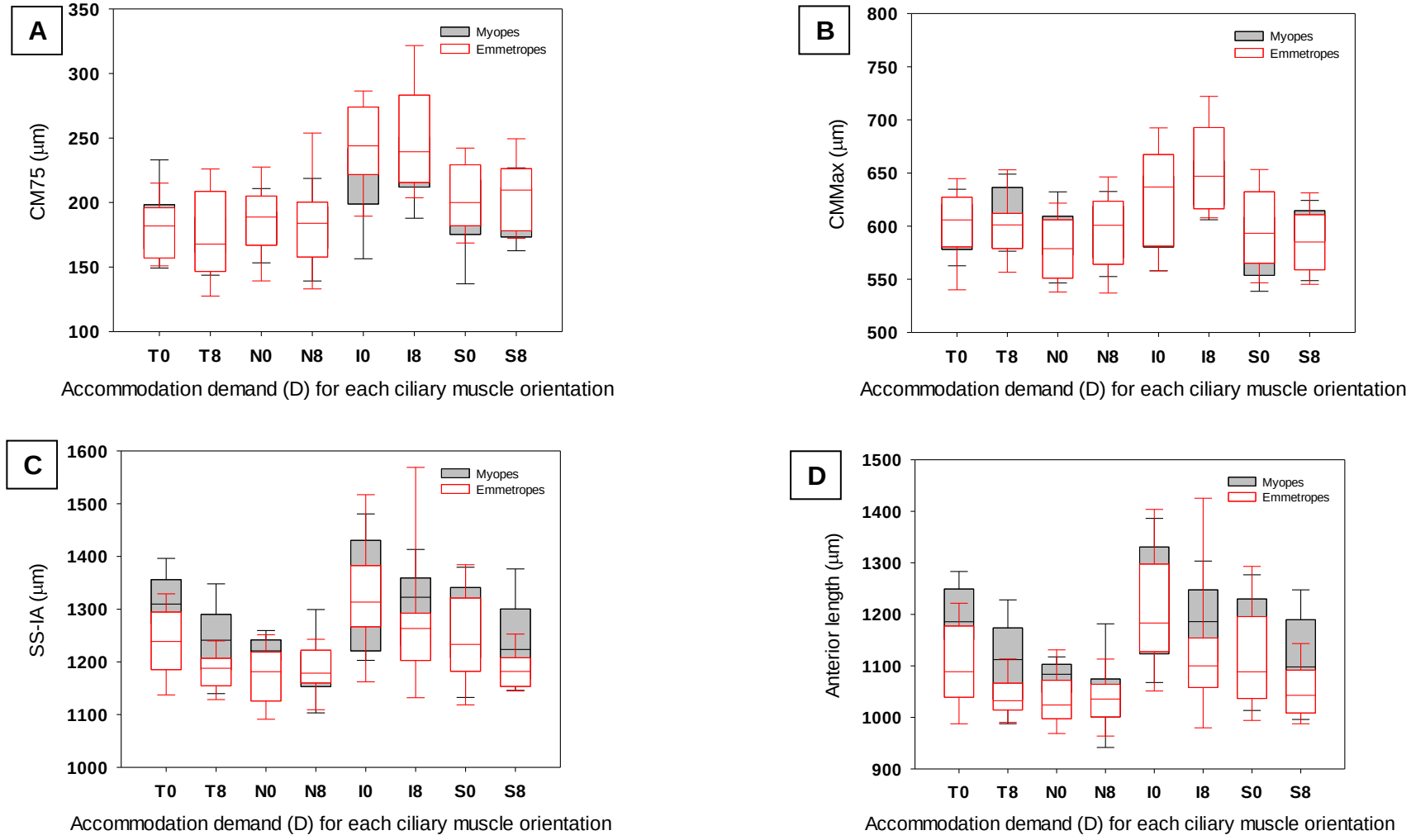

Figure 6-13. Box and whisker plot showing A) CM75, B) CMMax, C) SS-IA and D) anterior length during relaxed accommodation (0 D) and maximum accommodation (8D) for the temporal (T), nasal (N), inferior (I) and superior (S) ciliary muscle orientations, in emmetropes and myopes.

There was a negative correlation between CMT2 and CMT3 and mean spherical equivalent for all quadrants except the inferior, during relaxed accommodation, as shown in Figure 6-14 A and B, respectively. The results indicate eyes with longer axial lengths have a thicker ciliary muscle 2 mm and 3 mm posterior to the scleral spur within the nasal, temporal and superior quadrant although the correlation is not statistically significant for either quadrant (temporal CMT2: r= 0.208, r^2= 0.043, p= 0.20, CMT3: r= 0.123, r^2= 0.015, p= 0.45; nasal CMT2: r= 0.074, r^2= 0.005, p= 0.65, CMT3: r=0.155, r^2= 0.024, p= 0.34; superior CMT2 r= 0.174, r^2= 0.0302, p= 0.284, CMT3 r= 0.153, r^2= 0.024, p= 0.35), whereas shorter eyes have a longer inferior ciliary muscle length (CMT2: r= 0.175, r^2= 0.031, p= 0.279, CMT3: r= 0.247, r^2= 0.061, p= 0.124)

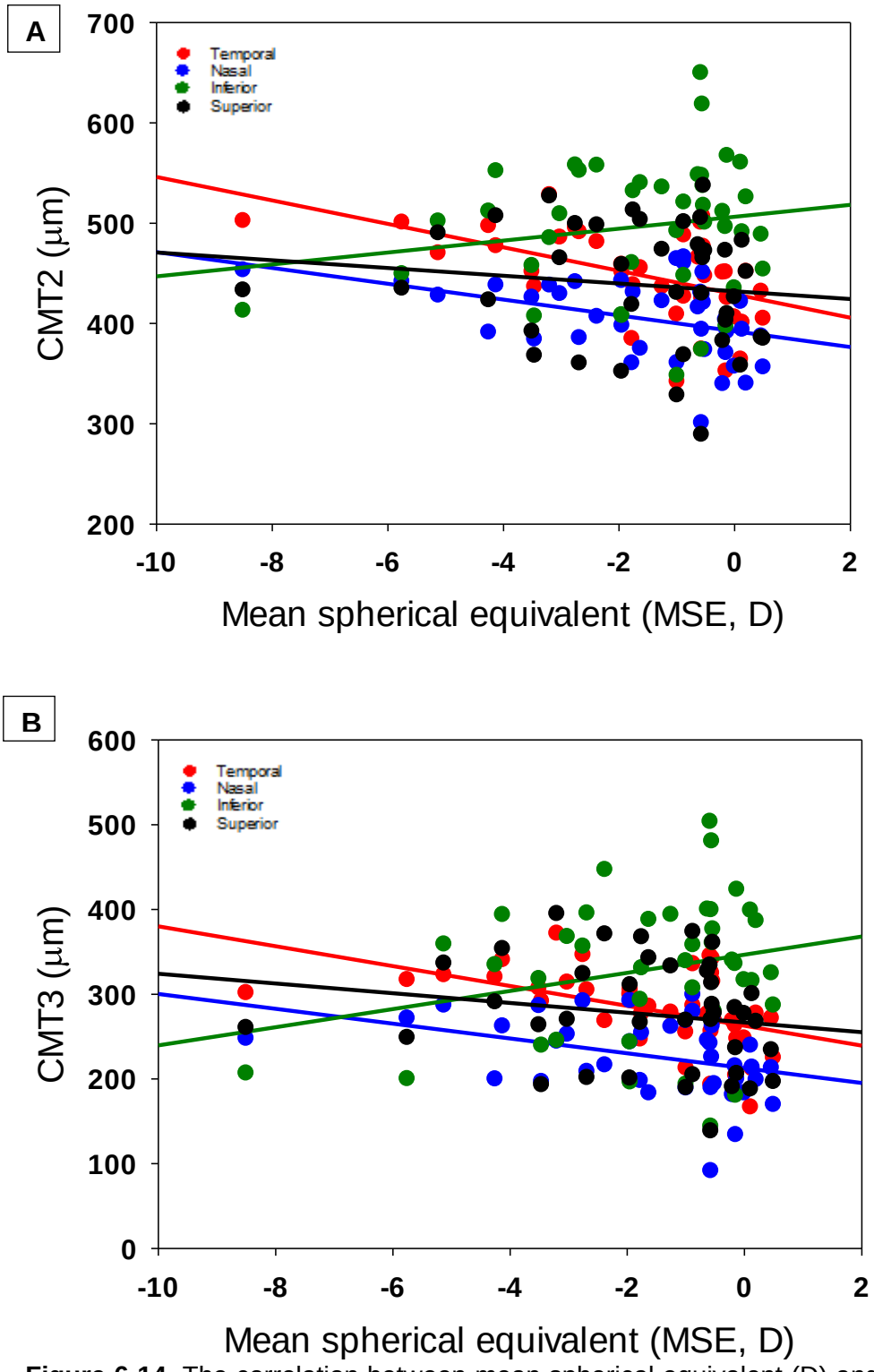

Figure 6-14. The correlation between mean spherical equivalent (D) and A: CMT2 (mm) and B: CMT3 (mm).

6.4. Discussion

This study reveals for the first time, there is variation to the ciliary muscle morphology within the horizontal and vertical meridians, in relation to accommodation and ametropia.

Relationship between ciliary muscle morphology, axial length and refractive error

The data from this study indicates that as the axial length increases, ciliary muscle length also increases but only within the temporal, nasal and superior quadrants, whereas, the inferior muscle length remains invariant with axial elongation. Interestingly, anterior ciliary muscle length increases within all four quadrants, however, this is only significant for the temporal ($r= 0.364$, $r^2= 0.13$, $p= 0.02$) and nasal ($r= 0.45$, $r^2= 0.20$, $p= 0.003$) quadrants. In addition, CMT2 increases significantly with axial length within the temporal and nasal quadrants, and there is a significant positive correlation between axial length and the location of maximum thickness (CMMax) within the nasal quadrant. Therefore, in accordance with previous research (e.g. Oliveira et al., 2005) these data suggest that longer eyes have longer ciliary muscle lengths, and there is an anterior thickening of the muscle as the axial length elongates. The thickening mainly occurs within the horizontal meridian, specifically, the nasal quadrant. Although the superior quadrant also becomes longer, there is a minimal alteration to the thickness of the ciliary muscle within the anterior and posterior locations. Moreover, the inferior ciliary muscle does not alter with axial elongation and remains stable in length and thickness as the axial length becomes greater.

Proportional measurements at CM25, CM50 and CM75 were independent of axial length which is in agreement with Sheppard and Davies (2010b), which was evident for both the horizontal and vertical meridians of the ciliary muscle. The finding indicates the growth of the muscle is restricted to the anterior region of the muscle which is evident by the increase in anterior length with axial elongation. The maximum thickness only increased within the anterior region for the nasal ciliary muscle, however considering the muscle within this quadrant was the thinnest, could explain why these findings are more evident compared to the other quadrants, where a similar process may also occur especially since an increase in anterior length was also identified. Such developmental changes may be due to the difference in vascular supply to the ciliary muscle. The anterior ciliary muscle receives blood supply from the major arterial circle, whereas the posterior regions are vascularised intramuscular circle of ciliary body

(Tamm et al., 1996; Bron et al., 1997), which suggests functional variation within the muscle.

Previous studies have only analysed the ciliary muscle parameters from the horizontal meridian, i.e. nasal and/ or temporal ciliary muscle. The findings of an increase in length for the temporal ciliary muscle in relation to increasing axial length are in agreement with previous studies (Sheppard and Davies, 2010b; Jeon et al., 2012). The current study revealed the nasal ciliary muscle was thinnest and shortest whilst the temporal muscle was the thickest and longest in the unaccommodated eye. The asymmetry is in agreement with Sheppard and Davies (2010b) who also used AS-OCT to obtain measurements from a cohort with similar axial lengths (24.49 mm (SD 1.13)) to those included in this study (24.18 mm (SD 0.91)). However, the authors calculated the ciliary muscle length as the horizontal measurement from the scleral spur to the posterior visible limit, and although this measurement (CMLength) was determined for this study, it was found the average for each quadrant was less than the average for the ciliary muscle length arc measurement (CMLength Arc). The measurement of the ciliary muscle length along the scleral arc provides a more accurate assessment of the length since the scleral curvature varies between individuals (Kao et al., 2011).

Comparing CMLength measurements obtained from this study with those found by Sheppard and Davies (2010b) reveals their average nasal ciliary muscle length were longer (4.630 mm (SD 0.470)) than in this study (4.408 mm (SD 0.401)) and temporal length shorter (4.810 mm (SD 0.690)) than found for this study (4.924 mm (SD 0.501)). In contrast, Jeon et al (2012) used ultrasound biomicroscopy (UBM) to determine the ciliary muscle length as measured along the ciliary muscle length arc on the scleral and vitreous side of the temporal muscle. Comparing the temporal measurements of the ciliary muscle along the scleral boundary of Jeon and colleagues (2012) to our CMLength Arc measures reveals longer lengths obtained with UBM (5.519 mm (SD 0.446)) compared to this study (4.987 mm (SE 0.081)). The possible underestimation of the ciliary muscle length found in this study could be attributed to the lack of visibility of the posterior zonular fibres with AS-OCT, which is identifiable with ultrasound biomicroscopy allowing better identification of the posterior limit of the ciliary muscle. Also, Jeon and colleagues recruited participants with higher myopic refractive errors (-3.10 D (SD 2.56)) in comparison to this study (MSE -1.66 D (SD 1.93)), which may explain the longer average ciliary muscle lengths reported.

A thicker ciliary body at 2 mm and 3 mm posterior to the scleral spur has been reported in myopic eyes (Oliveira et al., 2005; Bailey et al., 2008; Pucker et al., 2013). Oliveira et al (2005) evaluated the temporal ciliary body thickness in 75 eyes (mean age 51.8 years (SD 16.5), average axial length 23.2 ± 2.5 mm)) with UBM and reported thickness measurements at 2 mm (CBT2) and 3 mm (CBT3) posterior to the scleral spur during relaxed accommodation. Myopes had a significantly greater thickness at CBT2 in comparison to emmetropes (myopes: 490 µm (SD 115); emmetropes: 362 µm (SD 53)) and at CBT3 (myopes: 315 µm (SD 79); emmetropes: 247 µm (SD 49)), a finding which has also been documented for this study. However, for this study the magnitude of difference between emmetropes and myopes was smaller in comparison to those of Oliveira and colleagues (2005). The differences could be attributed to the presbyopic cohort recruited by Oliveira and colleagues as an anteroposterior ciliary muscle thickening is known to occur with increasing age (Strenk et al., 2010). Furthermore, the cohort consisted of participants with pathological conditions such as narrow angles and primary open angle glaucoma, which alter the ciliary body thickness in comparison to normals: a thinner ciliary body has been reported in eyes with narrow angles (Gohdo et al., 2000) and a thicker ciliary body for glaucoma patients using latanoprost (Marchini et al., 2003). The confounding effect of pathology on the ciliary body thickness may, therefore, have influenced the results. Also, it is unclear how the ciliary body data were quantified and the refractive index correction provided to the images. Overall, the present study showed a positive correlation for the thickness at the temporal ciliary muscle at CMT2 and CMT3 with axial length, which is in agreement with Oliveira et al (2005).

Muftuoglu et al (2009) also evaluated the temporal ciliary body thickness using ultrasound biomicroscopy within a highly myopic cohort (mean age 28.4 ± 10.4 years, average axial length 27.24 ± 1.52 mm). Using the in-built calipers, the thickness measurements were taken from the location of maximum thickness and the results indicated ciliary body thickness (CBT) and ciliary muscle thickness (CMT) were greatest in eyes with longer axial lengths (CBT: 1.350 ± 0.034 mm; CMT 0.698 ± 0.057 mm), which is in agreement with Jeon et al (2012). It seems myopic eyes have ciliary muscles with thicker anterior regions which may contract less during accommodation and produce the accommodative lag which could stimulate axial elongation (Jeon et al., 2012). However, the results from the current study do not reveal any significant differences in CMMax between emmetropes and myopes, which may be due to the shorter axial lengths included in comparison to Muftuoglu et al (2009). Nevertheless,

neither of the authors indicated the refractive indices used to correct for the speed of sound through the scleral and ciliary body tissue.

The thickness of the ciliary muscle at CMT2 was negatively correlated with refractive error for all quadrants, but positively correlated with axial length for the temporal, nasal and superior quadrants only. Therefore, axial length does not seem to be the only factor involved for altering ciliary muscle thickness, especially for the inferior quadrant. The ciliary muscle is the anterior extension of the choroid, and evidence from studies on Macaque monkeys (Hung et al., 2000) and humans (Read et al., 2010b) reveal a thinning of the choroid with hyperopic defocus. Therefore, the distribution of tissue mass from the choroid to the posterior regions of the ciliary muscle could result in the observed ciliary muscle thickness. The crystalline lens thins in childhood (Zadnik et al., 1995) therefore Muftuoglu and colleagues (2009) suggested the increased zonular tension from the lenticular changes could induce choroidal tension resulting in an increase to the ciliary muscle thickness.

In-vitro measurement for the ciliary muscle length treated with atropine indicates a mean length of 3.87 mm (SD 0.26) for an average age of 49.3 years (Pardue and Sivak, 2000) and approximately 4.0 mm for a 30 year old ciliary muscle (Tamm et al., 1990). The shorter lengths may be due to post-mortem changes to the ciliary muscle. However, the comparison of the *in-vivo* data for the pre-presbyopic cohort within this study and the older cohort from the histochemical studies provides support the ciliary muscle length decreases with age (Tamm et al., 1990). Furthermore, comparison of the ciliary muscle thickness measurements for the pre-presbyopic cohort within this present study and the presbyopic cohort recruited by Oliveira et al (2005) show a similar regression which is higher than reported for the ciliary body thickness data from children (Pucker et al., 2013), suggesting the refractive error for the cohort within the adult population recruited for our study is stable. Comparing the ciliary muscle thickness of children to the findings within this current study and to those of a presbyopic cohort investigated by Oliveira et al (2005) also indicates the ciliary muscle thickens with age (Tamm et al., 1992b).

The orbit of the eye possesses four walls which lie within the globe. The globe is flatter in the vertical meridian compared to the horizontal (Bron et al., 1997). The orbit of a child is rounder, however, the width and height of the orbital wall increases with age resulting in a greater width than height in the adult eye (Turvey et al., 2012). The dimensions of the ciliary body have been documented by Bron et al (1997) who reported a temporal width 7.5 – 8 mm, nasal width 6.5 – 7 mm, superior width 7 mm

and inferior width 7 mm within adult eyes. The thinner nasal ciliary muscle correlates with the findings from our study, although the overall findings are greater than the current study. However, the age range and the location from which the width measurements were obtained were not reported by the author. Moreover, the data clearly reveal variation within the quadrants of the ciliary muscle as found in the current study. The interesting finding from this study is the inferior ciliary muscle does not vary in length or thickness with increasing axial length. A possible cause may be because the inferior orbit is the shortest (Bron et al., 1997) therefore it may restrict ciliary muscle growth with axial elongation. However, it would be of interest to investigate the ratio change between the superior and inferior orbital walls in a longitudinal study to provide a clearer understanding of the ciliary muscle changes with orbital development. Furthermore, the sclera is thicker inferiorly (Buckhurst et al., 2015), which may restrict the ability of the muscle to expand with increasing axial length. Also, the thicker temporal ciliary muscle may be related to the thicker lateral wall which undergoes greater stress than the other aspects of the orbital wall (Bron et al., 1997).

Ciliary muscle and accommodation

This study is the first to quantify the changes in the vertical dimensions of the ciliary muscle during accommodation and compare the variation to the horizontal meridian. During accommodation, there was a contractile shortening and anterior thickening of the ciliary muscle in all quadrants, as well as a reduction to the anterior length and distance between the scleral spur and inner apex, indicating a forward and centripetal movement of the muscle as a unit. However, the changes to the ciliary muscle thickness and length during accommodation were dependent on quadrant. There was a significant interaction of quadrant and accommodation within CM25, CM50 and CMMax, indicating the accommodative changes to the ciliary muscle are confined to the anterior region which is also in agreement with previous studies (Sheppard and Davies, 2010b; Lewis et al., 2012; Lossing et al., 2012; Richdale et al., 2013; Shao et al., 2013; Ruggeri et al., 2014; Richdale et al., 2015). The anterior region of the muscle consists of circular fibres which are known to have a primary function in accommodation (Tamm et al., 1996). The forward and inward movement of all quadrants of the ciliary muscle as found from this study, indicates a mechanism for reducing zonular tension (Atchison, 1995).

Investigation of the temporal ciliary muscle thickness changes with accommodation in young adults suggested a thickening of CMTMax from 795.2 µm (SD 65.4) to 868.5 µm

(SD 83.3), and CMT1 from 774.8 µm (SD 66.3) to 813. 9 µm (SD 85.8), whereas a thinning was found at CMT2 from 557.8 µm (SD 80.8) to 535.5 µm (SD 98.2), and a reduction in thickness in CMT3 from 353.7 µm (SD 67.6) to 303.8 µm (SD 70.8) (Lossing et al., 2012). These measurements are greater than the unaccommodated data from the temporal ciliary muscle in our study where CMMax was 599 µm (SD 38.7), CMT1 634 µm (SD 44.1), CMT2 449 µm (SD 45.5) and CMT3 was 282 µm (SD 46.2). However, Lossing et al (2012) appeared to have included the thickness of the pigmented ciliary epithelium within the ciliary body results, whereas, only the ciliary muscle region was analysed within our current study. Nevertheless, the overall finding that the anterior muscle thickness with accommodation is evident for both studies. The suggestion that CMT2 is a fulcrum region during accommodation was not evident from the results reported here. Generally a reduction in thickness was identified for CMT2 from this study for the temporal, nasal and superior ciliary muscle quadrant but not the inferior which thickened with accommodation.

As the axial length increased, the contractile shortening of the inferior muscle reduced. Also, there was an asymmetry in contraction with the temporal ciliary muscle contracting more than the nasal side. Jeon et al (2012) measured the thickness of the ciliary muscle in myopic participants during accommodation to a 12.5 D stimulus. An anterior thickening and posterior thinning of the muscle was reported, however, the temporal ciliary muscle showed less contractility in longer eyes. In contrast, data from the current study suggests the contractility is less in the inferior but least for the nasal muscle whereas the temporal remains relatively unaffected in longer eyes with a thicker anterior muscle (CMMax). The anterior thickening of the muscle within the nasal quadrant may therefore reduce the ability of the muscle to contract with accommodation. However, using a greater accommodative demand level such as 12.5 D may possibly reveal greater changes therefore further investigation is required for comparison with Jeon and colleagues (2012) data.

Limitations

There are limitations to the study. To evaluate the ciliary muscle parameters within the relaxed state, cyclopentolate was not used to induce a pharmacological relaxation of the ciliary muscle. Rather it was presumed that the ciliary muscle was relaxed when measurements were obtained with AS-OCT as the changes between physiological accommodation were of interest. Although the semi-automated programme provided information about the ciliary muscle parameters, the programme required subjective

measurements of the posterior visible limit. Accurate location of the limit is possible with UBM where the posterior zonules are visible, but not with OCT (Bailey, 2011). However, the software is repeatable and accurately extracts data from the ciliary muscle parameters (Laughton et al., 2015). As evident from the results within this study, the ciliary muscle length was underestimated in comparison to UBM studies, however, the overall changes to the temporal and nasal ciliary muscle parameters with axial ametropia and accommodation were in agreement with previous studies. Perhaps, analysis of the ciliary muscle area would provide more detail on the overall gross changes which occur to the ciliary muscle during accommodation, for which the findings from the current study could elaborate on. Furthermore, the area of the ciliary muscle in emmetropic and myopic eyes would provide further information about whether significant changes occur during accommodation, and is of interest for further investigation.

In order to visualise the complete ciliary muscle for the temporal and nasal quadrant the participants were required to view a target 40° external to AS-OCT and vertical quadrants were imaged as the subject looked up or down. Therefore, the gaze direction may have altered the ciliary muscle morphology. However, peripheral refractions do not appear to alter with eye turn (Radhakrishnan and Charman., 2008), therefore the effect of eye turn is probably minimal on ciliary muscle morphology. In addition, the objective accommodative response was measured prior to ciliary muscle image acquisition therefore it was presumed the accommodative response was unaltered. A power refractor can measure the accommodative response as ciliary muscle images are acquired with the AS-OCT, however, a previous study has reported attrition of data due to the difficulty of acquiring ciliary muscle images alongside power refractor data (Lewis et al., 2012). The current study is the first to evaluate the changes to the muscle during accommodation in the vertical meridian and although the ciliary muscle images were clearly visible during acquisition, the repeatability for image analysis could have been determined.

In conclusion, the results from this study reveal the ciliary muscle length increases within the temporal, nasal and superior quadrants with axial elongation. Furthermore, the anterior muscle thickens particularly within the horizontal meridian as axial length increases. During accommodation, there was an anterior thickening of the ciliary muscle in all quadrants as well as a contractile shortening, possibly to reduce zonular tension, therefore supporting von Helmholtz's theory of accommodation.

6.5. Summary

- The study investigated the accommodative changes to the ciliary muscle along the horizontal (temporal and nasal) and vertical (superior and inferior) quadrants. Furthermore, the relationship between ciliary muscle morphology and ametropia and axial length were studied
- The main findings were:
    - During relaxed accommodation, the inferior ciliary muscle was the thickest and the temporal ciliary muscle was the longest
    - Temporal, nasal and superior CMLengthArc was significantly longer in eyes with longer axial lengths and inferior CMLengthArc was invariant with increasing axial length
    - As axial length increased, the anterior length increased in all quadrants which was significant for the temporal and nasal quadrants only
    - There was a significant positive correlation for CMMax within the nasal quadrant with increasing axial length
    - SS-IA increased increased significantly along the nasal and temporal quadrants, with axial elongation
    - During accommodation, the ciliary muscle length shortened which was greatest along the temporal and inferior quadrants
    - Changes to CMLengthArc and ciliary muscle thickness 2 mm posterior to the scleral spur during accommodation were dependant on quadrant
    - Changes to CM25 and CMLengthArc were dependent on accommodation
    - There was a statistically significant effect of quadrant on the thickness changes at CM75 during accommodation
    - The inferior ciliary muscle showed the greatest accommodative thickening at CMMax and there was a reduction to the anterior length and SS-IA during accommodation for all quadrants
    - The inferior ciliary muscle was longer in emmetropes and nasal, superior and temporal muscle was longer in myopes
    - No significant difference was found between refractive groups for CMMax, CMT2, CM25, CM50 and CM75
- The results suggest:
    - Longer eyes have longer ciliary muscle lengths and anterior thickening, particularly along the horizontal orientation

- The inferior ciliary muscle does not alter in morphology with axial elongation
- The thickness at CM25, CM50 and CM75 are independent of axial length in both the vertical and horizontal meridian and, thus suggests, the growth of the ciliary muscle is restricted to the anterior segment of the muscle since the anterior length increases with axial elongation
- During accommodation, the anterior thickening and contractile shortening of the muscle may reduce zonular tension and thus the findings support von Helmholtzs theory of accommodation

Chapter 7. Is the fovea the apposite location for investigating the effect of accommodation on posterior eye conformation?

7.1. Introduction

Our knowledge of the changes that occur within the anterior segment during accommodation has improved, nevertheless, there is a paucity of literature on the effect of accommodation on the posterior eye. There is evidence to suggest axial length does not alter with accommodation (Young, 1801; Beauchamp and Mitchell, 1985; Van der Heijde and Weber, 1989; Garner and Yap., 1997). However, techniques incorporating partial coherence interferometry (Drexler et al., 1998b; Mallen et al., 2006), optical low coherence reflectometry (Read et al., 2010a; Woodman et al., 2011; Woodman et al., 2012) and, more recently, ultra-long scan depth optical coherence tomography (resolution of 5.6 µm; Zhong et al., 2014) indicate axial length is modified during accommodation (Drexler et al., 1998b; Mallen et al., 2006; Read et al., 2010a; Woodman et al., 2011; Woodman et al., 2012; Zhong et al., 2014), although, the significance between refractive groups remains equivocal (see Table 7-1).

The relationship between accommodation and axial length has been of interest to elucidate the role of accommodation on the development of refractive error, especially since an association between near work and myopia has been suggested (e.g. Rosenfield and Gilmartin, 1998). During accommodation, a greater elongation of axial length has been documented in myopic eyes compared to emmetropic eyes (Mallen et al., 2006). However, axial length measurements obtained with the IOLMaster are overestimated during accommodation as a consequence of increased crystalline lens curvature and reduction in anterior chamber depth (Atchison and Smith, 2004b). Drexler et al (1998) measured axial length during accommodation using each participant's individually determined near point that was measured subjectively by placing a cross hair target at the position of their maximum amplitude of accommodation. Although the range of accommodative responses between the refractive groups was not statistically significant (emmetropes: 5.1 ± 1.2D; myopes: 4.1 ± 2.0 D), the authors found that the greatest increase in axial length occurred in emmetropic eyes (emmetropes: 12.7 ± 3.4 µm, myopes: 5.2 ± 2.0 µm). Read et al (2010a) used the LenStar to measure axial length during transient accommodation, to a 3 D and 6 D stimulus, which was a similar method to Mallen and colleagues (2006). The LenStar provides biometric measurements including axial length, crystalline lens thickness and anterior chamber depth (Buckhurst et al., 2009). The invaluable

biometric data enables correction of the measured axial length during accommodation, for each participant, which provides a representable estimate of the eye length change with accommodation. Although Read et al (2010a) found that there was a maximum increase to axial length for the 6 D stimulus, no significant differences were observed between the refractive error groups, which is in contrast to the data obtained by Mallen et al (2006). Nevertheless, as can be seen in Table 7-1, the refractive error of the myopic cohort in Mallen and colleagues study (2006) were of a greater magnitude than Read et al (2010a) therefore indicating eyes with higher myopic refractive errors may exhibit more noticeable changes. Furthermore, if myopes are subclassified as early onset (refractive error onset before 12 years) and late onset myopes, or stable (less than -0.50 DS increase in refractive error over two years) and progressing myopes, the transient axial elongation is greatest in myopes whose refractive error is progressing and whose refractive onset was in childhood (Woodman et al., 2012). Such findings indicate different mechanisms may be involved in axial elongation during accommodation in subgroups of myopes.

In addition, there are no significant differences to the axial length of the eye, between emmetropic and myopic groups, during a prolonged near task (Woodman et al., 2011; Woodman et al., 2012). Yet, during disaccommodation the axial length of myopes remains longer than baseline, which is independent of whether they are stable or progressing myopes, whereas for emmetropic eyes, axial length returns to baseline immediately post-task (Woodman et al., 2012). A potential limitation of these studies is that the data were collected along the visual axis; whether the same changes occur across eccentric retinal locations and whether the foveal location is the point where the maximum retinal elongation occurs with accommodation, is yet to be determined.

There are several factors which are known to influence the axial length of human eyes: axial elongation has been reported as a result of an increase in intraocular pressure (Hata et al., 2012) and transient hyperopic monocular defocus (Read et al., 2010b), whereas a reduction to the axial length has been documented with water drinking (Read and Collins., 2010), transient monocular myopic defocus (Read et al., 2010b), prolonged monocular myopic defocus (Chakraborty et al., 2012) and dynamic exercise (Read and Collins., 2011). Furthermore, axial length varies with the direction of gaze, specifically, an increase has been reported in the infero-nasal gaze during accommodation (Ghosh et al., 2012).

Ocular shape is known to vary between and within refractive groups (e.g. Atchison et al., 2004a). Instruments incorporating partial coherence interferometry have been used to measure retinal shape within the unaccommodated eye, assuming the retinal profile is homogenous and measurements are obtained for field angles less than 30˚, thereby minimising the effects of optical distortions (Atchison and Charman, 2011). Peripheral eye lengths have been obtained with the IOLMaster during relaxed accommodation (Faria-Ribeiro et al., 2013) or with the use of a cycloplegic drug (Logan et al., 2004; Mallen and Kashyap, 2007). Similar to the axial length, the peripheral eye length measurements for unaccommodated eyes are longer in myopic eyes than emmetropic eyes (Ehsaei et al., 2013). In addition, an asymmetry of peripheral eye lengths has been documented with a longer eye length within the nasal quadrant in caucasian anisomyopes (Logan et al., 2004) as well as low (refractive error -1.75 DS) and moderate myopes (refractive error -6.75 DS) (Mallen and Kashyap, 2007). Also, there is evidence of an asymmetry within the vertical field with the superior retina experiencing a steeper profile in comparison to the inferior retina (Mallen and Kashyap, 2007). Moreover, a study of the retinal contour in white and Chinese anisomyopes revealed that the axial length is greatest and the retinal shape is distorted into a prolate shape in the more myopic eye (Logan et al., 2004).

Furthermore, peripheral refraction studies indicate variation between the horizontal and vertical meridian, and an asymmetry between the temporal and nasal quadrants (Ehsai et al., 2011), as well as a superior-inferior asymmetry (Atchison et al., 2006), whether accommodation occurs (Lündstrom et al., 2009) or not. There is disagreement as to whether accommodation alters the peripheral refraction with some studies reporting a myopic shift (Ho et al., 2009; Lündstrom et al., 2009; Whatham et al., 2009), whereas other studies have not identified a difference (Calver et al., 2007, Davies and Mallen, 2009). However, it is clear ocular shape influences peripheral refraction (Verkicharla et al., 2012) and ocular shape depends upon retinal steepness (Schmid, 2003a).

Hitherto, researchers have assumed the visual axis is the apposite location for investigating the effect of accommodation on the posterior eye, although it is clear that the ocular shape varies between and within refractive groups. Furthermore, the fovea occupies a small region on the fundus compared to the peripheral retina, therefore, may not exclusively lengthen with accommodation. Additionally, asymmetry exists within the horizontal and vertical retinal hemispheres, but, it is unknown whether the elongation that has been documented to occur with accommodation is homogenous across the posterior eye.

Consequently, this study addresses three questions: 1) does peripheral eye length alter with accommodation; 2) is the effect of accommodation on eye length homogenous across the retina; and 3) does the maximum change in eye length occur at the fovea or at another eccentric location(s).

	Refractive error (mean spherical equivalent)		Method for stimulating accommodation	Axial length increase (statistical significant results)		Axial length difference between refractive groups	Instrumentation and error correction
	Emmetropes	Myopes		Emmetropes	Myopes		
Drexler et al (1998b)	-0.34 ± 0.30 D	-3.50 ± 2.80 D	Individual determined near point.	12.7 ± 3.4 µm	5.2 ± 2.0 µm	Yes: emmetropes > myopes	IOLMaster: axial length error corrected
Mallen et al (2006)	-0.07 ± 0.23 D	-3.59 ± 0.75 D	Accommodative stimuli levels: + 2 D, + 4 D and + 6 D	6 D stimulus: 37 ± 27 µm	6 D stimulus: 58 ± 37 µm	Yes: myopes > emmetropes	IOLMaster: axial length data uncorrected
Read et al (2010a)	-0.05 ± 0.27 D	-1.82 ± 0.84 D	Accommodative stimuli levels: + 3 D and + 6 D.	6 D stimulus: ~ 10 µm	6 D stimulus: ~ 10 µm	No	LenStar: axial length corrected
Zhong et al (2014)	Not specified	1.95 ± 0.88 D	Accommodative stimuli: +6 D	Emmetropic and myopic data collated: 26.1 ± 13.4 µm		N/A	Ultra-long scan depth optical coherence tomography
Deshpande (2012)	Not specified	-1.93 ± 1.39 D	N6 print at 33 cm N6 print at 12.5 cm	Accommodation at 12.5 cm: 80 µm	Accommodation at 12.5 cm: 70 µm	No	A-scan ultrasonography
Woodman et al (2011)	-0.10 ± 0.23 D	-3.11 ± 2.24 D	30 minute near vision task, + 5 D accommodative stimulus	10 ± 15 µm	20 ± 20 µm	No	IOLMaster: assumed axial length data were not overestimated. Data were collected immediately after the near task
Woodman et al (2012)	+0.16 ± 0.28 D	-2.90 ± 1.57 D	30 minute near vision task, accommodative stimulus +4 D	6 ± 22 µm	22 ± 34 µm	No	LenStar: axial length data corrected

Table 7-1. Summary of results found from research studies investigating the changes to the axial length with accommodation.

7.2. Methods

The study was conducted in accordance to the tenets of the Declaration of Helsinki. Written and verbal information was provided to participants before they provided written consent for their participation. A favourable opinion was provided by the Life and Health Sciences Ethics Committee at Aston University before the study commenced.

7.2.1. Sample size calculation

The number of participants required for the study was determined from a statistical power test based on a calculation using G*power (version 3.1.9.2; Universitat Kiel, Germany). In order to measure a medium effect size (f=0.25), based on a within-subject ANOVA design and a required statistical power (1-β) of 80% with an error probability (α) of 0.05, at least 24 participants were required.

7.2.2. Inclusion criteria

Fifty five participants were recruited from the undergraduate cohort at Aston University, to account for attrition. All participants were advised not to wear contact lenses 24 hours before the study to prevent corneal morphology alteration, which could influence axial length measurements. Participants were invited to answer questions relating to their ocular and general health to ensure they had no health concerns or using any medication which could modify accommodation. Participants who had not had an eye examination within the last two years had their ocular health examined. In addition, questions regarding refractive error history were asked to determine if the refractive error of myopes was stable (defined as a change in mean spherical equivalent (MSE) ± 0.25 D over the last two years), or progressing (defined as a change in MSE of at least -0.50 DS within two years). Participants were classified as emmetropic if MSE was within the range -0.75 D to + 0.50 D and myopic if MSE was less than -1.00 D. Exclusion criteria included astigmatism which was greater than 1.12 DC, participants who had an ocular or systemic disease, participants who had an ocular injury, ocular trauma or ocular surgery which affected the cornea, lens or ciliary apparatus, and those participants whose right eye monocular amplitude of accommodation was less than 8 D. Volunteers who were amblyopic or had a binocular vision condition were also excluded from the study. Anisometropes (MSE refractive error greater than 1 D difference between the eyes) were also excluded since interocular differences such as a thinner subfoveal choroidal thickness in the more myopic eye (Vincent et al., 2013b) and greater changes to the corneal astigmatism in the more myopic eye during near

work (Vincent et al., 2013a) have been reported which could confound the data from the study.

7.2.3. Procedure

Visual acuity and Refractive error

The same procedure was used as described in Chapter 6.

Amplitude of accommodation

Monocular amplitude of accommodation was measured with the Royal Air Force (RAF) rule using the push down method, which is known to have good repeatability (Rosenfield and Cohen, 1996). Briefly, the RAF rule rest was placed on the subject's cheeks whilst fixating on a line equivalent to N5 Times New Roman font. The target was moved towards the eye and the subject was asked to report when the font first became blurred. When they first reported that the font became blurred, they were asked if they could make it clear again, and if this was possible the target was moved towards the eye until it was reported it was blurred and could not be made clear. The target was then moved away from the subject who again reported when the print first became clear. The average of these values was recorded. The procedure was repeated three times monocularly and binocularly to obtain an overall average of the amplitude of accommodation. Subjects with a distance refractive error were asked to wear their spectacles during this procedure.

7.2.4. Axial and eccentric eye length measurements

7.2.4.1. Main study

Peripheral eye length and on-axis axial eye length measurements were obtained from the right eye (contralateral eye occluded with a patch) with the IOLMaster during relaxed accommodation and 4 D and 8 D accommodative demands. An aluminium gantry was placed around the forehead/ chin rest of the IOLMaster (Figure 7-1 A) onto which a Badal rig system (Figure 7-1 B) was attached using the same setup as described by Mallen and Kashyap (2007). The rig consisted of a +20.8 D Badal optometer (Edmund Optics), a high contrast Maltese target which was illuminated by an LED light, a beamsplitter (50% transmission/ 50% reflection) and a goniometer to vary target eccentricity in 5 degree increments.

Horizontal and vertical eye length measures were obtained by placing the Badal optometer on the top and side of the gantry, respectively (see Figures 7-1 A and 7-2).

The rig was adjusted to ensure the Maltese cross target was aligned with the pupil centre of the right eye, which was confirmed when the patient reported the beam from the IOLMaster coincided with the Maltese cross target. The Badal lens was used to focus the target to each individual's far point. The lens was slowly moved towards the beam splitter until the subject reported the Maltese cross target appeared clear. It was then moved away from the beam splitter until the subject reported it first became blurred and then moved towards the beam splitter until the subject reported it appeared clear again; this ensured there was no accommodation at the far point confirming accommodation was relaxed.

The goniometer was used to position the Maltese target at various eccentric locations for each accommodative demand. The eye length measurements were obtained for: 0˚ (axial length), + 5˚, + 15˚ and + 25˚ (temporal retina) and - 5˚, -15˚ and - 25˚ (nasal retina) along the horizontal meridian and 0˚ (axial length), - 5˚, -15˚ and - 25˚ (inferior retina) and - 5˚, -15˚ and - 25˚ (superior retina) along the vertical meridian. The subject rotated their eye to view the target, since no significant differences have been shown to occur between the influence of the extraocular muscles on the eye ball in peripheral directions of gaze during eye movement when compared with head movement (Radhakrishnan and Charman, 2008). During data collection, the accommodative demand level was randomised, as well as eccentricity. The meridian from which the data were collected was also randomly chosen. For each accommodative demand level the target was viewed for one minute before five measurements were recorded with the IOLMaster (with a signal-to-noise ratio >2.0) and the mean value noted. The light beam from the IOLMaster was directed towards the centre of the cornea, so there was a normal incidence of the beam at the anterior cornea (Atchison and Charman, 2011). Between each vergence level, the subject was allowed to relax their eyes for thirty seconds. All measurements were conducted in low illumination (to maximize pupil size) of 10^{-3} cd/m^2.

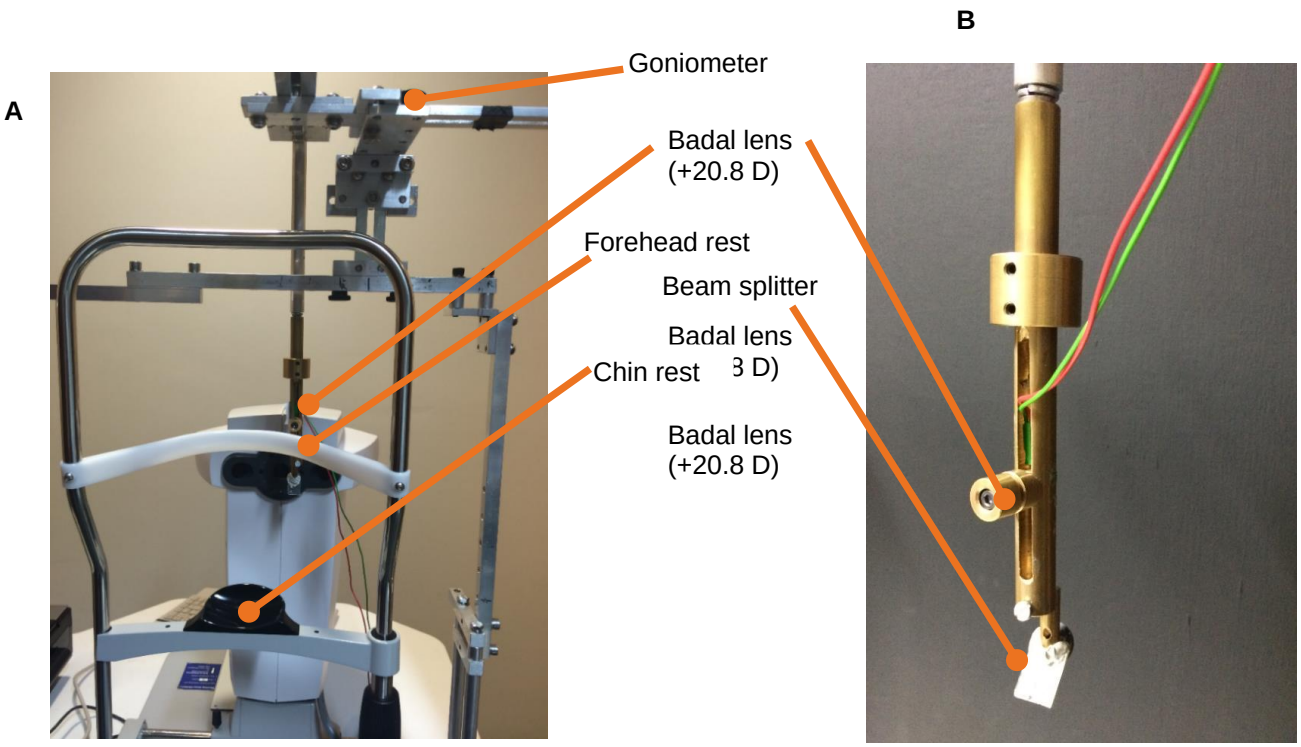

Figure 7-1. A shows the rig setup for the IOLMaster to obtain measurements for the horizontal meridian. **B** shows the rig consisting of a Badal lens used to correct the ametropia and stimulate accommodation, and the beam splitter. The beam splitter reflects the Maltese cross target viewed by the participant. The goniometer is used to alter the angle of gaze.

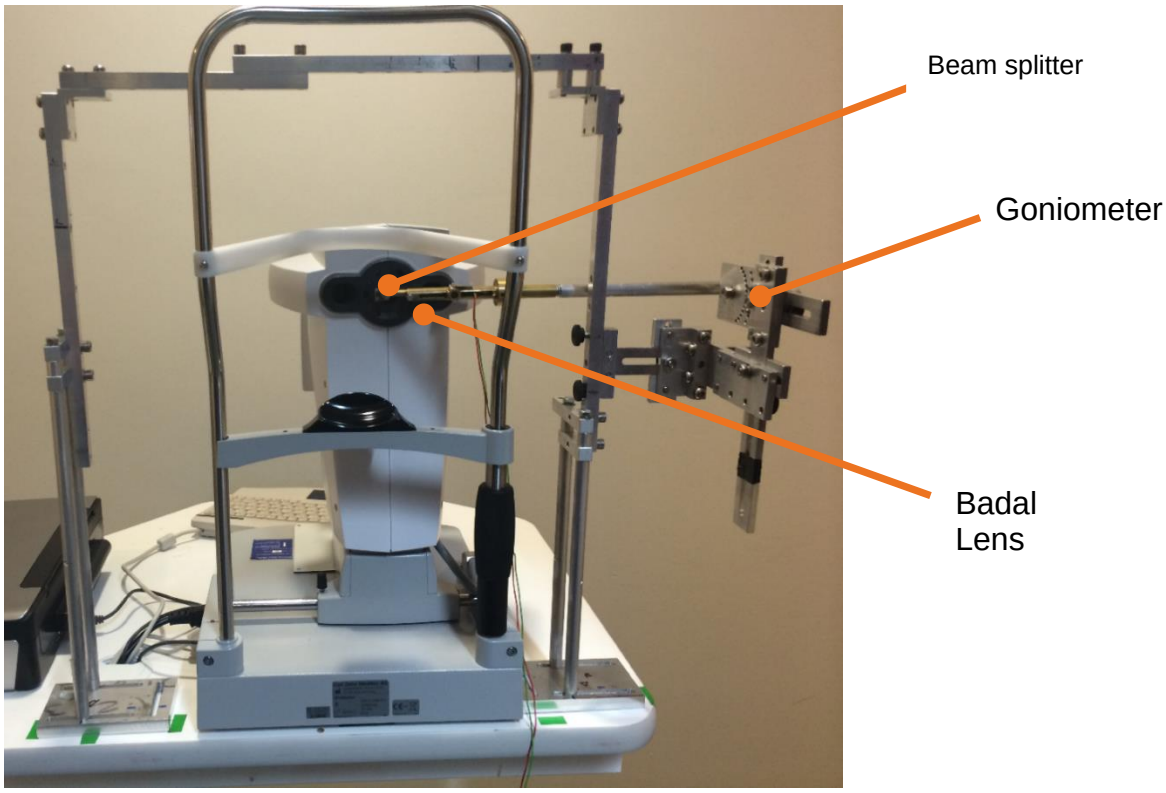

Figure 7-2. The rig setup to obtain measurements for the vertical meridian of the right eye. The beam splitter reflects the Maltese cross target that is viewed by the participant. The Badal lens corrects the refractive error and the goniometer is used to alter the angle of gaze.

Once the measurements were obtained, the health of the anterior eye was examined of the myopic participants, with a slit lamp prior to the correction of the myopic refractive error with a spherical daily soft contact lens (*Nelfilcon A*; water content 69%) to render participants functionally emmetropic. Once inserted, a settling time of five minutes was allowed. The contralateral eye was occluded with a patch and an over-refraction was performed with the Grand Seiko *WAM 5500* autorefractor whilst the participant viewed an external fixation target within a Badal lens system. The over-refraction results were within ±0.50 DS for all subjects. Subsequently, the monocular objective accommodative response of the right eye for the three demand levels (0.17 D, 4 D and 8 D) was determined for all emmetropic and myopic individuals as the subjects viewed a Maltese cross target in free space, as shown in Figure 7-3 and Figure 7-4. Three measurements were taken at each position and a final overall result was provided by the autorefractor, which was recorded. The order of the measurements for the accommodative response was randomised.

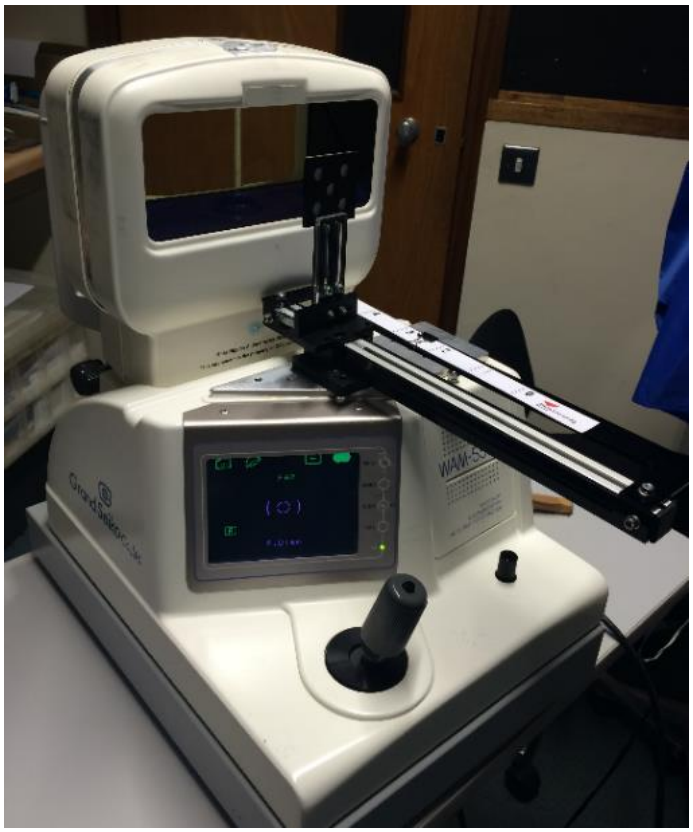

Figure 7-3. 4 D accommodative demand was simulated by placing the Maltese cross target 25 cm from the eye in free space.

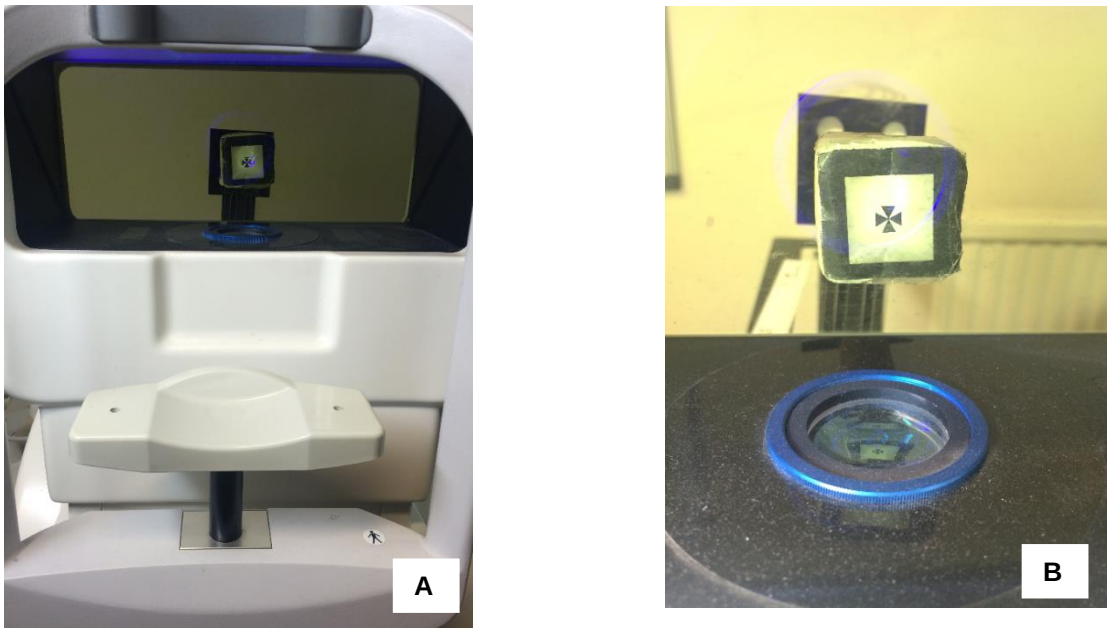

Figure 7-4. A For the 8 D accommodative demand level, a Maltese cross target was placed 12.5 cm from the eye in free space. B shows the magnified image of the Maltese cross target.

Following data collection, the contact lens was removed from the right eye of the myopic participants and the anterior eye health assessed with a slit lamp. Subsequently, corneal topography (Medmont) was obtained from the right eye.

7.2.5. Analysis

The beam of the IOLMaster was directed towards the centre of the cornea during axial and eccentric eye length measurements. The optical path length was calculated as the total distance from the cornea (anterior surface) to the posterior surface of the vitreous chamber. Corneal topography was essential to calculate the corneal sagittal height for each individual participant prior to calculating the retinal sagittal height. Model eyes that assume the corneal elevation is the same amongst individuals can produce an error for the retinal contour of 244 µm (Faria-Ribeiro et al., 2014).

Although eccentric measurements with the IOLMaster are possible (Ehsaei et al., 2013; Faria-Ribeiro et al., 2014), the path length of the beam at eccentric locations does not follow the same course when reflected from the retinal surface (Atchison and Charman, 2011). Therefore the optical path length data provided by the IOLMaster cannot be used to determine the exact position of the retina to estimate the retinal contour. As such, the average eye length measurements for each direction of gaze calculated with the IOLMaster were converted to the optical path length using the equation:

$$OPL = (GL + 1.367)/0.7711 \text{ (Haigis et al., 2000).} \quad \textbf{1.0}$$

The refractive index within the eye is assumed to remain homogenous for each eccentric measurement and with accommodation. The vitreous path length (PL) for each individual can be calculated by ray tracing to determine the direction and physical distance that the ray travels for the different media by using the following equation:

$$PL_{VITREOUS}(\theta) \times 1.3445 = PL_{CORNEA}(\theta) \times 1.385 + PL_{AQEUOUS}(\theta) \times 1.3459 + PL_{LENS}(\theta) \times 1.4070 - EL_{IOLMASTER}(\theta) \times 1.33549 \quad \textbf{1.1}$$

The data were used alongside a semi-customised eye model, based on the individual corneal topography and Navarro eye model, to compute the retinal intercept coordinates. Subsequently, the retinal sagittal height was calculated and a best conic curve was fitted (Faria-Ribeiro et al., 2014). Fitting errors that equated to the mean ± 3 SD were considered poor fits and excluded from the data to ensure a confidence interval of 99.6%, therefore only conic models with good accuracy have been included

in the results. The path of the light beam is not linear within the eye, especially at larger eccentricities, therefore all the results were normalized for the maximum distance of the conic section from the fovea (x) which was approximately ± 8 mm (average value of x for ± 30 degrees of incidence angle).

7.2.6. Axial length error during accommodation

During accommodation, the increased thickness of the crystalline lens alters the optical path length which alters the measured axial length found with the IOLMaster. As such, the axial length measurements were converted from the optical path length to the geometric path length using the equations listed in Chapter 6. The IOLMaster was only used to collect axial length data, therefore, the values for the crystalline lens thickness and anterior chamber depth during accommodation were initially obtained with the LenStar. However, complete data for all accommodative stimulus levels was only possible from 6 of the 29 participants. Therefore, as described in Chapter 6, the equations derived by Norrby (2005) have been used to calculate the lens thickness and anterior chamber during accommodation.

7.2.7. Statistical analysis

A Shapiro-Wilk test (SPSS Statistics 21; SPSS Inc., Illinois, USA) revealed normal distribution of the data for the axial length at relaxed accommodation, and with 4 D and 8 D accommodative demand levels. Therefore, assumptions of normality and homogeneity of variance were met. To explore the changes to the retinal sag depth and the axial length with accommodation, a repeated measures analysis of variance (ANOVA) was performed with one within subject factor (i.e. accommodation) and one between subject factor (i.e. refractive error).

7.3. Results

Repeatability

The intersessional repeatability of the rig that was used to obtain eye length measurements within the horizontal and vertical meridians, was assessed from 9 participants who attended two separate visits. Eye length measurements were obtained from all angles analysed in the present study. The bias for each each eye length measurement was calculated from the mean difference in measures between both visits, and paired t-tests were used to determine whether the differences were significantly different. The limits of agreement (the interval where 95% of the mean

differences lie (Altman and Bland, 1983; Bland and Altman, 1986)), were found by using the formula:

$$LoA = bias \pm (1.96 \times SD \text{ of differences})$$

There were no significant differences in eye length measurements obtained between both visits for the horizontal meridian (Table 7-2, Figure 7-5) and vertical meridian (Table 7-3, Figure 7-6).

Angle (degree)	Bias (mm)	SD of differences (mm)	95% LoA (mm)	t-test	p
-25	0.08	0.16	+ 0.40, - 0.23	1.60	0.15
-15	0.14	0.27	+ 0.68, - 0.40	1.55	0.16
-5	-0.07	0.48	+ 0.41, - 0.56	-0.91	0.39
0	-0.007	0.038	+ 0.67, - 0.08	-0.59	0.57
5	-0.06	0.18	+ 0.29, -0.42	-1.03	0.33
15	-0.02	0.18	+ 0.32, - 0.36	-0.38	0.71
25	0.05	0.29	+ 0.63, -0.52	0.58	0.58

Table 7-2. Intersession repeatability data of the eye length measurements along the horizontal meridian obtained with the rig at two seperate visits. Minus angles refer to the nasal retina and positive angles refer to the temporal retina.

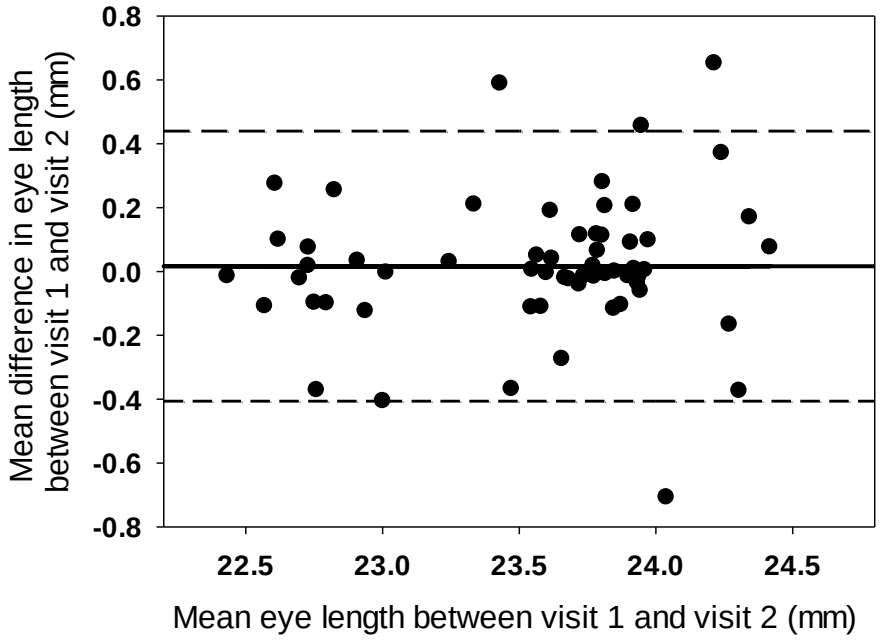

Figure 7-5. Bland-Altman plot representing the intersession repeatability data of the eye length measurements along the horizontal meridian obtained with the rig at two separate visits.

Angle (degree)	Bias (mm)	SD of differences (mm)	95% LoA (mm)	t-test	p
-25	-0.05	0.08	+ 0.24, - 0.10	1.70	0.13
-15	0.02	0.08	+ 0.20, - 0.14	0.96	0.36
-5	0.06	0.11	+ 0.28, - 0.15	1.77	0.12
0	0.01	0.07	+ 0.15, -0.12	0.52	0.62
5	0.04	0.11	+ 0.27, -0.17	1.32	0.22
15	0.01	0.10	+ 0.22, -0.20	0.24	0.81
25	0.15	0.59	+1.32, - 1.07	0.90	0.39

Table 7-3. Intersession repeatability data of the eye length measurements along the vertical meridian obtained with the rig at two seperate visits. Minus angles refer to the inferior retina and positive angles refer to the superior retina.

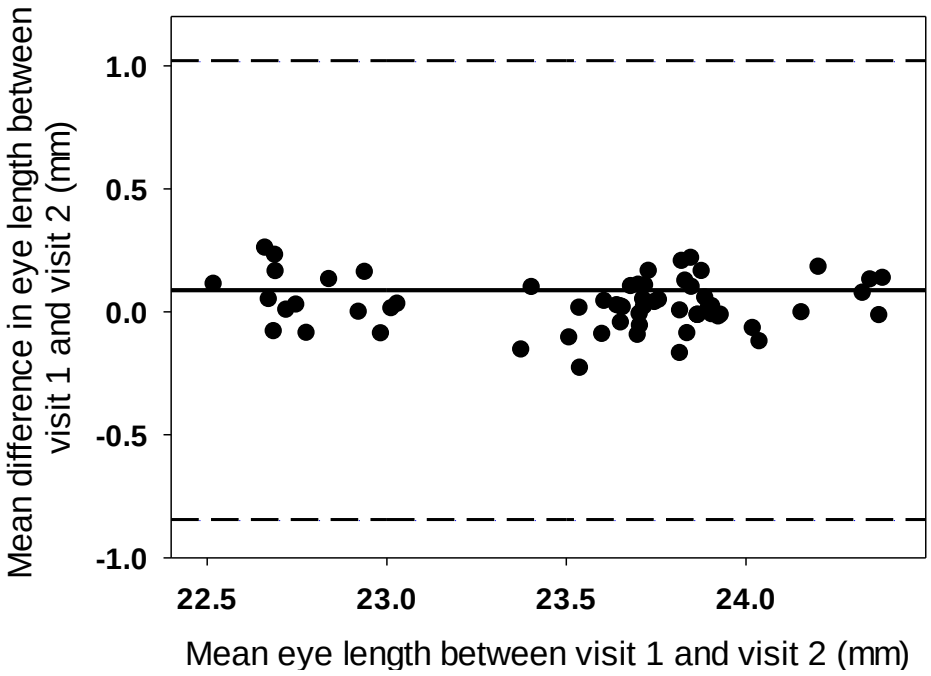

Figure 7-6. Bland-Altman plot representing the intersession repeatability data of the eye length measurements along the vertical meridian obtained with the rig at two separate visits.

Intrasessional repeatability was assessed by obtaining eye length measurements for both meridians at all field angles analysed for the present study, from one participant 10 times.

Table 7-4 shows the results and it is evident the intrasessional repeatability was good, since there was minimal variance in the data.

	Angle (degree)	Mean eye length (mm)
Horizontal	-25	22.82 (SD 0.10)
	-15	23.07 (SD 0.10)
	-5	23.04 (SD 0.5)
	0	23.02 (SD 0.08)
	5	22.92 (SD 0.12)
	15	22.88 (SD 0.16)
	25	22.71 (SD 0.16)
Vertical	-25	22.67 (SD 0.01)
	-15	22.75 (SD 0.01)
	-5	22.81 (SD 0.05)
	0	23.02 (SD 0.08)
	5	22.88 (SD 0.01)
	15	22.92 (SD 0.02)
	25	22.90 (SD 0.04)

Table 7-4. Intrasessional repeatability for the rig used to obtain eye length measurements. The negative angles refer to the nasal retina (horizontal) and inferior retina (vertical).

Retinal contour (main study)

Due to attrition (inability to collect data at all eccentricities for each accommodative stimuli level because of pupil miosis with accommodation n = 9; accommodative response less than 5 D for an 8 D stimulus n =5; errors greater than the mean ± 3 SD for the fitting curves during analysis n= 12), data are presented for 29 participants (age 20.9 years (SD 2.10) consisting of 13 myopes (age 21.2 (SD 2.1) years, MSE -2.81 D (SD 0.98)) and 16 emmetropes (age 20.7 (SD 2.2) years, MSE -0.14 D (SD 0.38)). Eight males and twenty one females participated in the study (emmetropic males n=4,

females n=12; myopic males n=4, females n=9). Twenty five participants were of an Asian ethnic background and four participants were White.

Retinal sagittal height

Data for the retinal sag height for the horizontal and vertical meridian is shown in Table 7-5 and Table 7-6, respectively. During relaxed accommodation, the values for the location referring to the visual axis (0°) show slight elevation since the conic curve apex is displaced on average by (x, y) -0.00067, -0.01061 along the horizontal meridian, and (x, y) 0.115, -0.008 along the vertical meridian rather than located at the location where the retinal sag= 0. Thus, the results indicate there is slight elevation of the retinal sagittal height at the fovea.

During accommodation, an increase of approximately 0.2 mm to the sagittal height was evident along the horizontal meridian for the whole cohort particularly between 1.5 mm and 7 mm of the nasal retina, as shown in Figure 7-7 A. The radius of the apex (R) and conic constant (Q) between 0 D (R = 12.77 mm, Q= -0.99) and 8 D (R= 13.08 mm, Q= -1.41) indicates the retinal shape alters from a prolate ellipse to a hyperboloid during accommodation.

Analysing the retinal shape with accommodation for the emmetropic subjects indicates minimal change to the initial prolate ellipse between 0 D (R= 13.03 mm, Q= -0.63) and 8 D (R= 12.93 mm, Q= -0.91) demand level. In contrast, there was an increase to the sagittal height for the myopic cohort with accommodation indicating a change from a hyperboloid retinal shape to a prolate ellipse with accommodation (0 D: R= 12.43 mm, Q= -1.46, 8 D: R= 13.29 mm, Q= -0.23).

However, the effect of accommodation on the retinal sag height was not statistically significant along the horizontal meridian for the whole cohort ($F_{1.091}$, p= 0.34), emmetropic subgroup ($F_{0.219}$, p= 0.79) or myopic subgroup ($F_{1.435}$, p=0.26). The interaction effect between the accommodation demand levels and eccentricity along the horizontal meridian was not statistically significant for the whole cohort ($F_{0.707}$ p= 0.62) nor for the emmetropic sub-group ($F_{0.995}$, p=0.43) or myopic subgroup ($F_{0.599}$, p= 0.62).

Accommodation Demand Level (D)		Distance from fovea (mm)						
		Nasal						Temporal
		-7	***-4.5***	***-1.5***	***0***	***1.5***	***4.5***	***7***
All	0 D	-1.94 (SE 0.051)	-0.81 (SE 0.054)	-0.13 (SE 0.026)	6.1×10^{-5} (SE 4.4×10^{-5})	-0.13 (SE 0.041)	-0.82 (SE 0.039)	-1.95 (SE 0.058)
	4 D	-1.88 (SE 0.055)	-0.81 (SE 0.049)	-0.083 (SE 0.028)	5.9×10^{-6} (SE 1.6×10^{-5})	-0.045 (SE 0.027)	-0.79 (SE 0.045)	-1.94 (SE 0.064)
	8 D	-1.93 (SE 0.05)	-0.77 (SE 0.043)	-0.12 (SE 0.023)	-3.30×10^{-6} (SE 1.0×10^{-5})	-0.095 (SE 0.023)	-0.82 (SE 0.036)	-1.95 (SE 0.0056)
Myopes	0 D	-1.96 (SE 0.060)	-0.85 (SE 0.065)	-0.17 (SE 0.032)	1.1×10^{-4} (SE 6.4×10^{-5})	-0.17 (SE 0.054)	-0.85 (SE 0.050)	-1.95 (SE 0.062)
	4 D	-1.88 (SE 0.070)	-0.78 (SE 0.065)	-0.06 (SE 0.031)	-1.9×10^{-6} (SE 1.7×10^{-5})	-0.024 (SE 0.028)	-0.77 (SE 0.061)	-1.93 (SE 0.084)
	8 D	-1.91 (SE 0.059)	-0.77 (0.057)	-0.07 (SE 0.022)	1×10^{-5} (SE 1.4×10^{-5})	-0.083 (SE 0.023)	-0.79 (SE 0.043)	-1.99 (SE 0.070)
Emmetropes	0 D	-1.92 (SE 0.044)	-0.79 (SE 0.045)	-0.11 (SE 0.020)	2.6×10^{-5} (SE 1.2×10^{-5})	-0.093 (SE 0.026)	-0.80 (SE 0.027)	-1.96 (SE 0.057)
	4 D	-1.88 (SE 0.040)	-0.83 (SE 0.033)	-0.11 (SE 0.026)	2.6×10^{-5} (SE 1.5×10^{-5})	-0.061 (SE 0.027)	-0.80 (SE 0.028)	-1.95 (SE 0.045)
	8 D	-1.95 (SE 0.044)	-0.78 (SE 0.030)	-0.15 (SE 0.023)	2.5×10^{-6} (SE 7.5×10^{-6})	-0.11 (SE 0.025)	-0.84 (SE 0.030)	-1.92 (SE 0.042)

Table 7-5. Data for the average retinal sagittal depth (mm) along the horizontal meridian for the three accommodative demand levels for all participants (n=29), myopes (n=13) and emmetropes (n=16).

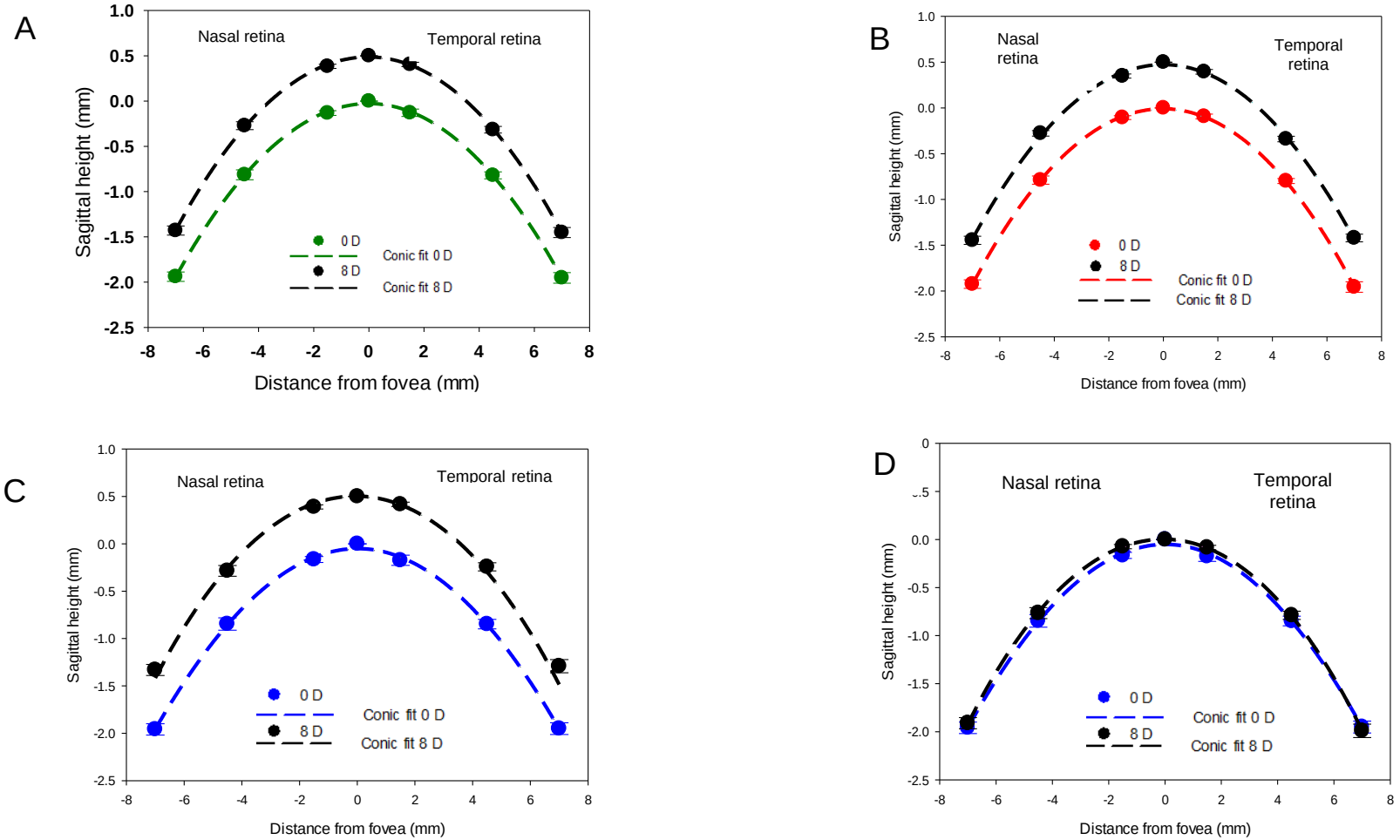

Figure 7-7. Average sagittal values fitted with a conic curve for 0 D demand and 8 D demand level along the horizontal meridian for all participants (A), 16 emmetropic participants (B) and 13 myopic participants (C and D) . Negative distance from the fovea represents the nasal retina. The error bars represent the SEM. Only the 0 D and 8 D demand level data are shown for clarity and the conic fits have been separated by +0.5 mm for clarity.

Along the vertical meridian, the retinal shape for the whole cohort indicated an oblate ellipse, which became prolate as the retinal sagittal height increased with accommodation for all subjects as seen in Figure 7-8 A (0 D: R= 13.91 mm, Q= 0.50, 8 D: R= 13.64 mm, Q= -0.78), which was in contrast to the horizontal meridian. The retinal shape of the emmetropic cohort altered from a prolate ellipse to a hyperboloid the 0 D (R= 13.96 mm, Q= -0.80) and 8 D (R= 13.20 mm, Q= -1.42) accommodative demand level, which can be seen on Figure 7-7 B. The myopic cohort showed the greatest increase in retinal sagittal specifically within 1.5 mm of the superior retina to 7 mm of the inferior retina, as shown in Figure 7-7 C and D. During accommodation, the retinal shape changed from prolate ellipse to oblate ellipse (0 D: R= 13.85 mm, Q= -0.17; 8 D: R= 14.24 mm, Q= 0.044), However, the effect of accommodation on the retinal sag height was not statistically significant along the vertical meridian (whole cohort $F_{0.965}$, p= 0.39; emmetropic subgroup $F_{1.886}$, p= 0.17; myopic subgroup $F_{1.285}$, p= 0.30).

Also, there was no statistical significance interaction between the accommodation demand levels and eccentricity along the vertical meridian for the whole cohort ($F_{1.529}$, p=0.11), the emmetropic subgroup ($F_{1.452}$, p=0.21) or myopic subgroup ($F_{1.316}$, p= 0.27). Overall, the effect of eccentricity on the retinal sag depth was highly statistically significant for both meridians for the whole cohort as well as the emmetropic and myopic refractive subgroups considered separately ($p<0.001$).

Accommodative Demand Level (D)		Distance from fovea (mm)						
		-7	***-4.5***	***-1.5***	***0***	***1.5***	***4.5***	***7***
All participants	0 D	-1.89 (SE 0.056)	-0.78 (SE 0.035)	-0.13 (SE 0.025)	6.1×10^{-5} (SE 4.4×10^{-5})	-0.079 (SE 0.016)	-0.71 (SE 0.027)	-1.78 (SE 0.052)
	4 D	-1.95 (SE 0.053)	-0.81 (SE 0.030)	-0.091 (SE 0.015)	5.9×10^{-6} (SE 1.6×10^{-5})	-0.089 (SE 0.021)	-0.74 (SE 0.030)	-1.79 (SE 0.053)
	8 D	-1.88 (SE 0.053)	-0.78 (SE 0.036)	-0.091 (SE 0.016)	-3.30×10^{-6} (SE 1.0×10^{-5})	-0.075 (SE 0.022)	-0.72 (SE 0.038)	-1.77 (SE 0.054)
Myopes	0 D	-2.02 (SE 0.060)	-0.85 (SE 0.042)	-0.15 (SE 0.023)	1.1×10^{-4} (SE 6.4×10^{-5})	-0.094 (SE 0.015)	-0,69 (SE 0.021)	-1.78 (SE 0.048)
	4 D	-2.02 (SE 0.060)	-0.83 (SE 0.039)	-0.086 (SE 0.016)	-1.9×10^{-6} (SE 1.7×10^{-5})	-0.084 (SE 0.024)	-0.71 (SE 0.028)	-1.78 (SE 0.051)
	8 D	-1.93 (SE 0.055)	-0.76 (SE 0.041)	-0.067 (SE 0.016)	1×10^{-5} (SE 1.4×10^{-5})	-0.066 (SE 0.020)	-0.69 (SE 0.035)	-1.75 (SE 0.055)
Emmetropes	0 D	-1.78 (SE 0.045)	-0.73 (SE 0.026)	-0.11 (SE 0.026)	2.6×10^{-5} (SE 1.2×10^{-5})	-0.066 (SE 0.017)	-0.73 (SE 0.031)	-1.78 (SE 0.057)
	4 D	-1.90 (SE 0.047)	-0.80 (SE 0.020)	-0.095 (SE 0.015)	2.6×10^{-5} (SE 1.5×10^{-5})	-0.093 (SE 0.019)	-0.76 (SE 0.030)	-1.79 (SE 0.055)
	8 D	-1.83 (SE 0.052)	-0.79 (SE 0.032)	-0.11 (SE 0.015)	2.5×10^{-6} (SE 7.5×10^{-6})	-0.083 (SE 0.024)	-0.74 (SE 0.041)	-1.79 (SE 0.056)

Table 7-6. Data for the average retinal sagittal depth (mm) along the vertical meridian for the three accommodative demand levels for all participants (n=29), myopes (n=13) and emmetropes (n=16).

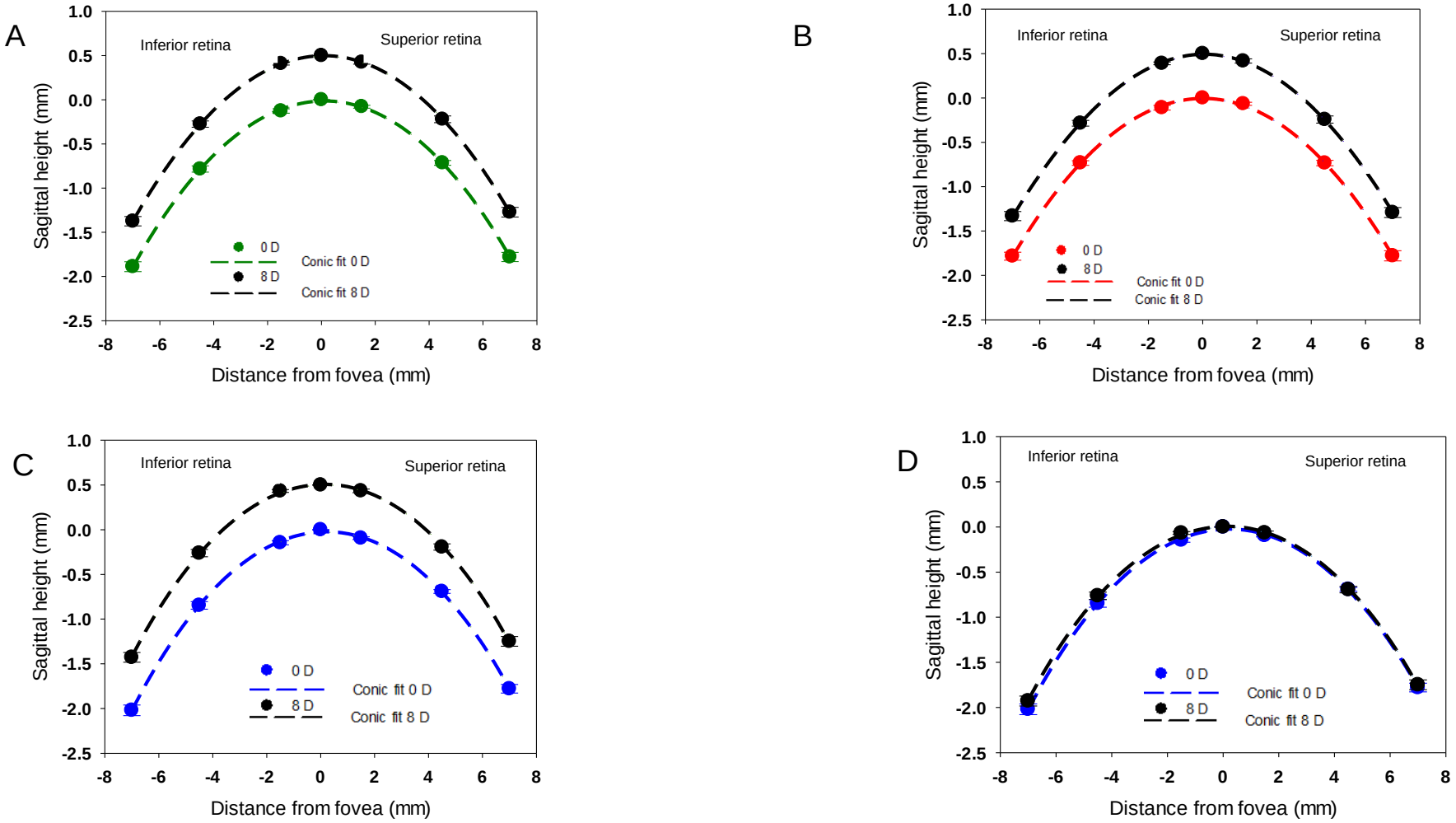

Figure 7-8. Average sagittal values fitted with a conic curve for 0 D demand and 8 D demand level along the vertical meridian for all participants (A), 16 emmetropic participants (B) and 13 myopic participants (C and D). Negative distance from the fovea represents the inferior retina. The error bars represent the SEM. Only the 0 D and 8 D demand level data are shown for clarity and the conic fits have been separated by +0.5 mm for clarity.

Between the refractive error groups, there was no significant effect of accommodation on the retinal sag depth in either the horizontal ($F_{0.002}$, p= 0.97) or vertical ($F_{0.162}$, p= 0.69) meridians.

Moreover, the retinal sagittal height did not alter significantly between meridians during relaxed accommodation (whole cohort $F_{3.623}$, p= 0.062; emmetropes $F_{3.017}$, p= 0.093; myopes $F_{1.005}$, p= 0.326) and at the maximum accommodative demand level of 8 D (whole cohort $F_{3.234}$, p= 0.077; emmetropes $F_{2.086}$, p= 0.159; myopes $F_{1.110}$, p= 0.303).

Axial length

The average baseline axial length of the myopes was longer than the emmetropes (myopes 24.52 mm (SD 0.76), emmetropes 23.67 mm (SD 0.84) ($F_{4.590}$, p= 0.05)). For all participants, the group mean increase in axial length between the 0 D and 8 D stimulus levels was 0.01 mm, however, there was a reduction to the axial length between 0 and 4 D of accommodation with a mean decrease of 0.01 mm. Table 7-7 shows the change to the axial length with accommodation for all participants, as well as the emmetropic and myopic subgroups. The greatest elongation occurred between 0 D and 8 D stimulus level for the whole cohort as well as the emmetropic, however, there was a reduction to the axial length with accommodation in the myopic cohort, as shown in Figure 7-9. A repeated measures ANOVA with one within subject factor (i.e. accommodation) revealed no significant effect of accommodation on the axial length within the whole cohort, emmetropic subgroup or the myopic subgroup separately. Moreover, there was no significant refractive error effect of the change to axial length with accommodation ($F_{8.131}$, p= 0.08), indicating the magnitude of the elongation of emmetropes was not statistically significant compared to the myopes.

The myopic cohort consisted of four progressing myopes (MSE -3.60 D (SD 0.69)) and nine myopes with stable refractive errors (MSE -2.46 D (SD 0.82)). The axial length of the progressing and stable myopes were 24.14 mm (SD 0.66) and 24.68 mm (SD 0.77), respectively. As shown in Table 7-8, there was a general increase in axial length with accommodation for the progressing myopes, whereas there was a general shortening of the axial length with accommodation for the stable myopes. The mean accommodative response was similar between both groups for the 4 D and 8 D demand level.

	Age (years)	MSE (D)	Accommodative response			'Measured' AXL (mm)			'Corrected' AXL (mm)	
			0 D	*4 D*	*8 D*	*0 D*	*4 D*	*8 D*	*4 D*	*8 D*
All participants	20.9 (SD 2.1)	-1.33 (SD 1.52)	0.19 (SD 0.30)	3.56 (SD 0.48)	6.52 (SD 0.91)	24.05 (SD 0.90)	24.05 (SD 0.85)	24.08 (SD 0.87)	24.04 (SD 0.85)	24.06 (SD 0.87)
Myopes	21.2 (SD 2.1)	-2.81 (SD 0.98)	0.12 (SD 0.28)	3.79 (SD 0.49)	6.63 (SD 0.82)	24.52 (SD 0.76)	24.51 (SD 0.85)	24.53 (SD 0.87)	24.50 (SD 0.72)	24.51 (SD 0.72)
Emmetropes	20.7 (SD 2.2)	-0.14 (SD 0.38)	-0.14 (SD 0.38)	3.38 (SD 0.39)	6.43 (SD 0.99)	23.67 (SD 0.84)	23.67 (SD 0.85)	23.72 (SD 0.83)	23.66 (SD 0.78)	23.70 (SD 0.83)

Table 7-7. The average age, refractive error and biometric measurements for the three accommodative demand levels for all participants (n=29), myopes (n=13) and emmetropes (n=16).

	Axial length (mm)			Accommodative response MSE (D)		
	0 D	4 D	8 D	0 D	4 D	8 D
Progressing Myopes (n=4)	24.14 (SD 0.66	24.19 (SD 0.60)	24.17 (SD 0.59)	0.30 (SD 0.28)	3.80 (SD 0.57)	6.76 (SD 0.69)
Stable Myopes (n=11)	24.68 (SD 0.77)	24.63 (SD 0.76)	24.66 (SD 0.75)	0.04 (SD 0.22)	3.79 (SD 0.42)	6.57 (SD 0.82)

Table 7-8. Comparison of the axial length (mm) and accommodative response (D) between the progressive myopes and stable myopes Included in the myopic cohort.

	Measured			Calculated			p value
	0 D	4 D	8 D	0 D	4 D	8 D	
Crystalline lens thickness (mm)	3.38 (SE 0.07)	3.68 (SE 0.09)	3.8 (SE 0.11)	3.42 (SE 0.02)	3.61 (SE 0.02)	3.80 (SE 0.02)	0.064
Anterior chamber depth (mm)	3.15 (SE 0.15)	2.94 (SE 0.16)	2.94 (SE 0.18)	3.66 (SE 0.01)	3.50 (SE 0.01)	3.34 (SE 0.01)	0.013*
Error in axial length (µm)	N/A	11	23	N/A	10	22	0.363
'Corrected' axial length (mm)	23.92 (SE 0.35)	23.90 (SE 0.31)	23.87 (SE 0.33)	23.92 (SE 0.35)	23.90 (SE 0.31)	23.87 (SE 0.33)	0.428

Table 7-9. Comparison of the average 'measured' (data from *LenStar* LS900) and the average 'calculated' crystalline lens thickness and anterior chamber depth (using equations 1.1 and 1.2 provided by Norrby (2005)) from 6 participants. The axial length has been calculated using equation 1.3 - 1.7, listed above. Statistically significant results are indicated with an asterisk.

The axial length was calculated using the equations listed in Chapter 6. However, using the LenStar LS900, the crystalline lens thickness and anterior chamber depth measurements could only be obtained from 6 of the 29 participants within the study. Thus, the data for the lens thickness and anterior chamber depth were calculated using the equations provided by Norrby (2005) (refer to equation 1.0 and 1.1, respectively in Chapter 6). The values were then used to calculate the error of the axial length with accommodation for all participants. Nevertheless, it was of interest to determine whether the 'measured' crystalline lens thickness and anterior chamber depth measurements for the 6 participants, produced any significant differences in the axial length error, which was determined from the 'calculated' biometric values. Therefore, a repeated measures ANOVA with one within factor (i.e. accommodation) and one between factor (i.e. measured and calculated values) was conducted for the 6 participants whose crystalline lens thickness and anterior chamber depth biometric data could be obtained. Table 7-9 shows that only the anterior chamber depth values were statistically significant between the measured and calculated data, however, the

error to the axial length was not statistically different between the 'measured' and 'calculated' value as determined from a paired t-test.

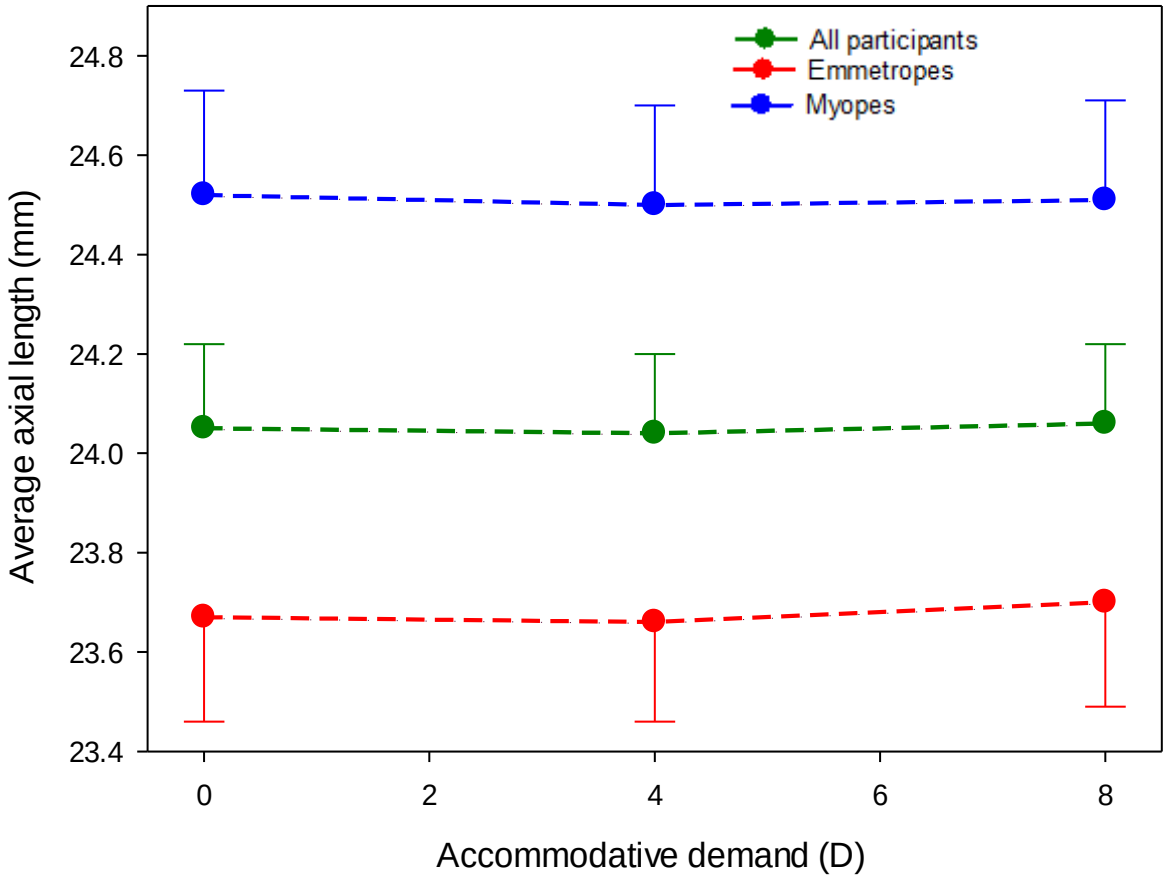

Figure 7-9. Average axial length for the three accommodative demand levels for all participants, emmetropes and myopes. Error bars represent SEM.

As expected, there was a lag of accommodation at the 4 D and 8 D demand levels, as shown in Figure 7-10. On average the accommodative response of the myopes was greater for each accommodative demand level when compared to the emmetropes (average accommodative response for 4 D stimulus: emmetropes 3.37 D (SD 0.39), myopes 3.79 D (SD 0.49); average accommodative response to an 8 D stimulus emmetropes 6.43 D (SD 0.99), myopes 6.63 D (SD 0.82)).

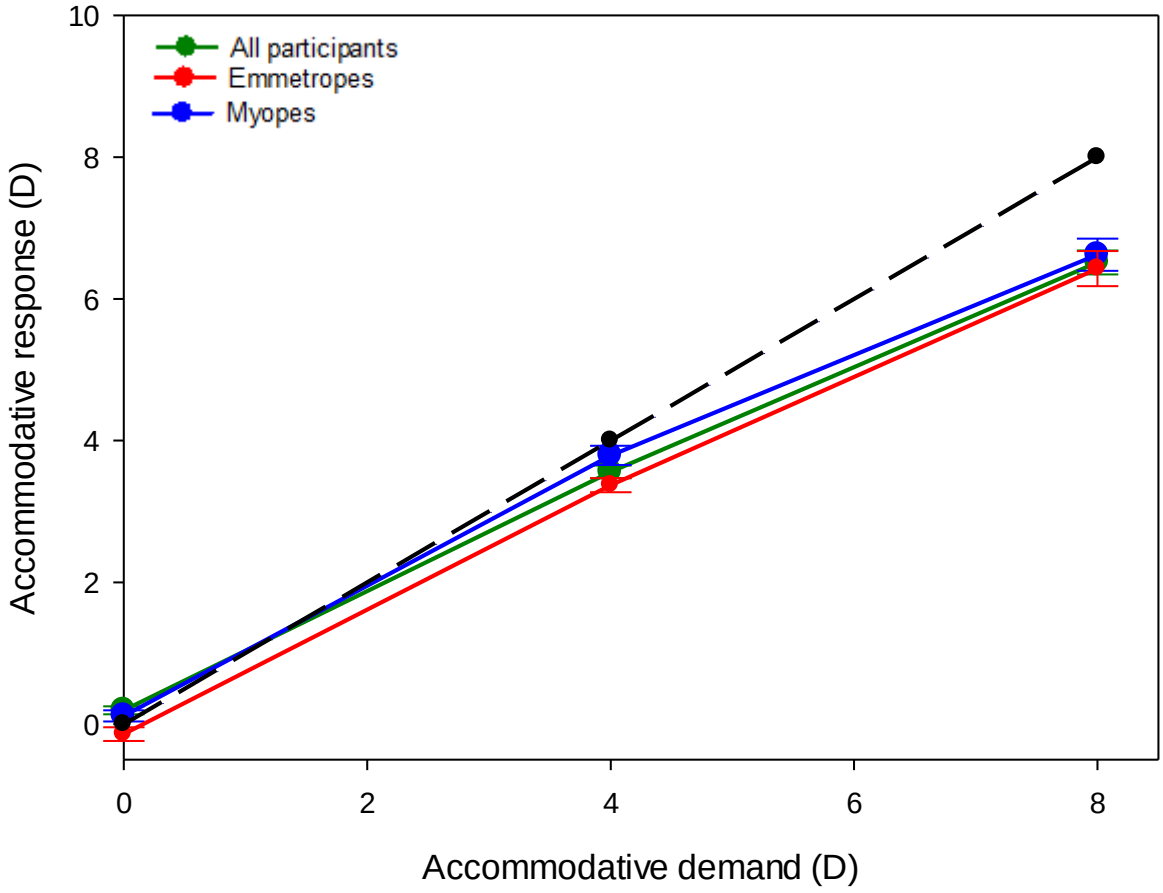

Figure 7-10. Average stimulus-response curve for the whole cohort (green), myopes (blue) and emmetropes (red). The linear line (black) represents the condition where the accommodative response is equal to the accommodative demand.

7.4. Discussion

The present investigation is the first to document the changes to retinal contour during accommodation. The findings reveal an invariant homogenous increase in retinal sagittal height during accommodation along the central 14 mm of the posterior pole, for both the horizontal and vertical meridians, which was independent of refractive error. Furthermore, accommodation revealed an insignificant effect on axial length changes. Overall, the results suggest that maximum elongation does not appear to occur at the fovea, a datum that is often used as the location for investigating the effect of accommodation at the posterior eye, but rather within the inferior-nasal retina.

The mechanism of accommodation has generally been discussed in relation to the anterior eye and the changes to the accommodative apparatus, as highlighted in

Chapter 1 (section 1.3). However, our knowledge of the consequential changes to the posterior eye during accommodation, is limited. The results in the present study have highlighted that the posterior pole is also influenced by accommodation, and although the alteration is evident along the complete posterior pole, the greatest elongation is apparent within the inferior nasal region. Such a finding is of interest especially since inferior gaze and convergence occurs during every day near vision tasks. Indeed, a significant increase in axial length has been demonstrated during infero-nasal gaze for both emmetropic and myopic refractive groups (Ghosh et al., 2012), and thus, is further supported by the present investigation.

Interestingly, the results reveal an invariant effect of accommodation on axial length changes, which is in contrast to the findings of previous researchers (Drexler et al., 1998b; Mallen et al., 2006; Read et al., 2010a; Deshpande, 2012; Woodman et al., 2011; Woodman et al., 2012; Zhong et al., 2014). Although a transient axial *elongation* was evident during accommodation between the 0 D and 8 D demand level for the whole cohort, sub-dividing the cohort into refractive groups indicated a general *shortening* of axial length during accommodation in the myopic group, which is in agreement with Drexler et al (1998b). Moreover, the variation in axial length changes further support previous research by Deshpande (2012) who also reported a reduction in the axial length with accommodation in twenty participants, although the refractive error of the cohort was not reported. In addition, the data reported by Mallen et al (2006) also suggest a reduction to the axial length during accommodation, specifically for the lowest accommodative level tested (2 D).

Furthermore, the lack of significance for refractive error effect on axial length changes during accommodation is in agreement with Woodman and colleagues (2011, 2012) whose myopic cohort (see Table 7-1) had a magnitude similar to that in the present study. The authors did not find a significant difference to the axial length changes between refractive error groups when using the LenStar (average myopic refractive error -2.90 ± 1.57 D; Woodman et al., 2012), or the IOLMaster (average refractive error of the myopic subjects -3.11 ± 2.24 D; Woodman et al., 2011). Subdividing the data for the myopic cohort in the current investigation, into stable and progressing myopes, revealed the axial length of stables myopes reduced between relaxed and 8 D accommodative demand level, whereas the progressing myopes showed an axial elongation. However, Woodman and colleagues (2011) reported greater axial length changes 10 minutes after a *prolonged* near task for progressing myopes (-0.002 ± 0.017 mm). These differences in results could be attributed to the duration of the near

task, although, further analysis of the Woodman and colleagues (2011) data suggest there was a greater reduction in the axial length within the stable myopes immediately post-task as well as 10 minutes after (stable myopes: 0 minutes post-task 0.014 ± 0.018 mm, 10 minutes post task 0.001 mm ± 0.021; progressing myopes: 0 minutes post-task 0.031 mm ± 0.022, 10 minutes post-task -0.002 mm ± 0.017).

The IOLMaster obtains the path length from the anterior corneal surface to the retinal pigment epithelium, and thus, the results from the present study can be used to describe the retinal shape across the horizontal and vertical meridians. Overall, during relaxed accommodation, data for both emmetropic and myopic eyes considered together along the horizontal meridian, showed the retinal shape was a prolate ellipse ($-1 < Q < 0$), whereas considering refractive groups separately indicated emmetropes have a prolate ellipse and myopes a hyperboloid ($Q < -1$) retinal shape. In contrast, the data for the whole cohort considered together along the vertical meridian revealed a retinal shape which was a prolate ellipse. The difference in retinal shape along the horizontal and vertical meridians is attributed to the differences in retinal shape for myopic eyes alone, which exhibited a prolate shape whereas emmetropic eyes remained prolate along the vertical meridian. These results differ from previous research which have used a range of optical (Cheng et al., 1992; Schmid, 2003b) and non-optical methods (Mutti et al., 2000; Logan et al., 2004) to measure ocular shape, and generally report myopic eyes exhibit a prolate shape. Also, a study which investigated retinal shape using MRI suggests myopic and emmetropic retinal surfaces are oblate and become less oblate, as myopia progresses, especially within the horizontal meridian (Atchison et al., 2005). Perhaps the lack of agreement for ocular shape between the current research and previous studies may be due to the techniques employed. Mutti et al. (2000) concluded their findings based on two peripheral refraction measurements, and perhaps, their results may not provide information about the overall profile for ocular shape. Logan and colleagues (2004) also obtained measurements of ocular shape derived from peripheral refraction along the horizontal meridian, therefore, their data are likely to represent retinal shape. They obtained data up to 60° field angles, which was greater than possible for the present study. The authors reported a greater prolate shape in eyes with the greatest level of myopia, but, interestingly, the authors also reported ethnic differences, with larger and more symmetrical changes in the ocular shape of Chinese participants, when compared to White adults. Indeed, moderate myopes (ametropia less than -2.50 D) of East Asian ethnicity show a more prolate ocular shape in comparison to moderate myopes of White ethnicity, along the horizontal meridian, whereas low myopes

(ametropia between -0.50 D and -2.49 D) exhibit a spherical ocular shape (Kang et al., 2010). Interestingly, ethnic variation and the degree of myopia studied may also explain the lack of agreement in the findings for ocular shape between the current investigation and previous research.

Between relaxed and active accommodation, there was an alteration to retinal shape across the horizontal and vertical meridians. Results for the whole cohort, along the horizontal meridian, reveal the retinal shape became hyperboloid during accommodation. Subdivision of the cohort into refractive groups indicates a change to the retinal shape for the myopic cohort from a hyperboloid to a prolate ellipse, whereas the retinal shape of the emmetropic eyes remains prolate. During accommodation, the retinal shape of the myopic eyes also alters along the vertical meridian to an oblate ($Q > 0$) retinal shape. Interestingly, the ocular shape of the emmetropic cohort also varies from the initial prolate ellipse to a hyperboloid during accommodation. A prolate ocular shape during accommodation has been reported by Walker and Mutti (2002), who observed a hyperopic shift in the peripheral refraction from 30° of the nasal retina when 3 D accommodative demand was stimulated in 22 subjects. Therefore, in agreement with Walker and Mutti (2002), the present study also generally shows a change to a prolate retinal shape during accommodation along the horizontal meridian for the emmetropic and myopic participants. However, it is interesting that a greater accommodative effect appears to occur along the vertical meridian for emmetropic eyes, whereas accommodation alters the retinal shape for both meridians within myopic eyes. Therefore, further research is warranted to establish the importance of the vertical meridian during accommodation.

Hitherto, the exact mechanisms responsible for the structural ocular changes, which lead to axial length changes during accommodation, are still unknown. The findings from Chapter 6, indicated a contractile shortening and anterior thickening of the ciliary muscle, which was asymmetric along the horizontal and vertical meridian. Yet, the asymmetry in ciliary muscle morphology during accommodation is not evident at the posterior pole, as found from the present investigation. The results reported for the current investigation indicate a homogenous elongation across the posterior pole with accommodation, across both the horizontal and vertical meridians, therefore suggesting an exertion of vitreous pressure on the sclera. Although Coleman (1970) proposed a vitreal involvement during accommodation, the author hypothesised the vitreous would move forward rather than towards the posterior pole. However, the results from this present study disprove Coleman's theory, since an elongation rather

than a homogenous shortening was observed. Nevertheless, it is possible that the vitreous is involved in accommodation especially since evidence from recent research has revealed zonular fibres are present within the vitreous (Croft et al., 2013a). Moreover, recent evidence suggests vitrectomy in pre-presbyopic eyes reduces the accommodative amplitude (Kim et al., 2015). The possible mechanism resulting in the findings reported for this study are probably due to a combination of accommodative changes within the anterior segment and their influence on the vitreous. Studies have indicated a backward movement of the posterior lens surface, during accommodation (e.g. Garner and Yap, 1997). Therefore, one may hypothesise that the posterior movement of the lens could exert pressure onto the vitreous which applies a force to the retinal surface and, thus, producing the homogenous elongation evident from this study. This seems likely considering a backward movement of the anterior hyaloid has been reported during accommodation (Croft et al., 2013a).

It is plausible that the increase in axial length during accommodation reported in the literature could result from the centripetal movement of the choroid and sclera during contraction of the ciliary muscle, therefore, leading to elongation of the posterior pole in order to maintain a constant ocular volume (Drexler et al., 1998b; Mallen et al., 2006). However, the results in the current study did not reveal a significant effect of accommodation on the retinal sagittal height across 14 mm of the posterior pole, and no change to the sagittal height at the fovea, indicating the reduction to the scleral circumference during ciliary muscle contraction is unlikely to produce the increased axial elongation observed during accommodation. Also, Woodman et al (2012) suggested such a mechanism is unlikely, since their results for axial length changes during a prolonged near vision task, did not reveal a direct correlation between the ciliary muscle contraction and crystalline lens thickness between accommodation and disaccommodation; rather their results indicated the lens thickness returned to baseline levels with disaccommodation, whereas the axial length did not for myopic subjects, Therefore, other mechanisms such as alterations to the choroidal thickness during accommodation maybe be involved.

It is difficult to discern whether the increase in sagittal height as well as the axial elongation are due to scleral or choroidal biomechanics. Choroidal thinning at the visual axis in response to hyperopic defocus has been documented in humans (Read et al., 2010b), however, only a 38% contribution of the choroidal thickness to the magnitude of the axial length increase with accommodation, has been reported (Woodman et al., 2012) with significant thinning of the choroid only occurring in myopic

subjects. Animal studies have shown that the thickness of the choroid can change depending on the visual stimulus presented (e.g. Wildsoet and Wallman, 1995). Chick (Wallman et al., 1995), rhesus monkeys (Hung et al., 2000) and tree-shrews (McBrien et al., 2000) are able to compensate for blur and defocus by modifying the axial length which can be achieved through physiological processes either by remodelling the sclera at the posterior pole (McBrien et al., 2000) or altering the choroidal thickness (Wallman et al., 1995; Wildsoet and Wallman, 1995; Troilo et al., 2000), therefore, moving the retina towards the image plane. For example, a chick eye is able to recover from myopic defocus or form deprivation myopia via thickening of the choroid. Wallman and colleagues (Wallman et al., 1995) located the thickness variations of the choroid to the outer choroid, which is adjacent to the sclera, and revealed that thicker choroids have larger lacunae and a greater cross-sectional area. Although it appears that the choroid regulates the scleral response in avian eyes (Wallman et al., 1995), the magnitude of the choroidal changes seem to be smaller in primates than in chick eyes possibly due to anatomical variances between the species (Hung et al., 2000). Thus, other biomechanical properties may contribute to the elongation of the retinal contour observed in our study, particularly between the emmetropic and myopic cohort, such as scleral properties.

The greater increase to the sagittal height during accommodation within the nasal and inferior retina may be due to the greater elasticity of the sclera (Phillips and McBrien, 1995) in these quadrants, in combination of the presumed choroidal thinning which has been shown to result from hyperopic defocus. The thickness of the sclera is not uniform and varies across the globe; the greatest thickness occurs at the posterior pole (Watson and Young, 2004; Norman et al., 2010; Vurgese et al., 2012) and thinnest regions at the insertion of the extraocular muscles (Watson and Young, 2004) and the equator. Eyes with longer axial lengths have been shown to have a thinner sclera (McBrien and Gentle, 2003; Norman et al., 2010; Vurgese et al., 2012) and choroid (Fujiwara et al., 2009), specifically at the posterior pole. Although the sclera is comprised of various protein components including collagen fibrils and elastin (McBrien and Gentle, 2003; Watson and Young, 2004, Pijanka et al., 2012), there are suggestions that mechanical stretching or compression of the sclera probably does not produce the scleral thinning in axially longer eyes, but rather there may be an alteration to the scleral volume and a possible loss of tissue within the posterior region of the eye (Norman et al., 2010). Animal models for myopia suggest the scleral thinning may occur from a reduced production of extracellular matrix within the sclera (Norton and Rada, 1995) and an alteration in regulatory factors of the myofibroblasts which contract

the scleral matrix (McBrien et al., 2009). Furthermore, scleral resistance may also correlate with scleral thickness (Patel, 2010) Thus, the differences in scleral structure between emmetropic and myopic eyes could have produced the differences noted in this study.

In-vitro studies of monkey scleral tissue suggests it is anisotropic (Girard et al., 2009; Girard et al., 2011), whereas there is conflict as to whether the human sclera is isotropic (Eilaghi et al., 2010) or anisotropic (Bisplinghoff et al., 2009; Pijanka et al., 2012) possibly due to the tissue samples used in the studies (glaucomatous or normal tissue). Nevertheless, the vertical meridian of the sclera has been shown to withstand more strain and compressing the sclera is easier than stretching the structure longitudinally (Battaglioli and Kamm, 1984). Also, the equatorial region of the human sclera has a greater stiffness (Bisplinghoff et al., 2009), although an animal model for scleral stiffness suggests the stiffness is similar along the horizontal and vertical meridian (Lari et al., 2012). Considering, there were no differences to the sagittal height between the horizontal and vertical meridians for all participants or between the refractive error groups, suggests the stiffness of the sclera is similar in both meridians. It could also be that similar mechanisms regulate the change to the retinal sagittal height with accommodation in both meridians. However, measurement of the axial length during inferior gaze alone, also produces a significant increase when compared to head movement alone, suggesting axial length measurements at different angles of gaze may be influenced by extraocular muscles (Ghosh et al., 2012).

Having considered the principle findings from the data, it is also important to recognise the potential limitations of the study. A semi-customised eye model based on the Navarro eye model was used in combination with the participants' corneal topography to calculate the conic curves of the retina assuming the profiles were regular for each participant. Furthermore, the assumption of a regular retinal profile has also been made when collecting peripheral eye length measurements with the IOLMaster. Such assumptions resulted in the exclusion of 12 participants since the sagittal heights were greater than ±3 SD of the mean, which may have been due to irregular retinal profiles. The IOLMaster can be used to estimate the retinal contour if the light beam is aimed at the central cornea, since the path of light is more likely to pass through the nodal points, and is the method adopted within the current investigation. Therefore, it is assumed for axial length measurements that the beam from the IOLMaster is undeviated in its path through the eye. However, it was also assumed that the path of the beam passed through the nodal points for all eccentric locations measured and that

the instrument is able locate the retinal surface for each eccentric location, with the depth of the reflected light beam constant for all locations from which the eye length was measured.

The equations stated by Norrby (2005) were used to calculate the lens thickness and anterior chamber depth to determine the error associated with the axial length during accommodation. The error calculated for the axial length was a good approximation, since the comparison of the axial length error revealed no statistical significance whether actual biometric values or the calculated biometric values were used. Furthermore, the error associated with the axial length during accommodation was similar to that of Read et al (2010a; reported error ~ 5 µm for 3 D stimulus, ~ 7 µm for 6 D stimulus) who used biometric data from the LenStar to estimate a corrected axial length. In accordance with previous authors (Read et al., 2010a) an average refractive index for the crystalline lens thickness during accommodation based on the Gullstrand simplified eye was also used for the present investigation, since the change to the refractive index during accommodation is unclear.

Moreover, it would be of interest to further investigate the accommodative changes within the vertical and horizontal ciliary muscle simultaneously alongside the changes in retinal sagittal height, to determine whether any significant relationships between the morphology of the anterior and posterior eye exist during accommodation.

In conclusion, the results from this study indicate that accommodation produces an increase to the retinal sagittal height suggesting there is an elongation of the central 14 mm of the posterior eye with accommodation, particularly in myopic eyes. Although the higher accommodative demand levels resulted in an axial increase when the data from the cohort was considered together, there was no significant refractive error effect on the axial changes during accommodation. Furthermore, there was no statistical significance of accommodation on the retinal sagittal profile, although accommodation produces a homogenous elongation within 14 mm of the central retina suggesting the pressure of the vitreous on the posterior eye during accommodation may be involved. It seems unlikely that a reduced scleral circumference occurs with accommodation to produce the axial elongation which has been suggested by previous researchers, since the results from our study do not indicate the maximum stretch occurs at the fovea, but rather the inferior-nasal quadrant. Thus, the lack of agreement between researchers regarding the axial elongation between refractive error groups may be a result of the

axial length not being the appropriate location for investigating the changes to the posterior eye with accommodation.

7.5. Summary

- The aims of the study were to investigate whether peripheral eye length alters with accommodation, whether the effect of accommodation is homogenous across the retina and if the maximum change in eye length occurs at the fovea or at another eccentric location, within emmetropic and myopic eyes
- The main findings were:
    - There is an invariant homogenous elongation of the posterior pole in the vertical and horizontal meridians
    - However, the results suggest the greatest elongation during accommodation does not occur at the fovea, but rather the inferior-nasal retina
    - There was no significant effect of accommodation on axial length
    - There were no significant differences in the axial elongation or the homogenous expansion along the posterior pole between emmetropes and myopes
- The findings suggest:
    - Peripheral eye length alters with accommodation although the homogenous elongation is not significant between the horizontal and vertical meridian or between refractive error groups
    - The homoegenous expansion of the posterior pole suggests thre is a vireal involvement during accommodation, however, the results disproves Coleman's theory for accommodation. Rather, the results indicate the vitreous is likely to push against the sclera/choroid
    - The greatest effect of accommodation occurs within the inferior-nasal quadrant rather than the fovea

Chapter 8. Conclusions and future research

8.1. General conclusion

The accommodative apparatus has been investigated for over a century, and although our understanding of the mechanisms involved which elicit an accommodative response has improved, the exact process is still unknown. The ciliary muscle is a primary structure within the accommodative apparatus, however, there is still a paucity of literature relating to the *in-vivo* structural changes that occur during accommodation. The primary aim of this thesis was to explore the ocular changes which during physiological and pharmacological stimulation of the accommodative aparatus, with particular interest in the morphology of the ciliary muscle. In addition, the ciliary muscle assymetry was investigated to determine whether differences in the morphology and contractility occurs between the vertical and horizontal meridian. Moreover, the possible effect of accommodation at the posterior eye was also studied.

Prior to the studies investigating ciliary muscle morphology, it was of interest to determine the most appropriate target for eliciting accurate accommodative responses, considering various targets are often used in accommodation research. Accommodative responses to the most commomly used targets in research relating to ocular accommodation (letter or Maltese cross) have not been investigated before, yet, the suggestion of differences in accommodative amplitude with different target choices has previously been reported (Win-Hall et al., 2007). Consequently, the aim of Chapter 3 was to establish whether accommodative responses to a Maltese cross were significantly different to a letter target, for youthful emmetropic and myopic participants. Objective accommodative responses were obtained with the Grand Seiko WAM 5500 autorefractor, for each dioptre of accommodative demand level between 1 and 8 D. The results suggested both a letter target and Maltese cross target are adequate choices for accommodation research, nevertheless, there is a greater lag of accommodative responses in myopic eyes when a Maltese cross target is used.

AS-OCT was utilised to image the ciliary muscle *in-vivo* enabling acquisition of high resolution images, which were analysed using semi-automated software (Laughton et al., 2015). In Chapter 4, the contractility and mobility of the ciliary muscle was investigated in emmetropic participants during relaxed and active accommodation. Furthermore, ocular biometry was analysed and the findings of an increased lenticular thickness and reduced anterior chamber depth (Charman, 2008) was documented,

which supported previous studies (e.g. Dubbelman et al., 2001). An anterior thickening and contractile shortening of the ciliary muscle was also reported which is in agreement with previous research that has also employed AS-OCT (Sheppard and Davies, 2010b). The effect of the pharmacological agents tropicamide 1% and cyclopentolate hydrochloride 1% were investigated to determine which regions of the muscle are primarily involved in accommodation. The findings revealed both anti-muscarinic agents reduced the mobility of the muscle, with the greatest effect evident with cyclopentolate. Interestingly, a centripetal movement of the muscle was still possible when tropicamide was used, which possibly explains the greater residual accommodation that was found after tropicamide instillation, in comparison to cyclopentolate. However, both agents reduced the ability of the muscle to thicken and shorten, when accommodation was simulated. The findings suggests circular fibres produce the anterior thickening and centripetal movement of the muscle, and the radial and longitudinal fibres also have a role in accommodation to produce the forward shift of the muscle during accommodation.

The contraction and mobility of the pre-presbyopic and presbyopic ciliary muscle of emmetropic participants was investigated using pilocarpine in Chapter 5. Pilocarpine has often been inferred as a super-stimulus for accommodation (Koeppl et al., 2005a), therefore the agent was employed in this study to induce maximum ciliary muscle contractility. The data highlighted variability in accommodative responses between participants, but, it was evident that pilocarpine produced a significant anterior thickening and posterior thinning of the muscle in pre-presbyopic eyes, but not presbyopic eyes. The findings support von Helmholtz's theory of accommodation, and also suggest the contractility of the presbyopic ciliary muscle is preserved, which further provides support for lenticular theories for the pathogenesis of presbyopia. Comparison of pilocarpine data from a sub-group of pre-presbyopic participants from Chapter 4, indicated that the forward movement of the ciliary muscle seems to have an essential role during accommodation, which may be essential for high accommodative amplitudes.

Ciliary muscle asymmetry has previously been documented *in-vivo* for rhesus monkeys (Glasser et al., 2001) and humans (Sheppard and Davies, 2010b). Hitherto, the research on the ciliary muscle during accommodation has generally been documented for the horizontal meridian. Chapter 6 explored the morphology of the ciliary muscle within the nasal, temporal, inferior and superior quadrants using AS-OCT, and interestingly, the findings indicated that the thickness and length of the ciliary muscle

varies with axial length within all quadrants, except the inferior. The findings were related to the globe shape and dimensions. Moreover, the anterior thickening and contractile shortening was evident within all regions of the ciliary muscle during accommodation suggesting the asymmetry documented in morphology, does not alter the ability of the muscle to contract in response to an accommodative stimulus.

Minimal research has been conducted relating to the effect of accommodation at the posterior eye. Recent studies (e.g. Woddman et al., 2012) have investigated changes to the axial length with accommodation, presuming the axial length is the main location for accommodative changes. The effect of accommodation on posterior eye conformation was studied in Chapter 7, to determine whether the axial length is the most approprtiate location to investigate accommodative changes. The results suggest there is an invariant homogenous elongation of the retinal contour along the horizontal and vertical meridians during accommodation, which is evident for myopic and emmetropic eyes. Furthermore, the greatest elongation appears to occur within the inferior nasal quadrant. Previous research has proposed the vitreous has a role in acommodation (Coleman, 1986), and considering recent evidence has also documented the existence of vitreous zonules (Croft et al., 2013a), the homogenous expansion reported in this chapter, may be due to the vitreous exerting pressure onto the retina, during accommodation.

8.2. Future research

Phamacological agents and their effect on the ciliary muscle contractility and mobility has provided further insights into the role of the ciliary muscle during accommodation. The studies within the thesis have revealed that a forward movement of the ciliary muscle, rather than centripetal movement alone, is required to elicit high accommodative amplitudes. Evidence from rhesus monkeys suggests the mobility of the ciliary muscle reduces with increasing age due to the stiffening of the choroid. Consequently, reports of vitreous zonules in human eyes indicates the posterior eye has a role in accommodation, and further research is required to determine whether alteration to the posterior eye morphology occurs with increasing age in humans, which may restrict the anterior movement of the ciliary muscle. Such reseach may elucidate a vitreal role in the pathogenesis of presbyopia. Considering the ciliary muscle morphology was investigated with pharmacological agents in emmetropic eyes, further research is required for individuals with ametropia. Of particular interest would be the comparison of emmetropic data to myopic participants, especially since reports of differences have been documented in children.

Further investigation of the differences in ciliary muscle contractility between anti-muscarinic agents and pilocarpine, is required, to confirm the findings of the sub-group data in Chapter 4. Comparison with presbyopes is also warranted to further establish the ciliary muscle fibre groups that are involved in accommodation.

Moreover, the vitreous may have a greater role in the accommodative mechanism than previously thought. Future research investigating whether the homogenous expansion is evident in presbyopes would be of interest, and comparison with the pre-presbyopic data reported herein, would enhance our understanding for the relevance of the posterior eye in accommodation. Moreover, the cause for the variation in the ciliary muscle within the inferior, nasal, superior and temporal quadrants, should be further explored especially in relation to ocular shape and ametropia.

8.3. Concluding statement

The studies presented in this thesis are the first to document the *in-vivo* alteration to the ciliary muscle morphology with pharmacological agents, as well as exploring the ciliary muscle asymmetry and providing support for the role of the posterior eye in accommodation.The significance of the anterior thickening and forward movement of the ciliary muscle has been demonstrated, which supports von Helmholtz's theory of accommodation. Most interestingly, the findings suggest further research is required to determine whether a similar mechanism for presbyopia development occurs in humans as it does in rhesus monkeys. Considering current methods of presbyopia reversal have generally been unsuccessful, the outcomes of the thesis will inform future research for the development of newer methods for presbyopia correction.

References

Abbott, M. L., Schmid, K. L., Strang, N. C. (1998). Differences in the accommodation stimulus response curves of adult myopes and emmetropes. *Ophthalmic and Physiological Optics*, **18** (1), 13-20.

Abramson, D. H., Coleman, D. J., Forbes, M., Franzen, L. A. (1972). Pilocarpine: effect on the anterior chamber and lens thickness. *Archives of Ophthalmology*, **87** (6), 615.

Abramson, D. H., Franzen, L. A., Coleman, D. J. (1973). Pilocarpine in the presbyope: demonstration of an effect on the anterior chamber and lens thickness. *Archives of Ophthalmology*, **89** (2), 100-102.

Adler, G., Shahar, J., Kesner, R., Rosenfeld, E., Fischer, N., Loewenstein, A., Kurtz, S. (2015). Effect of Pupil Size on Biometry Measurements Using the IOLMaster. *American Journal of Ophthalmology*, **159** (5), 940-944.

Adnan Efron, N., Mathur, A., Edwards, K., Pritchard, N., Suheimat, M. and Atchison, D.A. (2014). Amplitude of Accommodation in Type 1 DiabetesType 1 Diabetes and Amplitude of accommodation. *Investigative Ophthalmology and Visual Science*, **55** (10), 7014-7018.

Aggarwala, K. R., Nowbotsing, S., Kruger, P. B. (1995). Accommodation to monochromatic and white-light targets. *Investigative Ophthalmology and Visual Science*, **36** (13), 2695-2705.

Aldaba, M., Gómez-López, S., Vilaseca, M., Pujol, J., Arjona, M. (2015). Comparing Autorefractors for Measurement of Accommodation. *Optometry and Vision Science*, **92** (10), 1003-1011.

Aldaba, M., Pujol, J., Otero, C. (2016). On the usefulness of Badal optometer to stimulate accommodation. *Investigative Ophthalmology and Visual Science*, ARVO E-abstract #3957.

Allouch, C., Touzeau, O., Kopito, R., Borderie, V., Laroche, L. (2005). Crystalline lens biometry using A-scan ultrasound and the Orbscan device .*Journal Francais d'Ophtalmologie*, **28** (9), 925-932.

Altman, D. G., Bland, J. M. (1995). Statistics notes: Absence of evidence is not evidence of absence. *British Medical Journal*, **311**, 485.

Amos, D. M. (1978). Cycloplegics for refraction. *Optometry and Vision Science*, *55*(4), 223-226.

Anderson, H. A., Stuebing, K. K. (2014). Subjective vs Objective Accommodative Amplitude: Preschool to Presbyopia. Optometry and vision science: official publication of the American Academy of Optometry, **91** (11), 1290.

Arici, C., Turk, A., Ceylan, O. M., Kola, M. (2014). The Effect of Topical 1% Cyclopentolate on IOLMaster Biometry. *Optometry & Vision Science*, **91** (11), 1343-1347.

Armstrong, R. A., Davies, L. N., Dunne, M., Gilmartin, B. (2011). Statistical guidelines for clinical studies of human vision. *Ophthalmic and Physiological Optics*, **31** (2), 123-136.

Atchison, D. A. (1995). Accommodation and presbyopia. *Ophthalmic and Physiological Optics*, **15** (4), 255-272.

Atchison, D. A., Bradley, A., Thibos, L. N., Smith, G. (1995). Useful variations of the Badal Optometer. *Optometry and Vision Science*, **72** (4), 279-284.

Atchison, D. A., Jones, C. E., Schmid, K. L., Pritchard, N., Pope, J. M., Strugnell, W. E., Riley, R. A. (2004a). Eye shape in emmetropia and myopia. *Investigative Ophthalmology and Visual Science,* **45** (10), 3380-3386.

Atchison, D. A., Smith, G. (2004b). Possible errors in determining axial length change during accommodation with the IOLMaster. *Optometry and Vision Science,* **81** (4), 283-286.

Atchison, D. A., Pritchard, N., Schmid, K. L., Scott, D. H., Jones, C. E., Pope, J. M. (2005). Shape of the retinal surface in emmetropia and myopia. *Investigative Ophthalmology and Visual Science,* **46** (8), 2698-2707.

Atchison, D. A., Pritchard, N., & Schmid, K. L. (2006). Peripheral refraction along the horizontal and vertical visual fields in myopia. *Vision research*, **46** (8), 1450-1458.

Atchison, D. A., Markwell, E. L., Kasthurirangan, S., Pope, J. M., Smith, G., Swann, P. G. (2008). Age-related changes in optical and biometric characteristics of emmetropic eyes. *Journal of Vision*, **8** (4), 29-29.

Atchison, D. A., Charman, W. N. (2010). Thomas Young's contribution to visual optics: The Bakerian lecture “On the mechanism of the eye”. *Journal of Vision*, **10** (12), 16.

Atchison, D.A., Charman, W.N. (2011). Can partial coherence interferometry be used to determine retinal shape? *Optometry and Vision Science,* **88** (5), E601-E607.

Augusteyn, R.C. (2010). On the growth and internal structure of the human lens. *Experimental Eye Research*, **90** (6), 643-654.

Bacskulin, A., Bergmann, U., Horoczi, Z., Guthoff, R. (1995). Continuous ultrasound biomicroscopic imaging of accommodative changes in the human ciliary body. *Klinische Monatsblatter fur Augenheilkunde*, **207** (4), 247-252.

Baïkoff, G., Lutun, E., Wei, J., Ferraz, C. (2004a). Anterior chamber optical coherence tomography study of human natural accommodation in a 19-year-old albino. *Journal of Cataract and Refractive Surgery*, **30** (3), 696-701.

Baikoff, G., Lutun, E., Wei, J., Ferraz, C. (2004b). Contact between 3 phakic intraocular lens models and the crystalline lens: an anterior chamber optical coherence tomography study. *Journal of Cataract and Refractive Surgery*, **30** (9), 2007-2012.

Baïkoff, G. (2006). Anterior segment OCT and phakic intraocular lenses: a perspective. *Journal of Cataract and Refractive Surgery*, **32** (11), 1827-1835.

Bailey, M. D., Sinnott, L. T., Mutti, D. O. (2008). Ciliary body thickness and refractive error in children. *Investigative Ophthalmology and Visual Science*, **49** (10), 4353-4360.

Bailey, M. D. (2011). How should we measure the ciliary muscle? *Investigative Ophthalmology and Visual Science*, 52 (3), 1817-1818.

Bakbak, B., Koktekir, B. E., Gedik, S., Guzel, H. (2013). The effect of pupil dilation on biometric parameters of the Lenstar 900. *Cornea*, **32** (4), e21-e24.

Barbee, R. F., Smith, W. O. (1957). A comparative study of mydriatic and cycloplegic agents: In human subjects without eye disease. *American Journal of Ophthalmology*, **44** (5), 617-622.

Bassnett, S. (2002). Lens organelle degradation. *Experimental Eye Research*, **74**, 1-6.

Battaglioli, J. L., Kamm, R. D. (1984). Measurements of the compressive properties of scleral tissue. *Investigative Ophthalmology and Visual Science*, **25** (1) 59-65.

Beauchamp, R., Mitchell, B. (1985). Ultrasound measures of vitreous chamber depth during Ocular accommodation. *American Journal of Optometry and Physiological Optics*, **62** (8), 523-532.

Bee, K., Kiat, L. T. (1984). The use of ultrasound in ocular biometry. *Med. J. Malaysia*, **39** (4), 280-284.

Beebe. D.C. (1986). Development of the Ciliary Body: A brief review. *Transaction of the Ophthalmological Society, U.K,* **105**, 123-129.

Beebe, D.C., Vasiliev, O., Guo, J., Shui, Y-B., Basnnet, S (2001). Changes in adhesion complexes define stages in the differentiation of lens fiber cells. *Investigative Ophthalmology and Vision Science*, **42** (3)**,** 727-734.

Bernal, A., Parel, J-P., Manns, F. (2006). Evidence for posterior zonular fibre attachment on anterior hyaloid membrane. *Investigative Ophthalmology and Visual Science*, **47** (11), 4708-4713.

Bisplinghoff, J. A., McNally, C., Manoogian, S. J., Duma, S. M. (2009). Dynamic material properties of the human sclera. *Journal of Biomechanics*, **42** (10), 1493-1497.

Bito, L. Z., DeRousseau, C. J., Kaufman, P. L., Bito, J. W. (1982). Age-dependent loss of accommodative amplitude in rhesus monkeys: an animal model for presbyopia. *Investigative Ophthalmology and Visual Science*, **23** (1), 23-31.

Bito, L. Z., Kaufman, P. L., DeRousseau, C. J., Koretz, J. (1987). Presbyopia: an animal model and experimental approaches for the study of the mechanism of accommodation and ocular ageing. *Eye*, **1** (2), 222-230.

Bland, J. M., Altman, D. (1986). Statistical methods for assessing agreement between two methods of clinical measurement. *The lancet*, **327**, 2-18.

Bourge. J-L., Robert. A.M., Robert. L., Renard, G. (2007). Zonular fibres, multimolecular composition as related to function (elasticity) and pathology. *Pathologie Biologie*, **55**, 347-359.

Brezinski M.E., Fujimoto J.G. (1999). Optical Coherence Tomography: High-resolution imaging in nontransparent tissue. *IEEE Journal of Selected topics in Quantum Electronics,* **5** (4), 1185.

Bron, A. J. (1997). Wolff's Anatomy of the Eye and Orbit. *Chapman and Hall Medical*, 8th Edition

Brown, N. (1973). The change in shape and internal form of the lens of the eye on accommodation. *Experimental Eye Research*, **15** (4), 441-459.

Brown, N. P., Koretz, J. F., Bron, A. J. (1999). The development and maintenance of emmetropia. *Eye*, **13** (1), 83-92.

Buckhurst, P. J., Wolffsohn, J. S., Shah, S., Naroo, S. A., Davies, L. N., Berrow, E. J. (2009). A new optical low coherence reflectometry device for ocular biometry in cataract patients. *British Journal of Ophthalmology*, **93** (7), 949-953.

Buckhurst, H., Gilmartin, B., Cubbidge, R. P., Nagra, M., Logan, N. S. (2013). Ocular biometric correlates of ciliary muscle thickness in human myopia. *Ophthalmic and Physiological Optics*, **33** (3), 294-304.

Busby, A., Ciuffreda, K. J. (2005). The effect of apparent depth in pictorial images on accommodation. *Ophthalmic and Physiological Optics*, **25** (4), 320-327.

Burns, D.H., Evans, B. J.W., Allen, P.M. (2014). Clinical measurement of amplitude of accommodation: a review. *Optometry in Practice*, **15** (3), 75-86.

Calver, R., Radhakrishnan, H., Osuobeni, E., O'Leary, D. (2007). Peripheral refraction for distance and near vision in emmetropes and myopes. *Ophthalmic and Physiological Optics,* **27** (6), 584-593.

Campbell, F. W., Westheimer, G. (1960). Dynamics of accommodation responses of the human eye. *The Journal of Physiology*, **151** (2), 285-295.

Caulfield, M. P., Birdsall, N. J. (1998). International Union of Pharmacology. XVII. Classification of muscarinic acetylcholine receptors. *Pharmacological Reviews*, **50** (2), 279-290.

Chakraborty, R., Read, S. A., Collins, M. J. (2012). Monocular myopic defocus and daily changes in axial length and choroidal thickness of human eyes. *Experimental Eye Research*, **103**, 47-54.

Chan, F. L., Choi, H. L., Underhill, C. B. (1997). Hyaluronan and chondroitin sulfate proteoglycans are colocalized to the ciliary zonule of the rat eye: a histochemical and immunocytochemical study. *Histochemistry and Cell Biology*, **107** (4), 289-301.

Chang, Y-C., Ruggeri, M., Kontadakis, G., Yoo, S.H., Parel, J-M., Manns, F. (2016). Dynamic changes of the internal structure of the lens with accommodation. *Investigative Ophthalmology and Visual Science*, Abstract # 3964.

Charman, W. N., Radhakrishnan, H. (2009). Accommodation, pupil diameter and myopia. *Ophthalmic and Physiological Optics*, **29** (1), 72-79.

Charman, N., Radhakrishnan, H. (2010). Peripheral refraction and the development of refractive error: a review. *Ophthalmic and Physiological Optics*, **30** (4), 321-338.

Chen, X., Sankaridurg, P., Donovan, L., Lin, Z., Li, L., Martinez, A., Holden, B., Ge, J. (2010). Characteristics of peripheral refractive errors of myopic and non-myopic Chinese eyes. *Vision Research*, **50** (1), 31-35.

Cheng, H. M., Singh, O. S., Kwong, K. K., Xiong. G, J., Woods, B. T., Brady, T. J. (1992). Shape of the myopic eye as seen with high-resolution magnetic resonance imaging. *Optometry and Vision Science*, **69** (9), 698-701.

Cogan, D. G. (1937). Accommodation and the autonomic nervous system. *Archives of Ophthalmology*, **18** (5), 739-766.

Cohen, A. (1965). Electron microscopy of normal human lens. *Investigative Ophthalmology and Visual Science*, **4** (4), 433-446.

Cole, D. F. (1977). Secretion of the aqueous humour. *Experimental Eye Research*, **25**, 161-176.

Coleman, D. J. (1969). Ophthalmic biometry using ultrasound. *International Ophthalmology Clinics*, **9** (3), 667-683.

Coleman, D. J. (1970). Unified model for accommodative mechanism. *American Journal of Ophthalmology*, **69** (6), 1063-1079.

Coleman, D. J. (1986). On the hydraulic suspension theory of accommodation. *Transactions of the American Ophthalmological Society,* **84,** 846-68.

Collison, D.J., Coleman, R.A., James, R.S., Carey, J., Duncan, G. (2000). Characterization of Muscarinic Receptors in Human Lens Cells by Pharmacologic and Molecular Techniques. *Investigative Ophthalmology and Visual Science*, **41** (9), 2633-2641.

Collison, D. J., Duncan, G. (2001). Regional differences in functional receptor distribution and calcium mobilization in the intact human lens. *Investigative Ophthalmology and Visual Science*, **42** (10), 2355-2363.

Cook, C. A., Koretz, J. F., Pfahnl, A., Hyun, J., Kaufman, P. L. (1994). Aging of the human crystalline lens and anterior segment. Vision Research, **34** (22), 2945-2954.

Cuiffreda, K.J., Kenyon, R. V. (1983). Accommodaitve vergence and accommodation in normals, amblyopes, and strabismics. In Schor CM, Cuiffreda KJ. Ed. Vergence Eye movements: Basic and Clinical Aspects. *Boston: Butterworths*, 102-103.

Ciuffreda, K. J. (1998) Accommodation, the pupil, and presbyopia. In: Borish's Clinical Refraction (ed. W. Benjamin), W.B. Saunders Co., Philadelphia, PA, pp. 77–120.

Crawford, K., Terasawa, E., & Kaufman, P. L. (1989). Reproducible stimulation of ciliary muscle contraction in the cynomolgus monkey via a permanent indwelling midbrain electrode. Brain Research, **503**, 265–272.

Croft, M. A., Glasser, A., Heatley, G., McDonald, J., Ebbert, T., Nadkarni, N. V., Kaufman, P. L. (2006a). The zonula, lens, and circumlental space in the normal iridectomized rhesus monkey eye. *Investigative Ophthalmology and Visual Science*, **47** (3), 1087-1095.

Croft, M. A., Glasser, A., Heatley, G., McDonald, J., Ebbert, T., Dahl, D. B., Nadkarni, N.V., Kaufman, P. L. (2006b). Accommodative ciliary body and lens function in rhesus monkeys, I: normal lens, zonule and ciliary process configuration in the iridectomized eye. *Investigative Ophthalmology and Visual Science*, **47** (3), 1076-1086.

Croft, M. A., Mcdonald, J. P., James, R. J., Heatley, G. A., Lin, T. L., Lütjen-Drecoll, E., Kaufman, P. L. (2008). Surgical intervention and accommodative responses: I. Centripetal ciliary body, capsule and lens movement in rhesus monkeys of varying age. *Investigative Ophthalmology and Visual Science*, **49** (12), 5484.

Croft, M. A., Nork, T. M., McDonald, J. P., Katz, A., Lütjen-Drecoll, E., Kaufman, P. L. (2013a). Accommodative Movements of the Vitreous Membrane, Choroid, and Sclera in Young and Presbyopic Human and Nonhuman Primate Eyes: Vitreous Membrane, Choroid, and Sclera. *Investigative Ophthalmology and Visual Science*, **54** (7), 5049-5058.

Croft, M. A., McDonald, J. P., Katz, A., Lin, T. L., Lütjen-Drecoll, E., Kaufman, P. L. (2013b). Extralenticular and Lenticular Aspects of Accommodation and Presbyopia in Human Versus Monkey Eyes: Zonula and Ciliary Muscle Function. *Investigative Ophthalmology and Visual science*, **54** (7), 5035-5048.

Croft, M. A., Heatley, G., McDonald, J. P., Katz, A., Kaufman, P. L. (2016). Accommodative movements of the lens/capsule and the strand that extends between the posterior vitreous zonule insertion zone and the lens equator, in relation to the vitreous face and aging. *Ophthalmic and Physiological Optics*, ***36*** (1), 21-32.

Croft, M.A., Nork, M., McDonald, J., Heatley, G.A., Lütjen-Drecoll, E., Kaufman, P.L. (2016). Accommodative apparatus: movements in phakic and aphakic eyes, interconnections with the vitreous and presbyopia. *Investigative Ophthalmology and Visual Science*, abstract #1378.

Cruysberg, L. P., Doors, M., Verbakel, F., Berendschot, T. T., De Brabander, J., Nuijts, R. M. (2010). Evaluation of the Lenstar LS 900 non-contact biometer. *British Journal of Ophthalmology*, **94** (1), 106-110.

Culhane, H.M, Winn, B., Gilmartin, B. (1999). Human Dynamic Closed-Loop Accommodation Augmented by Sympathetic Inhibition. *Investigative Ophthalmology and Visual Science*, **40**, 1137-1143.

Cumming, J. S., Slade, S. G., Chayet, A., and AT-45 Study Group. (2001). Clinical evaluation of the model AT-45 silicone accommodating intraocular lens: results of feasibility and the initial phase of a Food and Drug Administration clinical trial. *Ophthalmology*, **108** (11), 2005-2009.

Dafna, Z., Lahav, M., Melamed, E. (1979). Localization of the β-adrenoceptors in the anterior segment of the albino rabbit eye using a fluorescent analog of propranolol. *Experimental Eye Research*, **29**, 327-330.

Davies, L. N., Mallen, E. A. H., Wolffsohn, J. S., Gilmartin, B. (2003). Clinical evaluation of the Shin-Nippon NVision-K 5001/Grand Seiko WR-5100K autorefractor. *Optometry and Vision Science*, **80** (4), 320-324.

Davies, L. N., Bartlett, H., Mallen, E. A., Wolffsohn, J. S. (2006). Clinical evaluation of rebound tonometer. *Acta Ophthalmologica Scandinavica*, **84** (2), 206-209.

Davies, L. N., Mallen, E. A. H. (2009). Influence of accommodation and refractive status on the peripheral refractive profile. *The British Journal of Ophthalmology,* **93** (9), 1186-1190.

Davis. E.C., Roth. R.A., Heuser. J.E., Mecham, R.P. (2002). *Journal of Structural Biology*, **139**, 65-75.

Davson, H. (1980). The physiology of the eye. *Academic Press, New York, ed*, *4*, 218-219.

Davson, H. (2012). Physiology of the eye, 4th Edition. *Elsevier*, pg 116-117.

Day, M., Seidel, D., Gray, L. S., Strang, N. C. (2009). The effect of modulating ocular depth of focus upon accommodation microfluctuations in myopic and emmetropic subjects. *Vision research*, **49** (2), 211-218.

de Graaf, P., Barkhof, F., Moll, A. C., Imhof, S. M., Knol, D. L., van der Valk, P., Castelijns, J. A. (2005). Retinoblastoma: MR Imaging Parameters in Detection of Tumor Extent 1. *Radiology*, **235** (1), 197-207.

de Graaf, P., Knol, D. L., Moll, A. C., Imhof, S. M., Schouten-van Meeteren, A. Y., Castelijns, J. A. (2007). Eye Size in Retinoblastoma: MR Imaging Measurements in Normal and Affected Eyes 1. *Radiology*, **244** (1), 273-280.

Deshpande, S. (2012). Ocular biometric study during accommodation. *International Journal of Medical and Clinical Research*, **3** (4), 150-153.

Dillon, J. R., Tyhurst, C. W., Yolton, R. L. (1977). The mydriatic effect of tropicamide on light and dark irides. *Journal of the American Optometric Association*, **48** (5), 653-658.

Ding, X., Li, J., Zeng, J., Ma, W., Liu, R., Li, T., Yu, S., Tang, S. (2011). Choroidal thickness in healthy Chinese subjects. *Investigative Ophthalmology and Visual Science*, **52** (13), 9555-9560.

Dirckx J.J., Kuypers L.C., Decraemer W.F. (2005). Refractive index of tissue measured with confocal microscopy. *Journal of Biomedical Optics*, **10**, 44014.

Donders, F. C., Moore, W. D. (1864). On the anomalies of accommodation and refraction of the eye: With a preliminary essay on physiological dioptrics, **22**. *New Sydenham Society*.

Drexler, W., Baumgartner, A., Findl, O., Hitzenberger, C. K., Fercher, A. F. (1997). Biometric investigation of changes in the anterior eye segment during accommodation. *Vision Research*, **37** (19), 2789-2800.

Drexler, W., Findl, O., Menapace, R., Rainer, G., Vass, C., Hitzenberger, C. K., Fercher, A. F. (1998a). Partial coherence interferometry: a novel approach to biometry in cataract surgery. *American Journal of Ophthalmology*, **126** (4), 524-534.

Drexler, W., Findl, O., Schmetterer, L., Hitzenberger, C. K., Fercher, A. F. (1998b). Eye elongation during accommodation in humans: Differences between emmetropes and myopes. *Investigative Ophthalmology and Visual Science,* **39** (11), 2140-2147.

Drexler, W., Morgner, U., Ghanta, R. K., Kärtner, F. X., Schuman, J. S., Fujimoto, J. G. (2001). Ultrahigh-resolution ophthalmic optical coherence tomography. *Nature Medicine*, **7** (4), 502-507.

Duane, A. (1912). Normal values of the accommodation at all ages. *Journal of the American Medical Association*, **59** (12), 1010-1013.

Duane, A. (1922). Studies in monocular and binocular accommodation with their clinical applications. *American Journal of Ophthalmology*, **5** (11), 865-877.

Duane, A. (1925). Are the current theories of accommodation correct? *American Journal of Ophthalmology*, **8** (3), 196-202.

Dubbelman, M., Van der Heijde, G. L., Weeber, H. A. (2001). The thickness of the aging human lens obtained from corrected Scheimpflug images. *Optometry & Vision Science*, **78** (6), 411-416.

Dubbelman, M., Van der Heijde, G. L. (2001). The shape of the aging human lens: curvature, equivalent refractive index and the lens paradox. *Vision Research*, **41** (14), 1867-1877.

Dubbelman, M., Van der Heijde, G. L., Weeber, H. A., Vrensen, G. F. J. M. (2003). Changes in the internal structure of the human crystalline lens with age and accommodation. *Vision Research*, **43** (22), 2363-2375.

Dubbelman, M., Van der Heijde, G. L., Weeber, H. A. (2005). Change in shape of the aging human crystalline lens with accommodation. *Vision Research,* **45** (1), 117-132.

Dunne, M. C., Davies, L. N., Wolffsohn, J. S. (2007). Accuracy of cornea and lens biometry using anterior segment optical coherence tomography. *Journal of Biomedical Optics*, **12** (6), 064023-064023.

Ebersberger, A., Flügel, C., Lütjen-Drecoll, E. (1993). Abstract: Ultrastructural and enzyme histochemical studies of regional structural differences within the ciliary muscle in various species. *Klinische Monatsblatter fur Augenheilkunde*, **203** (1), 53-58.

Egashira, S. M., Kish, L. L., Twelker, J. D., Mutti, D. O., Zadnik, K., Adams, A. J. (1993). Comparison of cyclopentolate versus tropicamide cycloplegia in children. *Optometry and Vision Science*, **70** (12), 1019-1026.

Eglen, R.M., Hegde, S.S., Watson, N. (1996). Muscarinic receptor type subtypes and smooth muscle function. *Pharmacological reviews*, **48** (4), 549.

Ehinger, B., Falck, B., Persson, H. (1968). Function of cholinergic nerve fibres in the cat iris dilator. *Acta physiologica Scandinavica*, **72** (1-2), 139-147.

Ehsaei, A., Mallen, E. A., Chisholm, C. M., Pacey, I. E. (2011). Cross-sectional sample of peripheral refraction in four meridians in myopes and emmetropes. *Investigative Ophthalmology and Visual Science*, **52** (10), 7574-7585.

Ehsaei, A., Chisholm, C. M., Pacey, I. E., Mallen, E. A. (2013). Off-axis partial coherence interferometry in myopes and emmetropes. *Ophthalmic and Physiological Optics*, **33** (1), 26-34.

Eilaghi, A., Flanagan, J. G., Tertinegg, I., Simmons, C. A., Brodland, G. W., Ethier, C. R. (2010). Biaxial mechanical testing of human sclera. *Journal of Biomechanics*, **43** (9), 1696-1701.

Eleftheriadis, H. I. O. L. (2003). IOLMaster biometry: refractive results of 100 consecutive cases. *British Journal of Ophthalmology*, **87** (8), 960-963.

Enoch, I.M. (1976). Retinal stretch and accommodation. In: *Current Concepts in Ophthalmology*, Vol. 5. H.E. Kaufman and T.J. Zimmerman, eds. C.V. Mosby Co., St. Louis, pp. 59-78.

Fan, D. S., Lam, D. S., Chan, C. K., Fan, A. H., Cheung, E. Y., Rao, S. K. (2007). Topical atropine in retarding myopic progression and axial length growth in children with moderate to severe myopia: a pilot study. *Japanese Journal of Ophthalmology*, **51** (1), 27-33.

Faria-Ribeiro, M., Queirós, A., Lopes-Ferreira, D., Jorge, J., González-Méijome, J. M. (2013). Peripheral refraction and retinal contour in stable and progressive myopia. *Optometry and Vision Science*, **90** (1), 9-15.

Faria-Ribeiro, M., López-Gil, N., Navarro, R., Lopes-Ferreira, D., Jorge, J., González-Méijome, J. M. (2014). Computing retinal contour from optical biometry. *Optometry and Vision Science*, **91** (4), 430-436.

Farnsworth, P. N., Burke, P. (1977). Three-dimensional architecture of the suspensory apparatus of the lens of the rhesus monkey. *Experimental Eye Research*, **25** (6), 563-576.

Farnsworth, P. N., Shyne, S. E. (1979). Anterior zonular shifts with age. *Experimental Eye Research*, **28** (3), 291-297.

Fercher, A. F. (1996). Optical coherence tomography. *Journal of Biomedical Optics*, **1** (2), 157-173.

Ferree, C. E., Rand, G., Hardy, C. (1931). Refraction for the peripheral field of vision. *Archives of Ophthalmology*, **5** (5), 717-731.

Fincham, E. F. (1937). The coincidence optometer. *Proceedings of the Physical Society*, **49** (5), 456.

Fincham, E. F. (1925). The changes in the form of the crystalline lens in accommodation. *Transactions of the Optical Society*, **26** (5), 239.

Fincham, E. F. (1951). The accommodation reflex and its stimulus. *The British Journal of Ophthalmology*, **35** (7), 381.

Fincham, E. F. (1955). The proportion of ciliary muscular force required for accommodation. *The Journal of Physiology*, **128** (1), 99.

Findl, O., Kiss, B., Petternel, V., Menapace, R., Georgopoulos, M., Rainer, G., Drexler, W. (2003). Intraocular lens movement caused by ciliary muscle contraction. *Journal of Cataract and Refractive Surgery*, **29** (4), 669-676.

Findl, O., Kriechbaum, K., Menapace, R., Koeppl, C., Sacu, S., Wirtitsch, M., Buehl, W., Drexler, W. (2004). Laserinterferometric assessment of pilocarpine-induced movement of an accommodating intraocular lens: a randomized trial. *Ophthalmology*, **111** (8), 1515-1521.

Fisher, R. F. (1969). Elastic constants of the human lens capsule. *The Journal of physiology*, **201** (1), 1-19.

Fisher, R. F. (1973). Presbyopia and the changes with age in the human crystalline lens. *The Journal of Physiology*, **228** (3), 765-779.

Fisher, R. F. (1977). The force of contraction of the human ciliary muscle during accommodation. *The Journal of Physiology*, **270** (1), 51-75.

Fisher, R. F. (1982). The vitreous and lens in accommodation. *Transactions of the Ophthalmological Society,U.K.,* **102,** 318-322.

Fisher, R. F. (1983). Is the vitreous necessary for accommodation in man? *British Journal of Ophthalmology*, **67** (3), 206.

Fledelius, H. C. (1997). Ultrasound in ophthalmology. *Ultrasound in Medicine & Biology*, **23** (3), 365-375.

Flitcroft, D. I. (2012). The complex interactions of retinal, optical and environmental factors in myopia aetiology. *Progress in Retinal and Eye Research*, **31** (6), 622-660.

Flügel C., Bàràny. E.H., Lütjen-Drecoll. E. (1990). Histochemical differences within the ciliary muscle and its function in accommodation. *Experimental Eye Research.* **50**, 219-226.

Flügel-Koch, C., May, C. A., Lütjen-Drecoll, E. (1996). Presence of a contractile cell network in the human choroid. *Ophthalmologica*, **210** (5), 296-302.

Flügel-Koch, C., Neuhuber, W. L., Kaufman, P. L., Lütjen-Drecoll, E. (2009). Morphologic indication for proprioception in the human ciliary muscle. *Investigative Ophthalmology and Visual Science*, **50** (12), 5529-5536.

Flügel-Koch, C. M., Croft, M. A., Kaufman, P. L., Lütjen-Drecoll, E. (2016). Anteriorly located zonular fibres as a tool for fine regulation in accommodation. *Ophthalmic and Physiological Optics*, **36** (1), 13-20.

Forrester, J.V., Dick. A.D., McMenamin. P.G., Roberts. F. (2008). The Eye Basic Sciences in Practice, 3rd edition. *Elsevier,* pg 130.

Foster, C. S., de la Maza, M. S. (Eds.). (2013). The sclera. *Springer Science and Business Media*, 1-33.

Fraunfelder, F. T., Scafidi, A. F. (1978). Possible adverse effects from topical ocular 10% phenylephrine. *American Journal of Ophthalmology*, **85** (4), 447-453.

Freddo TF, Gong H. (1971). Anatomy of the ciliary body and outflow pathways. In: Hogan, M., Alvarado, J., Weddell, J., eds. Histology of the human eye. Vol 3, chapter 43. *Philadelphia, WB Saunders.*

Freddo, T. F. (1996). Ultrastructure of the iris. *Microscopy research and technique*, **33** (5), 369-389.

Freeman, G., Pesudovs, K. (2005). The impact of cataract severity on measurement acquisition with the IOLMaster. *Acta Ophthalmologica Scandinavica*, **83** (4), 439-442.

Fryer, A.D., Christopoulos, A., Nathanson, N.M. (2012). Muscarinic receptor agonists and antagonists: effects on ocular function. In Muscarinic Receptors Handbook of Experimental Pharmacology. *Springer* Berlin Heidelberg, **208**, 3.

Fujimoto, J. G., Pitris, C., Boppart, S. A., Brezinski, M. E. (2000). Optical coherence tomography: an emerging technology for biomedical imaging and optical biopsy. *Neoplasia*, **2** (1), 9-25.

Fujiwara, T., Imamura, Y., Margolis, R., Slakter, J. S., Spaide, R. F. (2009). Enhanced depth imaging optical coherence tomography of the choroid in highly myopic eyes. *American Journal of Ophthalmology*, **148** (3), 445-450.

Gabelt, B. T., Kaufman, P. L., Polansky, J. R. (1990). Ciliary muscle muscarinic binding sites, choline acetyltransferase, and acetylcholinesterase in aging rhesus monkeys. *Investigative Ophthalmology and Visual Science*, **31** (11), 2431-2436.

Gabriele, M. L., Wollstein, G., Ishikawa, H., Xu, J., Kim, J., Kagemann, L.Folio, L.S., Schuman, J. S. (2010). Three dimensional optical coherence tomography imaging: advantages and advances. *Progress in Retinal and Eye Research*, **29** (6), 556-579.

Garner, L.F., Brown, B., Baker, R., Colgan, M. (1983). The effect of phenylephrine hydrochloride on the resting point of accommodation. *Investigative Ophthalmology and Visual Science*. **24** (4), 393-395.

Garner, L. F., Yap, M. K. H. (1997). Changes in ocular dimensions and refraction with accommodation. *Ophthalmic and Physiological Optics,* **17** (1), 12-17.

Garner, L. F., Smith, G. (1997). Changes in equivalent and gradient refractive index of the crystalline lens with accommodation. *Optometry and Vision Science*, **74** (2), 114-119.

German, E. J., Wood, D., Hurst, M. A. (1999). Ocular effects of antimuscarinic compounds: Is clinical effect determined by binding affinity for muscarinic receptors or melanin pigment?. *Journal of Ocular Pharmacology and Therapeutics*, **15** (3), 257-269.

Gettes, B. C., Leopold, I. H. (1953). Evaluation of five new cycloplegic drugs. *AMA Archives of Ophthalmology*, **49** (1), 24-27.

Gettes, B. C. (1954). Three new cycloplegic drugs: clinical report. *AMA Archives of Ophthalmology*, **51** (4), 467-472.

Gettes, B. C., Belmont, O. (1961). Tropicamide: comparative cycloplegic effects. *Archives of Ophthalmology*, **66** (3), 336-340.

Gerometta, R., Zamudio, A. C., Escobar, D. P., Candia, O. A. (2007). Volume change of the ocular lens during accommodation. *American Journal of Physiology - Cell Physiology,* **293** (2), C797-C804.

Ghosh, A., Collins, M. J., Read, S. A., Davis, B. A. (2012). Axial length changes with shifts of gaze direction in myopes and emmetropes. *Investigative Ophthalmology and Visual Science*, **53** (10), 6465 - 6471.

Gil, D. W., Krauss, H. A., Bogardus, A. M., WoldeMussie, E. (1997). Muscarinic receptor subtypes in human iris-ciliary body measured by immunoprecipitation. *Investigative Ophthalmology and Visual Science*, **38** (7), 1434-1442.

Gilmartin, B., Hogan, R. E., Thompson, S. M. (1984). The effect of Timolol Maleate on tonic accommodation, tonic vergence, and pupil diameter. *Investigative Ophthalmology and Visual Science*, **25** (6), 763-770.

Gilmartin, B., Hogan. R.E. (1985). The relationship between tonic accommodation and ciliary muscle innervation. *Investigative Ophthalmology and Visual Science*, **26** (7), 1024-1028.

Gilmartin, B. (1986). A review of the role of sympathetic innervation of the ciliary muscle in ocular accommodation. *Ophthalmic and Physiological Optics*, **6** (1), 23-37.

Gilmartin, B. (1995). The aetiology of presbyopia: a summary of the role of lenticular and extralenticular structures. *Ophthalmic and Physiological Optics*, **15** (5), 431-437.

Gilmartin, B., Nagra, M., Logan, N. S. (2013). Shape of the Posterior Vitreous Chamber in Human Emmetropia and Myopia. *Investigative Ophthalmology and Visual Science*, **54** (12), 7240-7251.

Girard, M. J., Suh, J. F., Bottlang, M., Burgoyne, C. F., Downs, J. C. (2009). Scleral biomechanics in the aging monkey eye. *Investigative Ophthalmology and Visual Science*, **50** (11), 5226.

Girard, M. J., Suh, J. K. F., Bottlang, M., Burgoyne, C. F., Downs, J. C. (2011). Biomechanical changes in the sclera of monkey eyes exposed to chronic IOP elevations. *Investigative Ophthalmology and Visual Science*, **52** (8), 5656.

Glasser, A., Campbell, M. C. (1998). Presbyopia and the optical changes in the human crystalline lens with age. *Vision Research*, **38** (2), 209-229.

Glasser, A., Campbell, M. C. (1999). Biometric, optical and physical changes in the isolated human crystalline lens with age in relation to presbyopia. *Vision Research*, **39** (11), 1991-2015.

Glasser, A., Kaufman, P. L. (1999). The mechanism of accommodation in primates. *Ophthalmology*, **106** (5), 863-872.

Glasser, A., Campbell, M. C. (1999). Biometric, optical and physical changes in the isolated human crystalline lens with age in relation to presbyopia. *Vision Research*, **39** (11), 1991-2015.

Glasser, A., Croft, M. A., Brumback, L., Kaufman, P. L. (2001). Ultrasound biomicroscopy of the aging rhesus monkey ciliary region. *Optometry and Vision Science*, **78** (6), 417-424.

Gohdo, T., Tsumura, T., Iijima, H., Kashiwagi, K., Tsukahara, S. (2000). Ultrasound biomicroscopic study of ciliary body thickness in eyes with narrow angles. *American Journal of Ophthalmology*, **129** (3), 342-346.

Graw. J. (2010). Organogensis in Development. Chapter ten – eye development. *Current Topics in Developmental Biology*, **90**, 343-386.

Green, K., Tonjum, A. (1971). Influence of various agents on corneal permeability. *American Journal of Ophthalmology*, **72** (5), 897-905.

Gupta, N., Drance, S. M., McAllister, R., Prasad, S., Rootman, J., Cynader, M. S. (1994). Localization of M3 muscarinic receptor subtype and mRNA in the human eye. *Ophthalmic Research*, *26*(4), 207-213.

Gustafsson, J., Terenius, E., Buchheister, J., Unsbo, P. (2001). Peripheral astigmatism in emmetropic eyes. *Ophthalmic and Physiological Optics,* **21** (5), 393-400.

Haddad, D. E., Rosenfield, M., Portello, J. K., Krumholz, D. M. (2007). Does prior instillation of a topical anaesthetic alter the pupillary mydriasis produced by tropicamide (0.5%)?. *Ophthalmic and Physiological Optics*, **27**(3), 311-314.

Hamilton, D. R., Davidorf, J. M., Maloney, R. K. (2002). Anterior ciliary sclerotomy for treatment of presbyopia: a prospective controlled study.*Ophthalmology*, **109** (11), 1970-1976.

Hammer, R., Berrie, C. P., Birdsall, N. J. M., Burgen, A. S. V., Hulme, E. C. (1980). Pirenzepine distinguishes between different subclasses of muscarinic receptors. *Nature* **283**, 90 – 92.

Hanssen, E., Franc, S., Garrone, R. (2001). Synthesis and structural organization of zonular fibers during development and aging. *Matrix Biology*, **20** (2), 77-85.

Harper, D. G. (2014). Bringing Accommodation Into Focus: The Several Discoveries of the Ciliary Muscle. *JAMA Ophthalmology*, **132** (5), 645-648.

Hata, M., Hirose, F., Oishi, A., Hirami, Y., Kurimoto, Y. (2012). Changes in choroidal thickness and optical axial length accompanying intraocular pressure increase. *Japanese Journal of Ophthalmology*, **56** (6), 564-568.

He L., Donnelly W. J. III, Stevenson S. B. Glasser A. (2010). Saccadic lens instability increases with accommodative stimulus in presbyopes. *Journal of Vision*. **10**, 1–16.

Hermans, E., Dubbelman, M., Van der Heijde, R., Heethaar, R. (2007). The shape of the human lens nucleus with accommodation. *Journal of Vision*, **7** (10), 1-10.

Hermans, E. A., Pouwels, P. J., Dubbelman, M., Kuijer, J. P., Van der Heijde, R. G., Heethaar, R. M. (2009). Constant volume of the human lens and decrease in surface area of the capsular bag during accommodation: an MRI and Scheimpflug study. *Investigative Ophthalmology and Visual Science*, **50** (1), 281-289.

Heys, K. R., Cram, S. L., Truscott, R. J. (2004). Massive increase in the stiffness of the human lens nucleus with age: the basis for presbyopia? *Molecular Vision*, **10**, 956-63.

Hiraoka, M., Inoue, K. I., Ohtaka-Maruyama, C., Ohsako, S., Kojima, N., Senoo, H., Takada, M. (2010). Intracapsular organization of ciliary zonules in monkey eyes. *The Anatomical Record*, **293** (10), 1797-1804.

Hiraoka, M., Kuroda, T., Inoue, K., Senoo, H., Takada, M. (2013). Developmental anatomy in the zonular connection with lens capsule in macaque monkey. *The Anatomical Record*, **296**, 726-735.

Hirsch, M. J., Weymouth, F. W. (1949) Pupil size in ametropia. *Journal of Applied Physiology.* **1**, 646–648.

Hitzenberger, C. K. (1991). Optical measurement of the axial eye length by laser Doppler interferometry. *Investigative Ophthalmology and Visual Science*, **32** (3), 616-624.

Hitzenberger, C. K., Drexler, W., Dolezal, C., Skorpik, F., Juchem, M., Fercher, A. F., Gnad, H. D. (1993). Measurement of the axial length of cataract eyes by laser Doppler interferometry. *Investigative Ophthalmology and Visual Science*, **34** (6), 1886-1893.

Ho, A., Zimmermann, F., Whatham, A., Martinez, A., Delgado, S., de la Jara, P. L., Sankaridurg, P. (2009) Change in peripheral refraction and curvature of field of the human eye with accommodation. In *SPIE BiOS: Biomedical Optics*. 716318-716318.

Hoerauf, H., Scholz, C., Koch, P., Engelhardt, R., Laqua, H., Birngruber, R. (2002). Transscleral optical coherence tomography: a new imaging method for the anterior segment of the eye. *Archives of Ophthalmology*, **120** (6), 816-819.

Hoffer, K. J. (1980). Biometry of 7,500 cataractous eyes. *American Journal of Ophthalmology*, **90** (3), 360-368.

Hoffer, K. J. (1993). Axial dimension of the human cataractous lens .*Archives of Ophthalmology*, **111** (7), 914-918.

Hoffer, K. J., Shammas, H. J., Savini, G. (2010). Comparison of 2 laser instruments for measuring axial length. *Journal of Cataract & Refractive Surgery*, **36** (4), 644-648.

Holden, B.A., Fricke, T.R., Ho, S.M., Wong, R., Schlenther, G., Cronje, S., Burnett, A., Papas, E., Naidoo, K.S., Frick, K.D (2008). Global vision impairment due to uncorrected presbyopia. *Archives of Ophthalmology*, **126** (12), 1731-1739.

Holzer, M. P., Mamusa, M., Auffarth, G. U. (2009). Accuracy of a new partial coherence interferometry analyser for biometric measurements. *British Journal of Ophthalmology*, **93** (6), 807-810.

Honkanen, R.E., Howard, E.F., Abdel-Larif, A.A. (1990) M3-Muscarinic Receptor Subtype Predominates in the Bovine Iris Sphincter Smooth Muscle and Ciliary Processes. *Investigative Ophthalmology and Visual Science*, **31** (3), 590-596.

Hoogerheide. J, Rempt, F., Hoogenboom, W.P. (1971). Acquired myopia in young pilots. *Ophthalmologica*, **163** (4), 209-215.

Hopkins, G., Richard M.. Pearson. (2007). *Ophthalmic Drugs*. Butterworth Heinemann/Elsevier. Fifth edition.

Horwood, A. M., Riddell, P. M. (2010). Differences between naïve and expert observers' vergence and accommodative responses to a range of targets. *Ophthalmic and Physiological* Optics, **30** (2), 152–159.

Huang, D., Swanson, E. A., Lin, C. P., Schuman, J. S., Stinson, W. G., Chang, W., Hee. M.R.., Flotte. T., Gregory, K., Puliafito, C. A., Fujimoto J.G. (1991). Optical coherence tomography. *Science*, **254** (5035), 1178-1181.

Huang, J., McAlinden, C., Su, B., Pesudovs, K., Feng, Y., Hua, Y., Feng, Y., Chao, P., Wang, Q. (2012). The effect of cycloplegia on the lenstar and the IOLMaster biometry. *Optometry and Vision Science*, **89** (12), 1691-1696.

Huang, J., Hung, L. F., Smith, E. L. (2011). Effects of foveal ablation on the pattern of peripheral refractive errors in normal and form-deprived infant rhesus monkeys (Macaca mulatta). *Investigative Ophthalmology and Visual Science,* ***52*** (9), 6428-6434.

Hung, L. F., Wallman, J., Smith, E. L. (2000). Vision-dependent changes in the choroidal thickness of macaque monkeys. *Investigative Ophthalmology and Visual Science,* **41** (6), 1259-1269.

Hurwitz, B.S., Davidowitz, J., Chin, N.B., Breinin, G.W. (1972). The effects of the sympathetic nervous system on accommodation. *Archives Ophthalmology*, **87**, 668-674.

Ikuno, Y., Kawaguchi, K., Nouchi, T., Yasuno, Y. (2010). Choroidal thickness in healthy Japanese subjects. *Investigative Ophthalmology and Visual Science*, *51*(4), 2173-2176.

Ishikawa, T. (1962). Fine structure of the human ciliary muscle. *Investigative Ophthalmology and Visual Science*, **1** (5), 587-608.

Izatt, J. A., Hee, M. R., Swanson, E. A., Lin, C. P., Huang, D., Schuman, J. S., Puliafito. C.A., Fujimoto, J. G. (1994). Micrometer-scale resolution imaging of the anterior eye in vivo with optical coherence tomography. *Archives of Ophthalmology*, **112** (12), 1584-1589.

Jasvinder, S., Khang, T. F., Sarinder, K. K. S., Loo, V. P., Subrayan, V. (2011). Agreement analysis of LENSTAR with other techniques of biometry. *Eye*, **25** (6), 717-724.

Jones, L. W., Modes, D. T. (1991). Possible allergic reactions to cyclopentolate hydrochloride: case reports with literature review of uses and adverse reactions. *Ophthalmic and Physiological Optics*, **11** (1), 16-21.

Jones, C. E., Atchison, D. A., Pope, J. M. (2007). Changes in lens dimensions and refractive index with age and accommodation. *Optometry and Vision Science*, **84** (10), 990-995.

Jones, R. (1990). Do women and myopes have larger pupils? *Investigative Ophthalmology and Visual Science*, **31** (7), 1413-1415.

Jeon, S., Lee, W. K., Lee, K., Moon, N. J. (2012). Diminished ciliary muscle movement on accommodation in myopia. *Experimental Eye Research*, **105**, 9-14.

Kamikawatoko, S., Tokoro, T., Ishida, A., Masuda, H., Hamasaki, H., Sato, J., Azuma, H. (1998). Nitric oxide relaxes bovine ciliary muscle contracted by carbachol through elevation of cyclic GMP. *Experimental Eye Research*, **66** (1), 1-7.

Kang, P., Gifford, P., McNamara, P., Wu, J., Yeo, S., Vong, B., Swarbrick, H. (2010). Peripheral refraction in different ethnicities. *Investigative Ophthalmology and Visual Science*, **51** (11), 6059-6065.

Kao, C. Y., Richdale, K., Sinnott, L. T., Ernst, L. E., Bailey, M. D. (2011). Semi-Automatic Extraction Algorithm for Images of the Ciliary Muscle. *Optometry and Vision Science*, **88** (2), 275.

Kara, N., Demircan, A., Karatas, G., Ozgurhan E.B., Tatar, G., Karakucuk, Y., Basci, A., Demirok, A. (2014). Effects of two commonly used mydriatics on choroidal thickness: direct and crossover effects. *Journal of Ocular Pharmacology and Therapeutics,* **30** (4) 366-370.

Kaschke, M., Donnerhacke, K-H., Rill, M.S. Optical devices in ophthalmology and optometry: Technology, Design Principles and Clinical Applications. Published 2014.

Kasthurirangan, S., Markwell, E. L., Atchison, D. A., Pope, J. M. (2011). MRI study of The changes in crystalline lens shape with accommodation and aging in humans. *Journal of Vision,* **11** (3), 1-16.

Kaufman, P. L., Bito, L. Z., DeRousseau, C. J. (1981). The development of presbyopia in primates. *Transactions of the Ophthalmological Societies of the United Kingdom*, **102**, 323-326.

Kiernan, D. F., Mieler, W. F., Hariprasad, S. M. (2010). Spectral-domain optical coherence tomography: a comparison of modern high-resolution retinal imaging systems. *American Journal of Ophthalmology*, **149** (1), 18-31.

Kim, M., Kwon, H. J., Lee, S. C. (2012). Influence of mydriatics on choroidal thickness measurement using enhanced depth imaging-OCT. *Optometry and Vision Science*, **89** (8), 1150-1155.

Kim, M., Kim, S. S., Koh, H. J., Lee, S. C. (2014). Choroidal thickness, age, and refractive error in healthy Korean subjects. *Optometry and Vision Science*, **91**(5), 491-496.

Kim, J. H., Moon, T. H., Chae, J. B., Hyung, S. (2015). Changes of Accommodative Power in Vitrectomized Eyes with Crystalline Lenses. *Optometry and Vision Science*, **92** (12), 1148-1153.

Koeppl, C., Findl, O., Kriechbaum, K., Drexler, W. (2005a). Comparison of pilocarpine-induced and stimulus-driven accommodation in phakic eyes. *Experimental Eye Research*, **80** (6), 795-800.

Koeppl, C., Findl, O., Menapace, R., Kriechbaum, K., Wirtitsch, M., Buehl, W.,Stacu, S., Drexler, W. (2005b). Pilocarpine-induced shift of an accommodating intraocular lens: AT-45 Crystalens. *Journal of Cataract and Refractive Surgery*, **31** (7), 1290-1297.

Kohnen, T., Thomala, M. C., Cichocki, M., Strenger, A. (2006). Internal anterior chamber diameter using optical coherence tomography compared with white-to-white distances using automated measurements. *Journal of Cataract and Refractive Surgery*, **32** (11), 1809-1813.

Koretz, J. F., Handelman, G. H., Brown, N. P. (1984). Analysis of human crystalline lens curvature as a function of accommodative state and age. *Vision Research*, **24** (10), 1141-1151.

Koretz, J. F., Handelman, G. H. (1986). Modeling age-related accomodative loss in the human eye. *Mathematical Modelling*, 7, 1003-1014.

Koretz, J. F., Neider, M. W., Kaufman, P. L., Bertasso, A. M., DeRousseau, C. J., Bito, L. Z. (1987a). Slit-lamp studies of the rhesus monkey eye: I. Survey of the anterior segment. *Experimental Eye Research*, **44** (2), 307-318.

Koretz, J. F., Bertasso, A. M., Neider, M. W., True-Gabelt, B., Kaufman, P. L. (1987b). Slit-lamp studies of the rhesus monkey eye. II Changes in crystalline lens shape, thickness and position during accommodation and aging. *Experimental Eye Research*, **45**, 317–326.

Koretz, J. F., Cook, C. A., Kaufman, P. L. (1997). Accommodation and presbyopia in the human eye. Changes in the anterior segment and crystalline lens with focus. *Investigative Ophthalmology and Visual Science*, **38** (3), 569-578.

Koretz, J. F., Cook, C. A., Kaufman, P. L. (2002). Aging of the human lens: changes in lens shape upon accommodation and with accommodative loss. *Journal of the Optical Society of America A,* **19** (1), 144-151.

Krag, S., Andreassen, T. T. (2003). Mechanical properties of the human lens capsule. *Progress in Retinal and Eye Research*, **22** (6), 749-767.

Kriechbaum, K., Findl, O., Kiss, B., Sacu, S., Petternel, V., Drexler, W. (2003). Comparison of anterior chamber depth measurement methods in phakic and pseudophakic eyes. *Journal of Cataract & Refractive Surgery*, **29** (1), 89-94.

Kriechbaum, K., Findl, O., Koeppl, C., Menapace, R., Drexler, W. (2005). Stimulus-driven versus pilocarpine-induced biometric changes in pseudophakic eyes. *Ophthalmology*, **112** (3), 453-459.

Kruger, P. B., Pola, J. (1986). Stimuli for accommodation: blur, chromatic aberration and size. *Vision Research*, **26** (6), 957-971.

Kuszak, J.R. (1995a). The ultrastructure of epithelial and fibre cells in the crystalline lens. *International Review of Cytology: a survey of cell biology*, **163**, 310-312.

Kuszak, J.R. (1995b). Chapter 9: The development of lens sutures. *Progress in Retinal and Eye Research* **14** (2), 567-590.

Kuszak, J.R., Zoltoski, R.K., Sivertson, C. (2004). Fibre cell organization in crystalline lenses. *Experimental Eye Research*, **78** (3), 673-687.

Land, M. (2015). Focusing by shape change in the lens of the eye: a commentary on Young (1801) 'On the mechanism of the eye'. *Philosophical Transactions of the Royal Society B,* 370.

Langenbucher, A., Huber, S., Nguyen, N. X., Seitz, B., Gusek-Schneider, G. C., Küchle, M. (2003). Measurement of accommodation after implantation of an accommodating posterior chamber intraocular lens. *Journal of Cataract and Refractive Surgery*, **29** (4), 677-685.

Lari, D. R., Schultz, D. S., Wang, A. S., Lee, O. T., Stewart, J. M. (2012). Scleral mechanics: comparing whole globe inflation and uniaxial testing. *Experimental Eye Research*, **94** (1), 128-135.

Laughton, D. S., Coldrick, B. J., Sheppard, A. L., Davies, L. N. (2015). A program to analyse optical coherence tomography images of the ciliary muscle. *Contact Lens and Anterior Eye*, **38** (6), 402-408.

Laughton, D. S., Sheppard, A. L., Davies, L. N. (2016). A longitudinal study of accommodative changes in biometry during incipient presbyopia. *Ophthalmic and Physiological Optics*, **36** (1), 33-42.

Lee, J. J., Fang, P. C., Yang, I. H., Chen, C. H., Lin, P. W., Lin, S. A., Kuo, H.K., Wu, P. C. (2006). Prevention of myopia progression with 0.05% atropine solution. *Journal of Ocular Pharmacology and Therapeutics*, **22** (1), 41-46.

León, A. Á., Medrano, S. M., Rosenfield, M. (2012). A comparison of the reliability of dynamic retinoscopy and subjective measurements of amplitude of accommodation. *Ophthalmic and Physiological Optics*, **32** (2), 133-141.

Leng, L., Yuan, Y., Chen, Q., Shen, M., Ma, Q., Lin, B., Zhu, D., Qu, J., Lu, F. (2014). Biometry of anterior segment of human eye on both horizontal and vertical meridians during accommodation imaged with extended scan depth optical coherence tomography. *PloS one*, **9** (8), e104775.

Leitgeb, R., Hitzenberger, C. K., Fercher, A. F. (2003). Performance of fourier domain vs. time domain optical coherence tomography. *Optics Express*, **11** (8), 889-894.

Leung, C. K. S., Li, H., Weinreb, R. N., Liu, J., Cheung, C. Y. L., Lai, R. Y. K.., Pang. C.P., Lam, D. S. C. (2008). Anterior chamber angle measurement with anterior segment optical coherence tomography: a comparison between slit lamp OCT and Visante OCT. *Investigative Ophthalmology and Visual Science*, **49** (8), 3469-3474.

Levin. A.L., Nilsson. S.F.E., Ver Hoeve, J., Wu. S.M., Kaufman. P.L., Alm. A (2011). Adlers Physiology of the Eye, 11th Edition. *Elsevier Saunders*, pg 145.

Lewis, H. A., Kao, C. Y., Sinnott, L. T., Bailey, M. D. (2012). Changes in ciliary muscle thickness during accommodation in children. *Optometry and Vision Science*, **89** (5), 727.

Liampa, Z., Kynigopoulos, M., Pallas, G., Gerding, H. (2010). Comparison of two partial coherence interferometry devices for ocular biometry. *Klinische Monatsblatter fur Augenheilkunde*, **227** (4), 285-288.

Lim, L. S., Yang, X., Gazzard, G., Lin, X., Sng, C., Saw, S.-M., Qiu, A. (2011). Variations in Eye Volume, Surface Area, and Shape with Refractive Error in Young Children by Magnetic Resonance Imaging Analysis. *Investigative Ophthalmology and Visual Science,* **52** (12), 8878-8883.

Lim, L. S., Chong, G. H., Tan, P. T., Chong, Y.-S., Kwek, K., Gluckman, P. D., Fortier, M.V., Saw, S-M., Qiu, A. (2013). Distribution and Determinants of Eye Size and Shape in Newborn Children: A Magnetic Resonance Imaging Analysis. *Investigative Ophthalmology and Visual Science*, **54** (7), 4791-4797.

Lin, L. L. K., Shih, Y. F., Hsiao, O, C. H., Su, T. C., Chen, C. J., Hung, P. T. (1998). The cycloplegic effects of cyclopentolate and tropicamide on myopic children. *Journal of Ocular Pharmacology and Therapeutics*, **14**(4), 331-335.

Lin, Z., Vasudevan, B., Liang, Y.B., Zhang, Y.C., Zhao, S.Q., Yang, X.D., Wang, N.L., Gilmartin, B. Ciuffreda, K.J. (2013). Nearwork-induced transient myopia (NITM) in anisometropia. *Ophthalmic and Physiological Optics*, **33** (3), pp.311-317.

Logan, N. S., Gilmartin, B., Wildsoet, C. F., Dunne, M. C. (2004). Posterior retinal contour in adult human anisomyopia. *Investigative Ophthalmology and Visual Science*, **45** (7), 2152-2162.

Lograno, M.D., Reibaldi, A. (1986). Receptor-responses in fresh human ciliary muscle. *British Journal of Pharmacology*, **87**, 379-385.

Lossing, L. A., Sinnott, L. T., Kao, C. Y., Richdale, K., Bailey, M. D. (2012). Measuring changes in ciliary muscle thickness with accommodation in young adults. *Optometry and Vision Science*, **89** (5), 719.

Lovasik, J. V. (1986). Pharmacokinetics of Topically Applied Cyclopentolate HCI and Tropicamide. *Optometry and Vision Science*, **63** (10), 787-803.

Lovasik, J. V., Kergoat, H., Kothe, A. C. (1987). The influence of letter size on the focusing response of the eye. *Journal of the American Optometric Association*, **58** (8), 631-639.

Love, J., Gilmartin, B., Dunne, M.C.M. (2000) Relative peripheral refractive error in adult myopia and emmetropia *Investigative Ophthalmology and Visual Science*, **41**, S302.

Lowe, R. F. (1970). Anterior lens displacement with age. *The British Journal of Ophthalmology*, **54** (2), 117-121.

Ludwig, K., Wegscheider, E., Hoops, J.P., Kampik, A. (1999). In vivo imaging of the human zonular apparatus with high-resolution ultrasound biomicroscopy. *Graefe's Archives for Clinical and Experimental Ophthalmology*, **237**, 361-371.

Lündstrom, L., Mira-Agudelo, A., Artal, P. (2009). Peripheral optical errors and their change with accommodation differ between emmetropic and myopic eyes. *Journal of Vision,* **9** (6), 17.11-11.

Lütjen-Drecoll, E., Tamm, E., Kaufman, P. L. (1988a). Age changes in rhesus monkey ciliary muscle: light and electron microscopy. *Experimental Eye Research*, **47** (6), 885-899.

Lütjen-Drecoll, E., Tamm, E., Kaufman, P. L. (1988b). Age-related loss of morphologic responses to pilocarpine in rhesus monkey ciliary muscle. *Archives of Ophthalmology*, **106** (11), 1591-1598.

Lütjen-Drecoll, E., Kaufman, P. L., Wasielewski, R., Ting-Li, L., Croft, M. A. (2010). Morphology and accommodative function of the vitreous zonule in human and monkey eyes. *Investigative Ophthalmology and Visual Science*, **51** (3), 1554.

Maceo, B. M., Manns, F., Borja, D., Nankivil, D., Uhlhorn, S., Arrieta, E., Ho. A., Augusteyn R.C, Parel, J. M. (2011). Contribution of the crystalline lens gradient refractive index to the accommodation amplitude in non-human primates: in vitro studies. *Journal of Vision*, **11** (13), 1-13.

Macsai, M. S., Padnick-Silver, L., Fontes, B. M. (2006). Visual outcomes after accommodating intraocular lens implantation. *Journal of Cataract and Refractive Surgery*, **32** (4), 628-633.

Maheshwari, R., Sukul, R.R., Gupta, Y., Gupta, M., Phougat, A., Dey, M., Jain, R., Srivastava, G., Bhardwaj, U. and Dikshit, S. (2011). Accommodation: Its relation to refractive errors, amblyopia and biometric parameters. *Nepalese Journal of Ophthalmology*, **3** (2), 146-150.

Majaj, N. J., Pelli, D. G., Kurshan, P., Palomares, M. (2002). The role of spatial frequency channels in letter identification. *Vision Research*, **42** (9), 1165-1184.

Malecaze, F. J., Gazagne, C. S., Tarroux, M. C., Gorrand, J. M. (2001). Scleral expansion bands for presbyopia. *Ophthalmology*, **108** (12), 2165-2171.

Mallen, E. A., Gilmartin, B., Wolffsohn, J. S. (2005). Sympathetic innervation of ciliary muscle and oculomotor function in emmetropic and myopic young adults. *Vision Research*, **45** (13), 1641-1651.

Mallen, E. A. H., Kashyap, P., Hampson, K. M. (2006). Transient axial length change during the accommodation response in young adults. *Investigative Ophthalmology and Visual Science,* **47** (3), 1251-1254.

Mallen, E. A., Kashyap, P. (2007). Technical note: measurement of retinal contour and supine axial length using the Zeiss IOLMaster. *Ophthalmic and Physiological Optics*, **27** (4), 404-411.

Manny, R. E., Fern, K. D., Zervas, H. J., Cline, G. E., Scott, S. K., White, J. M., Pass, A. F. (1993). 1% Cyclopentolate hydrochloride: another look at the time course of cycloplegia using an objective measure of the accommodative response. *Optometry and Vision Science*, **70** (8), 651-665.

Manny, R. E., Hussein, M., Scheiman, M., Kurtz, D., Niemann, K., Zinzer, K. (2001). Tropicamide (1%): an effective cycloplegic agent for myopic children. *Investigative Ophthalmology and Visual Science*, **42** (8), 1728-1735.

Marchini, G., Ghilotti, G., Bonadimani, M., Babighian, S. (2003). Effects of 0.005% latanoprost on ocular anterior structures and ciliary body thickness. *Journal of Glaucoma*, **12** (4), 295-300.

Margolis, R., Spaide, R. F. (2009). A pilot study of enhanced depth imaging optical coherence tomography of the choroid in normal eyes. *American Journal of Ophthalmology*, *147*(5), 811-815.

Masuda, H., Goto, M., Tamaoki, S., Kamikawatoko, S., Tokoro, T., Azuma, H. (1998). M 3-type muscarinic receptors predominantly mediate neurogenic quick contraction of bovine ciliary muscle. *General Pharmacology: The Vascular System*, **30** (4), 579-584.

Mathews, S. (1999). Scleral expansion surgery does not restore accommodation in human presbyopia. *Ophthalmology*, **106** (5), 873-877.

Mathur, A., Atchison, D. A. (2013). Peripheral Refraction Patterns Out to Large Field Angles. *Optometry and Vision Science,* **90** (2), 140-147.

Matsumoto, S., Yorio, T., DeSantis., L., Pang. I-H. (1994). Muscarinic effects on cellular functions in cultured human ciliary muscle cells. *Investigative Ophthalmology and Visual Science*, **35** (10), 3732-3738.

Matsui, M., Motomura, D., Karasawa, H., Fujikawa, T., Jiang, J., Komiya, Y., Takahashi. S-I., Taketo, M. M. (2000). Multiple functional defects in peripheral autonomic organs in mice lacking muscarinic acetylcholine receptor gene for the M3 subtype. *Proceedings of the National Academy of Sciences*, **97** (17), 9579-9584.

McAlinden, C., Wang, Q., Pesudovs, K., Yang, X., Bao, F., Yu, A., Lin, S., Feng, Y. and Huang, J. (2015). Axial length measurement failure rates with the IOLMaster and Lenstar LS 900 in eyes with cataract. *PloS one*, **10** (6), p.e0128929.

McBrien, N. A., and Millodot, M. (1986). Amplitude of accommodation and refractive error. *Investigative Ophthalmology and Visual Science*, *27*(7), 1187-1190.

McBrien, N. A., Lawlor, P., Gentle, A. (2000). Scleral remodelling during the development of and recovery from axial myopia in the tree shrew. *Investigative Ophthalmology and Visual Science,* **41** (12), 3713-3719.

McBrien, N. A., Gentle, A. (2003). Role of the sclera in the development and pathological complications of myopia. *Progress in Retinal and Eye Research*, **22** (3), 307-338.

McBrien, N. A., Jobling, A. I., Gentle, A. (2009). Biomechanics of the sclera in myopia: extracellular and cellular factors. *Optometry and Vision Science*, **86** (1), E23-E30.

Mimouni, M., Zoller, L., Horowitz, J., Wygnanski-Jaffe, T., Morad, Y., Mezer, E. (2016). Cycloplegic autorefraction in young adults: is it mandatory? *Graefe's Archive for Clinical and Experimental Ophthalmology*, **254** (2), 395-8.

Milder, B., and Riffenburgh, R. S. (1953). An evaluation of Cyclogyl. American Journal of Ophthalmology, **36**, 1724- 1726.

Milder, B. (1961). Tropicamide as a cycloplegic agent. *Archives of Ophthalmology*, **66** (1), 70-72.

Millodott, M. (2009). Dictionary of Optometry and Visual Science, Seventh edition, Oxford, *Butterworth Heinemenn*, pg 4

Millodot, M. (2015). The effect of refractive error on the accommodative response gradient: a summary and update. *Ophthalmic and Physiological Optics*, **35**, 607-612.

Miller, J. M., Wildsoet, C. F., Guan, H., Limbo, M., Demer, J. L. (2004). Refractive error and eye shape by MRI. *Investigative Ophthalmology and Visual Science*, **45** (13), 2388-2388.

Miwa, T. (1992). Instrument myopia and the resting state of accommodation. *Optometry & Vision Science*, **69** (1), 55-59.

Moffat, B. A., Atchison, D. A., Pope, J. M. (2002a). Age-related changes in refractive index distribution and power of the human lens as measured by magnetic resonance micro-imaging in vitro. *Vision Research*, **42** (13), 1683-1693.

Moffat, B. A., Atchison, D. A., Pope, J. M. (2002b). Explanation of the lens paradox. *Optometry and Vision Science,* **79** (3), 148-150.

Molins, C.O., Aldaba, M., Martinez-Navarro, B., Pujol, J. (2016). Peripheral depth cues for accommodation stimulation. *Investigative Ophthalmology and Visual Science*, ARVO E-abstract #1381.

Mordi, J., Tucker, J., Charman, W. N. (1986b). Effects of 0.1% cyclopentolate or 10% phenylephrine on pupil diameter and accommodation. *Ophthalmic and Physiological Optics*, **6** (2), 221-227.

Mordi, J. A., Lyle, W. M., Mousa, G. Y. (1986a). Does Prior Instillation of a Topical Anesthetic Enhance the Effect of Tropicamide?. *Optometry and Vision Science*, **63** (4), 290-293.

Morgan, I. G., Iribarren, R., Fotouhi, A., Grzybowski, A. (2015). Cycloplegic refraction is the gold standard for epidemiological studies. *Acta Ophthalmologica*, **93** (6), 581-585.

Moriyama, M., Ohno-Matsui, K., Hayashi, K., Shimada, N., Yoshida, T., Tokoro, T., Morita, I. (2011). Topographic analyses of shape of eyes with pathologic myopia by high-resolution three-dimensional magnetic resonance imaging. *Ophthalmology*, **118** (8), 1626-1637.

Mrejen, S., Spaide, R.F. (2013). Optical coherence tomography: imaging of the choroid and beyond. *Survey of Ophthalmology*, **58** (5), 387-429.

Muftuoglu, O., Hosal, B. M., Karel, F., Zilelioglu, G. (2005). Drug-induced intraocular lens movement and near visual acuity after AcrySof intraocular lens implantation. *Journal of Cataract and Refractive Surgery*, **31** (7), 1298-1305.

Muftuoglu, O., Hosal, B. M., Zilelioglu, G. (2009). Ciliary body thickness in unilateral high axial myopia. *Eye*, **23** (5), 1176-1181.

Munro, R. J., Fulton, A. B., Chui, T. Y., Moskowitz, A., Ramamirtham, R., Hansen, R. M., Prabhu. S.P., Akula, J. D. (2015). Eye Growth in Term-And Preterm-Born Eyes Modeled From Magnetic Resonance Images. *Investigative Ophthalmology and Visual Science*, **56** (5), 3121-3131.

Mutti, D. O., Zadnik, K., Egashira, S., Kish, L., Twelker, J. D., Adams, A. J. (1994). The effect of cycloplegia on measurement of the ocular components. *Investigative Ophthalmology and Visual Science*, **35** (2), 515-527.

Mutti, D. O., Zadnik, K., Fusaro, R. E., Friedman, N. E., Sholtz, R. I., Adams, A. J. (1998). Optical and structural development of the crystalline lens in childhood. *Investigative Ophthalmology and Visual Science*, **39** (1), 120-133.

Mutti, D. O., Sholtz, R. I., Friedman, N. E., Zadnik, K. (2000). Peripheral refraction and ocular shape in children. *Investigative Ophthalmology and Visual Science,* **41** (5), 1022-1030.

Mutti, D. O., Mitchell, G. L., Hayes, J. R., Jones, L. A., Moeschberger, M. L., Cotter, S. A., Kleinstein, R.N., Manny, R.E., Twelker, J.D., Zadnik, K. (2006). Accommodative lag before and after the onset of myopia. *Investigative Ophthalmology and Visual Science*, **47** (3), 837-846.

Mutti, D. O., Hayes, J. R., Mitchell, G. L., Jones, L. A., Moeschberger, M. L., Cotter, S. A., Kleinstein. R.N., Manny, R. E., Twelker,J.D., Zadnik, K. (2007). Refractive Error,

Axial Length , and Relative Peripheral Refractive Error before and after the Onset of Myopia. *Investigative Ophthalmology and Visual Science,* **48** *(6)* 2510-2519.

Nagra, M., Gilmartin, B., Dunne, M. C., Logan, N. S. (2012). Concordance of Retinal Shape Profiles derived using 3D MRI and Peripheral Refraction in Adult Human Eyes. *Investigative Ophthalmology and Visual Science*, **53** (14), 4435-4435.

Nakaizumi, H., Sasaki, K., Sakamoto, Y. (1992). In vivo observation of the axial movement of intraocular lenses through an anterior eye segment analysis system. Ophthalmic Research, **24**, 21-25.

Nathanson, J. A., McKee, M. (1995). Identification of an extensive system of nitric oxide-producing cells in the ciliary muscle and outflow pathway of the human eye. *Investigative Ophthalmology and Visual Science*, **36** (9), 1765-1773.

Neider, M. W., Crawford, K., Kaufman, P. L., Bito, L. Z. (1990). In vivo videography of the rhesus monkey accommodative apparatus: age-related loss of ciliary muscle response to central stimulation. *Archives of Ophthalmology*, **108** (1), 69-74.

Nemati. B, Rylander. H.G., Welch A. (1997). Optical properties of conjunctiva, sclera, and the ciliary body and their consequences for transscleral cyclophotocoagulation: erratum. *Applied Optics*, **36**, 416-416.

Nemati, B., Dunn. A., Welch. A.J., Rylander H.G. (1998). Optical model for light distribution during transscleral cyclophotocoagulation. *Applied Optics*, **37**, 764–71.

Nemeth, G., Lipecz, A., Szalai, E., Berta, A., & Modis, L. (2013). Accommodation in phakic and pseudophakic eyes measured with subjective and objective methods. *Journal of Cataract & Refractive Surgery*, **39** (10), 1534-1542.

Neuheuber, W., Schrödl, F. (2011). Autonomic control of the eye and the iris. *Autonomic neuroscience: basic and clinical*, **165**, 67-79.

Neider, M. W., Crawford, K., Kaufman, P. L., Bito, L. Z. (1990). In vivo videography of the rhesus monkey accommodative apparatus: age-related loss of ciliary muscle response to central stimulation. *Archives of Ophthalmology*, **108** (1), 69-74.

Nickla, D.L. and Wallman, J. (2010). The multifunctional choroid. *Progress in Retinal and Eye Research*, **29** (2), 144-168.

Nietgen, G. W., Schmidt, J., Hesse, L., Hönemann, C. W., Durieux, M. E. (1999). Muscarinic receptor functioning and distribution in the eye: molecular basis and implications for clinical diagnosis and therapy. *Eye*, **13**, 285-300.

Nordmann, J., Mack, G. (1974). Nucleus of the human lens. *Ophthalmic Research*, ***6***, 216-222.

Norman, R. E., Flanagan, J. G., Rausch, S. M., Sigal, I. A., Tertinegg, I., Eilaghi, A., Portnoy, S., Sled. J.G., Ethier, C. R. (2010). Dimensions of the human sclera: thickness measurement and regional changes with axial length. *Experimental Eye Research*, **90** (2), 277-284.

Norrby, S. (2005). The Dubbelman eye model analysed by ray tracing through aspheric surfaces. *Ophthalmic and Physiological Optics*, **25** (2), 153-161.

Norton, T. T., Rada, J. A. (1995). Reduced extracellular matrix in mammalian sclera with induced myopia. *Vision Research*, **35** (9), 1271-1281.

Oliveira, C., Tello, C., Liebmann, J. M., Ritch, R. (2005). Ciliary body thickness increases with increasing axial myopia. *American Journal of Ophthalmology*, **140** (2), 324-325.

Olsen, T. (1989). The accuracy of ultrasonic determination of axial length in pseudophakic eyes. *Acta ophthalmologica*, **67** (2), 141-144.

Olsen, T. (1992). Sources of error in intraocular lens power calculation. *Journal of Cataract and Refractive Surgery*, **18** (2), 125-129.

Olsen, T., Thorwest, M. (2005). Calibration of axial length measurements with the Zeiss IOLMaster. *Journal of Cataract and Refractive Surgery*, **31** (7), 1345-1350.

O' Rahilly, R. (1975). The prenatal development of the human eye. *Experimental Eye Research*, **2**, 93-112.

Ostrin, L. A., Glasser, A. (2004). Accommodation measurements in a prepresbyopic and presbyopic population. *Journal of Cataract and Refractive Surgery*, **30** (7), 1435-1444.

Ostrin, L.A., Kasthurirangan, S., Glasser, A. (2004). Evaluation of a satisfied bilateral scleral expansion band patient. *Journal of Cataract and Refractive Surgery*, **30**, 1445-1453.

Ostrin LA, Glasser A. (2005). Comparisons between pharmacologically and Edinger-Westphal-stimulated accommodation in rhesus monkeys. *Investigative Ophthalmology and Visual Science*, **46**, 609–17.

Ostrin, L. A., Glasser, A. (2007). Edinger-Westphal and pharmacologically stimulated accommodative refractive changes and lens and ciliary process movements in rhesus monkeys. *Experimental Eye Research*, **84** (2), 302-313.

Ostrin, L. A., Garcia, M. B., Choh, V., Wildsoet, C. F. (2014). Pharmacologically Stimulated Pupil and Accommodative Changes in Guinea Pigs. *Investigative Ophthalmology and Visual Science*, **55** (8), 5456-5465.

Owens, D. A. (1980). A comparison of accommodative responsiveness and contrast sensitivity for sinusoidal gratings. *Vision Research*, **20** (2), 159-167.

Owens, H., Garner, L. F., Yap, M. K., Frith, M. J., Kinnear, R. F. (1998). Age dependence of ocular biometric measurements under cycloplegia with tropicamide and cyclopentolate. *Clinical and Experimental Optometry*, **81** (4), 159-162.

Oyster, C.W. (1999). The Human Eye: Structure and Function. *Sinauer Associates Inc*, 447.

Pardue, M. T., Sivak, J. G. (2000). Age-related changes in human ciliary muscle. *Optometry and Vision Science*, **77** (4), 204-210.

Park, K. A., Yun, J. H., Kee, C. (2008). The effect of cataract extraction on the contractility of ciliary muscle. *American Journal of Ophthalmology*, **146** (1), 8-14.

Patel, H. (2011). *Biomechanical aspects of the anterior segment in human myopia* (Doctoral dissertation, Aston University).

Pau, H., Kranz, J. (1991). The increasing sclerosis of the human lens with age and its relevance to accommodation and presbyopia. Graefe's Archive for Clinical and Experimental Ophthalmology, **229** (3), 294-296.

Pedrigi, R. M., Dziezyc, J., Humphrey, J. D. (2009). Altered mechanical behaviour and properties of the human anterior lens capsule after cataract surgery. *Experimental Eye Research*, **89** (4), 575-580.

Persson, H., Sonmark, B. (1971). Adrenoceptors and cholinoceptors in the rabbit iris. *European Journal of Pharmacology*, **2**, 240-244.

Phillips, J. R., McBrien, N. A. (1995). Form deprivation myopia: elastic properties of sclera. *Ophthalmic and Physiological Optics*, **15** (5), 357-362.

Pierscionek, B.K. (1993). In vitro alteration of human lens curvatures by radial stretching. *Experimental Eye Research*, **57** (5), 629-635.

Pierscionek, B.K. (1995). Age related response of human lenses to stretching forces. *Experimental Eye Research*, **60** (3), 325-332.

Pierscionek, B.K. (1997). Refractive index contours in the human lens. *Experimental Eye Research*, **64** (6), 887-893.

Pijanka, J. K., Coudrillier, B., Ziegler, K., Sorensen, T., Meek, K. M., Nguyen, T. D., Quigley. H.A., Boote, C. (2012). Quantitative mapping of collagen fibre orientation in non-glaucoma and glaucoma posterior human sclerae. *Investigative Ophthalmology and Visual Science*, **53** (9), 5258.

Piñero, D. P., Plaza, A. B., Alió, J. L. (2008). Anterior segment biometry with 2 imaging technologies: very-high-frequency ultrasound scanning versus optical coherence tomography. *Journal of Cataract and Refractive Surgery*, **34** (1), 95-102.

Plainis, S., Plevridi, E., Pallikaris, I. G. (2009). Comparison of the ocular wavefront aberration between pharmacologically-induced and stimulus-driven accommodation. *Ophthalmic and Physiological Optics*, **29** (3), 272-280.

Podoleanu, A., Charalambous, I., Plesea, L., Dogariu, A., Rosen, R. (2004). Correction of distortions in optical coherence tomography imaging of the eye. *Physics in Medicine and Biology*, **49** (7), 1277.

Podoleanu, A. G. (2012). Optical coherence tomography. *Journal of Microscopy*, **247** (3), 209-219.

Pollack, S. L., Hunt, J. S., Polse, K. A. (1981). Dose-Response Effects of Tropicamide HCI. *Optometry and Vision Science*, **58** (5), 361-366.

Poyer, J. F., B'Ann, T. G., Kaufman, P. L. (1994). The effect of muscarinic agonists and selective receptor subtype antagonists on the contractile response of the isolated rhesus monkey ciliary muscle. *Experimental Eye Research*, **59** (6), 729-736.

Priestley, B. S., Medine, M. M. (1951). A new mydriatic and cycloplegic drug: Compound 75 GT. *American Journal of Ophthalmology*, **34** (4), 572-575.

Pucker, A. D., Sinnott, L. T., Kao, C. Y., & Bailey, M. D. (2013). Region-Specific Relationships Between Refractive Error and Ciliary Muscle Thickness in Children: Apical Ciliary Muscle Thickness and Hyperopia. *Investigative Ophthalmology and Visual Science*, **54** (7), 4710-4716.

Pucker, A. D., Carpenter, A.R., McHugh, K.M., Mutti, D.O. (2014). Guinea pig ciliary muscle development. *Optometry and Vision Science*, **91** (7), 730-739.

Pucker, A. D., Jackson, A. R., Morris, H. J., Fischer, A. J., McHugh, K. M., Mutti, D. O. (2015). Ciliary muscle cell changes during guinea pig development. *Investigative Ophthalmology and Visual Science*, **56** (13), 7691-7696.

Qazi, M. A., Pepose, J. S., Shuster, J. J. (2002). Implantation of scleral expansion band segments for the treatment of presbyopia. *American Journal of Ophthalmology*, **134** (6), 808-815.

Queirós, A., González-Méijome, J., Jorge, J. (2008). Influence of fogging lenses and cycloplegia on open-field automatic refraction. *Ophthalmic and Physiological Optics*, **28** (4), 387-392.

Radhakrishnan, S., Rollins, A. M., Roth, J. E., Yazdanfar, S., Westphal, V., Bardenstein, D. S., Izatt, J. A. (2001). Real-time optical coherence tomography of the anterior segment at 1310 nm. *Archives of Ophthalmology*, **119** (8), 1179-1185.

Radhakrishnan, H., Charman, W. N. (2008). Peripheral refraction measurement: does it matter if one turns the eye or the head? *Ophthalmic and Physiological Optics*, **28** (1), 73-82.

Radhakrishnan, H., Hartwig, A., Charman, W. N., Llorente, L. (2015). Accommodation response to Chinese and Latin characters in Chinese-illiterate young adults. *Clinical and Experimental Optometry*, **98** (6), 527-534.

Rahman, W., Chen, F. K., Yeoh, J., Patel, P., Tufail, A., Da Cruz, L. (2011). Repeatability of manual subfoveal choroidal thickness measurements in healthy subjects using the technique of enhanced depth imaging optical coherence tomography. *Investigative Ophthalmology and Visual Science*, **52** (5), 2267-2271.

Ramasubramanian, V., Glasser, A. (2015). Distortion Correction of Visante Optical Coherence Tomography Cornea Images. *Optometry and Vision Science*, **92** (12), 1170-1181.

Ramos, J. L. B., Li, Y., Huang, D. (2009). Clinical and research applications of anterior segment optical coherence tomography–a review. *Clinical and Experimental Ophthalmology*, **37**(1), 81-89.

Ramrattan, R. S., van der Schaft, T. L., Mooy, C. M., De Bruijn, W. C., Mulder, P. G., Jong, P. T. D. (1994). Morphometric analysis of Bruch's membrane, the choriocapillaris, and the choroid in aging. *Investigative Ophthalmology and Visual Science*, **35** (6), 2857-2864.

Rajan, M. S., Keilhorn, I., Bell, J. A. (2002). Partial coherence laser interferometry vs conventional ultrasound biometry in intraocular lens power calculations. *Eye*, **16** (5), 552-556.

Raviola, G. (1971). The fine structure of the ciliary zonule and ciliary epithelium. With special regard to the organization and insertion of the zonular fibrils. *Investigative Ophthalmology and Visual Science*, **10** (11), 851-869.

Read, S. A., Collins, M. J., Woodman, E. C., Cheong, S. H. (2010a). Axial Length changes during accommodation in myopes and emmetropes. *Optometry and Vision Science,* **87** (9), 656-662.

Read, S. A., Collins, M. J., Sandler, B. (2010b). Human optical axial length and defocus. *Investigative Ophthalmology and Vision Science*, **51**(12), 6262-6269.

Read, S. A., Collins, M. J. (2010). Water drinking influences eye length and IOP in young healthy subjects. *Experimental Eye Research*, **91**(2), 180-185.

Read, S. A., Collins, M. J. (2011). The short-term influence of exercise on axial length and intraocular pressure. *Eye*, **25** (6), 767-774.

Read, S. A., Collins, M. J., Alonso-Caneiro, D. (2011). Validation of optical low coherence reflectometry retinal and choroidal biometry. *Optometry and Vision Science*, **88** (7), 855-863.

Read, S. A., Collins, M. J., Vincent, S. J., Alonso-Caneiro, D. (2013a). Choroidal Thickness in Childhood. *Investigative Ophthalmology and Visual Science*, **54** (5), 3586-3593.

Read, S. A., Collins, M. J., Vincent, S. J., Alonso-Caneiro, D. (2013b). Choroidal Thickness in Myopic and Nonmyopic Children Assessed With Enhanced Depth Imaging Optical Coherence Tomography. *Investigative Ophthalmology and Visual Science*, **54** (12), 7578-7586.

Rempt, F., Hoogerheide, J., Hoogenboom, W. P. H. (1971). Peripheral retinoscopy and the skiagram. *Ophthalmologica*, **162** (1), 1-10.

Richdale, K., Bullimore, M. A., Zadnik, K. (2008). Lens thickness with age and accommodation by optical coherence tomography. *Ophthalmic and Physiological Optics*, **28** (5), 441-447.

Richdale, K., Bailey, M. D., Sinnott, L. T., Kao, C. Y., Zadnik, K., Bullimore, M. A. (2012). The effect of phenylephrine on the ciliary muscle and accommodation. *Optometry and vision science: official publication of the American Academy of Optometry*, **89** (10), 1507

Richdale, K., Sinnott, L. T., Bullimore, M. A., Wassenaar, P. A., Schmalbrock, P., Kao, C. Y., Patz. S., Mutti. D.O., Glasser, A., Zadnik, K. (2013). Quantification of Age-Related and per Diopter Accommodative Changes of the Lens and Ciliary Muscle in the Emmetropic Human Eye. *Investigative Ophthalmology and Visual Science*, **54** (2), 1095-1105.

Richdale, K., Bullimore, M. A., Sinnott, L. T., Zadnik, K. (2015). The Effect of Age, Accommodation, and Refractive Error on the Adult Human Eye. *Optometry and Vision Science*, **93** (1), 3-11.

Rohen, J. W. (1979). Scanning electron microscopic studies of the zonular apparatus in human and monkey eyes. *Investigative Ophthalmology and Visual Science* **18** (2): 133-144.

Rosales, P., Dubbelman, M., Marcos, S., Van der Heijde, R. (2006). Crystalline lens radii of curvature from Purkinje and Scheimpflug imaging. *Journal of Vision*, **6** (10), 1057-1067.

Rosen, A. M., Denham, D. B., Fernandez, V., Borja, D., Ho, A., Manns, F., Parel. J.M., Augusteyn, R. C. (2006). In vitro dimensions and curvatures of human lenses. *Vision Research*, **46** (6), 1002-1009.

Rohrer, K., Frueh, B. E., Wälti, R., Clemetson, I. A., Tappeiner, C., Goldblum, D. (2009). Comparison and evaluation of ocular biometry using a new noncontact optical low-coherence reflectometer. *Ophthalmology*, **116** (11), 2087-2092.

Rosenfield, M., Linfield, P. B. (1986). A comparison of the effects of cycloplegics on accommodation ability for distance vision and on the apparent near point. *Ophthalmic and Physiological Optics*, **6** (3), 317-320.

Rosenfield, M. and Ciuffreda, K. J. (1991) Effect of surround propinquity on the open-loop accommodative response. *Investigative Ophthalmology and Visual Science,* 32, 142–147.

Rosenfield M, Ciuffreda KJ, Hung GK, Gilmartin B. (1994). Tonic accommodation: a review. II. Accommodative adaptation and clinical aspects. *Ophthalmic and Physiological Optics* , **14**, 265–77.

Rosenfield, M., Cohen, A. S. (1995). Push-up amplitude of accommodation and target size. *Ophthalmic and Physiological Optics*, **15** (3), 231-232.

Rosenfield, M., Cohen, A. S. (1996). Repeatability of clinical measurements of the amplitude of accommodation. *Ophthalmic and Physiological Optics*, **16** (3), 247-249.

Rosenfield, M., Gilmartin, B. (1998). Myopia and nearwork. *Butterworth and Heinemann.*

Rosenfield, M. (2009). Clinical assessment of accommodation. *Optometry: Science, techniques and clinical management*, 229-240.

Ruggeri, M., Hernandez, V., De Freitas, C., Manns, F., Parel, J. M. (2014). Biometry of the ciliary muscle during dynamic accommodation assessed with OCT. In *SPIE BiOS*, 89300W-89300W).

Ruggeri, M., De Freitas, C., Williams, S., Hernandez, V.M., Cabot, F., Alawa, K., Chang, Y-C., Gregori, G., Yoo, S.H., Parel, J-M., Manns, F. (2016). Dynamic interaction of the ciliary muscle and crystalline lens during accommodation evaluated with SD-OCT. *Investigative Ophthalmology and Visual Science*, abstract #3960.

Rutstein, R.P., Fuhr, P.D., Swiatocha, J. (1993). Comparing the amplitude of accommodation determined objectively and subjectively. *Optometry and Vision Science*, **70** (6), 496-500.

Ruskell, G.L. (1973). Sympathetic innervation of the ciliary muscle in monkeys. *Experimental Eye Research*, **16**, 183-190.

Sakabe, I., Oshika, T., Lim, S. J., Apple, D. J. (1998). Anterior shift of zonular insertion onto the anterior surface of human crystalline lens with age. *Ophthalmology*, **105** (2), 295-299.

Samuel, U., Lütjen-Drecoll. E., Tamm, E.R. (1996). Gap Junctions are found between iris sphincter smooth muscle cells but not in the ciliary muscle of human and monkey eyes. *Experimental Eye Research,* **63**, 187-192.

Sanchez-Cano, A., Orduna, E., Segura, F., Lopez, C., Cuenca, N., Abecia, E., Pinilla, I. (2014). Choroidal thickness and volume in healthy young white adults and the relationships between them and axial length, ammetropy and sex. *American Journal of Ophthalmology*, **158** (3), 574-583.

Sander, B. P., Collins, M. J., Read, S. A. (2014). The effect of topical adrenergic and anticholinergic agents on the choroidal thickness of young healthy adults. *Experimental eye research*, **128**, 181-189.

Santodomingo-Rubido, J., Mallen, E. A. H., Gilmartin, B., Wolffsohn, J. S. (2002). A new non-contact optical device for ocular biometry. *British Journal of Ophthalmology*, **86** (4), 458-462.

Schachar, R. A. (1992). Cause and treatment of presbyopia with a method for increasing the amplitude of accommodation. *Annals of Ophthalmology*, **24** (12), 445.

Schachar, R. A., Tello, C., Cudmore, D. P., Liebmann, J. M., Black, T. D., Ritch, R. (1996). In vivo increase of the human lens equatorial diameter during accommodation. *American Journal of Physiology-Regulatory, Integrative and Comparative Physiology*, **271** (3), R670-R676.

Schachar, R. A., Bax, A. J. (2001). Mechanism of accommodation. *International Ophthalmology Clinics*, **41** (2), 17-32.

Schachar, R. A. (2005). References are required for measurement of OCT images. *Journal of Cataract & Refractive Surgery*, **31** (2), 257-258.

Schachar, R. A. (2006). The mechanism of accommodation and presbyopia. *International Ophthalmology Clinics*, **46** (3), 39-61.

Schachar RA. (2008). Equatorial lens growth predicts the age-related decline in accommodative amplitude that results in presbyopia and the increase in intraocular pressure that occurs with age. *International Ophthalmology Clinics*, **48** (1), 1-8.

Schmid, G. F. (2003a). Variability of retinal steepness at the posterior pole in children 7 – 15 years of age. *Current Eye Research,* **27** (1), 61-68.

Schmid, G. F. (2003b). Axial and peripheral eye length measured with optical low coherence reflectometry. *Journal of Biomedical Optics*, **8** (4), 655-662.

Schmid, K. L., Hilmer, K. S., Lawrence, R. A., Loh, S. Y., Morrish, L. J., Brown, B. (2005). The effect of common reductions in letter size and contrast on accommodation responses in young adult myopes and emmetropes. *Optometry and Vision Science*, **82** (7), 602-611.

Schulle, K. L., 9Berntsen, D. A. (2013). Repeatability of on-and off-axis eye length measurements using the LenStar. *Optometry and Vision Science*, *90*(1), 16.

Schultz, K. E., Sinnott, L. T., Mutti, D. O., Bailey, M. D. (2009). Accommodative fluctuations, lens tension, and ciliary body thickness in children. *Optometry and vision science: official publication of the American Academy of Optometry*, **86** (6), 677.

Seddon, J. M., Sahagian, C. R., Glynn, R. J., Sperduto, R. D., Gragoudas, E. S. (1990). Evaluation of an iris color classification system. The Eye Disorders Case-Control Study Group. *Investigative Ophthalmology and Visual Science*, **31** (8), 1592-1598.

Seidel, D., Gray, L. S., Heron, G. (2005). The effect of monocular and binocular viewing on the accommodation response to real targets in emmetropia and myopia. *Optometry and Vision Science*, **82** (4), 279-285.

Seidemann, A., Schaeffel, F., Guirao, A., Lopez-Gil, N., Artal, P. (2002). Peripheral refractive errors in myopic, emmetropic, and hyperopic young subjects. *Journal of the Optical Society of America,* **19** (12), 2363-2373.

Seidemann, A., Schaeffel, F. (2003). An evaluation of the lag of accommodation using photorefraction. *Vision Research*, **43** (4), 419-430.

Seland, J.H. (1974). Ultrastrucutural changes in the normal human lens capsule from birth to old age. *Acta Ophthalmologica*, **52**, 688-705.

Shade, D. L., Clark, A. F., Pang, I. H. (1996). Effects of muscarinic agents on cultured human trabecular meshwork cells. *Experimental Eye Research*, **62** (3), 201-210.

Shaffer, R. N., Hetherington, J. (1966). Anticholinesterase drugs and cataracts. *American Journal of Ophthalmology*, **62** (4), 613-618.

Shammas, H. J. F. (1982). Axial length measurement and its relation to intraocular lens power calculations. *American Intra-Ocular Implant Society Journal*, **8** (4), 346-349.

Shammas, H. J., Hoffer, K. J. (2012). Repeatability and reproducibility of biometry and keratometry measurements using a noncontact optical low-coherence reflectometer and keratometer. *American Journal of Ophthalmology*, **153** (1), 55-61.

Shao, Y., Tao, A., Jiang, H., Shen, M., Zhong, J., Lu, F., Wang, J. (2013). Simultaneous real-time imaging of the ocular anterior segment including the ciliary muscle during accommodation. *Biomedical Optics Express*, **4** (3), 466-480.

Shao, Y., Tao, A., Jiang, H., Mao, X., Zhong, J., Shen, M., Xu, Z., Karp, C.L., Wang, J. (2015). Age-Related Changes in the Anterior Segment Biometry During Accommodation. *Investigative Ophthalmology and Visual Science*, **56** (6), 3522-3530.

Shen, P., Zheng, Y., Ding, X., Liu, B., Congdon, N., Morgan, I., He, M. (2013). Biometric measurements in highly myopic eyes. *Journal of Cataract and Refractive Surgery*, **39** (2), 180-187.

Sheng, H. U. A. N., Bottjer, C. A., Bullimore, M. A. (2004). Ocular component measurement using the Zeiss IOLMaster. *Optometry and Vision Science*, **81** (1), 27-34.

Sheppard, A. L., Davies, L. N. (2010a). Clinical evaluation of the Grand Seiko Auto Ref/Keratometer WAM-5500. *Ophthalmic and Physiological Optics*, **30** (2), 143-151.

Sheppard, A. L., Davies, L. N. (2010b). In vivo analysis of ciliary muscle morphologic changes with accommodation and axial ametropia. *Investigative Ophthalmology and Visual Science*, **51** (12), 6882-6889.

Sheppard, A. L., Davies, L. N. (2011). The effect of ageing on in vivo human ciliary muscle morphology and contractility. *Investigative Ophthalmology and Visual Science*, **52** (3), 1809-1816.

Sheppard, A. L., Evans, C. J., Singh, K. D., Wolffsohn, J. S., Dunne, M. C., Davies, L. N. (2011). Three-dimensional magnetic resonance imaging of the phakic crystalline lens during accommodation. *Investigative Ophthalmology and Visual Science*, **52** (6), 3689-3697.

Sheng, H. U. A. N., Bottjer, C. A., Bullimore, M. A. (2004). Ocular component measurement using the Zeiss IOLMaster. *Optometry and Vision Science*, **81** (1), 27-34.

Shum, P. J. T., Ko, L. S., Ng, C. L., Lin, S. L. (1993). A biometric study of ocular changes during accommodation. *American Journal of Ophthalmology*,**115** (1), 76-81.

Singh, M. (1985). Miotic-induced retinal detachment: a case report. *Medical Journal of Malaysia*, **40** (2), 136-138.

Singh, K. D., Logan, N. S., Gilmartin, B. (2006). Three-dimensional modeling of the human eye based on magnetic resonance imaging. *Investigative Ophthalmology and Visual Science*, *47*(6), 2272-2279.

Siu, A. W., Sum, A. C., Lee, D. T., Tam, K. W., Chan, S. W. (1999). Prior topical anesthesia reduces time to full cycloplegia in Chinese. *Japanese Journal of Ophthalmology*, **43** (6), 466-471.

Smith, G. (1983). The accommodative resting states, instrument accommodation and their measurement. *Journal of Modern Optics*, **30** (3), 347-359.

Smith, G., Atchison, D. A., Pierscionek, B. K. (1992). Modeling the power of the aging human eye. *JOSA A*, **9** (12), 2111-2117.

Smith, E. L. III., Kee, C.-S., Ramamirtham, R., Qiao-grider, Y. (2005). Peripheral Vision Can Influence Eye Growth and Refractive Development in Infant Monkeys. *Investigative Ophthalmology and Visual Science,* **46** (11), 3965-3972.

Smith, E. L., III, Hung, L. F., & Huang, J. (2009). Relative peripheral hyperopic defocus alters central refractive development in infant monkeys. *Vision Research,* **49** (19), 2386-2392.

Sng, C. C. A., Lin, X.-Y., Gazzard, G., Chang, B., Dirani, M., Lim, L. Selvaraj, P., Ian, K., Drobe, B., Wong, T-Y., Saw, S-M. (2011). Change in Peripheral Refraction over Time in Singapore Chinese Children. *Investigative Ophthalmology and Visual Science,* **52** (11), 7880-7887.

Song, H. T., Kim, Y. J., Lee, S. J., Moon, Y. S. (2007). Relations between age, weight, refractive error and eye shape by computerized tomography in children. *Korean Journal of Ophthalmology*, **21** (3), 163-168.

Sparrow, J. M., Bron, A. J., Brown, N. A. P., Ayliffe, W., Hill, A. R. (1986). The Oxford clinical cataract classification and grading system. *International Ophthalmology*, **9** (4), 207-225.

Steinert. R.F., Huang, D. (2008) Anterior segment optical coherence tomography. Slack, 2008.

Stephens, K.G. (1985). Effect of the sympathetic nervous system on accommodation. *American Journal of Optometry and Physiological Optics*, **62** (6), 402-406.

Streeten, B.W. (1977). The zonular insertion: a scanning electron microscopic study. *Investigative Ophthalmology and Visual Science*, **16** (4), 364-375.

Streeten, B.W. (2006). Duane's Ophthalmology Foundation Volume 1: Chapter 13. The Ciliary Body. *Lipincott Williams and Wilkins.*

Strenk, S. A., Semmlow, J. L., Strenk, L. M., Munoz, P., Gronlund-Jacob, J., DeMarco, J. K. (1999). Age-related changes in human ciliary muscle and lens: a magnetic resonance imaging study. Investigative Ophthalmology and Visual Science, **40** (6), 1162-1169.

Strenk, S. A., Strenk, L. M., Semmlow, J. L., DeMarco, J. K. (2004a). Magnetic resonance imaging study of the effects of age and accommodation on the human lens cross-sectional area. *Investigative Ophthalmology and Visual Science*, **45** (2), 539-545.

Strenk, S. A., Strenk, L. M., Semmlow, J. L. (2004b). MRI study of the effect of age and accommodation on ciliary muscle location. *Investigative Ophthalmology and Visual Science*, **45** (13), 2395-2395.

Strenk, S. A., Strenk, L. M (2005). MRI Study of the Aging Uveal Tract: The Modified Geometric Theory of Presbyopia and Its Implications for Posterior Chamber Phakic IOLs. *Investigative Ophthalmology and Visual Science,* **46** (13):4232.

Strenk, S. A., Strenk, L. M., Guo, S. (2006). Magnetic resonance imaging of aging, accommodating, phakic, and pseudophakic ciliary muscle diameters. *Journal of Cataract and Refractive Surgery*, **32** (11), 1792-1798.

Strenk, S. A., Strenk, L. M., Guo, S. (2010). Magnetic resonance imaging of the anteroposterior position and thickness of the aging, accommodating, phakic, and pseudophakic ciliary muscle. *Journal of Cataract and Refractive Surgery*, **36** (2), 235-241.

Suheimat, M., Verkicharla, P. K., Mallen, E. A., Rozema, J. J., Atchison, D. A. (2015). Refractive indices used by the Haag-Streit Lenstar to calculate axial biometric dimensions. *Ophthalmic and Physiological Optics*, **35** (1), 90-96.

Suzuki. R. (1983). Neuronal influence on the mechanical activity of the ciliary muscle, *British Journal of Pharmacology*, **78** (3), 591-597.

Suzuki, R., Kobayashi, S. (1983). Response of bovine intra-ocular muscles to transmural stimulation in the presence of various prostaglandins. *Experimental Eye Research*, **36** (6), 789-798.

Tabernero, J., Schaeffel, F. (2009). Fast scanning photoretinoscope for measuring

peripheral refraction as a function of accommodation. *Journal of the Optical Society of America,* **26** (10), 2206-2210.

Tabernero, J., Chirre, E., Hervella, L., Prieto, P., Artal, P. (2016). The accommodative ciliary muscle function is preserved in older humans. *Scientific Reports*, *6*.

Tamm, E., Flügel, C., Baur, A., Lütjen-Drecoll, E. (1991a). Cell cultures of human ciliary muscle: growth, ultrastructural and immunocytochemical characteristics. *Experimental Eye Research*, **53** (3), 375-387.

Tamm, E., Lütjen-Drecoll, E., Jungkunz, W., Rohen, J. W. (1991b). Posterior attachment of ciliary muscle in young, accommodating old, presbyopic monkeys. *Investigative Ophthalmology and Visual Science*, **32** (5), 1678-1692.

Tamm, E., Flügel, C., Stefani, F. H., Rohen, J. W. (1992a). Contractile cells in the human scleral spur. *Experimental Eye Research*, **54** (4), 531-543.

Tamm, S., Tamm, E., Rohen, J. W. (1992b). Age-related changes of the human ciliary muscle. A quantitative morphometric study. *Mechanisms of ageing and development*, **62** (2), 209-221.

Tamm, E., Croft, M. A., Jungkunz, W., Lütjen-Drecoll, E., Kaufman, P. L. (1992c). Age-related loss of ciliary muscle mobility in the rhesus monkey: role of the choroid. *Archives of Ophthalmology*, **110** (6), 871-876.

Tamm, E.R., Flügel-Koch, C., Mayer, B., Lütjen-Drecoll, E. (1995). Nerve cells in the human ciliary muscle: Ultrastructural and immunocytochemical characterization. *Investigative Ophthalmology and Visual Science*, **36** (2), 414-426.

Tan, D. T., Lam, D. S., Chua, W. H., Shu-Ping, D. F., Crockett, R. S., Asian Pirenzepine Study Group. (2005). One-year multicenter, double-masked, placebo-controlled, parallel safety and efficacy study of 2% pirenzepine ophthalmic gel in children with myopia. *Ophthalmology*, **112** (1), 84-91.

Tamm. E. R., Lütjen-Drecoll. E. (1996). Ciliary Body. *Microscopy Research and Technique*, **33**, 390-439.

Taylor, V.L., Al-Ghoul, K.J., Wesley Lane, C., Andrew Davis, V., Kuszak, J.R., Joseph Costello, M. (1996). Morphology of the normal human lens. *Investigative Ophthalmology and Visual Science*, **37** (7), 1396-1410.

Tearney G.J., Brezinski M.E., Southern J.F., Bouma B.E., Hee M.R., Fujimoto J.G. (1995). Determination of the refractive index of highly scattering human tissue by optical coherence tomography. *Optics Letters*, **20** (21), 2258-2260.

Tedesco, R.C., Da Silva Calabrese, K., Luiz Smith, R. (2005). Architecture of the Ciliary Muscle of *Gallus domesticus.* The anatomical record part A, 284a, 544-549.
Testoni, P. A. (2007). Optical coherence tomography. *The Scientific World Journal*, **7**, 87-108.

Tehrani, M., Krummenauer, F., Blom, E., Dick, H. B. (2003). Evaluation of the practicality of optical biometry and applanation ultrasound in 253 eyes. *Journal of Cataract and Refractive Surgery*, **29** (4), 741-746.

Testoni, P. A. (2007). Optical coherence tomography. *The Scientific World Journal*, **7**, 87-108.

Thomas, G. R., Williams, M. R., Sanderson, J., Duncan, G. (1997). The human lens possesses acetylcholine receptors that are functional throughout life. *Experimental Eye Research*, **64**(5), 849-852.

Thut, C.J., Rountree, R.B., Hwa, M., Kingsley, D.M. (2001). A large-scale *in situ* screen provides molecular evidence of the induction of eye anterior segment strucutres by the developing lens. *Developmental Biology*. **231** (1), 63-76.

Tornqvist, G. (1967). The relative importance of the parasympathetic and sympathetic nervous systems for accommodation in monkeys. *Investigative Ophthalmology*, **6** (6), 612-617

Tomlins, P. H., Wang, R. K. (2005). Theory, developments and applications of optical coherence tomography. *Journal of Physics D: Applied Physics*, **38** (15), 2519.

Troilo, D., Nickla, D. L., Wildsoet, C. F. (2000). Choroidal thickness changes during altered eye growth and refractive state in a primate. *Investigative Ophthalmology & Visual Science,* **41** (6), 1249-1258.

Tucker, J., Charman, W. N. (1975). The depth of focus of the human eye for Snellen letters. *Optometry and Vision Science*, ***52*** (1), 3-21.

Turvey, T. A., Golden, B. A. (2012). Orbital anatomy for the surgeon. *Oral and maxillofacial surgery clinics of North America*, *24*(4), 525-536.

Twelker, J. D., Mutti, D. O. (2001). Retinoscopy in infants using a near noncycloplegic technique, cycloplegia with tropicamide 1%, and cycloplegia with cyclopentolate 1%. *Optometry and Vision Science*, **78** (4), 215-222.

Uga, S. (1968). Abstract: Electron microscopy of the ciliary muscle. II. On the fine structure of the anterior terminal portion of the ciliary muscle. *Nippon Ganka Gakkai zasshi*, **72** (7), 1019.

Unno, T., Matsuyama, H., Komori, S. (2003). Interaction between the M2-and M3-receptor subtypes in muscarinic electrical and mechanical responses of intestinal smooth muscles. *Neurophysiology*, **35** (3-4), 262-273.

Ustundag, C., Bahcecioglu, H., Ozdamar, A., Aras, C., Yildirim, R., Ozkan, S. (2000). Optical coherence tomography for evaluation of anatomical changes in the cornea after laser in situ keratomileusis. *Journal of Cataract and Refractive Surgery*, **26** (10), 1458-1462.

Van Alphen. G.W.H.M., Kern, R., Robinette, S.L. (1965). Adrenergic receptors of the intraocular muscles: Comparision to cat, rabbit and monkey. *Archives of Ophthalmology*, **74**, 253-259.

Van Alphen, G. W. (1976). The adrenergic receptors of the intraocular muscles of the human eye. *Investigative Ophthalmology and Visual Science*, **15** (6), 502-505.

Van Alphen, G. W. H. M. (1986). Choroidal stress and emmetropisation. *Vision Research*, **26** (5), 723-734.

Van der Heijde, G. L., Weber, J. (1989). Accommodation used to determine ultrasound velocity in the human lens. *Optometry and Vision Science*, **66** (12), 830-833.

Vasudevan, B., Ciuffreda, K. J., Gilmartin, B. (2009). Sympathetic inhibition of accommodation after sustained nearwork in subjects with myopia and emmetropia. *Investigative Ophthalmology and Visual Science*, **50** (1), 114-120.

Verkicharla, P. K., Mallen, E. A., Atchison, D. A. (2013). Repeatability and comparison of peripheral eye lengths with two instruments. *Optometry and Vision Science*, **90** (3), 215-222.

Verkicharla, P. K., Mathur, A., Mallen, E. A., Pope, J. M., Atchison, D. A. (2012). Eye shape and retinal shape, and their relation to peripheral refraction. *Ophthalmic and Physiological Optics,* **32** (3),184-199.

Verkicharla, P. K., Mallen, E. A. H., Atchison, D. A. (2013). Repeatability and Comparison of Peripheral Eye Lengths With Two Instruments. *Optometry and Vision Science,* **90** (3), 215-222.

Vilupuru, A. S., Glasser, A. (2002). Dynamic accommodation in rhesus monkeys. *Vision Research*, **42** (1), 125-141.

Vilupuru, A. S., Glasser, A. (2005). The relationship between refractive and biometric changes during Edinger–Westphal stimulated accommodation in rhesus monkeys. *Experimental Eye Research*, **80** (3), 349-360.

Vincent, S. J., Collins, M. J., Read, S. A., Carney, L. G., Yap, M. K. (2013a). Corneal changes following near work in myopic anisometropia. *Ophthalmic and Physiological Optics*, **33** (1), 15-25.

Vincent, S. J., Collins, M.J., Read, S.A., Carney, L.G. (2013b). Retinal and choroidal thickness in myopic anisometropia. *Investigative Ophthalmology and Vision Science,* **54** (4), 2445-2456.

Vogel, A., Dick, H. B., Krummenauer, F. (2001). Reproducibility of optical biometry using partial coherence interferometry: intraobserver and interobserver reliability. *Journal of Cataract and Refractive Surgery*, **27** (12), 1961-1968.

Von Helmholtz, H. (1962). Mechanism of accommodation. *Helmholtz's Treatise on Physiological Optics, translated from the third German edition*, **1**, 143-173.

Vohra, S. B., Good, P. A. (2000). Altered globe dimensions of axial myopia as risk factors for penetrating ocular injury during peribulbar anaesthesia. *British Journal of Anaesthesia*, **85** (2), 242-245.

Vurgese, S., Panda-Jonas, S., Jonas, J. B. (2012). Scleral thickness in human eyes. *PloS one*, **7** (1), e29692.

Walker, T. W, Mutti, D. O. (2002). The effect of accommodation on ocular shape. *Optometry and Vision Science*, **79** (7), 424-430.

Wallman, J., Wildsoet, C., Xu, a., Gottlieb, M. D., Nickla, D. L., Marran, L., Krebs, W., Christensen, A. M. (1995). Moving the retina: choroidal modulation of refractive state. *Vision Research,* **35** (1), 37-50.

Walsh, A. C. (2011). Binocular optical coherence tomography. *Ophthalmic Surgery, Lasers and Imaging Retina*, **42** (4), S95-S105.

Wang, Q., Klein, B. E., Klein, R., Moss, S. E. (1994). Refractive status in the Beaver Dam Eye Study. *Investigative Ophthalmology and Visual Science*, **35** (13), 4344-4347.

Wang, X., Zhang, C., Zhang, L., Xue, L., Tian, J. (2002). Simultaneous refractive index and thickness measurements of bio tissue by optical coherence tomography. *Journal of Biomedical Optics*, **7** (4), 628-632.

Wang, B., Ciuffreda, K. J. (2006). Depth-of-focus of the human eye: theory and clinical implications. *Survey of Ophthalmology*, **51** (1), 75-85.

Wang, J., Shousha, M. A., Perez, V. L., Karp, C. L., Yoo, S. H., Shen, M., Cui, L., Hurmeric, V., Du, C., Zhu, d., Chen, Q., Li, M. (2011). Ultra-high resolution optical coherence tomography for imaging the anterior segment of the eye. *Ophthalmic Surgery, Lasers and Imaging Retina*, **42** (4), S15-S27.

Wanko, T., Gavin, M. A. (1959). Electron microscope study of lens fibers. *The Journal of Biophysical and Biochemical Cytology*, **6** (1), 97.

Warwick, R. (1954). The ocular parasympathetic nerve supply and its mesencephalic sources. *Journal of Anatomy*, **88** (1) 95-203.

Wasilewski, R., McDonald, J. P., Heatley, G., Lütjen-Drecoll, E., Kaufman, P. L., Croft, M. A. (2008). Surgical intervention and accommodative responses, II: forward ciliary body accommodative movement is facilitated by zonular attachments to the lens capsule. *Investigative Ophthalmology and Visual Science*, **49**(12), 5495-5502.

Watson, P. G., Young, R. D. (2004). Scleral structure, organisation and disease. A review. *Experimental Eye Research*, **78** (3), 609-623.

Wax, M.B., P.B. Molinoff. (1987). Distribution and Properties β - Adrenergic Receptors in Human Iris-Ciliary Body. *Investigative Ophthalmology and Visual Science*, **28** (3), 420-430.

Wendt, M., Glasser, A. (2008). Topical Pilocarpine Stimulated Accommodation in Anesthetized Rhesus Monkeys. *Investigative Ophthalmology and Visual Science*, **49** (13), 3787-3787.

Wendt, M., Glasser, A. (2010). Topical and intravenous pilocarpine stimulated accommodation in anesthetized rhesus monkeys. *Experimental Eye Research*, **90** (5), 605-616.

Weale, R. (1989). Presbyopia toward the end of the 20th century. Survey of ophthalmology, **34** (1), 15-30.

Weale, R. A. (2000). Why we need reading-glasses before a zimmer-frame. *Vision Research*, **40** (17), 2233-2240.

Weeber, H. A., Van der Heijde, R. G. (2007). On the relationship between lens stiffness and accommodative amplitude. *Experimental Eye Research*, **85** (5), 602-607.

Weeber, H. A., Eckert, G., Pechhold, W., Van der Heijde, R. G. (2007). Stiffness gradient in the crystalline lens. *Graefe's Archive for Clinical and Experimental Ophthalmology*, **245** (9), 1357-1366.

Whatham, A., Zimmermann, F., Martinez, A., Delgado, S., de la Jara, P. L., Sankaridurg, P., Ho, A. (2009). Influence of accommodation on off-axis refractive errors in myopic eyes. *Journal of Vision,* **9** (3), 14.11-13.

Wildsoet, C., and Wallman, J. (1995). Choroidal and scleral mechanisms of compensation for spectacle lenses in chicks. *Vision Research,* **35** (9), 1175-1194.

Win-Hall, D. M., Ostrin, L. A., Kasthurirangan, S., Glasser, A. (2007). Objective accommodation measurement with the Grand Seiko and Hartinger coincidence refractometer. *Optometry and Vision Science*, **84** (9), 879-887.

Win-Hall, D. M., Houser, J., Glasser, A. (2010). Static and Dynamic Measurement of Accommodation using the Grand Seiko WAM-5500 Autorefractor. *Optometry and Vision Science,* **87** (11), 873-882.

Wei, W. B., Xu, L., Jonas, J. B., Shao, L., Du, K. F., Wang, S., Chen, C.X., Xu, J., Wang, Y. W., Zhou, J.Q., You, Q. S. (2013). Subfoveal choroidal thickness: the Beijing eye study. *Ophthalmology*, **120** (1), 175-180.

Westphal, V., Rollins, A., Radhakrishnan, S., Izatt, J. (2002). Correction of geometric and refractive image distortions in optical coherence tomography applying Fermats principle. *Optics Express*, **10** (9), 397-404.

Wiederholt, M., Sturm, A., Lepple-Wienhues, A. (1994). Relaxation of trabecular meshwork and ciliary muscle by release of nitric oxide. *Investigative Ophthalmology and Visual Science*, **35** (5), 2515-2520.

Wiederholt, M., Schäfer, R., Wagner, U., Lepple-Wienhues, A. (1996). Contractile response of the isolated trabecular meshwork and ciliary muscle to cholinergic and adrenergic agents. *German Journal of Ophthalmology*, **5** (3), 146-153.

Wilson, R. S. (1997). Does the lens diameter increase or decrease during accommodation? Human accommodation studies: a new technique using infrared retro-illumination video photography and pixel unit measurements. *Transactions of the American Ophthalmological Society*, **95**, 261.

Williams, S., Ruggeri, M., Manns, F., Gregoris, G., Chang, Y-C., Yo, S.H., Parel, J-M. (2016). OCT biometry of the crystalline lens during dynamic accommodation. *Investigative Ophthalmology and Visual Science*, abstract #3959.

Winn, B., Whitaker, D., Elliott, D. B., Phillips, N. J. (1994). Factors affecting light-adapted pupil size in normal human subjects. *Investigative Ophthalmology and Visual Science*, **35** (3), 1132-1137.

Wold, J. E., Hu, A., Chen, S., Glasser, A. (2003). Subjective and objective measurement of human accommodative amplitude. *Journal of Cataract and Refractive Surgery*, **29** (10), 1878-1888.

Woldemussie, E., Feldmann, B. J., Chen, J. (1993). Characterization of muscarinic receptors in cultured human iris sphincter and ciliary smooth muscle cells. *Experimental Eye Research*, **56** (4), 385-392.

Wolfe, J. M., Owens, D. A. (1981). Is accommodation colorblind? Focusing chromatic contours. *Perception*, **10** (1), 53-62.

Woodman, E. C., Read, S. A., Collins, M. J., Hegarty, K. J., Priddle, S. B., Smith, J. M., Perro, J. V. (2011). Axial elongation following prolonged near work in myopes and emmetropes. *British Journal of Ophthalmology*, **95**, 652-656.

Woodman, E. C., Read, S. A., Collins, M. J. (2012). Axial length and choroidal thickness changes accompanying prolonged accommodation in myopes and emmetropes. *Vision Research,* **72**, 34-41.

Yeo, C. H., Kang, K. K., Tang, W. (2006). Accommodative stimulus response curve of emmetropes and myopes. Annasl- Academy of Medicine Singapore, **35** (12), 868.

Young, T. (1801). The Bakerian Lecture: on the mechanism of the eye. *Philosophical Transactions of the Royal Society of London*, **91**, 23-88.

Yoshitomi, T., Ito, Y., Inomata, H. (1985). Adrenergic excitatory and cholinergic inhibitory innervations in the human iris dilator. *Experimental Eye Research*, **40**, 453-459.

Yu, Y., Koss, M. (2003). Studies of α-adrenoceptor antagonists on sympathetic mydriasis in rabbits. *Journal of Ocular Pharmacology and Therapeutics*, **19** (3), 255-263.

Yuan, Y., Zhang, Z., Zhu, J., He, X., Du, E., Jiang, K., Zheng, W., Ke, B. (2015). Responses of the Ocular Anterior Segment and Refraction to 0.5% Tropicamide in Chinese School-Aged Children of Myopia, Emmetropia, and Hyperopia. *Journal of Ophthalmology*, **ID 612728**.

Zadnik, K., Mutti, D. O., Fusaro, R. E., Adams, A. J. (1995). Longitudinal evidence of crystalline lens thinning in children. *Investigative Ophthalmology and Visual Science*, **36** (8), 1581-1587.

Zamudio, A. C., Candia, O. A., Kong, C. W., Wu, B., Gerometta, R. (2008). Surface change of the mammalian lens during accommodation. *American Journal of Physiology-Cell Physiology*, **294** (6), C1430-C1435.

Zetterstrom, C., Hahnenberger, R. (1988). Pharmacological characterization of human ciliary muscle adrenoceptors in vitro. *Experimental eye research*, **46** (3), 421-430.

Zhang, X., Hernandez, M. R., Yang, H., Erickson, K. (1995). Expression of muscarinic receptor subtype mRNA in the human ciliary muscle. *Investigative Ophthalmology and Visual Science*, **36** (8), 1645-1657.

Zhao, J., Chen, Z., Zhou, Z., Ding, L., Zhou, X. (2013). Evaluation of the repeatability of the Lenstar and comparison with two other non-contact biometric devices in myopes. *Clinical and Experimental Optometry,* **96** (1), 92-99.

Zhong, J., Tao, A., Xu, Z., Jiang, H., Shao, Y., Zhang, H., Liu, C., Wang, J. (2014). Whole eye axial biometry during accommodation using ultra-long scan depth optical coherence tomography. *American Journal of Ophthalmology*, **157** (5), 1064-1069.

Ziebarth, N. M., Manns, F., Uhlhorn, S. R., Venkatraman, A. S., Parel, J. M. (2005). Noncontact optical measurement of lens capsule thickness in human, monkey, and rabbit postmortem eyes. *Investigative Ophthalmology and Visual Science*, **46** (5), 1690-1697.

APPENDICES

Appendix 1.

Tables showing the data obtained for Chapter 4.

Ciliary muscle parameter	Time (mins)				
	Baseline (0)	10 minutes post-instillation	20 minutes post instillation	30 minutes post-instillation	40 minutes post-instillation
CMT1	618.5 (SE 5.1)	622.4 (SE 6.8)	626.6 (SE 4.8)	630.2 (SE 7.0)	628.2 (SE 5.9)
CMT2	418.6 (SE 6.7)	419.0 (SE 6.8)	426.8 (SE 5.5)	426.6 (SE 7.1)	426.0 (SE 7.2)
CMT3	256.2 (SE 8.0)	256.0 (SE 6.7)	263.6 (SE 7.0)	263.6 (SE 7.9)	262.4 (SE 8.0)
CM25	523.0 (SE 8.2)	531.7 (SE 7.5)	544.9 (SE 7.8)	533.9 (SE 5.9)	541.9 (SE 6.5)
CM50	272.9 (SE 10.0)	283.1 (SE 8.8)	298.3 (SE 9.4)	278.1 (SE 7.6)	289.7 (SE 8.5)
CM75	111.4 (SE 6.3)	120.0 (SE 5.7)	126.2 (SE 6.0)	113.1 (SE 4.9)	122.0 (SE 6.7)
CMMAX	601.4 (SE 4.1)	599.1 (SE 5.3)	605.8 (SE 4.1)	610.3 (SE 5.8)	607.4 (SE 5.1)
SS-IA	1178.6 (SE 11.5)	1203.3 (SE 14.2)	1190.2 (SE 9.4)	1191.6 (SE 13.1)	1185.1 (SE 13.8)
SS-CM	1036.0 (SE 13.3)	1059.5 (SE 18.0)	1046.9 (SE 12.8)	1049.6 (SE 14.4)	1044.0 (SE 15.0)
CMLength Arc	5884.6 (SE 149.5)	5698.9 (SE 128.2)	5613.8 (SE 149.8)	5865.1 (SE 141.8)	5691.7 (SE 133.8)

Table A1-1. The measurement of ciliary muscle parameter (μm) during relaxed accommodation at baseline (0) and every 10 minutes post-instillation of tropicamide. The results are shown as the mean ± 1 SEM.

Ciliary muscle parameter	Time (mins)					
	Baseline (0)	10 minutes post-instillation	20 minutes post instillation	30 minutes post-instillation	40 minutes post-instillation	50 minutes post-instillation
CMT1	618.5 (SE 5.1)	609.2 (SE 8.9)	622.5 (SE 6.9)	623.0 (SE 6.9)	627.6 (SE 6.5)	625.6 (SE 6.4)
CMT2	418.6 (SE 6.7)	412.5 (SE 7.8)	418.5 (SE 6.9)	423.2 (SE 6.3)	426.4 (SE 6.8)	425.8 (SE 6.9)
CMT3	256.2 (SE 8.0)	254.2 (SE 8.5)	254.9 (SE 7.5)	262.7 (SE 7.4)	263.5 (SE 7.3)	260.3 (SE 8.2)
CM25	523.0 (SE 8.2)	530.9 (SE 8.2)	543.8 (SE 7.4)	537.7 (SE 6.7)	542.8 (SE 6.8)	543.4 (SE 7.2)
CM50	272.9 (SE 10.0)	288.3 (SE 8.9)	298.7 (SE 9.6)	292.3 (SE 9.1)	292.6 (SE 8.7)	296.0 (SE 8.9)
CM75	111.4 (SE 6.3)	126.6 (SE 6.4)	134.1 (SE 7.1)	128.7 (SE 6.8)	126.1 (SE 5.9)	125.3 (SE 5.9)
CMMAX	601.4 (SE 4.1)	591.2 (SE 6.9)	603.3 (SE 5.9)	600.7 (SE 5.4)	605.5 (SE 4.9)	605.2 (SE 5.5)
SS-IA	1176.3 (SE 12.0)	1168.7 (SE 15.5)	1183.2 (SE 10.0)	1192.8 (SE 12.1)	1198.4 (SE 10.7)	1189.2 (SE 11.4)
SS-CM	1036.0 (SE 13.3)	1031.5 (SE 16.4)	1039.8 (SE 10.1)	1056.1 (SE 13.3)	1057.1 (SE 11.4)	1047.6 (SE 12.8)
CMLength Arc	5884.6 (SE 149.5)	5572.7 (SE 117.0)	5477.9 (SE 130.0)	5646.1 (SE 121.6)	5655.6 (SE 137.9)	5594.0 (SE 109.9)

Table A1-2. The measurement of ciliary muscle parameter (μm) during relaxed accommodation at baseline (0) and every 10 minutes post-instillation of cyclopentolate. The results are shown as the mean ± 1 SEM.

Change in ciliary muscle parameter (µm) between maximum accommodation and relaxed accommodation	**Time (mins)**				
	Baseline (0)	10 minutes post-instillation	20 minutes post instillation	30 minutes post-instillation	40 minutes post-instillation
CMT1	6.1 (SE 7.0)	-5.3 (SE 6.2)	-19.0 (SE 5.1)	-14.1 (SE 7.1)	-4.9 (SE 8.9)
CMT2	-19.3 (SE 6.3)	0.7 (SE 4.4)	-14.0 (SE 3.9)	-9.0 (SE 5.2)	-1.1 (SE 5.9)
CMT3	-31.9 (SE 6.1)	2.4 (SE 4.1)	-11.2 (SE 4.0)	-9.4 (SE 5.3)	-5.8 (SE 6.2)
CM25	22.2 (SE 9.7)	-0.2 (SE 7.5)	-25.5 (SE 6.1)	-7.0 (SE 5.9)	-7.5 (SE 10.5)
CM50	12.5 (SE 11.5)	1.1 (SE 9.3)	-24.8 (SE 9.3)	-2.0 (SE 8.2)	-5.7 (SE 12.3)
CM75	8.0 (SE 8.0)	-0.4 (SE 6.5)	-12.6 (SE 6.3)	-1.2 (SE 5.1)	-5.4 (SE 8.9)
CMMAX	8.9 (SE 5.2)	0.5 (SE 5.1)	-9.3 (SE 3.9)	-5.7 (SE 5.9)	3.6 (SE 6.7)
SS-IA	-14.0 (SE 13.7)	-25.3 (SE 10.7)	-33.4 (SE 9.2)	-34.9 (SE 14.1)	-15.3 (SE 17.9)
SS-CM	-25.2 (SE 14.9)	-24.7 (SE 12.8)	-34.4 (SE 11.7)	-40.2 (13.9)	-27.0 (SE 17.0)
CMLength Arc	-520.3 (SE 140.5)	21.7 (SE 136.9)	178.3 (SE 135.1)	-115.3 (SE 104.8)	70.5 (SE 158.3)

Table A1-3. The change to the ciliary muscle parameter (measurement at the maximum objective accommodative amplitude - measurement during relaxed accommodation; µm) at baseline and every 10 minutes post-instillation of tropicamide. The results are shown as the mean ± 1 SEM.

Change in ciliary muscle parameter (µm) between maximum accommodation and relaxed accommodation		**Time (mins)**				
	Baseline (0)	10 minutes post-instillation	20 minutes post instillation	30 minutes post-instillation	40 minutes post-instillation	50 minutes post-instillation
CMT1	6.0 (SE 7.0)	12.5 (SE 7.3)	-6.0 (SE 6.9)	-1.9 (SE 5.3)	-12.3 (SE 7.5)	-3.2 (SE 6.6)
CMT2	-19.3 (SE 6.3)	7.8 (SE 6.1)	-3.1 (SE 4.7)	-2.1 (SE 3.8)	-8.2 (SE 4.7)	-5.1 (SE 5.9)
CMT3	-31.8 (SE 6.1)	2.8 (SE 5.3)	0.4 (SE 4.8)	-4.6 (SE 4.1)	-5.9 (SE 4.2)	-2.9 (SE 5.9)
CM25	22.2 (SE 9.7)	5.6 (SE 7.1)	-17.8 (SE 6.1)	-1.8 (SE 5.8)	-4.2 (SE 6.0)	-7.5 (SE 5.1)
CM50	12.5 (SE 11.5)	-3.1 (SE 8.4)	-21.0 (SE 8.3)	-6.5 (SE 7.0)	0.8 (SE 7.5)	-8.4 (SE 7.2)
CM75	8.0 (SE 8.0)	-6.8 (SE 5.3)	-16.1 (SE 5.5)	-7.3 (SE 4.5)	0.5 (SE 5.2)	-2.7 (SE 5.0)
CMMAX	8.9 (SE 5.2)	14.3 (SE 5.4)	-5.8 (SE 5.7)	4.0 (SE 3.9)	-6.0 (SE 4.6)	-2.5 (SE 5.2)
SS-IA	-14.0 (SE 14.1)	7.7 (SE 13.9)	-0.4 (SE 9.7)	-12.8 (SE 11.7)	-29.6 (SE 14.1)	-1.5 (SE 12.2)
SS-CM	-25.2 (SE 14.9)	-1.1 (SE 15.0)	0.7 (SE 10.5)	-21.7 (SE 14.1)	-33.1 (SE 15.1)	-4.1 (SE 13.7)
CMLength Arc	-520.3 (SE 140.5)	94.0 (SE 102.4)	293.9 (SE 88.0)	27.0 (SE 87.0)	-104.1 (SE 99.2)	64.4 (SE 103.0)

Table A1-4. The change to the ciliary muscle parameter (measurement at the maximum objective accommodative amplitude - measurement during relaxed accommodation; µm) at baseline and every 10 minutes post-instillation of cyclopentolate. The results are shown as the mean (± 1 SEM).

Appendix 2.

Tables showing the data obtained for Chapter 5.

Ciliary muscle parameter (μm)	Accommodative demand (D)							
	0	1	2	3	4	5	6	7
CMT1	610.3 (SE 8.9)	609.6 (SE 7.8)	612.7 (SE 8.6)	622.6 (SE 8.0)	617.5 (SE 7.8)	615.7 (SE 7.3)	628.1 (SE 9.3)	617.0 (SE 6.3)
CMT2	420. 1 (SE 9.5)	416.9 (SE 9.8)	414.3 (SE 10.5)	421.2 (SE 9.6)	415.8 (SE 8.3)	415.3 (SE 9.9)	417.7 (SE 10.6)	410.1 (SE 9.8)
CMT3	254.6 (SE 10.5)	253.0 (SE 10.2)	249.5 (SE 10.5)	250.7 (SE 10.1)	243.6 (SE 8.6)	238.7 (SE 10.4)	234.9 (SE 11.5)	225.9 (SE 10.1)
CM25	575.7 (SE 6.9)	572.8 (SE 6.8)	575.9 (SE 7.9)	589.6 (SE 6.0)	581. 4 (SE 7.2)	588.3 (SE 5.9)	600.9 (SE 7.3)	594.0 (SE 6.3)
CM50	356.6 (SE 6.3)	351.4 (SE 5.9)	352.5 (SE 8.4)	364.4 (SE 6.9)	357.6 (SE 8.0)	366.5 (SE 6.5)	371.0 (SE 8.1)	367.6 (SE 8.3)
CM75	176.0 (SE 4.7)	173.3 (SE 3.7)	176.2 (SE 5.6)	182.5 (SE 5.1)	173.9 (SE 6.1)	178.2 (SE 4.8)	179.9 (SE 7.2)	174.2 (SE 6.1)
CMMax	580.2 (SE 7.3)	581.3 (SE 6.7)	586.5 (SE 7.6)	597.5 (SE 6.9)	593.1 (SE 6.4)	595.4 (SE 6.5)	602.0 (SE 7.6)	596.3 (SE 5.6)
SS-IA	1226.0 (SE 17.4)	1215.8 (SE 15.9)	1208.3 (SE 13.1)	1208.3 (SE 14.5)	1199.5 (SE 12.0)	1188.9 (SE 12.5)	1211.0 (SE 15.6)	1180.4 (SE 11.7)
SS-CM	1103.1 (SE18.1)	1092.5 (SE 16.6)	1081.1 (SE 13.5)	1072.1 (SE 15.9)	1012.9 (SE 63.3)	1053.4 (SE 13.2)	1076.6 (SE 16.5)	1046.7 (SE 13.6)
CMLength Arc	4761.1 (SE 88.3)	4800.6 (SE 101.3)	4737.8 (SE 90.8)	4670.2 (SE 102.3)	4685.4 (SE 85.9)	4597.1 (SE 95.2)	4527.3 (SE 98.3)	4481.2 (SE 91.1)

Table A2-1. The ciliary muscle parameter during physiological accommodation for each accommodative demand level for 27 pre-presbyopic participants (mean ± 1 SEM).

Ciliary muscle parameter (µm)	Accommodative Demand (D)					
	0	1	2	3	4	5
CMT1	591.8 (SE 21.1)	588.6 (SE 34.2)	579.7 (SE 18.5)	575.3 (SE 14.9)	595.4 (SE 21.2)	586.2 (SE 21.1)
CMT2	378.4 (SE 34.1)	365.2 (SE 38.6)	356.3 (SE 39.7)	341.9 (SE 34.2)	358.1 (SE 38.2)	361.3 (SE 37.0)
CMT3	206.0 (SE 29.8)	204.9 (SE 28.9)	193.0 (SE 34.0)	175.0 (SE 33.4)	181.7 (SE 31.0)	180.6 (SE 31.2)
CM25	570.0 (SE 22.1)	559.8 (SE 34.6)	562.4 (SE 22.1)	573.7 (SE 19.3)	592.2 (SE 22.6)	574.8 (SE 21.3)
CM50	348.4 (SE 34.4)	319.9 (SE 31.5)	333.9 (SE 42.0)	338.7 (SE 19.2)	357.6 (SE 33.9)	342.7 (SE 26.6)
CM75	174.6 (SE 24.0)	155.9 (SE 14.1)	164.5 (SE 31.0)	164.9 (SE 14.6)	177.8 (SE 26.8)	149.5 (SE 15.2)
CMMax	555.0 (SE 31.8)	549.5 (SE 29.3)	543.4 (SE 24.4)	557.2 (SE 22.8)	567.4 (SE 27.8)	563.2 (SE 23.7)
SS-IA	1218.9 (SE 40.4)	1243.1 (SE 49.9)	1222.9 (SE 37.7)	1154.8 (SE 52.0)	1185.7 (SE 69.7)	1181.3 (SE 45.9)
SS-CM	1100.7 (SE 59.9)	1137.0 (SE 56.6)	1116.3 (SE 51.7)	1038.8 (SE 72.4)	1059.4 (SE 83.1)	1058.6 (SE 54.5)
CMLength Arc	4342.8 (SE 69.1)	4503.2 (SE 125.6)	4276.9 (SE 127.3)	4069.4 (SE 180.4)	4086.0 (SE 180.4)	4247.8 (SE 198.8)

Table A2-2. The ciliary muscle parameter during physiological accommodation for each accommodative demand level for 4 presbyopic participants. (mean ± 1 SEM).

Ciliary muscle parameter (µm)	Time (mins)					
	10	20	30	40	50	60
CMT1	624.9 (SE 8.2)	615.0 (SE 9.9)	616.8 (SE 6.7)	614.5 (SE 8.1)	608.6 (SE 7.4)	606.6 (SE 8.5)
CMT2	412.3 (SE 9.3)	415.2 (SE 9.4)	405.1 (SE 10.4)	411.1 (SE 8.9)	401.4 (SE 8.2)	403.5 (SE 8.7)
CMT3	229.1 (SE 9.5)	225.9 (SE 9.5)	223.0 (SE 10.9)	229.8 (SE 9.1)	220.6 (SE 9.6)	224.4 (SE 9.0)
CM25	599.2 (SE 6.8)	595.7 (SE 8.8)	597.0 (SE 5.7)	597.2 (SE 7.1)	591.1 (SE 6.1)	584.4 (SE 7.1)
CM50	370.1 (SE 6.5)	382.1 (SE 8.6)	367.5 (SE 7.0)	377.2 (SE 7.4)	369.5 (SE 5.2)	362.6 (SE 6.3)
CM75	177.6 (SE 4.1)	185.7 (SE 6.9)	176.0 (SE 5.7)	186.6 (SE 5.9)	180.5 (SE 4.2)	175.9 (SE 4.7)
CMMax	601.6 (SE 6.7)	593.8 (SE 8.3)	595.7 (SE 5.9)	593.3 (SE 7.4)	589.3 (SE 5.9)	587.5 (SE 7.5)
SS-IA	1193.9 (SE 13.3)	1184.7 (SE 13.2)	1187.9 (SE 10.0)	1187.9 (SE 11.9)	1178.1 (SE 11.9)	1175.3 (SE 11.6)
SS-CM	1057.9 (SE 13.6)	1051.9 (SE 12.7)	1054.6 (SE 10.2)	1054. 8 (SE 9.8)	1042.3 (SE 12.8)	1042.3 (SE 11.6)
CMLength Arc	4468.1 (SE 83.92	4367.1 (SE 77.8)	4432.1 (SE 89.4)	4380.2 (SE 75.9)	4377.0 (SE 81.5)	4459.1 (SE 81.9)

Table A2-3. The ciliary muscle parameter (mean ± 1 SEM) during pilocarpine stimulated accommodation for each time interval for 27 pre-presbyopic participants.

Ciliary muscle parameter (μm)	Time (mins)					
	10	20	30	40	50	60
CMT1	579.5 (SE 16.7)	571.8 (SE 28.4)	578.7 (SE 9.0)	572.0 (SE 25.0)	557.5 (SE 29.9)	560.6 (SE 28.0)
CMT2	336.3 (SE 36.0)	337.2 (SE 37.2)	330.9 (SE 37.5)	332.6 (SE 39.1)	335.1 (SE 43.7)	334.7 (SE 43.8)
CMT3	163.9 (SE 34.0)	157.8 (SE 26.4)	181.8 (SE 23.2)	162.8 (SE 27.4)	157.0 (SE 34.7)	173.4 (SE 34.4)
CM25	583.9 (SE 16.0)	580.2 (SE 26.0)	604.5 (SE 20.1)	579.1 (SE 23.6)	569.1 (SE 18.9)	563.2 (SE 24.9)
CM50	338.3 (SE 25.5)	358.9 (SE 21.6)	378.5 (SE 29.7)	345.3 (SE 32.2)	358.2 (SE 14.4)	328.4 (SE 26.0)
CM75	161.9 (SE 20.2)	169.9 (SE 8.0)	195.9 (SE 22.9)	176.3 (SE 22.5)	167.1 (SE 6.7)	156.3 (SE 14.4)
CMMax	564.5 (SE 20.0)	571.2 (SE 26.2)	569.5 (SE 8.7)	560.9 (SE 27.4)	556.2 (SE 26.4)	548.7 (SE 22.6)
SS-IA	1128.9 (SE 8.6)	1089.4 (SE 26.9)	1114.2 (SE 21.5)	1103.5 (SE 14.7)	1082.3 (SE 29.4)	1123.1 (SE 43.6)
SS-CM	1008.0 (SE 8.2)	954.8 (SE 17.0)	981.8 (SE 15.4)	977.8 (SE 27.2)	961.3 (SE 18.6)	1002.2 (SE 40.6)
CMLength Arc	4031.9 (SE 268.5)	3896.4 (SE 229.8)	3660.6 (SE 225.9)	3901.1 (SE 103.9)	3836.8 (SE 254.2)	4116.0 (SE 278.2)

Table A2-4. The ciliary muscle parameter (mean ± 1 SEM) during pilocarpine simulated accommodation over time for 4 presbyopic participants.

Ciliary muscle parameter (µm)	Time (mins)												
	Baseline (0)	10 minutes post-instillation		20 minutes post instillation		30 minutes post-instillation		40 minutes post-instillation		50 minutes post-instillation		60 minutes post-instillation	
		C	**P**	C	**P**	C	**P**	C	**P**	C	**P**	C	**P**
CMT1	601.2 (SE 5.9)	605.0 (SE 21.0)	**615.7 (SE 13.4)**	602.4 (SE 16.8)	**620.1 (SE 19.2)**	607.9 (SE 13.8)	**613.9 (SE 11.0)**	613.0 (SE 15.9)	**603.6 (SE 14.0)**	600.1 (SE 12.7)	**602.3 (SE 13.0)**	-	**604.4 (SE 14.0)**
CMT2	404.4 (SE16.3)	408.9 (SE 18.5)	**404.7 (SE 17.8)**	41.8 (SE 15.9)	**405.8 (SE 19.7)**	424.2 (SE 13.0)	**400.0 (SE 18.2)**	417.1 (SE 15.1)	**409.8 (SE 18.6)**	418.3 (SE 13.5)	**388.3 (SE 17.8)**	-	**398.1 (SE 17.3)**
CMT3	247.4 (SE 19.78)	250.8 (SE 19.3)	**220.1 (SE 17.9)**	256.4 (SE 15.3)	**210.4 (SE 17.1)**	268.5 (SE 15.8)	**212.7 (SE 21.3)**	257.3 (SE 15.5)	**229.1 (SE 20.0)**	258.6 (SE 15.3)	**208.5 (SE 20.0)**	-	**219.0 (SE 17.5)**
CM25	516.6 (SE 15.8)	527.1 (SE 14.7)	**595.8 (SE 6.1)**	530.8 (SE 14.2)	**601.2 (SE 16.3)**	532.5 (SE 10.4)	**602.1 (SE 7.6)**	536.0 (SE 15.7)	**591.3 (SE 10.5)**	527.3 (SE 16.2)	**586.7 (SE 8.8)**	-	**582.2 (SE 8.8)**
CM50	260.7 (SE 18.7)	282.5 (SE 15.6)	**367.2 (SE 8.1)**	295.0 (SE 17.9)	**375.0 (SE 18.4)**	292.9 (SE 17.6)	**372.6 (SE 11.5)**	290.7 (SE 19.6)	**380.4 (SE 12.0)**	293.6 (SE 19.3)	**361.1 (SE 9.0)**	-	**358.04 (SE 11.01)**
CM75	107.8 (SE 1.3)	129.3 (SE 11.0)	**176.0 (SE 7.0)**	140.9 (SE 14.3)	**176.5 (SE 13.7)**	139.3 (SE 14.8)	**180.7 (SE 12.1)**	134.4 (SE 12.6)	**187.6 (SE 10.2)**	131.0 (SE 11.7)	**175.2 (SE 6.9)**	-	**171.1 (SE 9.3)**
CMMAX	591.0 (SE 4.3)	592.5 (SE 17.7)	**593.9 (SE 10.7)**	587.9 (SE 14.3)	**596.8 (SE 16.0)**	592.4 (SE 10.4)	**592. 7 (SE 8.2)**	595.8 (SE 13.2)	**584.1 (SE 13.6)**	585.2 (SE 10.4)	**581.2 (SE 10.6)**	-	**581.9 (SE 12.2)**
SS-IA	1140.0 (SE 19.8)	1153.2 (SE 25.2)	**1187.5 (SE 26.7)**	1165.09 (SE 23.7)	**1189.1 (SE 23.2)**	1177.6 (SE 27.8)	**1190.3 (SE 18.46)**	1177.0 (SE 20.5)	**1182.9 (SE 12.8)**	1167.2 (SE 21.7)	**1182.3 (SE 18.4)**	-	**1187.5 (SE 21.6)**
SS-CM	1008.8 (SE 21.0)	1012.0 (SE 22.3)	**1058.7 (SE 28.2)**	1025.67 (SE 22.2)	**1054.8 (SE 22.3)**	1045.8 (SE 29.7)	**1063.9 (SE 18.4)**	1039.3 (SE 20.5)	**1061.6 (SE 12.3)**	1034.2 (SE 22.3)	**1056.0 (SE 18.2)**	-	**1059.5 (SE 22.1)**
CMLength Arc	5832.3 (SE 326.3)	5517.9 (SE 260.8)	**4395.2 (SE 162.2)**	5539.39 (SE 257.4)	**4315.0 (SE 142.7)**	5585.6 (SE 265.4)	**4339.9 (SE 209.4)**	5542.5 (SE 316.7)	**4327.0 (SE 140.9)**	5541.0 (SE 230.9)	**4344.6 (SE 181.6)**	-	**4443.0 (SE 166.9)**

Table A2-5. The ciliary muscle parameter (mean ± 1 SEM) at each time interval post-instillation of cyclopentolate (C) and pilocarpine (P) for 10 participants.

Appendix 3.

Ciliary muscle parameter (μm)	Ciliary muscle quadrant							
	Temporal		Nasal		Inferior		Superior	
	0 D	8 D	0 D	8 D	0 D	8 D	0 D	8 D
CM LENGTH	4924.0 (SE 79.2)	4720.2 (SE 79.1)	4408.4 (SE 63.4)	4335.4 (SE 58.4)	4858.9 (SE 88.6)	4954.4 (SE 83.7)	4702.5 (SE 76.9)	4516.1 (SE 77.9)
CMT1	637.6 (SE 6.9)	631.4 (SE 5.9)	610.1 (SE 5.4)	614.7 (SE 5.8)	667.7 (SE 7.4)	682.3 (SE 7.3)	621.6 (SE 5.9)	617.2 (SE 4.6)
CMT2	448.5 (SE 7.2)	431.9 (SE 7.2)	405.4 (SE 6.1)	399.4 (SE 8.0)	496.5 (SE 10.3)	507.8 (SE 10.2)	438.6 (SE 9.4)	423.6 (SE 8.0)
CMT3	282.1 (SE 7.3)	255.7 (SE 8.1)	227.3 (SE 7.2)	221.9 (SE 7.2)	328.8 (SE 13.2)	326.5 (SE 12.5)	276.1 (SE 10.0)	253.4 (SE 9.4)
CM25	590.9 (SE 6.4)	594.9 (SE 5.6)	586.4 (SE 4.9)	595.2 (SE 5.2)	630.7 (SE7.1)	656.0 (SE 6.3)	588.5 (SE 5.9)	592.2 (SE 4.9)
CM50	367.5 (SE 6.3)	365.3 (SE 5.7)	367.2 (SE 4.9)	366.4 (SE 7.3)	428.2 (SE 7.8)	450.9 (SE 7.3)	379.9 (SE 7.4)	378.9 (SE 6.5)
CM75	182.2 (SE 4.0)	175.7 (SE 4.3)	184.2 (SE 3.9)	185.1 (SE 5.5)	231.1 (SE 6.0)	241.6 (SE 6.0)	200.3 (SE 4.8)	198.7 (SE 4.4)
CMMAX	599.0 (SE 6.1)	605.7 (SE 4.5)	586.2 (SE 4.7)	595.2 (SE 5.4)	622.9 (SE 6.7)	647.0 (SE 6.1)	587.9 (SE 5.8)	590.3 (SE 4.5)
SS-IA	1275.9 (SE 12.8)	1218.3 (SE 11.2)	1200.8 (SE 9.2)	1185.87 (SE 9.1)	1334.2 (SE 16.1)	1294.7 (SE 17.8)	1256.5 (SE 13.5)	1217.5 (SE11.8)
ANTERIOR LENGTH	1151.8 (SE 14.0)	1081.3 (SE 12.4)	1062.4 (SE 9.9)	1041.4 (SE 10.2)	1217.1 (SE 18.0)	1160.2 (SE 18.8)	1132.8 (SE 15.8)	1086.9 (SE 13.3.)
CM LENGTH ARC	4987.4 (SE 81.4)	4776.5 (SE 81.2)	4440.8 (SE 64.9)	4364.5 (SE 59.4)	4916.36 (SE 90.1)	4708.4 (SE 8.5)	4744.4 (SE 78.5)	4554.9 (SE 79.5)

Table A3-1. The mean (μm) values (±1 SEM) are shown for the ciliary muscle parameters for each quadrant, for the relaxed (0 D) and maximum accommodative demand (8 D) levels for Chapter 6.

	ciliary muscle parameter (µm)	Ciliary muscle quadrant							
		Temporal		Nasal		Inferior		Superior	
		0 D	8 D	0 D	8 D	0 D	8 D	0 D	8 D
EMMETROPES	CMT1	629.1 (SE 10.1)	617.9 (SE 7.1)	595.9 (SE 8.5)	614.4 (SE 10.2)	670.3 (SE 82.6)	686.3 (SE 14.7)	631.5 (SE 10.1)	605.8 (SE 6.1)
	CMT2	435.3 (SE10.8)	405.9 (SE 11.1)	387.5 (SE 9.1)	389.0 (SE 14.7)	512.1 (SE 16.3)	511.1 (SE 19.9)	433.4 (SE 14.1)	406.9 (SE 12.0)
	CMT3	261.1 (SE 11.7)	227.1 (SE 12.2)	203.5 (SE 10.4)	208.3 (SE 13.0)	347.2 (SE 21.2)	325.6 (SE 24.4)	260.2 (SE 13.9)	229.0 (SE 14.9)
	CM25	593.3 (SE 8.3)	594.8 (SE 7.1)	583.3 (SE 8.1)	602.5 (SE 6.6)	636.9 (SE 10.8)	665.0 (SE 12.0)	606.4 (SE 8.6)	593.4 (SE 8.0)
	CM50	370.3 (SE 7.3)	365.5 (SE 9.7)	370.1 (SE 9.2)	369.6 (SE 11.3)	443.4 (SE 11.0)	464.0 (SE 12.4)	389.8 (SE 10.2)	371.8 (SE 10.4)
	CM75	184.4 (SE 5.9)	175.1 (SE 8.4)	182.5 (SE 4.3)	185.4 (SE 8.9)	220.0 (SE 7.6)	250.8 (SE 10.6)	196.5 (SE 6.9)	205.9 (SE 6.6)
	CMMAX	599.6 (SE 8.9)	599.7 (SE7.1)	577.9 (SE 7.3)	595.3 (SE 9.8)	631.8 (SE 11.5)	656.6 (SE 11.5)	598.3 (SE 9.6)	583.2 (SE 7.3)
	SS-IA	1233.8 (SE 17.2)	1184.4 (SE 8.8)	1173.5 (SE 13.3)	1182.3 (SE 11.4)	1326.6 (SE 23.6)	1279.0 (SE 35.1)	1246.9 (SE 20.7)	1191.5 (SE 13.2)
	SS-CM	1100.4 (SE 19.1)	1042.8 (SE 9.5)	1035.6 (SE 13.8)	1036.7 (SE 11.3)	1205.2 (SE 25.6)	1136.8 (SE 36.2)	1113.6 (SE 23.8)	1057.9 (SE 16.7)
	CM LENGTH ARC	4745.6 (SE 94.8)	4496.9 (SE 112.7)	4208.9 (SE 90.8)	4218.5 (SE 89.3)	4933.2 (SE 132.7)	4615.1 (SE 148.8)	4506.9 (SE 112.7)	4300.0 (SE 131.5)
MYOPES	CMT1	644.5 (SE 9.5)	642.2 (SE 8.5)	621.8 (SE 6.0)	615.1 (SE 6.7)	664.7 (SE 8.8)	679.0 (SE 6.1)	613.6 (SE 6.7)	626.5 (SE 6.3)
	CMT2	459.3 (SE 9.1)	450.6 (SE 7.7)	420.0 (SE 6.9)	407.8 (SE 8.1)	483.8 (SE 12.8)	505.0 (SE 9.4)	442.8 (SE 12.8)	437.2 (SE 10.1)
	CMT3	299.2 (SE 7.5)	279.0 (SE 8.0)	246.7 (SE 8.0)	233.1 (SE 6.8)	313.7 (SE 16.2)	327.1 (SE 11.6)	289.1 (SE 13.9)	273.4 (SE 10.5)
	CM25	588.9 (SE 9.6)	595.0 (SE 8.5)	589.0 (SE 6.2)	589.2 (SE 7.6)	625.5 (SE 9.5)	648.6 (SE 6.0)	573.9 (SE 6.7)	591.1 (SE 6.3)
	CM50	365.1 (SE 9.9)	365.2 (SE 6.8)	364.7 (SE 5.0)	363.8 (SE 9.7)	415.7 (SE 10.6)	440.2 (SE 8.0)	371.8 (SE 10.4)	374.0 (SE 8.6)
	CM75	184.4 (SE 5.9)	176.2 (SE 4.1)	182.5 (SE	184.8 (SE 7.1)	220.0 (SE 7.6)	234.0 (SE 6.5)	196.5 (SE 6.9)	192.8 (SE 5.8)
	CMMAX	598.4 (SE 8.5)	610.5 (SE 5.7)	593.0 (SE 5.9)	595.2 (SE 5.9)	615.6 (SE 7.7)	639.2 (SE 5.5)	579.3 (SE 6.7)	596.2 (SE 5.4)
	SS-IA	1275.9 (SE 15.6)	1218.3 (SE 7.9)	1200.8 (SE 12.0)	1185.8 (SE 10.3)	1334.2 (SE 21.3)	1294.7 (SE 31.7)	1256.5 (SE 18.7)	1217.5 (SE 12.0)
	SS-CM	1193.9 (SE 15.3)	1112.8 (SE 18.9)	1084.4 (SE 12.5)	1045.19 (SE 16.3)	1226.9 (SE 25.5)	1179.3 (SE 17.1)	1148.5 (SE 21.1)	1106.1 (SE 18.9)
	CM LENGTH ARC	5185.2 (SE 110.9)	5005.8 (SE 90.2)	4630.5 (SE 70.4)	4484.0 (SE 71.6)	4902.5 (SE 125.4)	4784.8 (SE 97.2)	4938.7 (SE 91.8)	4763.4 (SE 72.7)

Table A3-2. The mean (± 1 SEM) for the four ciliary muscle quadrants at 0 D and 8 D demands level for emmetropes (n= 18) and myopes (n= 22) for Chapter 6.

Appendix 4.

Pilot study for retinal contour study (Chapter 7)

To determine the most appropriate technique for measuring on-axis and peripheral eye length, a pilot study was conducted using the LenStar LS900 (Haag Streit). Previous authors (Read et al., 2010a, Woodman et al., 2012) have used biometric data provided by the instrument to convert the axial length from the optical path length to the geometric length. Therefore, it was of interest to obtain biometric data at the various eccentricities at which eye lengths were measured to correct the eye length data. Sixteen subjects were recruited (age range 19-25 years) from the undergraduate cohort of Aston University. The LenStar reflects a mire consisting of several dots that form a circle, onto the cornea and within the pupil margins. Accurate focussing of the instrument enables automatic calculation of the biometric data. However, if the complete mire is not reflected within the pupil margin, the measurement is prohibited. Therefore, peripheral eye length measurements beyond 15° were not possible for four participants. Importantly, complete off-axis biometric measurements were difficult to obtain in half of the subjects recruited. Overall, peripheral eye length measures could only be obtained from 12 subjects (two emmetropes (mean MSE: +0.22 ± 0.02 D) and ten myopes (mean MSE: - 2.08 ± 1.77 D)).

In contrast, the IOLMaster (Zeiss) uses a series of catropic images consisting of a central and six peripheral Purkinje images, which form a hexagon shape. Eye length measurements up to 30° are possible with the IOLMaster, since a value will still be provided even if the central dot is on the pupil edge. Therefore, the data that was collected and discussed for the main study is that obtained with the IOLMaster. However, on-axis biometric data (lens thickness, central corneal thickness and anterior chamber depth) were obtained with the LenStar, where possible.